A proteomic investigation of multi-lineage differentiated adult adipose-derived stem cells

Doctoral thesis by

Jerran Santos

Bachelor of Biotechnolgy Honours

2013

This thesis is presented for the degree of Doctor of Philosophy.

This thesis is presented as a partial fulfilment to the requirements for the Doctor of Philosophy

Statement of Candidate

I certify that the work in this thesis entitled "*A proteomic investigation of multi-lineage differentiated adult adipose-derived stem cells*" has not previously been submitted for a degree nor has it been submitted as part of requirements for a degree to any other university or institution other than Macquarie University.
I also certify that the thesis is an original piece of research and it has been written by me. In addition, I certify that all information sources and literature used are indicated in the thesis. Any help and assistance that I have received in my research work and the preparation of the thesis itself have been appropriately acknowledged.

_____

Jerran Santos

42174678

Student number

23 August 2013

Date

Preface

This thesis is dedicated to Talia and Nick

Out of the night that covers me,
Black as the Pit from pole to pole,
I thank whatever gods may be
For my unconquerable soul.

In the fell clutch of circumstance
I have not winced nor cried aloud.
Under the bludgeonings of chance
My head is bloody, but unbowed.

Beyond this place of wrath and tears
Looms but the Horror of the shade,
And yet the menace of the years
Finds and shall find me unafraid.

It matters not how strait the gate,
How charged with punishments the scroll,
I am the master of my fate:
I am the captain of my soul.

William Ernest Henley

Acknowledgements

There have been a number of people who have directly and indirectly been part of this PhD thesis over the course of its lifespan.

Dr Ben Herbert thank you for taking me on as a student. I have learnt a tremendous amount about stem cells, protein chemistry and interaction network computing.

Dr Matt Padula you have been a friend and mentor who I will always be indebted to. Without your passion and drive for discovering new and wonderful things through our profession this thesis most likely would not have existed. I thank you for the incredible amount of faith you have had in me over the years and most importantly reading through my page long paragraphs. We only progress in this field by standing on the shoulders of giants.

The Proteomics Core Facility UTS, I have spent more time with all of you in the last 3 years in our lab than anywhere else. Jess Tacchi, Ben Raymond, Michael Widjaja, Krish Singh, Marcelo Moreno, Kate Harvey, Isabella Hajduk, Tom Cawsey and Iain Berry, all of you are an incredible people who will achieve great things with all the hard work you have done. Every one of you has been of some support for me in one way or another during this insane period of my life. I thank you all for being great friends, colleagues and students. I look forward to working and having a blast with you all in the future.

Prof. Steve Djordjevic you have been great support and a friend throughout the entirety of my time in your lab. I am so grateful to have someone so enthusiastic about our work and willing to take chances on the crazy ideas I've come up with. I look forward to more scientific adventures and working with you in the future.

Prof. Ian Charles, thank you for employing me to work on the genomics sequencer and the plentiful philosophical and educational conversations. My time on the Miseq has definitely broadened my horizons and allowed me to value all the work I have done.

A number of people at Macquarie University: Prof. Paul Haynes, Dr Bill Russell, Dr Tim Dably, Prof. Trish Fanning, Prof. Jim Piper, Andre Hallen, Michael Sivell, Michael Medynskyj, Sinead Blaber and Cameron Hill for various roles you have all played in my research and course of my PhD.

UTS Prof. Kevin Broady, Prof. Bruce Milthorpe, Prof. Besim Ben-Nissan, Harry Simpson, Dr Ian Garthwaite, Prof Graham Nicholson and Dr Josh Chou for the advice and assistance you have all offered in my research and course of my PhD.

Special mention to Prof David Green and Dr Mung Wang you two people made research a different kind of fun. The stories from your short stints in my lab will forever resonate with the people that you touched the hearts and minds of.

To the thousands (3240) of students that I demonstrated tutored and lectured during the entirety of my PhD. Thank you all for keeping me employed as I had no scholarship and no other form of income besides this. Your enthusiasm to learn has ever increased my passion for teaching.

To my family, Dad, Mum, Larissa, Alysa and our pup Sox, without all of you this would have never been possible. You all put up with my ups and downs (so many downs), you gave me a place to live, always a warm meal and unwavering love and support. Even though you all have had a rough time with various health issues, you stayed strong and resilient. If I could have one-tenth the strength you all have I would be invincible. You have taught me to be the very best I can be and always give everything never expecting anything in return. I do apologise for not being around as often as I should have been and for stressing you all out during the lulls. I will forever be in your debt. Thank you so much for being the greatest family anyone could ever ask for.

Veronica Jarocki you were present through one of the most stressful parts of my life thus far. The last year has been tough for me in so many ways but you changed the final year of my PhD from an endurance race to a journey. You have shown me that life isn't as dichotomous but varying shades of every spectrum. Thank you for having being a part of my life.

Table of Contents

Figures and tables

Chapter 3: Proteomic analysis of human adipose derived stem cells during *in vitro* neuronal differentiation with β-mercaptoethanol

Chapter 4 Proteomic analysis of human adipose derived stem cells during novel *in vitro* neuronal differentiation with cyclic ketamines

Chapter 5 Final summary, concluding remarks and future perspectives

Abbreviations

Acronym	Full word
1-D	One-dimensional
2-D	Two-dimensional
AA	Ascorbic acid
AAK1	AP2-associated protein kinase 1
ABAM	Antibiotics/antimycotics
ACN	Acetonitrile
ADSC	Adipose-derived stem cell
AECK	S- aminoethyl-L-cyesteine ketamine
AHNAK	Neuroblast differentiation-associated protein
ALP	Alkaline phosphatase
AMP	Adenosine monophosphate
BAT	Brown adipose tissue
BBB	Blood brain barrier
BCIP	5-bromo-4-chloro-3-indolyl phosphate
bFGF	Basic fibroblast growth factor
BHA	Butylated hydroxyanisole
BHT	Butylated hydroxytoluene
BME	β-mercaptoethanol
BMP	Bone morphological proteins
BMSC	Bone-derived stem cell
BN	Blue native
BSA	Bovine serum albumin
cAMP	Cyclic-adenosine monophosphate
CD	Cluster of differentiation
cfu	Colony forming units
CK	Cyclic ketamine
CKR	Cyclic ketamine derivatives
CN	Clear native
CNS	Central nervous system
CO_2	Carbon dioxide
CO6A3	Collagen alpha-3(VI)
dex	Dexamethasone
dH2O	Deionised water
DIGE	Differential in gel electrophoresis
DMEM	Dulbecco's modified eagle's medium
DMSO	Dimethylsulfoxide
DNA	Deoxyribonucleic acid
DPBS	Deionised phosphate buffered saline
EBI	European Bioinformatics Institute
ECM	Extracellular matrix

EGF	Epidermal growth factor
EPO	Erythropoietin
ESC	Embryonic stem cell
ESI	Electrospray ionisation
ExPASy	Expert protein analysis system
FBS	Fetal bovine serum
FGF-2	Fibroblast growth factor-2
g	Grams
G6PD	Glucose-6-phosphate 1-dehydrogenase
GAG	Glycoaminoglycan
GBCs	Glioblastoma cells
GCLM	Glutamate--cysteine ligase regulatory subunit
G-CSF	Granulocyte colony-stimulating factor
GFAP	Glial fibiral associated protein
GM-CSF	Granulocyte macrophage colony-stimulating factor
GO	Gene ontology
GRO/KC	Neutrophil-activating protein 3
H&E	Haematoxylin and eosin
HCl	Hydrochloric acid
hESCs	Human embryonic stem Cells
HO	Heme oxygenase
HSC	Hematopoietic stem cell
HSP-70	Heat shock protein-70
HSPB1	Heat shock protein beta-1
HSPB11	Heat shock protein beta-11
HSPE1	10 kDa heat shock protein
IBMX	Isobutyl-methylxanthine
ICAT	Isotope coded affinity tags
IDA	Intelligent Data Acquisition
IF	Immunofluorescent
IFN-g	Interferon-gamma
IGF-1	Insulin-like growth factor-1
IL	Interluekin
iPSCs	induced pluripotent stem cells
iTRAQ	Isobaric tagging for relative and absolute quantification
KCl	Potassium Chloride
kDa	Kilodalton
LC-MS	Liquid chromatography–mass spectrometry
LK	Lanthionine Ketamine
LKEE	Lanthionine Ketamine Ethyl Ester
LPS	Lipopolysaccharide
MALDI	Matrix-assisted laser desorption/ionization
MAPK	Mitogen-activated protein kinase
MCP-1	Monocyte chemoattractant protein-1

M-CSF	Macrophage colony-stimulating factor
mg	Milligrams
MIP-1a	Macrophage inflammatory protein 1a
MIP-3a	Macrophage inflammatory protein 3a
ml	Millilitres
mM	Millimolar
MMP14	Matrix metallopeptidase 14
MMTS	Methyl methanethiosulfonate
mRNA	Messenger Ribonucleic Acid
MS	Mass spectrometry
MSC	Mesencymal stem cell
NADPH	Nicotinamide adenine dinucleotide phosphate
NBT	Nitro blue tetrazolium chloride
NENF	Neudesin
NF-M	Neurofilament-M
NH4HCO3	Ammonium bicarbonate
nm	Nanometer
NSC	Neural stem cells
NSE	Neuron specific enolase
^{o}C	Degrees Celcius
PAGE	Polyacrylamide gel electrophoresis
PBS	Phosphate buffered saline
PC12	Pheochromocytoma
PDB	Protein Database
PDC	Primary derived counterparts
pg	picograms
PKC	Protein Kinase C
PLC	Phospholipase C
pNPP	Para-Nitrophenylphosphate
PNS	Peripheral Nervous System
PPARγ	peroxisome proliferator-activated receptor gamma
ppm	Parts per million
PTGS1	Prostaglandin G/H synthase 1
PVDF	Polyvinylidene fluroride
RA	Retinoic acid
RANTES	Regulated on Activation, Normal T Cell Expressed and Secreted
RHN	Rat Hippocampal Neurons
SC	Stem cell
SDS	Sodium Dodecyl Sulphate
SHMT	Serine Hydroxymethyltransferase
SIB	Swiss Institute of Bioinformatics
SILAC	Stable isotope labelling of amino acids
SRM	Selective Reaction Monitoring
SVF	Stromal vascular fraction

TBP	Tributylphosphine
TCEP	Tris(2-carboxyethyl)phosphine
TEAB	Triethyl ammonium bicarbonate
TFA	Trifluoroaceteic Acid
TGF-β	Transforming growth factor beta
TMTs	Tandem mass tags
TNF-a	Tumor necrosis factor-alpha
TOF	Time of flight
Tris	2-Amino-2-hydroxymethyl-propane-1,3-diol
v/v	Volume per volume
VD3	1,25-dihyroxyvitamin D3
VDR	Vitamin D receptor
VEGF	Vascular endothelial growth factor
w/v	Weight per volume
WAT	White Adipose Tissue
WHO	World Health Organisation
α-MEM	Alpha-Modified Eagle Medium
βGP	β-glycerophosphate
βT3	Beta-tubulin III
µg	Micrograms
µl	Microlitre

Abstract

Regenerative medicine and stem cell therapies has rapidly come into vogue and remained in the public and research spotlight for the last decade due to the bountiful applications it promises. A large number of clinical applications now exist for a wide variety of injuries or disease states, ranging from skin damage in burn victims to degenerative joints in aged patients and, in a limited capacity, the repair of neuronal tissue.

Notwithstanding these advances, there is an insufficiency in the knowledge base regarding a stem cell's fate and characterisation of the extent of differentiation. This thesis presents the first investigation of its type, a broad proteomic investigation of differentiated stem cells derived from both rat and human adipose tissue.

The breadth of this body of work investigated the cellular and secreted proteome changes of homogenous ADSC cultures directed toward various phenotypic lineages by means of induction media. These differentiated lineages included osteocytes, chondrocytes, myocytes, adipocytes and neuronal phenotypes. For a marked comparison, primary derived cells from the relevant mature tissue were used as a benchmark measure for the extent of differentiation in the majority of the differentiation experiments. These comparisons aimed to expand our current knowledge about the depth of change occurring during each ADSC differentiation with respect to the mature primary derived cells. Furthermore this study queried the validity of currently employed markers and the possible alternative proteins identified which could be considered for future work.

The core chapters focused on the extent of neurogenic differentiation with various chemical inducers. The initial chemical investigated, the previously published β-mercaptoethanol which acted as an inducer, was found to have an overall toxic effect on cells, indicated by the up-regulation of stress proteins, if in contact for up to 24 hours. However the chemical initiated a morphological change that mimicked neuronal cells which furthermore expressed key neuronal protective and

restructuring proteins. Nonetheless the cell's proteome indicated that β-mercaptoethanol induced an overall cellular distress.

Novel to this study was the investigation of a naturally occurring chemical alternative; cyclic ketamine class chemicals that was theorised to have a less toxic effect. The cyclic ketamines investigated proved to be a superior induction chemical producing a higher population of cells that exhibited neuronal morphological properties as well as a wide variety of neuronally related proteins. These differentiations proved to be far gentler with a marked decrease in expression of stress related proteins compared to the β-mercaptoethanol treated cells. Due to the novel application and findings of the cyclic ketamine based neuronal induction a patent was filed around the method for the future development into a clinical and pharmaceutical application.

Chapter 1

A review of *in vitro* differentiated adipose-derived stem cells and proteomic characterisation

1.1.0 INTRODUCTION

1.1.1 Regenerative Medicine

Regenerative medicine is dedicated to the process of replacing, repairing or regenerating tissue [2] and has expanded into a multidisciplinary science which has rapidly grown in the past decade [3-12]. The foundation of this evolving branch of medicine and technology is the utilisation of a combination of biocompatible materials, stem cells, growth factors and supporting chemical cocktails to repair damaged or failing tissue and organs [2, 13-17]. The term 'Regenerative Medicine' usually directs people toward thinking about stem cells, particularly embryonic stem cells. While embryonic stem cells are important for the understanding of developmental biology, it has not been a central aspect of regenerative therapies due to long standing public controversy and legislative bans in numerous countries [18]. There are however various other sources of stem cells which have and will continue to play a critical role in the development of therapeutics and regenerative medicine; this will be expanded on in subsequent sections in this review.

The scale and breadth of stem cell applications in regenerative medicine is continually increasing with various clinical treatments being developed. The early prototype of skin grafting was the application of stem cells on a bilayer matrix to assist the growth of new skin in burns victims. The success of this application in the form of a commercially available product like *INTEGRA*^{TM} [19, 20] prompted a push toward the development of more complex regenerative therapeutics [2, 21]. This included therapies for the repair of traumatic musculoskeletal injuries and congenital defects [22], the regeneration of bone and cartilage in degenerative diseases such as osteoarthritis, [23-26], and the repair of damaged central and peripheral neuronal tissue [27].

Despite these advances, there remains a distinct deficit in the knowledge base regarding a stem cell's fate and characterising the extent of their differentiation. This review explores the current

information available about adult stem cells and their differentiation, the characterisation conjecture spanning the literature, and the utilisation of tools such as proteomics to further our knowledge about the fundamental changes occurring too as stem cells differentiate.

1.1.2 Stem Cells

Stem cells have long been the hot and often controversial topic amongst scientists, the media and the general public, shrouded with confusion and conjecture primarily due to the application of a generic title to a diverse group of cells. The stem cell population, regardless of their source, possess two characteristic properties; 1) unlimited self-renewal with long-term viability under controlled conditions and 2) the potential to differentiate into a variety of more specialised cell lineages [1, 28]. The first group of stem cells identified were derived from the blastocyst stage of a mouse embryo by Evans and Kaufman in 1981 [29] and embryonic stem cells have been well documented for their vast potential for medical applications [30-33]. However, due to the nature of their source, there are enormous ethical and political issues associated with their use [34, 35]. The second class of stem cells are the induced pluripotent stem cells which are produced by a viral reprogramming of skin epithelial cells to cells with a the differentiation potential of embryonic stem cells [36]. The third and less well known group of stem cells are those derived from adult tissue and have been termed adult mesenchymal stem cells (MSCs). Originally discovered by Friedenstein *et al*., 1992 in the bone marrow as osteoprogenitor cells [37, 38], MSCs primarily function in the repair and regeneration of organs and tissues. MSCs were originally postulated to have a differentiation capacity limited to their tissue of origin [39, 40], but a number of recent studies have demonstrated that these cells possess pluripotent plasticity [28, 41-50]. This denotes a greater differentiation potential, permitting the genesis of cells of other dermal lineages. However this potential is more restricted than that of embryonic stem cells [51]. Complete differentiation of MSCs into cells of mesodermal, endodermal and ectodermal lineages has been achieved by the promotion of certain signalling pathways [39] and

MSCs have been shown to have the potential to differentiate into adipocytes, chondrocytes, osteoblasts, myoblasts and neural cells [52-56]. Adult MSCs have been identified in other specific organs such as the bone marrow, gastrointestinal tract, brain, lungs, liver, kidneys and most recently adipose tissue [57]. This thesis focuses on subcutaneous adipose tissue deposits which are an abundant and readily accessible source of adult MSCs or adipose derived stem cells (ADSCs).

1.1.3 Adipose Tissue

Adipose is a highly specialised connective tissue made up of two functionally different tissue types that are intricately involved in energy balance [58]. White Adipose Tissue (WAT) is primarily constituted of adipocytes, that store lipid through the uptake of free fatty acids or by triacylglycerol synthesis linked to the process of glycolysis [59]. WAT is considered an endocrine organ due to its ability to store energy and secret numerous endocrine and paracrine molecules [13, 58]. Brown Adipose Tissue (BAT) is highly vascularised and functions principally for the regulation of body heat [9]. Mature adipocytes in either type of adipose tissue account for only 40-60% of the whole cell population in fat. The remaining cell population is considered to consist of endothelial and haematopoietic cells, pre-adipocytes or stem cells [13, 60]. This is known as the stromal vascular fraction (SVF) of adipose tissue and up to 35% of the total cell harvest have the potential for multi-lineage differentiation compared to the total of 0.002% of bone marrow-derived mesenchymal stem cells [12]. Mature adipocytes are developed from a committed lineage of MSCs. These precursor cells maintain the cell population range within adipose tissue. Adult mesenchymal stem cells have been isolated from adipose tissue, expanded and differentiated into a variety of lineages *in vitro* by numerous groups [13, 28, 38, 53, 61, 62]. Thus, adipose represents a plentiful source of ADSCs and an attractive candidate for tissue regenerative therapies and disease management. Additionally, with population dynamics indicating a growing rate of obesity in first world countries, coupled with an increasing trend in cosmetic enhancement surgery, especially liposuction, a vast supply of stem

cells residing within the lipoaspirate is potentially available using routine and minimally invasive procedures [39].

1.2.0 CLASSIFICATION OF ADULT STEM CELLS

The classification of ADSC's relies on the verification of several conditions. Some of these conditions are often debated in the literature due to some conflicting publications which will be explored in subsequent sections. The first condition of the criteria is the *in vitro* cellular morphology. ADSCs have a distinct fibroblastic appearance with a branched cytoplasm focusing at two or three extensions at the poles of the cell enclosing an elliptical nucleus, as seen in figure 1.

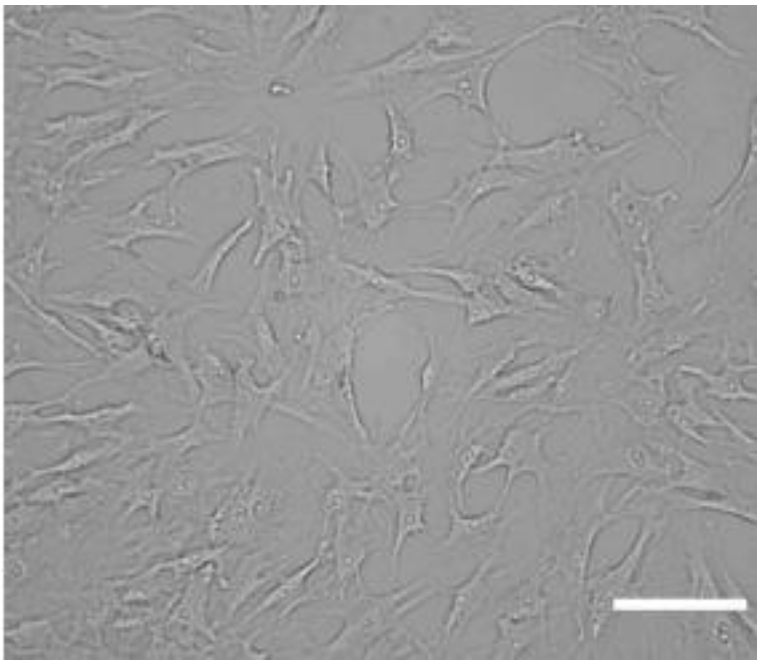

Figure 1 Adipose derived stem cells (ADSCs) live cell culture captured on an inverted microscope [1]

Successive passaging promotes the growth of a homogeneous population of cells which assumes a uniform morphology and directional growth. ADSCs can be cultured indefinitely. However, it is now well known and accepted that plasticity, or the differentiation potential of the cells, dissipates with aged cell lines and high passage number [63]. The optimal passage number for differentiation

studies is recommended between passages 3 to 7. Beyond passage 10 the differentiation potential is somewhat diminished [63]. Cryopreservation of cells should be routine after every passage.

1.2.1 Marker Characterisation

Traditional ADSC characterisation methods, such as histological stains, only qualitatively identify general cellular characteristics such as hematoxylin and eosin stain (H&E) [64, 65]. Fluorescent microscopy and flow cytometry are the most frequent and effectively utilised methods, especially the application of a combined approach of fluorescent antibodies and the adapted stem cell specific dyes such as Hoechst 33342. This Hoechst dye stains DNA and exploits a differential efflux function of a multi-drug-like transporter present in ADSCs [66]. Immunofluorescent (IF) staining is a straightforward method that works well when a target protein and its expression levels are known. Classically, a cluster of differentiation (CD) markers have been used in the phenotypic characterisation of leukocytes, including hematopoietic stem cells (HSCs). CD-markers are the most widely used cell surface molecules for characterisation by IF and haematopoietic and bone marrow stem cells have long been identified by the presence of CD34 and absence of CD31 [67-69]. CD34 is a surface adhesion molecule thought to play a role in cell localisation during inflammation [70]. This surface molecule is also prevalent in the small-vessel epithelium where its function remains to be deciphered [70]. Expression levels of CD34 are highest in early hematopoietic stem cells with levels decreasing in mature or differentiating cell populations and a similar phenomenon is observed in ADSCs [71]. The absence of CD31, a platelet endothelial cell adhesion molecule, confirms that the cells are not of a mature haematopoietic lineage. Paradoxically, while haematopoietic stem cells (HSCs) are easily identified and characterised utilizing specific sets of CD-markers, no such collection exists yet for ADSCs, however CD-markers are still used to characterise ADSCs. CD-marker characterisation is an immense area of conjecture across the literature on MSCs and ADSCs. Table 1

demonstrates the CD-marker uncertainty with several important CD markers studied and reported in a range of papers from the previous 10 years.

Table 1 Summarises different research group's positive and negative association of CD-markers present on Mesenchymal stem cells.

CD Marker	Name	Positive	Negative
CD11b	Integrin alpha M		Phinney and Prockop, 2007[38] Sanz-Ruiz *et al*., 2008 [72] Katz *et al*., 2005 [73]
CD14	Monocyte differentiation antigen		Phinney and Prockop, 2007[38] Sanz-Ruiz *et al*., 2008[72]
CD19	B-lymphocyte antigen		Sanz-Ruiz *et al*., 2008[72] Katz *et al*., 2005 [73]
CD29	Integrin beta-1 fibronectin receptor	Mitchell *et al* 2006 [74]	
CD31	Platelet/endothelial cell adhesion molecule	Mitchell *et al* 2006 [74]	Strem *et al*., 2005 [75] Cousin *et al.,*2009 [76]
CD34	Hematopoietic progenitor cell antigen	Casteilla & Dani, 2006 [13] Mitchell *et al* 2006 [74] Majumdar *et al.,*1998 [77], Young *et al*., 1999,[78]	Pittenger *et al.,* 1999 [40], Short *et al*., 2003 [79], Etheridge *et al*., 2004 [80], Song *et al* 2005 [81], Dicker *et al*., 2005 [82], Sethe *et al*., 2006 [83], Sanz-Ruiz *et al*., 2008[72] Tuli *et al*., 2003 [84]
CD44	Hyaluronic acid receptor	Phinney and Prockop, 2007[38] Mitchell *et al* 2006 [74]	
CD45	Protein tyrosine phosphatase, receptor type C	Sethe *et al*., 2006 [83], Casteilla & Dani, 2006 [13] Song *et al* 2005 [81],	Reyes *et al*., 2001 [85] Jones *et al*., 2002 [86] Zuk *et al.,* 2002 [28], Short *et al*., 2003 [79] Etheridge *et al*., 2004[80] Dicker *et al.*,2005 [82], Phinney and Prockop, 2007[38] Sanz-Ruiz *et al*., 2008[72] Tuli *et al*., 2003 [84]
CD49a-f		Phinney and Prockop, 2007[38] Mitchell *et al* 2006 [74] Katz *et al*., 2005 [73]	Katz *et al*., 2005 [73]
CD56	Neural Cell Adhesion Molecule	Young *et al*., 1999 [78]	Zuk *et al.,*2002 [28]
CD73	5'-nucleotidase	Phinney and Prockop, 2007 Sanz-Ruiz *et al*., 2008[72] Mitchell *et al* 2006 [74]	
CD79	CD79a molecule, Ig-associated alpha		Sanz-Ruiz *et al*., 2008[72]
CD90	Thy-1 cell surface antigen	Young *et al*., 1999[78] Pittenger *et al*., 1999 [40] Zuk *et al.,*2002 [28] Etheridge *et al*., 2004 [80] Song *et al* 2005 [81], Dicker *et al*, 2005 [82], Sanz-Ruiz *et al*., 2008[72] Mitchell *et al* 2006 [74] Katz *et al*., 2005 [73]	
CD105	Endoglin	Sanz-Ruiz *et al*., 2008[72] Mitchell *et al* 2006 [74] Tuli *et al*., 2003 [84]	
CD146	melanoma cell adhesion molecule	Lin *et al*., 2008 [87] Mitchell *et al* 2006 [74]	
CD166	Activated leukocyte cell adhesion molecule	Phinney and Prockop, 2007[38] Mitchell *et al* 2006 [74]	

Considering the wide discrepancies exhibited in Table 1, the question that needs to be asked is; why are different research groups confirming or occluding opposing marker sets from the same cell type? One may postulate that a number of variables may lead to marker expression. Do the varying isolation methods select for different subpopulations? Does a harvested heterogeneous cell population play a role in ADSCs ability to adhere and propagate? Are the ADSCs affected by the extraction method used? Does the high vascularisation of adipose influence the microenvironment of ADSCs, altering the expression and maturation of adhesion molecules which are routinely used as markers for MSCs from other tissues? Does the attempt to monoculture ADSCs alter their cell surface during proliferation in a new environment? Are there assays that can utilise a whole cell or component characterisation method? Can a proteomic approach assist in resolving these questions?

Exploring the range of CD-markers associated biological functions may elucidate a portion of the inconsistent findings established in table 1 and address a number of the above questions. The literature indicates the first three markers, CD11b, CD14 and CD9, are negative markers (table 1). CD11b, otherwise known as Integrin alpha M, is an adhesive molecule involved in the interactions of monocytes, macrophages and granulocytes [88]. CD14, or Monocyte differentiation antigen, is primarily expressed on peripheral blood monocytes and macrophages and is involved with the immune response to bacterial lipopolysaccharide (LPS) [89]. CD19 is expressed solely as a B-lymphocyte antigen with complex forming interactions [90]. The predominant shared feature among the three aforementioned CD-markers is their prevalence in mature leukocytes. The findings of Katz *et al*., Sanz-Ruiz *et al*., and Phinney and Prockop correlate in that ADSCs should not express these markers when undifferentiated [38, 72, 73]. Reviewing the biological role of CD29 or Integrin beta-1 shows that it is actively expressed in a dozen or more tissues and has several roles dependant on its location [91] such as a collagen receptor or an adhesive molecule [92]. Since adipose tissue is abundant in collagen, it is reasonable to presume that the ADSCs surface may harbour this marker to complement its environment. In consideration of its wide distribution, it would be inaccurate to label CD29 as a stem cell marker.

The previously mentioned CD31, a platelet/endothelial cell adhesion molecule, is employed as a negative marker in the characterisation of haematopoietic stem cells. Consequently it should not be present on the ADSC surface as confirmed by Strem *et al* and Cousin *et al* [75, 76]. Mitchell *et al* [74] presented a remarkably comprehensive list of the expression ratios of CD-markers at different passage number. The expression of CD31 at passage 1 and 2 significantly decreases to a third of its value in the initial culture, an expected outcome as the first passage removes the non-adherent RBCs. In an unanticipated outcome, the expression levels of CD31 in passage number 3 and 4 returns to the high levels of the initial culture. The cause of this is unknown and remains to be investigated.

Approximately 70% of reviewed papers conclude that CD34 and CD45 are not present on ADSCs. The confirmation of these markers by the remaining thirty percent is a perplexing circumstance particularly since CD34 is a positive marker for HSCs [67]. Scrutinizing the SVF constituents may reveal a minor population of HSCs derived from the highly vascularised adipose tissue. The Mitchell *et al* study revealed that the CD34 in 60% of cells in the SVF is eventually lost with *in vitro* expansion [74]. If the ADSCs are inherently CD34-positive *in vivo* in the presence of vascular endothelial cells and in early passage number *in vitro*, producing a monoculture of ADSCs may alter its environment enough that the cells have no functional need for CD34, decreasing its expression. Through continual clonal expansion, the CD34-negative ADSCs would eventually overcome any other population. Conversely CD45 should not exist on any MSCs, since its expression should be limited to mature leukocytes [93]. The SVF does indeed include a side population of haematopoietic cells of which CD45 expression is diminished with passage [74, 94].

A vast majority of papers corroborate CD90's presence in ADSCs. CD90 exists as a number of isoforms primarily expressed on all tissue derived MSCs and neuronal cells [95]. There are no known isoforms detected on adult tissues, and thus CD90 may be the quintessential mesenchymal stem cell marker. CD105, CD146 and CD166 have also been identified on ADSC surfaces with increasing levels in progressive passages. However these CD-markers cannot be used solely for stem cell identification

as they exist in a wide variety of tissues such as endothelial cells, muscle cells, fibroblasts and leukocytes [96-99]. There is no sufficient explanation for the above listed discrepancies between different studies. The definition and characterisation of something as specific as an adult stem cell and its diverse differentiated progeny will need to take into account the vast array changing mechanisms and variables.

1.3.0 STEM CELL DIFFERENTIATION

Differentiation is the process in which stem cells respond to local external stimuli by developing into the cell type caused by the signalling environment. The range of mature cell types a stem cell can differentiate into is known as plasticity, which is the inherent ability of stem cells to cross lineage barriers and adopt the phenotypic, biochemical and functional properties of cells unique to other tissues [39]. This plasticity potential can be subcategorised depending on the source of the stem cells. Embryonic stem cells (ESCs) are known to be able to differentiate into all cell and tissue types during foetal development and thus are referred to as pluripotent cells. MSCs have the innate potential to differentiate into cells within the mesodermal linage and are said to be multipotent. However numerous publications have shown that these cells when induced under specific conditions are capable of *in vitro* transdifferentiation [52, 100-103], effectively developing into cells of ectodermal and endodermal lineages [28, 104, 105]. Another commonly used class of cells are the oligopotent cells or progenitor cells that are committed to a tissue type and give rise to a defined set of cell types with a limited number of lineages [106].

Adipose-derived stem cells are multipotent adult MSCs which have been demonstrated, when induced, of being capable of differentiating morphologically and biochemically into neuronal cells [104, 107-109], osteocytes [28, 75, 110-112], chondrocytes [25, 113-116], adipocytes [52, 59, 116], myocytes [56] and cardiomyocytes [72, 117, 118] (figure 2). The two broad methods of inducing differentiation are chemical stimulation or biological stimulation. The overarching action of chemical

stimuli is due to simple small molecule additives acting directly on biochemical pathways promoting the desired differentiation pathway [119]. Biological stimulation uses cocktails of cytokines, growth factors and various bioactive components usually present in the tissue normally containing the desired differentiated cell [40, 120, 121]. These constituents not only promote differentiation pathways, but also have an active role in essential mineral and vitamin sequestration, driving the process forward. The subsequent sections detail the current differentiation methods and their clinical significance and potential.

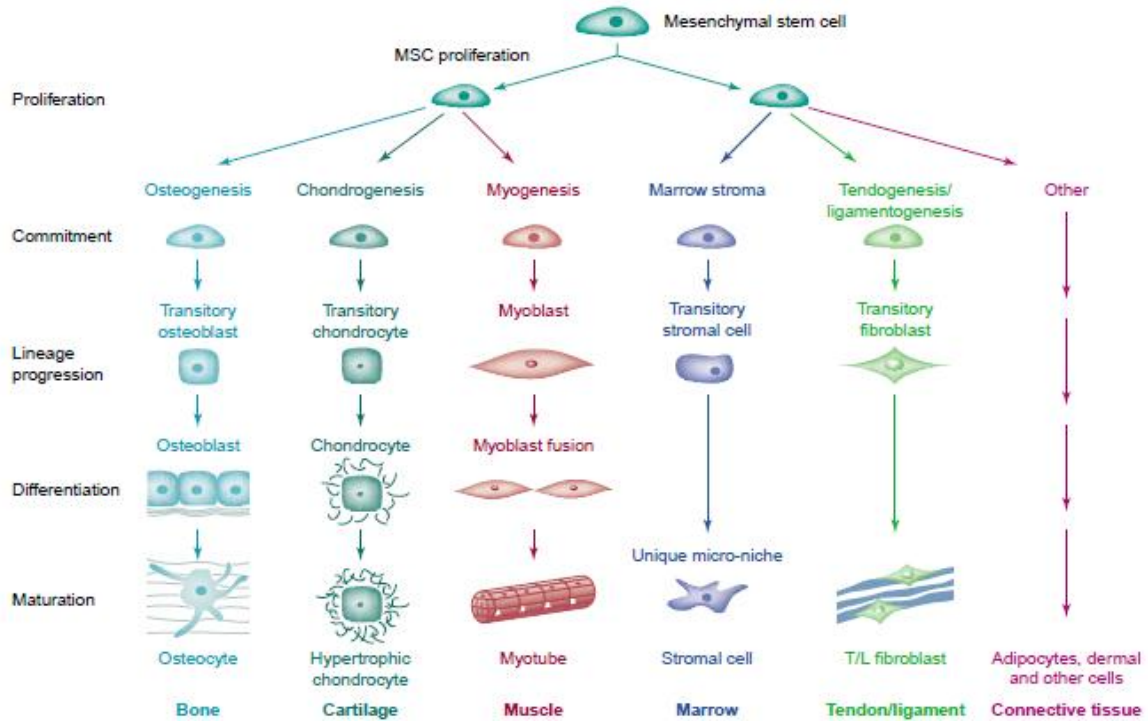

Figure 2 Mesogenic differentiation and maturation of differentiating adult mesenchymal stem cells adapted from Caplan *et al*., [122].

1.3.1 Adipogenic differentiation

The 'trilineage' differentiation of MSCs to adipogenic, osteogenic and chondrogenic cells has become a benchmark for determining the differentiation potential of tissue derived adult MSCs [28, 40]. Producing adipocytes from the ADSCs is no revelation considering the cell's source tissue, demonstrating an inherent potential for the development of adipocytes *in vivo* which can be

reproduced *in vitro* under the correct conditions. Producing adipocytes from MSCs has garnered much attention for their clinical importance in reconstructive surgeries and regenerative therapies. Patients suffering extensive tissue loss from burns, accidents and tumour removal in mastectomys have a source of autologous soft tissue for reconstructive surgeries. Several studies of *in vitro* adipose reconstruction have demonstrated the use of MSCs and precursor cells derived from bone and adipose tissue [49, 123, 124].

Current methodologies to achieve adipose reconstruction involve ADSCs cultured in serum containing adipogenic media supplemented with a combination of 0.5 mM isobutyl-methylxanthine (IBMX), 1 µM dexamethasone (dex), 10 µM insulin and 200 µM indomethacin. Following a 21 day differentiation period, the newly formed cells express adipocyte specific marker proteins and present visible accumulation of lipid, confirmed by Oil Red S staining. The adipogenic supplements have demonstrated critical roles in the development of adipocytes. The first component, IBMX, induces an increase in the intracellular concentrations of cAMP [125]. IBMX is an inhibitor of phosphodiesterase Gi complexes, which enzymatically convert cAMP to AMP [126]. IBMX also actively stimulates adenylyl cyclise promoting cAMP synthesis [125]. The increased intracellular cAMP is also known to mediate the stimulation of adipocyte differentiation [127]. The second supplement, Dex, is commonly utilised as it is known to regulate the metabolism of glucose and to stimulate the expression of the peroxisome proliferator-activated receptor γ (PPARγ), a transcription factor which is known to play an essential role in adipogenesis [128, 129]. The third component, indomethacin, binds and activates PPARγ which stimulates lipid uptake in adipogenesis [130]. The fourth and final component is the Insulin hormone which stimulates the uptake and storage of glucose in a variety of cells, especially adipose. The combination of these supplements provides the ideal stimulatory push for adipogenic induction. The expression and detection of markers such as the PPARγ, aP2 and Glut4 have been widely used as confirmation of adipogenesis [75, 131]. In further studies aimed at elucidating the pathway crossover and interactions during differentiation, Enomoto and colleagues [132] noted the inhibition of the RunX2 gene hinders chondrogenesis while

promoting adipogenesis. Dicker *et al's* study concluded that the adipocytes produced *in vitro* from differentiated BMSCs and ADSCs are phenotypically and functionally identical to the native adipocytes [82].

Both BMSCs and ADSCs have adipogenic capacity *in vivo* and are usually surgically implanted within scaffolds that possess a degree of biocompatibility [133, 134]. Nonetheless, several areas must be further developed before regenerated adipose tissue could be utilised in a clinical setting. These include the following: 1) proper vascularisation of tissue within a 3D scaffold; 2) producing a scaffold that is flexible and robust enough to be manipulated in surgery as well as being bioresorbable; 3) defining the complete proteomic characteristics of the adipogenic cells produced on the various scaffolds while comparing it to the native tissue, and 4) determining the stability of the cells as they do require pre-induction prior to implantation.

1.3.2 Osteogenic differentiation

Musculoskeletal conditions are the most common cause of severe long-term pain and physical disability affecting hundreds of millions of people around the world [22] while osteoporosis and osteoarthritis are the leading causes of skeletal and joint damage and the fourth leading cause of disability with a worldwide medical cost burden in the billions of dollars. The World Health Organisation (WHO) estimates that osteoarthritis effects 9.6% of men and 18.0% of women aged ≥60 years worldwide and estimate that 6.3 million people will suffer from osteoporosis by 2050 [135]. Cellular therapies for such afflictions have become popular in the last decade. Initially, BMSCs were used; however these cells are limited in number and estimated to be derived at a very dilute 1 per 10^5 cells using traumatic retrieval methods [136, 137]. Alternatively, primary isolation yields of ADSCs are often a thousand fold higher than that of BMSCs and the cells demonstrate a high capacity for bone formation *in vitro* and *in vivo* [138, 139]. In addition, using autologous cells negates the problem of immunological antigenic rejection [101].

There are now a plethora of methods that yield high numbers of differentiated osteogenic cells from a variety of tissue derived MSCs for research and clinical applications. In addition, numerous groups have demonstrated that ADSCs from various species can produce osteoblasts *in vitro* [25, 52, 75, 140, 141]. The most popular method of differentiating cells into osteogeneic lineages utilises the simple additives dexamethasone (Dex), ascorbic acid (AA), and β-glycerophosphate (βGP) to the basal media of *in vitro* cells [28]. Alternative induction medias do exist and contain combinations of hormones and growth factor supplements such as vitamin D [141] and Bone Morphological Proteins (BMP) 2 and 4 [142-144].

Dex is a synthetic glucocorticoid steroid that is often used interchangeably with naturally occurring 1,25-dihyroxyvitamin D3 (VD3) for *in vitro* differentiation studies [28]. The endogenous VD3 hormone is involved in a complex signalling cascade and is required for the maintenance of skeletal calcium balance by promoting calcium absorption during normal bone formation *in vivo* [145, 146]. VD3 deficiency decreases bone density and mineral deposition, usually manifesting as osteoporosis and structurally weak bones. Since Dex is structurally similar to VD3, it has been used in a number of *in vitro* studies and shown to increase vitamin D receptor (VDR) protein levels in a number of multipotent cell lines [147]. Dex has been also been utilised clinically to treat arthritis pain and inflammation. Furthermore Phillips *et al*. showed that Dex induces osteogenesis in primary dermal fibroblasts, confirmed by the presence of osteoblast markers, alkaline phosphatase activity, and mineral deposition [145]. When 100uM Dex is added to osteogenic media of MSCs it appears to initiate the mitogen-activated protein kinase (MAPK) pathway which activates Runx2/Cbfa1 by phosphorylation [28, 52, 136, 144]. The Runx2/Cbfa1 is an important transcription factor and is the functional partner of several bone morphogenetic proteins vital in osteoblast differentiation and skeletal morphogenesis [148-150].

The second additive, AA or Vitamin C, is an effective antioxidant and essential co-factor in collagen synthesis, however there is limited research detailing its effect on MSCs. Coelho and Fernandes

[151] showed that BMSCs grown in the absence of AA or Dex had a lower percentage of proliferative and differentiating cells *in vitro*, and failed to form calcium phosphate deposits. Jun-Beom's findings support this, detailing that AA and βGP induced osteodifferentiation with mineralisation increasing with Dex treatment in a dose-dependent manner [152]. The treatment of a mouse osteoblastic progenitor cell line with AA increased the hydroxylation of intracellular pro-collagen within one hour of treatment, stimulating the formation of collagenous ECM as well as a time dependant increase in alkaline phosphatase (ALP) and osteocalcin mRNA levels [153]. Franceschi concluded that the addition of AA is sufficient to initiate osteoblast maturation and induce early matrix-associated signals that positively regulate further osteoblast associated genes [153].

β-glycerophosphate (βGP) is a source of inorganic phosphate and is considered a likely mechanism for increasing mineral deposition [154, 155]. The addition of βGP has also been shown to decrease MSC proliferation and increase differentiation toward an osteoblast cell type [151]. Under normal cell culture conditions, MSCs and ADSCs in osteogenic media express morphological and phenotypic similarities to osteoblasts. The broadest changes are observed within 7 days of induction as cells assume a cuboidal and rigid planar morphology. At 14 days, the cells appear structurally similar to primary osteoblasts with very condensed and rigid cell bodies. At this time point, a significant up regulation in the expression of alkaline phosphatase, collagen type 1, osteopontin, osteonectin, osteocalcin, bone sialoprotein, and the receptors BMP-2 and BMP-4 is observed. Furthermore, the osteogenic cells are capable of mineralising calcium, confirmed by positive staining with alizarin red, in the newly formed collagen matrix [28, 152].

1.3.3 Chondrogenic differentiation

The development of cartilage regenerative therapies is complementary to bone regenerative therapies. Not surprisingly, the differentiation process of directing MSCs toward a chondrogenic lineage to produce cartilage is somewhat similar to that of osteogenesis. Many osteochondral degenerative diseases and injuries are often related, as are the repair mechanisms. The structural

difference between cartilage and other tissues is a main factor for the slower repair process. Cartilage is a unique tissue in that it lacks vascularisation and innervations, and as such the normal healing and tissue repair mechanisms do not apply as stem cells cannot be recruited to sites of damage [23, 156].

Cartilage is classified into three general types, hyaline, elastic and fibrocartilage. The damage to articular hyaline cartilage in joints disrupts the extracellular matrix (ECM) composed primarily of collagen type 2, hyaluranon and proteoglycans. The continuous wear on load bearing joints destroys the dense ECM material and this is most prevalent in osteoarthritis. The ECM is not readily restored and any normal repair by chondroblasts in the load bearing joints often yields structurally fallible fibrocartilage [157].

Cell transplantation [158-160], tissue engineering [7, 26, 161, 162] and biomaterial scaffolds [54, 114, 163-165] are in vogue and show much promise in repairing defective cartilage from traumatic injuries and degenerative diseases. The aforementioned approaches have proved that chondrocytes can be produced from MSCs in monolayers and three-dimensional culture systems that are clinically relevant. However, the ability of cells to generate ECM that is as mechanically robust as the native articular cartilage remains elusive. The cell transplant studies have provided minimal evidence of MSCs ability to produce cartilage *in vivo* compared to the success of *in vitro* studies [157, 166]. Mapping out the precise differentiation pathways *in vivo* is a daunting task as there are often hundreds of biochemical interactions and proteomic changes occurring in synchrony. These are initiated not only by differentiation supplements but also by heterogeneous cell populations, as well as physiological and mechanical signals [16, 43, 133, 167-170]. There is also the added difficulty of retrieving sufficient samples from non-experimental animals or human subjects. Defining these events *in vitro* allows for a controlled system for a clearer understanding of the cells produced.

Current standard *in vitro* culture techniques for promoting chondrogenesis *in vitro* consist of chemically defined media using synthetic serum replacements supplemented with recombinant

cytokines and growth factors. However, the use of serum-free media is a double edged sword and a challenging condition to culture cells. Stem cells produced under these conditions generally have a decreased adherence as well as a limited proliferation rate [156, 171]. The positive impact of not using serum is the reduced interbatch variation introduced by uncharacterised growth factors and differentiation factors which could potentially induce differentiation into multiple lineages. There are now numerous commercially available serum-free medias with synthetic serum substitutes. The latest research shows that newer serum-free media are proving to be as successful as serum-containing media compatible with chondrogenesis of MSCs [45, 172].

There have been at least a dozen published cytokines and growth factors which induce chondrogenesis [173, 174]. The most efficient and commonly used supplements are transforming growth factor beta (TGF-β), bone-morphogenetic protein-2 (BMP-2), fibroblast growth factor-2 (FGF-2), insulin-like growth factor-1 (IGF-1) and interleukin (IL)-1β [175-178]. The functional overlap of the supplements for differentiation into other lineages is not unexpected, especially within osteochondral differentiation, as many pathways are shared in normal biological processes. Investigating the supplements individually or in a combinatorial mixture allows for a delineated understanding of the chondral differentiation process in the presence of a differentiation induction media. The first component, TGF-β3, is part of a superfamily of highly conserved growth factors that are known to regulate cellular proliferation and differentiation of a variety of cells [179]. The TGF-β3 isoform is the most widely used supplement in chondrogenesis; however its role in the differentiation process is not implicit. It is hypothesised that TGF-β3 mode of action is directed through the TGF-β type-2 receptor. This activates the R-Smad cascade and Smad independent pathways such as the MEK1/2-Erk1/2 cascade [179] which play a prominent role in cartilage development. Interestingly TGF-β3 is also implicated in the inhibition of adipogenesis, osteogenesis and myogenesis through the functional repression of essential transcription factors that drive these differentiation pathways [179-181].

A group of functionally related cytokines to TGF-β3 are the BMPs which are well known for their role in bone formation. A large focus has been placed on the study of BMP-2, BMP-4 and BMP-7 which has been shown to induce MSCs differentiation toward cartilage formation inclusive of ECM synthesis [182-184]. A number of studies have shown that BMP-4 has the capacity to initiate chondrogenesis in a variety of tissue derived adult MSCs [185, 186]. Nakayama *et al's* study identified that BMP-4 synergistically acts with TGF-β3 in regulating chondrogenesis of MSCs through Smad pathways [187]. Chondrogenesis in MSCs is activated by several cytokines which often stimulate crosstalk between signalling pathways [156]. TGF-β3 has also been reported to act synergistically in chondrogenesis with other related cytokines such as FGF-2, regulating the MAPK cascade. Interestingly, FGF-2 is known to induce expression of the protein Gremlin1, which antagonises certain BMPs, therefore indirectly acting as an inhibitor in part of the TGFβ signalling pathway which is hypothesised to impede osteogenesis [188].

In monolayer chondrogenic cultures, morphological changes to the MSCs during differentiation are very limited throughout the 21 day incubation period. Cellular structural differences tend to manifest after 7 days as cells become more visibly polygonal in shape and grow in dense clusters resembling nodules. Differentiation is usually confirmed by histological staining and immunoblotting. Histological staining of these cells with alician blue shows a relative increase in the amount of the sulphated glycosaminoglycan, hyaluronan, over the culture period [164]. Hyaluranon is one of the chief components of the ECM of *in situ* cartilage. Complementing this is characterisation by immunoblotting by antibody-marker detection of ECM and collagen proteins. This has been widely conducted to investigate the expression levels for collagen type I and type II [54, 164].

1.3.4 Neurogenic differentiation

Neurogenic differentiation is one of the most sought after stem cell differentiation processes for the innumerable potential medical therapies and biotechnological applications it could be used for. It has also proven to be very difficult [189]. There are numerous reported chemical and biological

stimulation methods that have been shown to promote neural cell induction and differentiation both *in vivo* and *in vitro*. The chemical based differentiation methodologies vary greatly depending on the neuronal cell type required. The Woodbury [104] method to initiate differentiation of bone marrow stem cells into neurons utilises 1mM β-mercaptoethanol (BME) for 24hrs to serum-containing subconfluent cultures. Subsequently cells were placed in a differentiation induction media composed of serum free α-MEM and 1-10mM BME. Neuronal morphological manifestations reportedly appeared within 60 minutes of exposure to the induction media. As such the responsive cells assumed further neuronal traits over 3hours. Eventually cells presented a retracted cytoplasm directionally toward the nuclei as well as a multipolar cell body which formed dendrite-like extensions [104]. Confirmatory western blots found that at the 5 hour time point, the differentiated cells had a high propensity for Neuron specific enolase (NSE) and Neurofilament-M (NF-M) expression [104]. The NSE enzyme is exclusively expressed in mature neurons as a dimer in the alpha/gamma or gamma/gamma form, has neurotrophic and neuroprotective properties and has been found to promote cell survival in cultured neocortical neurons [190]. The NF-M protein is most abundantly located in the axons in which they appear to control axonal diameter. Identification of these early neuronal markers that have neuronal developmental functions has established a wider interest in simple chemical differentiation models.

Studies have shown that the neuronal like cells produced from such differentiations are capable of producing Schwann cells of which the functionality is still under investigation [191]. It has been hypothesised by Ishii *et al*, that the antioxidant properties of BME may play a key role in the neuronal survival and the differentiation process [192]. However, the exact initiating processes and extent of BME neuronal differentiation remains to be elucidated. As such, several related chemicals with similar reductive and antioxidant properties have also been investigated [193-195] such as dimethylsulfoxide (DMSO), butylated hydroxyanisole (BHA) and Butylated hydroxytoluene (BHT) alone or combined. Woodbury *et al.,* found the combination of 2% DMSO and 200mM BHA had a similar effect to BME, producing morphological neuronal-like cells *in vitro*.

Choi *et al*., revisited the DMSO differentiation method of BMSCs by performing immunocytochemistry, Western blotting, microarray gene expression and electrophysiology to evaluate the neuronal differentiation. From their broad array of data, it was determined that the DMSO method produced only neuron-like cells, as the cells resembled true neurons phenotypically but contained different genotypic and electrophysiological characteristics [193]. Barnebe *et al*. induced neurogenic differentiation of adult rat BMSCs using BME, DMSO and BHA in an effort to evaluate the electrophysiological potential of the produced cells through a patch clamp test [196]. In accordance with previous work, Barnebe and co-workers confirmed the neuronal-like morphology as well as the positive expression of the neuronal markers NF-200, S100, β-tubulin III, NSE and MAP-2 proteins. The patch clamp assays revealed that the produced cells did not show evidence of Na^+ or K^+ currents nor the ability to fire action potentials. Furthermore they claim that a disruption of the redox circuitry affects the biochemical pathways resulting in cellular damage which manifests as cytoskeletal modifications and loss of ion-gate function that ultimately causes cell death [196]. Understandably the extended exposure of any mammalian cells to high concentrations of strong reducing agents will undoubtedly damage the cells. Also, the unused excess chemical will non-preferentially reduce any protein it comes into contact with, leading to a toxic cellular stress event and eventually to apoptosis [197, 198]. Based on their findings, Barnebe *et al*. deemed induced rat BMSCs do not have basic functional neuronal properties [196].

In the assessment of a developing nervous system, the process of forming successful stable connections between functional neurons is a long and sensitive biological process. The expectation that these stem cells would develop into functional action potential firing neurons within 24 hours of exposure to a single chemical would be an over simplification of cell biology. The expression of neuronal-specific tissue markers does not necessarily imply that fully functional signal conducting neurons have been produced, especially since there are dozens of neuronal cell classes, some of which are non-axonal, and the expression of the listed shared markers are not mutually exclusive. As such, the neurogenic differentiation of MSCs could easily produce a wide range of supporting

neuronal cells, like astrocytes or glial cells which do not have the electrophysiological potential present in neurons. While the extended exposure to such chemicals may damage the MSCs, a time-limited treatment may be sufficient to initiate the differentiation process to a pre-neuronal stage [104, 199].

Woodbury *et al*., found that 5 hours post induction yielded the highest levels of NSE and NF-M markers while maintaining high cell population numbers. These chemical methods of differentiation certainly initiate differentiation toward a pre-neuronal stage however the induction media lacks the necessary supporting conditions to complete the differentiation process to a mature neuronal cell. Since the differentiation pathway has yet to be determined, it is highly probable that the current *in vitro* differentiation methods produce a mixed population of pre-neuronal cells and some differentiated neuronal-like cells. There remains a void in the field regarding the proteomic characterisation of the produced cells relative to their native counterparts. Examining the proteomic profiles will allow a complete comparative measurement of the extent of biological change occurring during the differentiation process. There has been no further research into the characterisation of alternate simple chemical effect on neurogenic differentiation on the wider range of stem cells now available, including ADSCs.

The use of additional growth factors for neurogenic differentiation has garnered some attention in recent years. Biological induction methods utilise bioactive molecules such as hormones and cytokines as the primary stimulatory additives. The extensive range of these components has been combined in several iterations of neurogenic induction media. Many have been optimised for the dynamic role of promoting differentiation while supporting the cell's nutrient acquisition. The most common additives are fibronectin [200], epidermal growth factor (EGF) [8, 109, 201, 202], basic fibroblast growth factor (bFGF) [8, 109, 202], retinoic acid [201], and interleukin IL-1α [203, 204]. These molecules active roles in biochemical and differentiation pathways have been investigated

more extensively than the chemical methods. This is generally attributed to relatively fewer interacting targets within these pathways [205-207].

Fibronectin can be found in numerous tissues intimately involved in a variety of cellular interactions especially within the extracellular matrix (ECM) [208]. In stem cells, fibronectin is most notable functional during growth and differentiation, mediating vital processes during mesodermal, neural and vascular development [205, 209]. The exact mechanisms of this complex interacting molecule and its role in differentiation have yet to be determined.

It is known the growth factors EGF and bFGF can induce ADSC differentiation to neuronal-like cells, such as neurospheres [210]. The EGF molecule binds to epidermal growth factor receptor (EGRF) stimulating the tyrosine kinase activity of the receptor. This initiates the signal transduction pathway for regulation of cell growth, proliferation and differentiation [211]. bFGF is known to maintain ES in an undifferentiated state *in vitro* as well as antagonise osteochondral differentiation [188].

Xu *et* al. [109] generated neurospheres which were subsequently further differentiated into functional Schwann-like cells presenting the morphological, phenotypic and functional capacities of their genuine counterparts. Neurite outgrowth and myelin sheath structures were developed by more than 90% of the adherent cells. Within 48 hours of induction, the Schwann cell markers nestin, p75, S-100 and Glial Fibiral Associated Protein (GFAP) were detected by immunostaining. Xu *et al* alluded the generated neurospheres were closer to neural stem cells. This idea was supported by Hermann et al [212] who proposed that neuronal-like cells propagated from bone marrow MSCs are real neural stem cells. These can be maintained undifferentiated *in vitro* with EGF and bFGF and when exposed to retinoic acid, terminally differentiate into nerve cells as seen in neuronal stem cells based on morphology and the presence of a handful of markers. Their patch clamping functional assays revealed their neurogenic induction protocol did not produce cells that were able to carry an action potential [212]. Bonilla *et al* [8] further supports Hermann *et al's* finding that a similar phenomenon occurs with BMSC *in vitro,* producing neurospheres in the presence of EGF and bFGF.

The neurospheres were shown to further differentiate into functional oligodendrocytes, neurons and astroglial cells both *in vitro* and *in vivo* presenting several known surface markers of the respective cells in both environments.

Radtke *et al*. [202] derived further evidence that peripheral glial cells are differentiated from neurospheres initiated from ADSCs. The action of retinoic acid (RA) was first observed to induce extensive neuronal differentiation in a clonal human EC cell line *in vitro* [213]. It has been confirmed that RA has a direct action on a number of targets within the *Wnt* pathway which actively promotes morphological and phenotypic neurogenic differentiation in embryonic stem cell lines [214]. The response of adult rat hippocampal derived neural stem cells (NSC) to the application of RA demonstrated the generation of both immature neurons and glial cells *in vitro*. This coupled with the sequential addition of neurotrophins subsequent to RA treatment yields mature neurons. The standing hypothesis is that RA determines an early neuronal fate while the neurotrophins allow maturation into functional neuronal cells [207]. Recent studies have confirmed the similar effect on BMSCs [199, 215].

The notion of transdifferentiation across dermal lineages is relatively recent and is still widely debated. However the mounting evidence supports that it is possible to direct mesodermal cells to neuroectodermal lineage [216]. In terms of future therapies, the abundance of ADSCs from lipoaspirates promises a wide range of autologous clinical applications for neuronal repair. The caveat that remains is the confirmation that the biological and functional similarities of the produced cells are the same as their genuine counterparts.

1.3.5 Myogenic Differentiation

The pinnacle of most regenerative research is the production of functional cells for clinical therapies. There is now ample evidence that ADSCs and BMSCs have the capacity for non-mesenchymal

differentiation toward skeletal and cardiac myogenesis [56, 217] and the applications of myogenic cells have a great potential for treating a variety of ailments. The production of skeletal myocytes has a broad application in treatments for musculoskeletal damage and degenerative diseases. *In vivo* implantation of ADSCs has proven to generate viable muscle in animal models [218-220], while *in vitro,* ADSCs can form myotubes under myogenic culture conditions, usually including 50µM hydrocortisone supplemented to serum containing growth media. The assumed morphology includes long multinucleated cells that are functionally contractile and phenotypically express SM-MHC, α-SMA, calponin, caldesmon, MyoD1, myf5, myf6 and myogenin [56, 75, 221]. Kang *et al*., [218] pre-induced human ADSCs *in* vitro and implanted them in an ischemic hindlimb mouse model. They detected within 14 days of implantation of the cells an increase in vascular density and reduced muscle atrophy. Furthermore the harvested cells from the mouse were confirmed by immunoblot to be differentiated myogenic human cells. Bacou *et al.,* [222] injected labelled, cultured ADSCs into the damaged tibialis anterior muscles of a rabbit and found within two weeks that regenerated myotubles were detected. These results are important stepping stones toward skeletal muscle regenerative therapies.

Similarly cardiomyogenesis has received much research interest, as cardiovascular diseases, myocardial infarction and congestive heart failure are a leading cause of mortality worldwide [223, 224]. Due to a greater donor organ waiting list, the prospect of receiving an autologous or allogenic regenerative therapy to restore blood flow and contractility would be an attractive alternative before the formation of scar tissue. The use of 5-azacytidine has been documented by Tang *et al's* [225] direct treatment of infracted mouse myocytes. The treatment reduced the amount of scar tissue formed and improved overall cardiac function when the newly differentiated myocytes were compared to the control groups. A dose dependant study of the effects of 5-azacytidine on ADSCs by Rangappa *et al* [226] found that, within 3 weeks of exposure to the chemical, terminally differentiated, extended binucleated, spontaneously beating cells were formed. In an alternate *in vitro* investigation by Planat-Benard and colleagues of ADSCs in a semi-solid methylcellulose media

not treated with 5-azacytidine, the cells were found to spontaneously differentiate toward functional beating cardiomyocytes [227]. Their ultrastructural and electrophysiological analysis revealed the presence of ventricle and atrial-like cells. Gaustad *et al*., induced cardiomyogenesis by culturing ADSCs in rat cardiomyocyte extract media with no further supplements. The produced cells were morphologically similar to the native counterpart forming striated beating cells and expressing several cardiomyocyte markers [228]. This provides sufficient evidence that ADSCs have the capability to form functional cardiomyocytes in an *in vitro* system in the presence of endogenous growth factors and thus, the ADSCs would not require a pre-induction prior to implantation.

1.4.0 PROTEOMIC CHARACTERISATION

Current stem cell characterisation techniques, such as flow cytometry and immunofluorescence, do not always offer a biological context for expressed proteins and merely relate to the presence or absence of several proteins. These techniques rely heavily on the quality of the antibodies utilised and if there is poor interaction or binding to the targeted proteins, the detection and quantitation would be skewed. This coupled with the previously mentioned non-definitive list of spontaneously changing surface or CD-markers can accumulate to numerous interpretation flaws. To adequately characterise a stem cell and their differentiating counterparts, a holistic approach of proteomics techniques investigating the proteome may assist in addressing or resolving these issues and furthermore will identify a number of functional and biological markers that can be relied upon when coupled with the classical techniques.

The proteome is the full complement of proteins present in a cell or organism at any given time point under a certain set of environmental conditions [229, 230]. The proteome of a cell is not static but constantly changing depending on the tissue or cell type and environmental factors occurring at any point in time. The term proteomics was coined by Wilkins *et al* (1995) and is a platform spanning

a vast array of methods and technologies. It allows a global investigation of the structure and function of thousands of proteins in a cell including how they interact within any cell type, tissue or organism. Protein complexes and interactions, rather than individual proteins, are responsible for most molecular and cellular processes and their study is therefore essential for understanding cellular organization and function. However, difficulties arise in their study as protein complexes are often labile, transient or in low concentration making isolation and analysis challenging. Despite their biological importance, protein complexes have not been the focus of most stem cell proteomic and dynamics research. Adult stem cells have not been well defined at the level of the proteome or protein interaction network [231]. Thus, a global stem cell proteome study would expand our understanding of how protein localisation, surface markers and metabolic pathways are actually changed during the *in vitro* expansion and the differentiation process. Furthermore, identifying how the experimental data fits into the integrated visualizations of protein complexes and interactions are key components in relating *in vitro* models to *in vivo* therapies. The field of proteomics and interaction networks is rapidly expanding and will be a cornerstone of increasing the understanding of cellular dynamics.

1.4.1 Denaturing proteomic techniques

Denaturing proteomic techniques are numerous, including a multitude of variations of the standard techniques of one-dimensional and two-dimensional polyacrylamide gel electrophoresis (1D and 2-D PAGE) and multidimensional chromatography coupled with tandem mass spectrometric analysis, and these have been extensively employed to analyse the proteomes of other cell types. Sample preparation can be derived from whole tissue or homogenous cell culture and there are numerous extraction methods based on very similar principles of sequestering as much soluble protein as possible while maintaining compatability with the separation technique being employed. This is achieved through the tailored use of chaotropes, surfactants, salts and buffers to minimise the

presence of non-protein components that would interfere with protein or peptide separation and ionisation into the mass spectrometer [232].

The choice of separation technique utilised is dependant on the aim of the experiment and the equipment and instrumentation available. Maximal proteome coverage is mainly achieved through so-called shotgun proteomic techniques utilising multidimensional chromatographic separation of peptides coupled directly to tandem mass spectrometry. However this maximal proteome coverage could come at the expense of protein isoform information if the peptide defining an isoform is not detected and fragmented. 2D-PAGE is able to resolve protein isoforms to discreet spots for analysis, but sample limitation and a lack of throughput often stop researchers from utilising 2D-PAGE for maximal proteome coverage. SDS-PAGE followed by LC/MS/MS occupies a middle ground, exploiting the power of SDS as a protein solubilising agent, retaining a protein's intact mass context and having sample throughput comparable to a multidimensional chromatography of peptides approach [233].

The successful application of the above mentioned techniques is dependant on the sample's dynamic range of protein concentration, refering to the relative concentration range of all proteins in a sample as not all proteins are in equal quantities in varying sample types. For example, in human serum the concentration of albumin is approximately 35-50g/L whereas ferritin is found at a concentration of 12-300 μg/L which is a six factor difference. There are known to be larger variances up to 10 orders of magnitude especially with low copy number proteins [234]. The detection of this group of proteins can be easily masked by much higher abundant proteins in gel based or chromatography analyses. Protein equalizer technology [235] can address this limitation, its design is based on a diverse library of combinatorial ligands attached to spherical porous beads which deplete abundant proteins and enrich the rare species in complex proteomes [236]. However, co-depletion of proteins bound to depleted proteins is an issue, as it is in all depletion techniques, as is difficulty in performing quantitative analysis. High-pressure liquid chromatography with strong cation

exchange columns followed by reversed phase fractionation of peptides is often coupled with MS in electrospray acquisition. Chromatography based methods for the separation of peptides prior to mass spectrometric analysis of tryptically digested peptides can allow for the highest proteome coverage [237].

1.4.2 Native proteomic techniques and interactomics

The interactions and complexes formed between all of the protein groups mentioned in section 3 are responsible for most molecular processes and vital cellular functions, such as DNA replication, transcription and mRNA translation, cell signalling, metabolic, transduction and differentiation pathways [238]. These biological processes are precisely coordinated and regulated by dynamic signalling networks of interacting proteins. Accordingly their analysis is essential to expand our knowledge of stem cells. Unlike conventional denaturing methods, the purification of interacting proteins must be performed using conditions that preserve their native environment to maintain the relevant protein interactions. There are numerous methods available for the detection and purification of stable protein-protein complexes which associate through strong interactions. Conversely the detection of very weak or transient protein-protein interactions remains a difficult task. Transient interactions are expected to control the majority of cellular processes [239]. They are temporary in nature and typically require a specific set of conditions that promote the interaction to fulfil their biological function. Blue native and clear native polyacrylamide gel electrophoresis (BN or CN-PAGE) allows for the study of stable intact and complete protein complexes or transient protein-protein interactions. To analyse the more elusive transient interactions the use of commercially available chemical cross-linking reagents to capture or freeze these momentary interactions is widely used [240-242]. Cross-linking reagents have been used in numerous studies to cross-link protein complexes in cells and tissue [243, 244]. This can help define the rare constituent proteins of some complexes, their stoichiometry and function.

It is now recognized that protein interactions are not random events, their interfaces are precisely coordinated spatially and temporally according to biological and environmental cues [245]. In stem cell biology, these signals affect protein-protein interactions which regulate the molecular processes of proliferation and differentiation. The systems biology approach of visualising interacting proteins within a proteome, termed the interactome, presents datasets as graphical representations at a global proteome scale and has become a significant tool in understanding the cellular context in which protein's function and localises to promote complex cellular events. Proteomics is a high throughput, non hypothesis driven approach producing vast data sets which cannot always elucidate context. The notion of biological context from classically obtained proteomic datasets is limited to identification and quantification to presence or absence of proteins within the cell type at that given point in time. The functionality and system implications of the detected proteins are not addressed at this point, hence the lack of biological context

1.4.3 Current technologies for quantitative proteomic applications to stem cells

Complementing the mechanistic interaction networks is the relative quantification of changes in protein expression that occurs as cells differentiate. Relative quantification of proteins can be achieved using instrument-time intensive label-free techniques or by a number of labelling technologies, which include the Differential In Gel Electrophoresis (DIGE) [246], isobaric tagging for relative and absolute quantification (iTRAQ) [247] , tandem mass tags (TMTs) [248], isotope coded affinity tags (ICAT) [249] and stable isotope labelling of amino acids in cell culture (SILAC) [250].

The DIGE approach involves the covalent derivatisation of all sample proteins with fluorophores prior to electrophoretic separation and thus enables detection and quantitation of differences in protein abundance between different biological samples within a single gel. The dyes react via either a maleimide group with cysteine residues or through succinimide reacting with lysine residues in the

protein sample. Because the dyes have a net zero charge, there is no alteration to the isoelectric points of the labeled proteins. A pooled internal standard can be created by mixing aliquots of all samples to be analysed. This substantially removes experimental gel-to-gel variation leading to improved accuracy of protein quantitation between samples from different gels [251, 252]. Barthéléry *et al*., employed the 2D DIGE approach to investigate and quantitate proteomic differences in the early commitment process of human Embryonic Stem Cells (hESCs) during directed neural differentiation. They compared hESC and NSC nuclear proteins and detected 1521 protein spots matched across three gels with less than a 2% densitometric signal variance and tandem mass spectrometry identified 15 differentially expressed proteins which were known to be involved in chromatin remodelling and mRNA processing. Early linage commitment would only identify a few detectable enzymes and cytoskeletal remodelling proteins [253]. The DIGE method is sensitive enough to detect expression differences in less than 1% of compared proteomes.

Kantawong *et* al investigated very biologically similar proteomes of osteoprogenitor cells expanded in varying small culture environments of a bioreactor and static slides. [254]. Due to the smaller culture environments the amount of protein produced would be too low for regular 2D PAGE, differential display analysis which typically requires 500µg of protein for detection with Coomassie stain. The DIGE technique was sensitive enough to detect and analyse 5µg of protein [246] finding at least eleven statistically and biologically significant expression regulation changes in Kantawong *et al's* proteome comparisons. While the method improves gel to gel comparisons the only technical drawback is that it does not address the issue of dynamic range, which decreases the analytical power for low abundant proteins.

The iTRAQ method allows a multiplexed stable isotope labelling of all peptides in either four or eight different biological sample configurations [255]. This allows for simultaneous relative quantitative analysis of expressed proteins. This has been used successfully in stem cell research for the quantitative analysis of expressed proteins [231, 247, 256-258]. Unwin and colleagues iTRAQ

labelled 1x10^6 long-term reconstituting hematopoietic stem cells and non–long-term reconstituting progenitor cells for relative peptide quantification of approximately 950 proteins, of which 145 were different. The comparison of the 145 changes in the proteomic data to the transcriptomic data revealed more than 50% of the proteins were not detected in the transcriptomic data set [257]. By combining proteomics with another dataset allowed greater access to cell state biological information. In another study, Ji *et al*. [259] iTRAQ labelled and compared an embryonic stem cell line C3H10T1/2 cells and their chondrogenic induced derivative line in *in vitro* cultures. The successful quantification of 1753 proteins revealed at least 100 protein's expressions were significantly altered in the differentiation process. The functional categorization presented 17 up-regulated chondrocyte specific proteins [259]. Ji and colleagues were also the first to identify the biological roles of BTF3l4 and fibulin-5, two novel chondrogenesis related proteins from their iTRAQ proteomic data. The iTRAQ method can be costly compared to LC-MS/MS of the same non-labelled sample types when investigating numerous biological samples; however the data derived can provide valuable quantitative information assisting with the definition of proteomic changes in stem cells and their progeny.

The TMT and ICAT methods are used in a similar fashion to iTRAQ for quantitative analysis during tandem MS analysis. The TMT process is functionally similar to iTRAQ labelling in that the labels contain heavy and light isotopes that give rise to reporter-ions at different masses after activation in the collision cell of a mass spectrometer [248, 260]. TMTs were utilised by Wang *et al*., [261] in establishing the protein interactions in embryonic stem cells (ES) differentiation potential to understand their properties and the process of cellular reprogramming. The ICAT chemical probes are isotypically differentiated by heavy or light tags which react with cysteine residues [262]. The two proteomes to be compared can be labelled with either probe then combined and digested with a protease. Subsequently the MS/MS signal ratio intensities of differentially mass-tagged peptide pairs are quantified.

SILAC is a stable isotope labelling technique that was developed by Matthias Mann and published by Ong *et al* in 2002 [250]. SILAC involves supplementing cell culture media with stable isotope versions of amino acids, typically $^{13}C_6$ or $^{13}C_6{}^{15}N_5$ Arginine or Lysine. When cells are grown in this modified medium, the 'heavy' amino acids are incorporated into proteins during the cell's normal protein synthesis pathways. A second population of cells is grown with a supplement of unlabelled amino acids. Perturbation of the growth conditions, such as differentiation, of one of these populations will result in changed protein expression, with the other, unperturbed cell population acting as a comparative control. The observed ion intensity ratio between the resulting peptides (figure 3) provides information regarding the differential expression of proteins in response to the changed growth conditions such as stem cell differentiation [250, 252, 263].

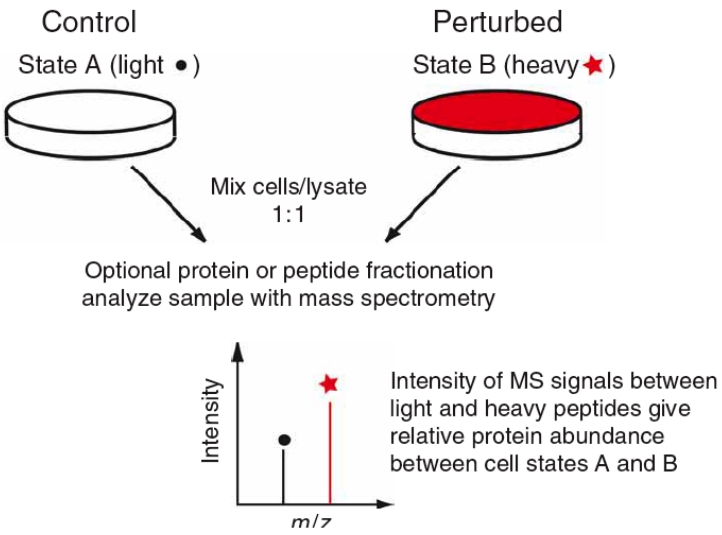

Figure 3 A schematic overview of SILAC comparisons. A 'Control' cell population is grown with a 'light' amino acid and a 'Perturbed' cell population with a 'heavy' stable isotope-labelled amino acid. Fold changes in proteins resulting from the specific perturbation of culture conditions can be calculated from resulting mass spectral analyses. Figure from [252]

1.5.0 CONCLUSION

The deficiencies of classical characterisation of ADSCs and their differentiated progeny are extensive, and are touched upon in Table 1 of the CD-marker conjecture. The surface marker profiling has also carried over in the characterisation of differentiated ADSCs. There are numerous issues presented in

this chapter detailing the short comings of the classical or reductionist characterisation of these cells utilising a handful of markers. The main deficit is that the extent of differentiation cannot be elucidated and there is no biological context for the expression of these surface markers relative to the massive changes occurring. By investigating the profoundly unique differentiations derived from the same homogenous *in vitro* MSCs culture by performing in-depth characterisation through the utilisation of proteomics and bioinformatics tools will ultimately reveal the broad spectrum of differences, relative similarities and stability of the produced differentiated cell populations. A directed comparative evaluation to their native counterparts will aid with the elucidation of induced pathways as well as the mechanisms involved in functional and morphological markers that queue post induction to produce phenotypically similar cells to their intended targets. This allows for a biological and temporal context for each individual up and down regulated proteins to be mapped and characterised for every specific differentiation. Through defining these events, the knowledge and functional behaviour of cells in adult stem cell biology and regenerative therapeutic applications will undoubtedly be expanded whilst advancing avenues for further applications.

The overall aim of this thesis is to profile differentiating adipose derived stem cells utilising current proteomic techniques.

Chapter 2

Preliminary proteomic comparison of multi-lineage differentiated adipose-derived stem cells (ADSCs)

2.1.0 INTRODUCTION

A range of questions have been raised in chapter one that essentially query the extent of ADSC differentiation as well as the robustness of the methods of characterisation of ADSCs and their progenies, which is a broad gap in the literature to date. These questions were raised due to the reliance on only a few surface markers for identification and the thinking that this may not be adequate to truly characterise a cell which has the potential of maturing into dozens of phenotypically varied cell lineages. ADSCs have been annotated as multipotent adult mesenchymal stem cells and they have been demonstrated, when induced, to differentiate morphologically and biochemically into osteocytes [28, 75, 110-112], chondrocytes [25, 113-116], adipocytes [52, 59, 116], myocytes [56] and neuronal cells [28, 100, 104, 264].

The uncertainty and concerns surrounding characterisation were outlined in the review of basal ADSC characterisation (chapter 1 section 3.1). That section detailed the variance in the literature and opposing conformational evidence of CD-marker presence and absence reported by different lab groups for basal ADSC characterisation. Further to this, the widespread application and acceptance of relatively few markers to characterise differentiated cells, markers thought as being true reflections of their actual mature counterparts, is a dubious approach to define such a complex variety of progeny [56, 100, 144, 217, 265-268]. While a number of these studies present certain activity assay data to prove functionality of the produced cells [269-273], there still remains some conjecture as to whether the cells are phenotypically and/or functionally mature or express a dozen cell specific markers but are merely masquerading as non-functional phenocopies [46, 196]. There is some data available that reveals that the basal ADSCs may spontaneously express a number of the expected (and widely used) markers for a particular cell type after a very short time *in vitro* without induction [47, 274].

The significance of defining the starting material and, more importantly, the elucidation of the extent of differentiation is vital for research and clinical applications alike. For afflictions such as osteoporosis and osteoarthritis which are the world's leading causes of skeletal and joint damage and the fourth leading cause of disability worldwide [135], cellular therapies have become popular in the last decade. Initially, bone marrow stem cells (BMSCs) were used in limited therapies [50, 275, 276] and are now banked and expanded prior to use [277]. Treatments using BMSCs were hindered by the limited source of cells at a very dilute 1 per 10^5 cells in traumatic retrieval methods [136, 137]. The utilisation of ADSCs has become very attractive as an alternative for autologous transplants. As the primary isolation often yields a thousand fold higher cells than for BMSCs and the cells demonstrate the still debateable high capacity for mutli-lineage maturation *in vitro* and *in vivo* [138, 139].

In recent years, adult stem cells have been successfully used to treat joint and muscle injuries in humans and animals [12, 62, 111, 278]. However, successful regenerative therapies utilising ADSCs have yet to be developed for organs such as the brain and central nervous system. Numerous studies show ADSCs, as well as other adult MSCs, has been induced toward a neural differentiated population *in vitro* [28, 104, 279]. Due to the reasonably easy access to an abundant source of ADSCs, stem cell therapies based on this cell source has the potential to instil significant change to personal regenerative therapies in healthcare and medicine.

To explore the definition of basal ADSCs and the degree of differentiation of induced cells, a global approach utilising various proteomic techniques investigating the expression differences of proteomes, may assist in explication and resolution of some of the stated queries outlined in chapter one. The proteome is not static and is constantly changing depending on the tissue or cell type and the state of a cell's environment at any point in time. This is particularly useful in terms of examining extensive changes to stem cells over time in the presence of the inducing agent/s.

This chapter employs a number of routinely employed proteomic methodologies for the preliminary investigation of the broad differentiation potential of rat basal ADSCs toward osteogenic, chondrogenic, myogenic, adipogenic and neurogenic with comparisons to the mature primary derived counterparts (PDC) where possible to ascertain the broad proteomic changes that occur during ADSC differentiation.

2.2.0 MATERIALS AND METHODS

2.2.1 Primary isolation and ADSC cell culture

Adult *Rattus norvegicus* (Fischer species) were used for the isolation of rat ADSCs. Animals were housed and cared for under standard conditions and were euthanized in a CO_2 chamber. Tissue was obtained as donated tissue (waste) from an unrelated project undertaken by staff at Regeneus Ltd. under Regeneus animal ethics committee approval number: RE001. After euthanasia, the inguinal fat pad was harvested and ADSCs were isolated using previously published methods [39]. All subsequent steps were conducted under sterile conditions. Fat pads were rinsed twice in Dulbecco's Modified Eagle's Medium (DMEM, Gibco). The fat pad was then minced with a pair of scissors briefly until afine slurry was formed. Connective tissue was then digested with collagenase type 1 (Gibco) for 45 minutes at 37^0 C. The suspension was then centrifuged at 1600 x g for 10 minutes at 4^o C to separate adipocytes from the SVF. Usually 3 layers are seen above the pellet. The upper most layer is the free lipid and appears as clear/white colour, the middle layer is usually a very small portion of undigested adipose tissue, then a red digestion solution. By carefully decanting all these layers the pellet was revealed. The pellet was then resuspended in 3 ml of DMEM and pipetted carefully on top of 3 ml of Ficoll Paque PLUS (Sigma-Aldrich). Centrifugation at 1600 x g for 20 minutes was then performed to remove red blood cells from the SVF. The ADSCs were then removed from the interface between the Ficoll and DMEM. The cells were then washed with 8 ml of DMEM to dilute out residual Ficoll. The cells were washed twice in DMEM and centrifuged at 1000 x g. Upon

completion of the final wash the pellet was resuspended in the basal growth media DMEM Glutmax/F12 (Gibco) with 10% Foetal Bovine Serum (FBS, Invitrogen) supplemented with 1% Antibiotics/Antimycotics (ABAM, Invitrogen). 2 mL of the suspension was then aliquoted into a T25 culture flask (Nunc) and incubated at 37^{o} C at 5% CO_2 for 48 hours until ADSCs adhered to the culture flask. Non-adherent cells are eliminated by aspirating floating cells and replacing the media. ADSCs were passaged 3-5 times for a homogenous adsc culture before being utilised in experiments.

2.2.2 Induction and differentiation

Primary MSC isolates were expanded in a basal growth media of DMEM Glutmax/F12 (Gibco) with 10% FBS and 1% ABAMin triplicate T175 until 80% confluent. Once cells reached 80% confluence media was aspirated to remove non-adhered cells. The monolayer was gently rinsed twice in 20 ml pre-warmed to 37^{o} C DPBS. 20 ml of pre-warmed differentiation media was placed on cells for induction incubated 37^{o} C at 5% CO_2 replacing media every 84 hours where necessary.

Table 1 Differentiation media supplement additives and days in culture adapted from Zuk et al [28]

Differentiation	Supplementation	Time in culture
Neurogenic	5–10 mM β-mercaptoethanol	1 day
Adipogenic	0.5 mM IBMX, 1 µM dex, 10 µM insulin, 200 µM indomethacin and 10% FBS	14 days
Osteogenic	0.1 µM dex , 50 µM ascorbate-2-phosphate, 10 mM β-glycerophosphate and 10% FBS.	14 days
Chondrogenic	StemPro Chondrogenesis Differentiation media (Invitrogen)	21 days
Myogenic	50 µM hydrocortisone and 10% FBS.	42 days

2.2.3 Primary isolation and cell culture

2.2.3.1 Chondrocytes

Chondocyte cells were isolated enzymatically from adult rat epiphyseal articular cartilage from the femoral long bones in the hind limbs [280]. The cartilage used in this experiment was dissected from

the femoral head, taking care to exclude subchondral bone or connective tissue. This tissue was finely minced into 1 mm^3 pieces using aseptic techniques. The pieces were then washed three times in sterile phosphate buffered saline. To liberate the chondrocytes from the cartilage extracellular matrix required sequential enzymatic digestion methods. The minced tissue was pre-digested in 10 ml of 0.05% trypsin (Gibco, UK) at 37^0C for 30 minutes. Subsequent to digestion, 10 ml of DMEM/F12 Glutmax (Gibco, UK) supplemented with 10% FBS (Gibco, UK) and 1% Penicillin/streptomycin, was added to the mixture to dilute the trypsin. The cartilage pieces were allowed to settle then centrifuged at 1500 rcf for 10 minutes. The supernatant was carefully removed and discarded. The partially digested cartilage pieces were washed twice in DMEM with 10% FBS to neutralise any remaining proteolytic enzymes. The cartilage pieces were then resuspended in 10 ml of 1.5 mg/ml of collagenase and agitated in a water bath at 27^0 C overnight to digest the connective tissue. After overnight digestion, the solution was filtered through a sterile 5 mm nylon mesh to remove undigested debris. The filtrate was centrifuged at 900 rcf for 5 minutes to pellet the cells. The supernatant was discarded and the pelleted cells were washed in DMEM/F12 Glutmax, supplemented with 10% FBS and 1% penicillin/streptomycin. The cells were then resuspended in 5 ml of the same media and placed in T25 culture flasks (Nunc) and maintained in a humidified incubator at 37^0 C with 5% CO_2 undisturbed for 48 hours to allow cells to adhere.

2.2.3.2 Osteoblasts

Osteoblastic cells were isolated either enzymatically or from explants cultures from adult rat hind femoral long bones. For the explant culture; the skin, connective tissue and muscle were removed. The diaphyses were cut free from the epiphyseal cartilage (which was used for chondrocyte isolation 2.3.1). The bone was cut in pieces approximately 2mm by 2mm and washed in 10 ml sterile phosphate buffered saline (PBS) by vortexing for 5 minutes and gentle inversion 10 times to remove blood and bone marrow. The bone pieces were placed on the bottom of a T25 culture flask (Nunc)

and incubated for 30 minutes to allow cells to adhere to the plastic prior to the addition of culture medium (DMEM, 10% FBS, 1% ABAM). The cells were cultured and maintained in a humidified incubator at 37^0 C with 5% CO_2 undisturbed for 48 hours to allow cells to adhere until 95% confluence.

Enzymatic isolations were performed using a variation of the method described in Bellows et al [281]. Femoral long bones were physically cut into 2 mm by 2 mm pieces and washed as described above. Subsequently the bone fragments were placed in 0.5% trypsin (Invitrogen) for 15 minutes at 37^0 C in a warm water bath. After which the trypsin solution was decanted carefully to not lose any bone fragments to which 10 ml of a solution of 1.5 mg/ml collagenase (Sigma) in PBS was added and incubated for 90 minutes at 37^0 C in a warm water bath. The digestion was then diluted to 30 ml with ADSC basal media and centrifuged at 1200 xg for 5minutes. The supernatant was discarded and the entire pellet was resuspended in 5 ml of ADSC media and placed in a T25 flask and incubated at 37^0 C with 5% CO_2 undisturbed for 48 hours to allow cells to adhere until 95% confluence

2.2.3.3 Hippocampal neurons

Two sources of primary adult rat hippocampal neurons were acquired for neuronal differentiation comparison. The first was a primary isolation from the brain of the adult rat utilised in section 2.3.1 and 2.3.2. The skin and connective tissue was removed from the cranium with a scalpel exposing the skull which was opened with a surgical scissor from the base near the spine to the front of the skull above the brow in the shape of an inverted "V" (Λ). This allowed the easy removal of the whole brain for dissection. The brain was sectioned and the hippocampus was located as per the diagram below (figure 2). The hippocampus was dissected into approximately 2-3 mm^2 pieces. The pieces were rinsed in 37^0 C sterile PBS and then incubated with 5 ml of a solution of 1.5 mg/ml collagenase to breakdown any collagen based connective tissue in the pieces. The digestion solution was discarded and the pieces were then placed in a T25 culture flask coated with lysine (Nunc) before

5ml of Neurobasal (Invitrogen) media supplemented with B-27® (Invitrogen) as added. The flask was incubated at 37^0 C with 5% CO_2 undisturbed for a week to allow cells to adhere.

The second source of neuronal cells was purchased as Rat Hippocampal Neurons (RHN) (Invitrogen). Culture conditions were followed as per supplier instructions after placing in a T25 culture flask coated with lysine (Nunc). The cells were cultured with 5ml of Neurobasal (Invitrogen) media supplemented with B27 (Invitrogen) and incubated at 37^0C with 5% CO_2 undisturbed for a week to allow cells to adhere.

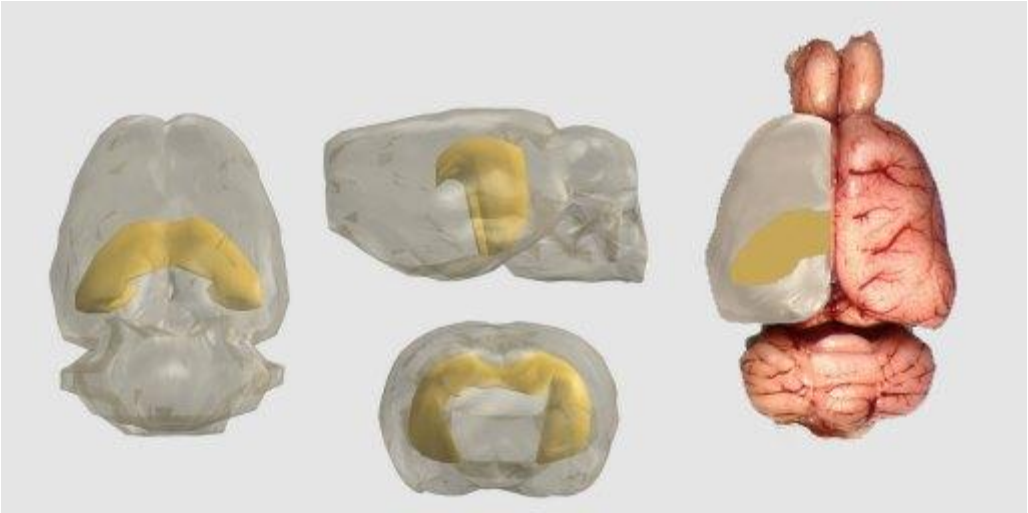

Figure 2 3D model of brain with highlighted Rat hippocampus showing approximate location for dissection reference (http://synapses.clm.utexas.edu/anatomy/hippo/hippo.stm)

2.2.4 Microscopy and histological staining

After differentiation end time points were reached, the basal cells, the produced differentiated cells and the primary isolated cells were aspirated and media collected for Bioplex assays (Section 2.9). Cells were then washed 2-3 times in sterile PBS before fixation in the flask with 4% formaldehyde for 30 minutes, followed by washing twice with PBS then twice with deionised water for histological staining (Section 2.4.1).

2.2.4.1 Haematoxylin and eosin (H&E) staining

Haematoxylin is a basic stain that colours basophilic structures and is generally used to visualise nuclei, producing a deep purple to blue colour. In conjunction with haematoxylin, eosin is used as a membrane counter stain which stains acidophilic structures red. Following general fixation in 4% formaldehyde, slides with cells were flooded with haematoxylin [Sigma, H3136 haematoxylin 6 g, absolute alcohol 300 ml, distilled water 300 ml, glycerol 300 ml, glacial acetic acid 30 ml, ammonium or potassium aluminium sulphate 30 g and sodium iodate 0.9 g] for 5 minutes, rinsed in water for 30 seconds and the slide submerged in acid alcohol for 15 seconds to remove excess stain. This was followed by a 30 second rinse in water, submersion in Harris bluing agent [0.5% w/v sodium acetate in distilled water] for 2 minutes, another rinse in water before counterstaining with Eosin Y (2% v/v in distilled water) for 30 seconds. The slide was then dehydrated by 30 second submersions in 75%, 95% and then 100% ethanol before the slide was sealed with clear xylene for 5 minutes followed by the addition of a coverslip. Stained cells were visualised on an Olympus IX51 inverted microscope and images captured with the attached Olympus DP70 camera.

2.2.4.2 Alcian Blue

Alcian Blue 1%w/v (Sigma) solution was prepared in 0.1M HCl. Cells fixed in formaldehyde as per section 2.4.2 were then flooded with the stain for 30 minutes. Subsequently the cells were rinsed three times with 0.1M HCl, washed with distilled water to neutralize the acidity, visualize under light microscope, and capture images for analysis as per the previous section (2.4.1) [282]. Blue staining indicates synthesis of proteoglycans by chondrocytes.

2.2.4.3 Alizarin Red

Alizarin Red S is a stain commonly used to identify the deposition of calcium in tissue and cells. It functions as a chelator of diatomic molecules where calcium is the most reactive and the most abundant in tissue sections. After normal formaldehyde fixation of the cells as per section 2.4.2, cell monolayers were flooded with 2% w/v Alizarin Red S made up in distilled water and pH adjusted to 4.1 – 4.3 with 10% ammonium hydroxide [282]. Cells with calcium deposition were stained orange –

red of varying intensities. Stained cells were visualised on an Olympus IX51 inverted microscope and images captured with the attached Olympus DP70 camera.

2.2.4.4 Oil Red

Oil Red S is a lipid stain commonly utilised to identify the accumulation of lipid in tissue and cells. Subsequent to normal formaldehyde fixation of cell monolayers, the cells were rinsed in 60% isopropanol. The cells were then treated for 15 minutes with 0.5% w/v Oil Red S suspended in isopropanol, then immediately rinsed in 60% isopropanol. Stained cells were visualised on an Olympus IX51 inverted microscope and images captured with the attached Olympus DP70 camera.

2.2.4.5 Immunofluroescence microscopy

Cells were fixed in 2% paraformaldehyde for 3^{o} min atues at 4^{o} C, then washed 3 times with PBS and rinsed with 100 mM glycine in PBS for 5 minutes to quench excess formaldehyde. After each subsequent step the sample was washed with PBS. Sample was then blocked with 2% bovine serum albumin (BSA) in PBS for 1 hour. The cells were then stained with Anti-CD45 or Anti-CD90 (1:500) in 2% BSA/PBS for 60 minutes. This was followed by staining with Alexa Fluor® 488 dye conjugate (1:1000) in 2% BSA/PBS fora further 60 minutes. Stained cells were visualised on an Olympus IX51 inverted microscope and images captured with the attached Olympus DP70 camera.

2.2.5 Alkaline phosphatase activity assay

ALP activity was determined by a commercially available assay. After differentiation commencement, on day 14, cell culture medium was collected and a colorimetric assay (Sigma Aldrich, Australia) based on the hydrolysis of 4-nitrophenyl phosphate into 4-nitrophenol was used. Formation of 4-nitrophenol was directly proportional to ALP activity and its absorbance could be detected at 405 nm by a microplate reader (BioTek SynergyTM HT Multi-Mode Microplate Reader).

2.2.6 Protein extraction

Harvesting cells for proteomic analysis by LC-MS/MS or iTRAQ and Western blot were generally completed at the desired end time point as per the following. Aspiration and collection of expended media for Bioplex analysis was followed by rinsing the cells with excess pre-warmed DMEM/F12 to

dilute out and remove FBS components. The cells were then exposed to TrypLE Express (Invitrogen) for 10-15 minutes at 37^{o} C. Cells were then collected in 10 ml DPBS, gently inverted to rinse cells, then centrifuged at 1000 x g for 10 minutes. The DPBS washes were carefully decanted not to disturb the pellet. The cells were resuspended again gently in DPBS to rinse and centrifuged again at 1000 x g for60 seconds. The DPBS was decanted and the cells were resuspended in 200 µl of 1% SDS and sonicated for 10 minutes for one dimensional (1-DE) SDS-PAGE or an extraction buffer (1% (w/v) C7bz0, 2 M Thiourea, 7 M Urea, and 40 mM Tris-HCl pH 8.8) for two dimensional electrophoresis (2DE). Lysates were centrifuged at 16000 x g for 10 minutes to pellet cell wall debris. The lysed cell proteins were then reduced and alkylated with 10 mM Tributylphosphine (TBP) (Sigma) and 20 mM Acrylamide (Sigma) for 90 minutes at room temperature [283]. Insoluble material was removed by centrifugation at 16000 x g for 10 minutes and the pellet was discarded. The supernatant was removed and the proteins were precipitated in five volumes of acetone for 30 minutes at room temperature. The precipitate was centrifuged at 4000 x g for 10 minutes, the acetonedecanted and the pellet was left to air dry briefly prior to resuspending in 100 µl of 1% SDS (1DE) or extraction buffer without Tris-HCl (2DE). All samples were assayed to determine protein concentration using 1D SDS-PAGE and densitometry. Protein concentrations were approximated against serial dilutions of 1 mg/mL BSA. BSA dilutions along with neat and 1:10 diluted samples underwent 1D SDS-PAGE though only electrophoresed for 5 minutes at 160 V, keeping all proteins stacked in a single band, before fixing the gel and staining with Flamingo (BioRad). Concentration was measured using densitometry available through QuantityOne software (BioRad). Each sample was diluted to 100 µg/100 µl. Samples were then frozen in liquid nitrogen and stored at minus 80^{o} C till required.

2.2.7 One-dimensional PAGE and Westernblots

Samples were diluted 1:1 with lithium dodecyl sulphate (LDS) loading buffer (Invitrogen), heated at 95^{o}C for 10 minutes then centrifuged. Samples were then loaded into 4-12% Bis-Tris Criterion gel (BioRad) in XT-MES (BioRad) running buffer then electrophoresed according to the standard product

protocol of 160 V for 50 minutes (BioRad). Upon completion of electrophoresis, unless required for western blot gels were placed in fix solution (40% methanol and 10% acetic acid) and incubated on a gentle rocker at room temperature for 60 minutes. Gels were then placed in Flamingo fluorescent protein stain (BioRad) and incubated for 60 minutesr. Gels were imaged using a PharosFX Plus (BioRad) imager and Quantity One software (BioRad). The gel was then placed in Coomassie Blue G stain [Reagent 1: 45% methanol, 10% glacial acetic acid, 45% deionised water (dH2O), and 3 g/L Coomassie Brilliant Blue G250. Reagent 2: 50% ammonium sulfate] overnight, post staining a solution of 1% acetic acid to remove background stain. The gel was then scanned with an Epson Perfection 4800 document scanner. Proteins of interest were excised from the gel for in-gel trypsin digestion (Section 2.9).

The western blot method as adapted from Jobbins *et al*., 2010 [284], buffers were prepared as following: 2 blot papers (BioRad) soaked in Buffer 1 [40 mL 10X stock (400 mM amino-caproic acid, 250 mM Tris), 40 mL methanol, 1 mL 20% SDS, 400 mL dH2O], 2 blot papers were soaked in Buffer 2 [20 mL 10X stock (250 mM Tris), 40 mL methanol, 200 mL dH2O] and 1 blot paper was soaked in Buffer 3 [10 mL 10X stock (3 M Tris), 100 mL dH2O]. Post 1D-SDS-PAGE of whole cell lysates as prepared in section 2.3, the gel was rinsed for 60 secondsin dH2O then equilibrated in buffer 1 for 5minutes. A piece of polyvinylidene fluroride (PVDF) membrane (BioRad) was cut to the same dimensions as the gel and placed in methanol for 2 minutes prior to equilibration in Buffer 2. The Western blot stack was assembled within an Owl HEP-1 Semi dry electroblotting cassette (Thermo Fisher Scientific) with Buffer 1 soaked papers at the cathode base, then the gel, PVDF membrane, Buffer 2 soaked papers, and lastly Buffer 3 soaked paper under the anode top. The stack was rolled to remove excess buffer and any air bubbles and the protein transferred to the membrane at 300 mA for 30minutes. Once the gel was electrophoretically transferred, the membrane was washed in PBS with 0.1% Tween [BioRad, USA] for 20 minutes and then blocked with PBS, 0.1% Tween and 5% skim milk powder for 60 minutes to prevent non-specific antibody binding. The membrane was then placed in a solution containing the one of the following primary monoclonal antibodies: mouse anti-

human NeuN/Fox3 (M377100 Biosensis 1:5000), mouse anti-human NF200 (M988100 Biosensis 1:500), rabbit anti-human β-TUBBIII (ab18207 Abcam 1:1000) or rabbit anti-human GFAP (ab7260 Abcam 1:50000) diluted in PBS respectively and incubated overnight at 4^{o} C on a gentle rocker. The blot was subsequently washed 3 times with PBS and probed with a secondary antibody, either anti-mouse IgG (A4416 Sigma) or anti-rabbit IgG (A4312 Sigma) dependant on the primary probe. Both secondary antibodies were ALP conjugated for visualisation with 5-bromo-4-chloro-3-indolyl phosphate/nitro blue tetrazolium chloride (BCIP/NBT) (Sigma).

2.2.8 Two -dimensional SDS-PAGE

All protein extraction was performed in the procedure outlined in section 2.6 and isoelectric focusing performed using a modified method from Jobbins *et al* [284]. The whole cell lysates protein extract was separated in the first dimension on an immobilised pH gradient (IPG) strip (11 cm, pH 4−7 or pH 3−10, BioRad) for at least 100kVhours. The focused IPG strip was equilibrated in 2% (w/v) SDS, 6 M Urea, 250 mM Tris-HCl (pH 8.5) and then separated in the second dimension on a 4−12% Bis-Tris gel using the 2-(N-morpholino)ethanesulfonic acid (MES) buffer system at 160 V. Following separation and fixation, gels were visualized by staining with either Flamingo Fluorescent Gel Stain (BioRad, Australia) or Coomassie Blue G-250 [284]. A differential display analysis utilising PDQuest (BioRad) software was utilised to identify difference in 2D-gel profiles. Proteins of interest were excised from the gel for in-gel trypsin digestion (Section 2.9).

2.2.9 Protein band excision and extraction for in-gel trypsin digestion and LC-MS/MS

Gel bands (1D) or spots (2D) stained with Coomassie Blue G250 were excised and destained with 50% acetonitrile (ACN) in 50 mM ammonium bicarbonate until the blue colour was no longer visible. Gel pieces were then dehydrated with 100% ACN for 5 minutes before removing ACN. Reduction and alkylation was then carried out by incubating the gel pieces with 100 µL 5 mM TBP and 20 mM acrylamide in 100 mM Am for 90 minutes. The solution was discarded and gel pieces washed first

with 100 µL 100 mM ammonium bicarbonate and then twice with 50% ACN in 50 mM ammonium bicarbonate followed by dehydration with 100 µL ACN. Once the gel pieces had shrunk and turned noticeably white, Trypsin Gold, MS grade [Promega USA] in 100 mM ammonium bicarbonate (12.5 ng/µL) was added and left to incubate for 30 minutes at 4^0 C. The sample was spun briefly and more 100 mM NH4HCO3 added to cover the pieces before digestion overnight at 37^0 C. Peptides were extracted by sonicating briefly and transferring the digestion solution into a new tube. To the gel pieces 50% ACN and 2% formic acid was added and incubated for 20 minutes before sonicating again and removing the liquid to combine with initial digest solution. This last step was repeated before the digestion solution was concentrated to approximately 15 µL using a VacufugeTM Concentrator 5301 [Eppendorf Germany] and then centrifuged at 14,000 xg for 10 minutes. The solution was then transferred to an autosampler vial for LC-MS/MS analysis.

Once samples were prepared for analysis, all subsequent MS operations were performed by Dr Matthew Padula from the Proteomics Core Facility at UTS using the Tempo/QSTAR Elite system and standardized automated methods. Samples were placed onto the autosampler of a TEMPO™ nanoLC system [Eksigent USA] and loaded at a rate of 20 µL per minute onto a Michrom reverse phase trapping cartridge before eluting onto a 75 µmID X 150 mm PicoFrit column [New Objective, USA] packed with Magic C18AQ chromatography resin [Bruker-Michrom, USA]. Peptides were separated using an increasing gradient of ACN at 300 nL/minute and ionised at 2300 V by the Micro-ionspray II head into the source for the QSTAR EliteTM quadrupole time of flight (TOF) MS [Applied Biosystems/MDS Sciex]. The QSTAR performs Information Dependent Acquisition (IDA) to analyse ions transmitted through the first quadrupole to the TOF analyser. If a multiply charged ion (2-5+) was detected at greater than 30 counts per scan, the ion was selected and transmitted to the second quadrupole collision cell to be fragmented and the fragment masses measured by the TOF analyser.
The MS/MS data files produced by the QSTAR were searched using Mascot Daemon (version 2.3.02, provided by the Walter and Elisa Hall Institute, Parkville, Vic. Perkins, D.N. 1999) and searched against the LudwigNR database (comprised of the UniProt, plasmoDB and Ensembl databases

(vQ212. 19375804 sequences, 6797271065 residues) with the following parameter settings: Fixed modifications: none; Variable modifications: propionamide, oxidised methionine, deamidated asparagine and glutamine; Enzyme: semitrypsin; Number of allowed missed cleavages: 3; Peptide mass tolerance: 100 ppm; MS/MS mass tolerance: 0.2 Da; Charge state: 2+ and 3+. The results of the search were then filtered by including only protein hits with at least one unique peptide and excluding proteins identified by a single peptide hit with a p-value > 0.05.

2.2.10 Bio-Plex

ADSCs secretion samples were collected at endpoint times for assay. Concentrations of rat IL-1A, IL-1β, IL-2, IL-4, IL-5, IL-6, IL-7, IL-10, IL-12p70, IL-13, IL-17A, IL-18, Erythropoietin (EPO), Granulocyte colony-stimulating factor (G-CSF), Granulocyte macrophage colony-stimulating factor (GM-CSF), Neutrophil-activating protein 3 (GRO/KC), Interferon-gamma (IFN-γ), M-CSF, Monocyte chemoattractant protein-1 (MCP-1), Macrophage inflammatory protein 1a and 3a (MIP-1a MIP-3a), Regulated on Activation, Normal T Cell Expressed and Secreted (RANTES), Tumor necrosis factor-alpha (TNF-α) and Vascular endothelial growth factor (VEGF) were simultaneously evaluated using commercially available multiplex bead-based sandwich immunoassay kits (Rat 24-plex, BioRad Laboratories). Assays were performed following the manufacturer's instructions. Briefly, 24 distinct sets of fluorescently dyed beads loaded with capture monoclonal antibodies specific for each cytokine to be tested, were used. Secretion samples (50 µl/well) or standards (50 µl/well) were incubated with 50 µl of pre-mixed bead sets into the wells of a pre-wet 96 well microtitre plate. After incubation and washing, 25 µl of fluorescent detection antibody mixture was added for 30 minutes and then the samples were washed and resuspended in assay buffer. High standard curves for each soluble factor were used, ranging from 2.00 to 32,000.00 pg/ml and the minimum detectable dose was <10 pg/ml. The formation of different sandwich immunocomplexes on distinct bead sets was measured and quantified using the Bioplex Protein Array System (BioRad Laboratories). A 50 µl volume was sampled from each well and the fluorescent signal of a minimum

of 100 beads per region (chemokine/cytokine) was evaluated and recorded. Values presenting a coefficient of variation beyond 10% were discarded before the final data analysis [285].

2.3.0 RESULTS

2.3.1 Microscopy

2.3.1.1 Basal ADSCs

Rat ADSCs were cultured in a monolayer by passaging three to five times therefore selecting for a morphologically homogenous culture corresponding with current literature for performing differentiation studies on primary MSCs including ADSCs [28, 39]. The morphological appearance of ADSCs *in vitro* is a distinctly fibroblastic appearance with branched cytoplasm focusing at two or three extensions at the poles of the cell enclosing an elliptical nucleus. Successive passaging promotes the growth of an adherent homogeneous population which assumes a uniform morphology and directional growth (figure 3). All differentiation inductions were performed with cells at sub-confluency. Primary derived chondrocytes, osteoblasts and hippocampal neurons were also cultured for histological, proteomic and various biochemical assay comparisons where possible.

Figure 3 Basal rat ADSCs formaldehyde fixed and stained with Haematoxylin and Eosin

2.3.1.2 Osteogenic Differentiation

Induction of ADSCs toward an osteogenic lineage is commonly carried out with the supplementation of dex, AA and β-glycerophosphate in the basal ADSC media *in vitro* for up to 14 days. Initial signs of differentiation are the morphological variation which the cells assume by 7 days post induction. The general structural alterations are immediately visible as the post induction ADSCs no longer exhibits the bi-/tri-polar appearance of the basal cells. Instead, the cells share a uniformly rigid and rounded exterior. The extent of differentiation is firstly determined by matrix mineralisation verified by the presence of calcium deposition easily distinguished histologically by Alizarin red. Secondly the detection of ALP activity is a relative measure of osteoblastic activity. The extracellular matrix synthesis and calcium deposition manifests at detectable levels after 7 days of induction with slights of calcium detected on the circumference of each cell and rarely a dense nodule which appears dark orange due to higher accumulation of calcium or clustered cells (fig 4). Post induction at 14 days, a deeper colouration and staining of the monolayer indicates a higher proportion of cells now harbour an increased concentration of calcium (fig 5). A morphological comparison of the 7 and 14 day osteogenic ADSCs reveals both osteogenic time points have structural resemblances to the primary osteoblasts (fig 6). The chief difference between the cell types is the increasing amount of calcium detected by the staining method which was seen to be relative to the maturity of the cell.

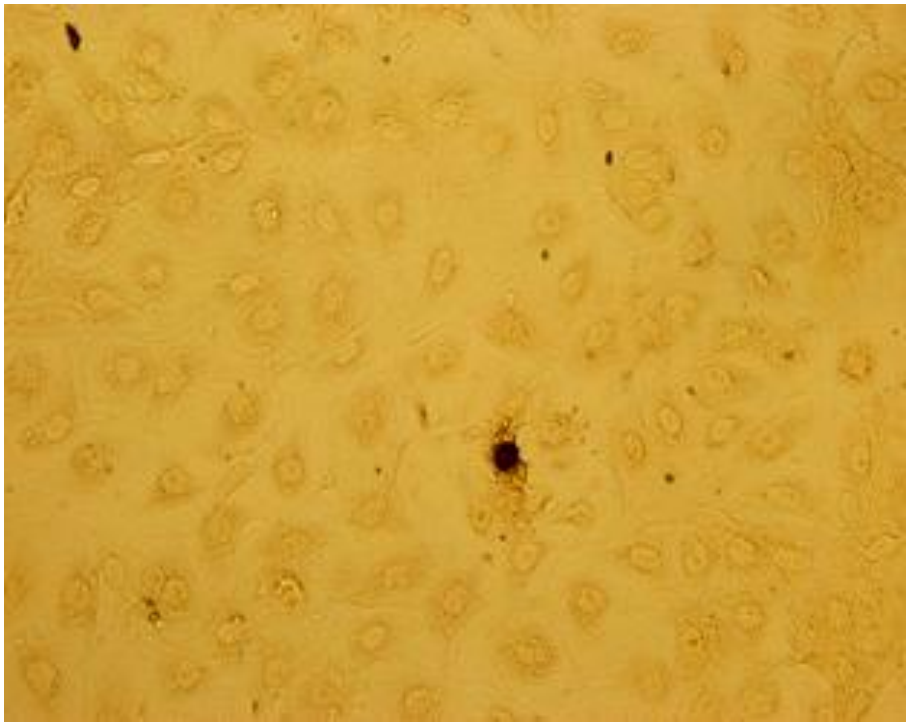

Figure 4 Osteogenic induced ADSCs 7 days post induction stained with Alizarin red. Faint orange colouring is visible in the cytoplasm.

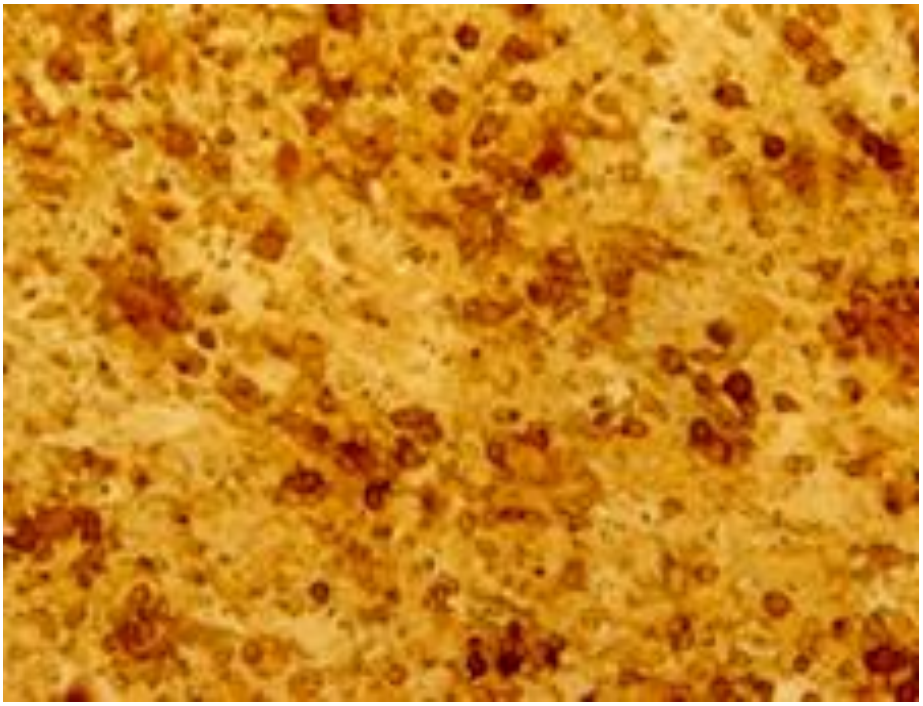

Figure 5 Osteogenic induced ADSCs 14 days post induction stained with Alizarin red. Faint orange colouring is visible in the cytoplasm

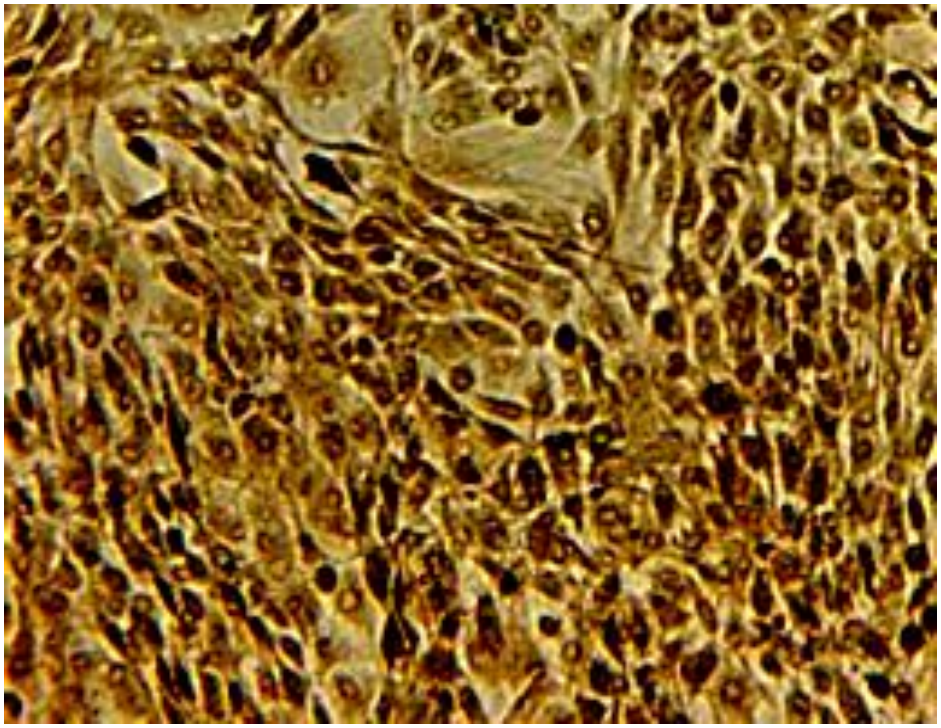

Figure 6 Primary osteoblasts maintained for the same length of time as the 14 day differentiated cells stained with Alizarin red, thus showing a high intensity of calcium deposition in the cytoplasm.

2.3.1.3 Chondrogenic Differentiation

To induce chondrogenesis, the StemPro Chondrogenesis Differentiation Kit (Gibco) was used to induce chondrogenesis in adipose tissue-derived stem cells. The accumulation of cartilage-specific macromolecules in chondrogenic differentiated ADSCs and chondrocytes was examined by microscopy and histological staining. Alcian blue dye staining of cells is predominantly used to identify mucopolysaccharides and glycoaminoglycan (GAG) content which are markers for collagen synthesis. The development of cartilaginous tissue in cultured ADSCs, chondrogenic and primary cartilage cultures were evaluated after 14 days by GAG staining with Alcian blue which formed an intense blue colour across the ECM of cells expressing GAG. Alcian blue staining revealed no GAG content in basal undifferentiated ADSCs (image not shown). After 14 days of exposure to chondrogenic media, the ADSCs induced toward a chondrogenic phenotype adopted a more rounded to polygonal morphological appearance and were embedded with significant amounts of GAGs, detected with Alcian blue staining (figure 7). The primary cultured chondrocytes (figure 8)

share the distinct polygonal rigid morphological appearance similar to that of the chondrogenic ADSCs presenting a higher density of GAGs in the ECM as detected with a greater intensity of alcian blue indicating the cells have been induced toward a chondrogenic lineage.

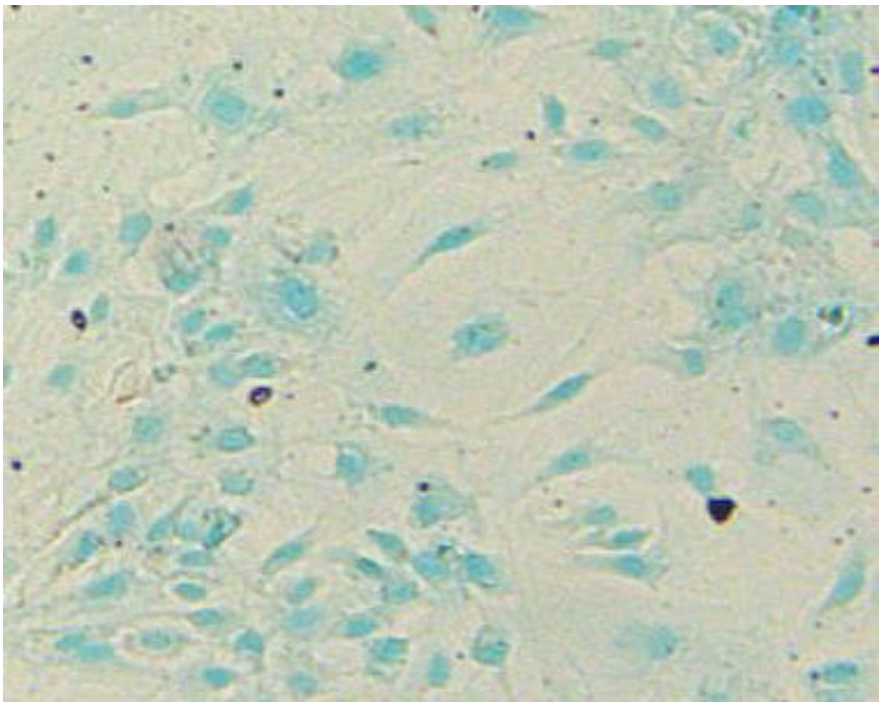

Figure 7 ADSCs differentiated for 14days in chondrogenic media then fixed and stained with Alcian blue shows and increased content of hyaluronan content in chondrogenic cells.

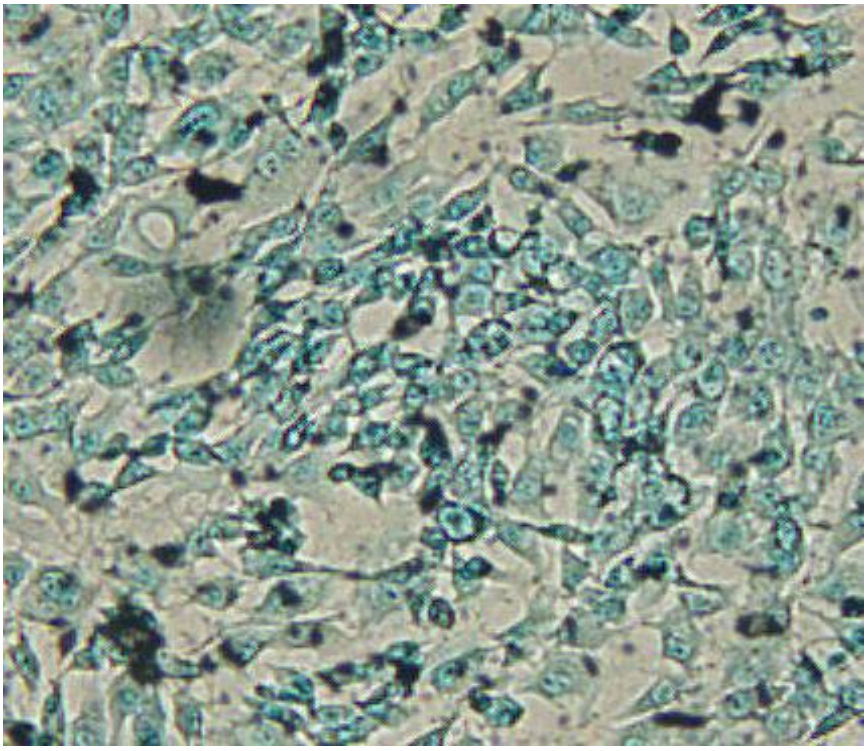

Figure 8 Primary cultured chondrocytes fixed and stained with Alcian blue shows hyaluronan content greater than ADSCs and a much more uniform and widespread content than the chondrogenic cells

2.3.1.4 Neurogenic and Myogenic Differentiation

Neurogenic differentiation by means of BME media supplementation instigates morphological changes within 3 hours of induction and exhibits a near complete transition within 24 hours. There was a loss of more than 50% of the cell population during the differentiation process; however the majority of the surviving cells no longer resemble basal ADSCs and present extensive neuronal-like structural similarities (fig 9 and 10). The morphological changes are predominantly the retraction of the membrane and cytoplasm toward the nucleus and the growth of multi-polar extensions with evidence of processes linking separate cell bodies which resemble primary hippocampal neurons (fig 11) [109, 202, 286].

Myogenic differentiation required approximately 6 weeks for the cells to be morphologically distinct from the basal ADSCs. The resultant cells somewhat resembled smooth muscle epithelium however the extent of differentiation could not be determined directly from microscopic examination and required further investigation (fig 12).

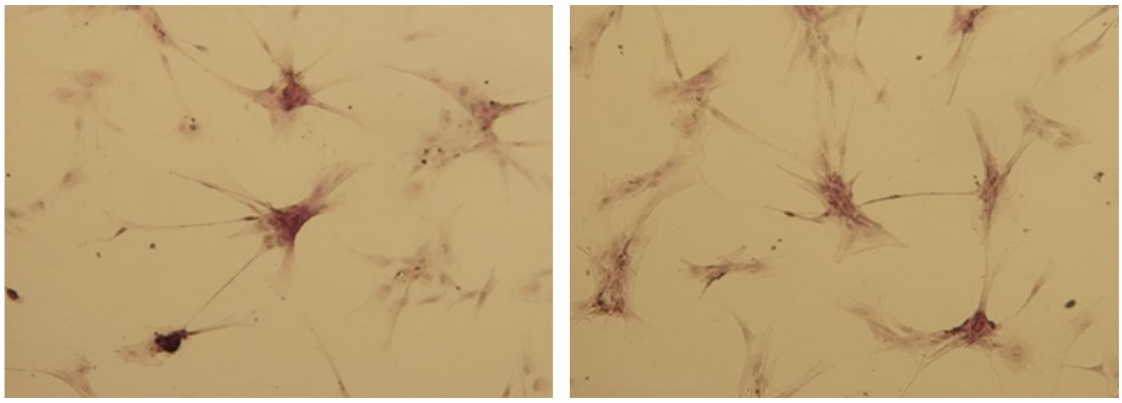

Figure 9 and 10 Neurogenic differentiated ADSCs treated for 24 hours with BME supplemented media fixed and stained with H&E.

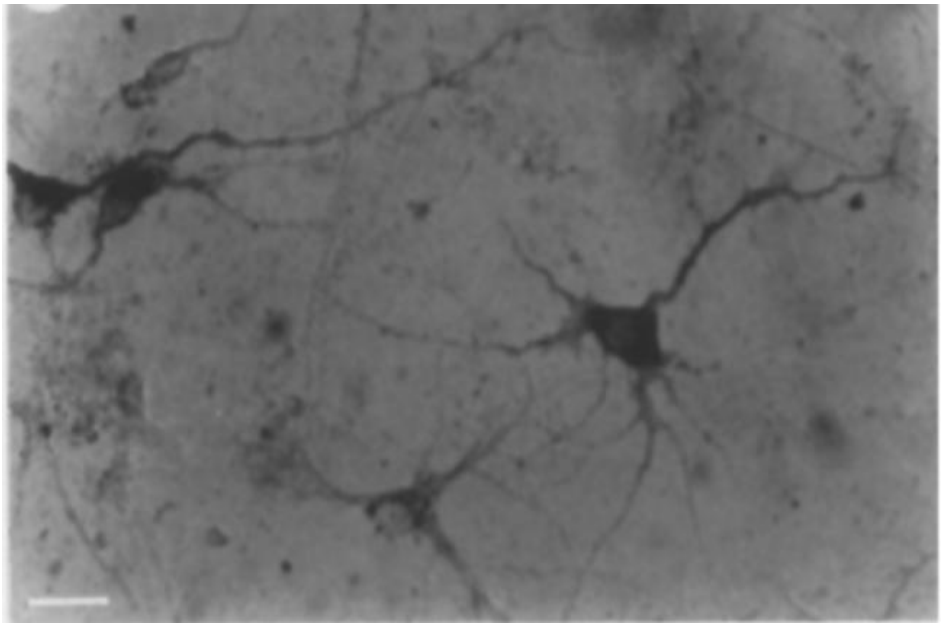

Figure 11 Primary cultured hippocampal neurons from Alderson *et al* [287] showing similar structures are present in the in the BME treated ADSCs in figure 8.

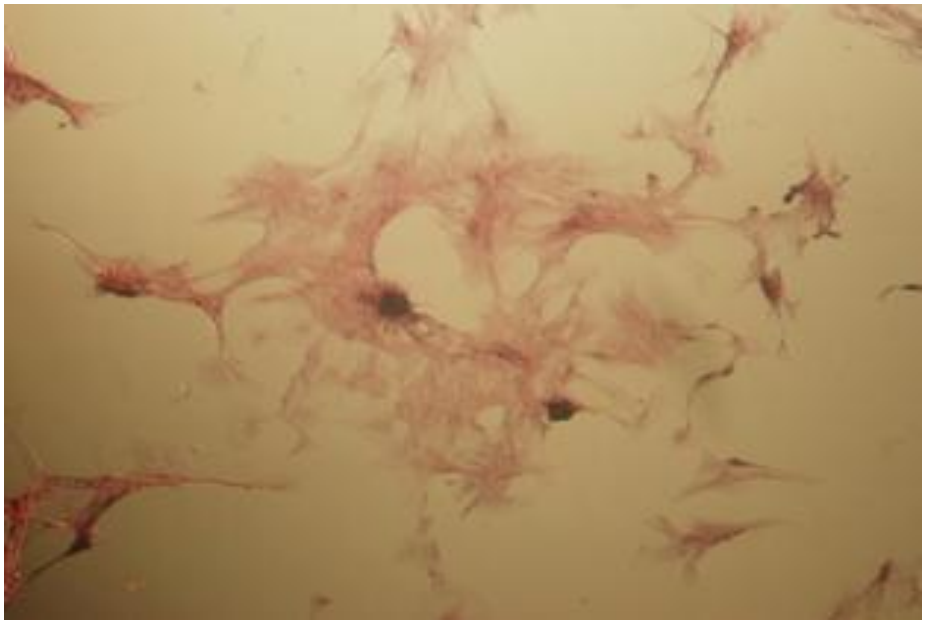

Figure 4 Myogenic Differentiation of ADSCs after 6 weeks of *in vitro* maintenance presents a diffuse however clustered and conjoined cell bodies.

2.3.1.5 Immunofluorescence of basal ADSCs

Pursuing the inquiry about marker variation observed by numerous research groups (as described in chapter one), an interesting result was revealed by immunofluorescence localisation of CD45 and CD90 at passage 1 and passage 5. These two markers were chosen because of the vast literature disparity about their presence or absence. A vast majority of papers corroborate the presence of CD90 in ADSCs (chapter 1, section 3.1, table 1). CD90 is not expressed on any adult tissues and has been utilised as the ideal surface marker [95]. Conversely CD45 should not exist on ASCs, since its expression should be limited to mature leukocytes [93] Figure 11 A and B are images of ADSCs at passage 1 and 5 both probed with fluorescent anti-CD90 antibodies. Passage 1 is brightly illuminated with a definite positive presence of the CD-marker. However at passage 5 the amount of fluorescence is equivalent to the background showing a stark decrease in the expression of CD90. Figure 11 C and D show the same ADSCs at the exact same passage probed with a fluorescent anti-CD45 antibody, where the converse was detected. The passage 1 displayed minimal traces of CD45 and the passage 5 revealed a much higher level of expression of CD45 than its earlier passage

counterpart. It is now largely accepted that the marker phenotype may change in culture according to passage number [288], this has been corroborated by preliminary immunofluorescent microscopy experiments seen in figure 13 A-D. This shows that marker characterisation is not a definitive method for characterising ADSCs as the markers relied on can change spontaneously in culture. This reinforces the approach of a proteome wide analysis for characterisation.

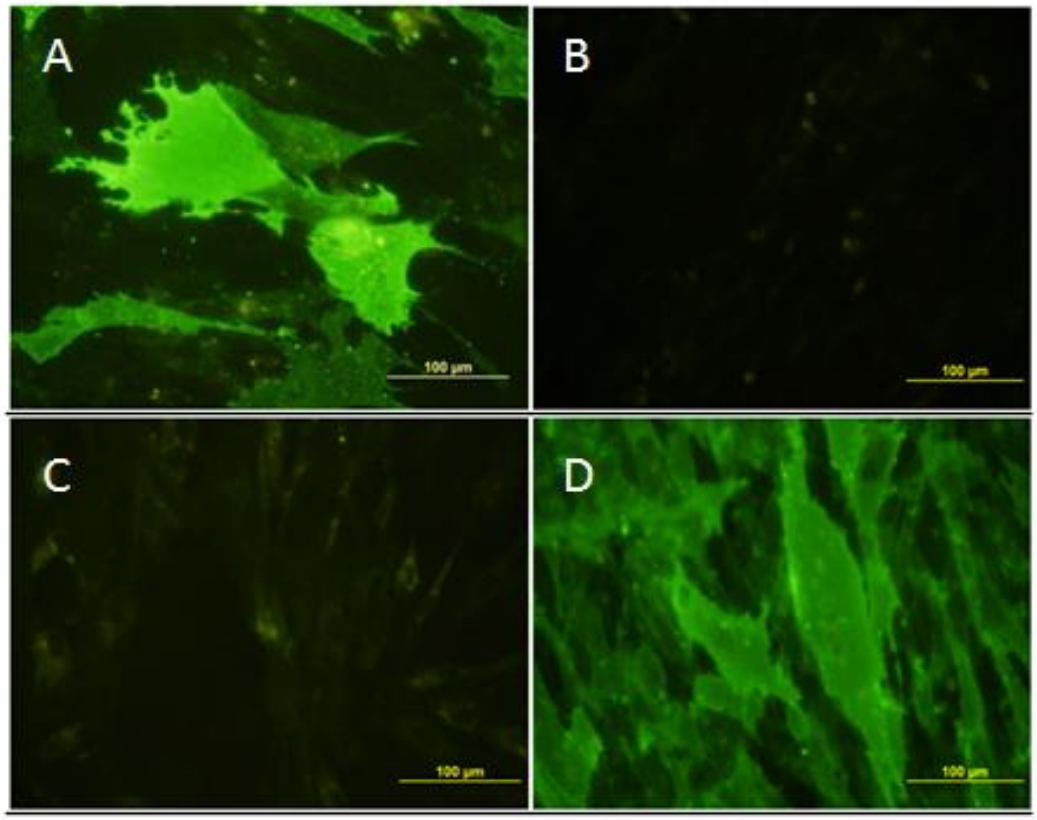

Figure 13 Rat adipose derived stem cells *in vitro* cultured probed with Rabbit Anti-Rat CD90 FITC or Rabbit Anti-Rat CD45 FITC. A. ADSCs at Passage 1 stain positively for CD90. B. ADSCs at Passage 5 are CD90 negative. C. ADSCs at Passage 1 are CD45 negative. D. ADSCs at Passage 5 are CD45 Positive. Image was captured on a Nikon Eclipse Ti

2.3.2 Alkaline phosphatase activity assay

ALP activity was measured in collected media from DMEM/F12 control blank, ADSCs, Osteogenic, Osteocytes, Chondrogenic and Chondrocytes (figure 12). Para-Nitrophenylphosphate (pNPP) is a chromogenic substrate for ALP used in Western blot, ELISA and alkaline phosphatase activity assays. ALP breaks down pNPP to yellow *para*-nitrophenol. This product can be measured with a 405 nm

spectrophotometer which can then be equated against standard curve to determine the amount enzyme present or the activity rate. Detected ALP is widely used to indicate the development of osteoblasts. Therefore primary osteoblast cultures were used as a positive control against all tested cell types. The recorded ALP activities demonstrate that the chondrogenic and chondrocytes have approximately the same levels of ALP activity relative to ADSCs and negligible levels when compared to osteogenic and osteoblast cells. The osteogenic differentiated cells presented the highest amount of ALP activity which was second to the primary osteoblasts (fig 14). This shows that the osteogenic cells are indeed in the process of differentiating toward an osteocyte linage as the relative comparison between osteogenic and osteoblasts are quite similar.

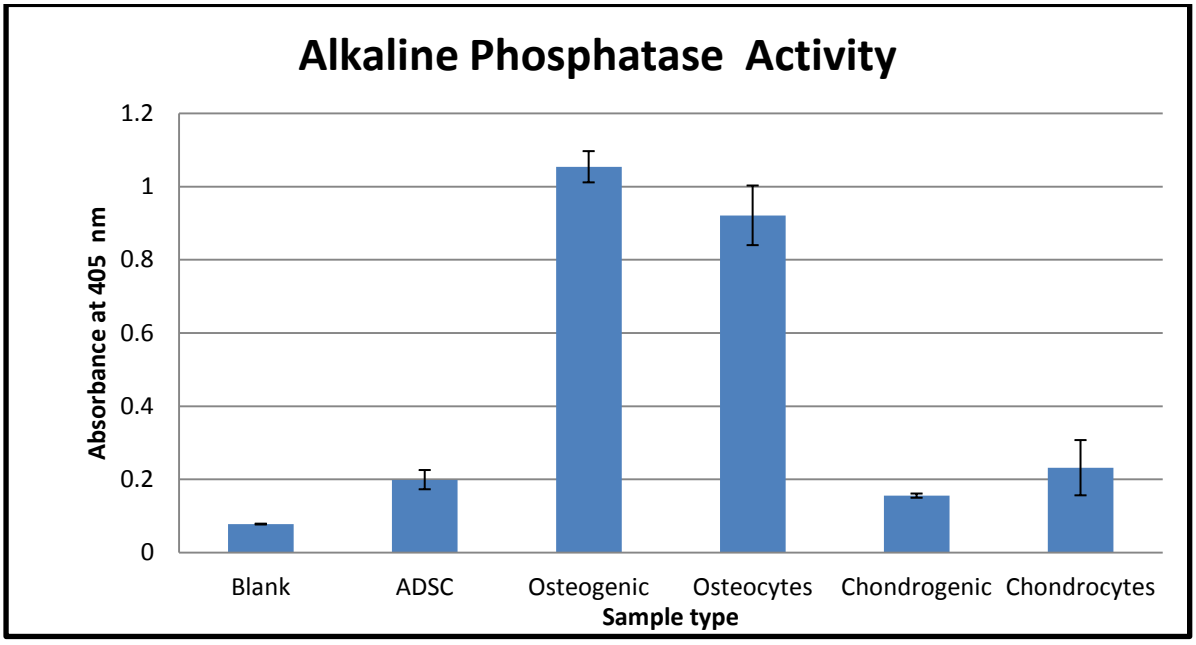

Figure 54 Alkaline Phosphatase activity expression difference across ADSCs, osteogenic, osteocytes, chondrogenic and chondrocytes. Minimal detected ALP activity of chondrogenic and chondrocytes is a positive indicator for non-osteogenic differentiation.

2.3.3 Two-dimensional PAGE

The 2-DE PAGE (figures 15-22) of ADSCs and its differentiated progenies were the foundation of the preliminary investigation to inspect the range of changes occurring in the acquired soluble fraction of the proteome of the differentiating cells. The initiative of utilising a 2-DE approach prior to engaging other techniques was to rapidly identify the range of changes in the proteome, relative to basal ADSCs, at their optimal differentiation end time point. The premise of employing this method was that any substantial changes to the proteome will be immediately identifiable by visual inspection and the subtle variances would be detected by 2D gel image analysis software PDQuest (BioRad). Thus the cells with the most significant visual proteome changes and most robust differentiation were pursued for further research. In addition, 2-DE allows resolution and identification of individual isoforms of a protein; something only possible in “shotgun” LC-MS/MS methodologies of the peptide defining the isoform is detected and efficiently fragmented.

Inter gel comparisons of differentiated cells relative to the basal ADSCs show a clear change in proteomic profiles meaning the cells were differentiated. The gels of the neurogenic cellular proteins (figures 17 and 18), while having unique protein spots, shared the most similar profiles to the ADSCs. The PDQuest evaluation of the ADSCs and the Neurogenic pH 3-10 gradient gels found a 79 protein spot differences of which 38 spots from the former and 19 from the latter were excised and prepared for MS/MS. The remaining 22 spots were not excised for tandem MS/MS as the spots were too faint and small. Table 1 summaries the proteins identified. The range of proteins identified did not match the number of spots analysed as a numerous analysed samples returned results with insufficient scores or no peptide matches for a positive identification this is due to the faintness of these spots.

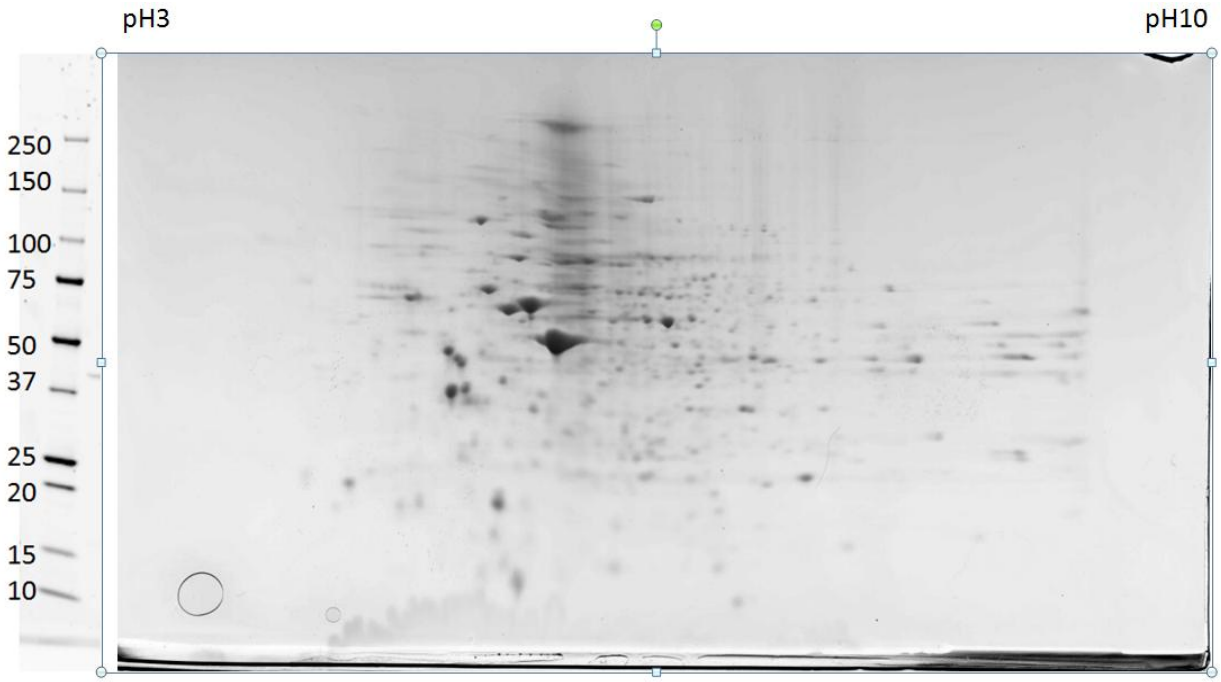

Figure 15 ADSCs 2D SDS-PAGE run in a 3-10 pH IPG strip for the first dimension and a 4-20% Bis-Tris second dimension.

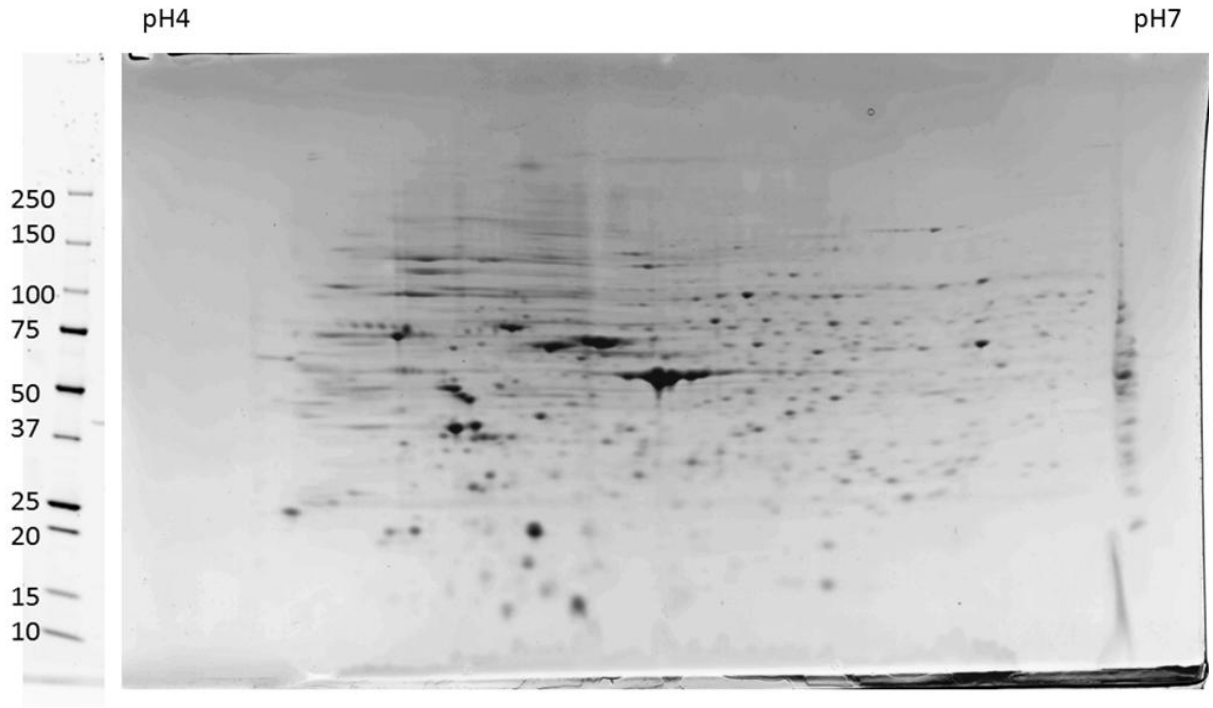

Figure 16 ADSCs 2D SDS-PAGE run in a 4-7 pH IPG strip for the first dimension and a 4-20% Bis-Tris second dimension.

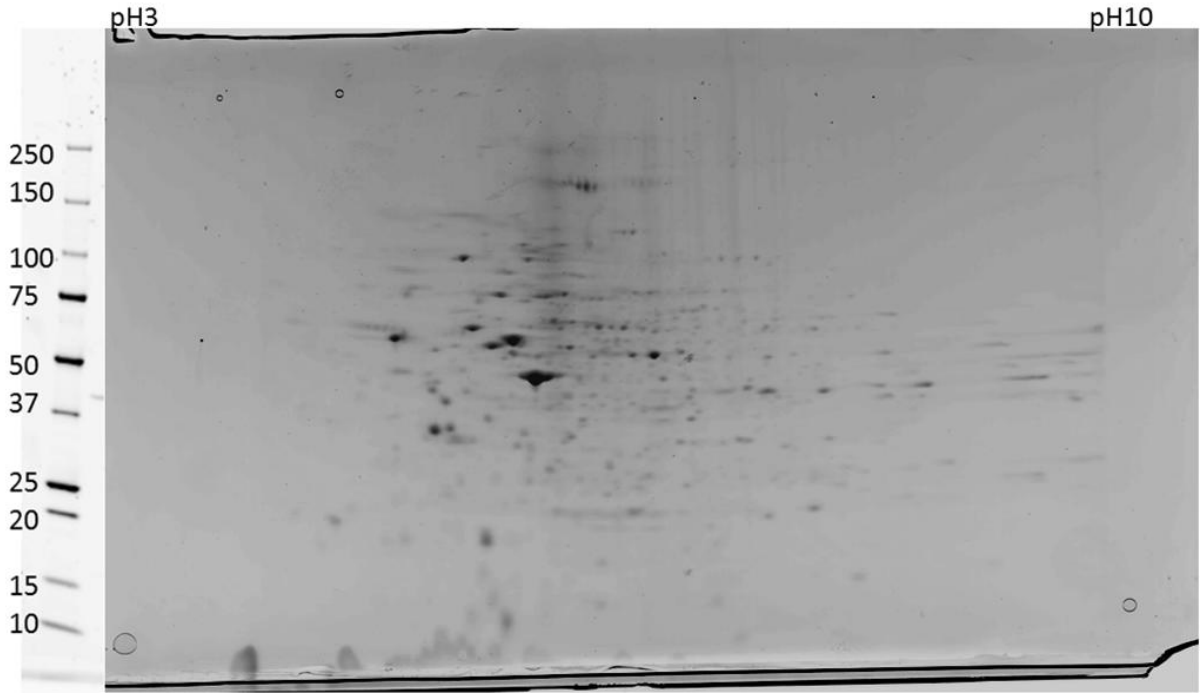

Figure 17 Neurogenic ADSCs 2D SDS-PAGE run in a 3-10 pH IPG strip for the first dimension and a 4-20% Bis-Tris second dimension

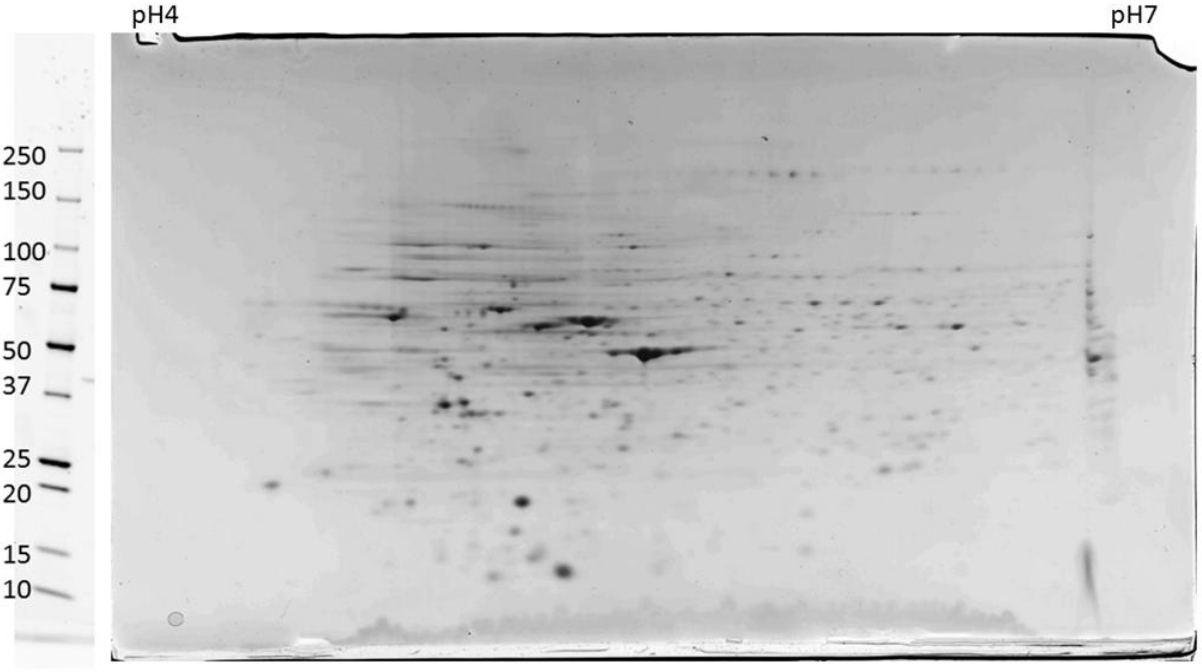

Figure 18 Neurogenic ADSCs 2D SDS-PAGE run in a 4-7 pH IPG strip for the first dimension and a 4-20% Bis-Tris second dimension

Table 2 Protein identification of spots excised from Neurogenic induced ADSCs

Protein	Accession number	Mass	Score	Unique peptides
Vcp Transitional endoplasmic reticulum ATPase	P46462	89293	143	2
Abcc8 ATP-binding cassette sub-family C member 8	F1LS70	177589	41	1
Eno1 Enolase 1, (Alpha)	Q5EB49	47128	260	2
Eno3 Beta-enolase	P15429	46984	409	5
Vat1 Synaptic vesicle membrane protein VAT-1 homolog	Q3MIE4	43091	92	1
Cct2 T-complex protein 1 subunit beta	Q5XIM9	57422	82	1
Vcl Vinculin	P85972	116542	256	6
LOC500959 Triosephosphate isomerase	Q6SA19	26850	170	3
Stip1 Stress-induced-phosphoprotein 1	O35814	62530	77	1
Prdx5 Peroxiredoxin-5	D3ZEN5	22256	782	10
Glyceraldehyde-3-phosphate dehydrogenase	D3ZGY4	35800	139	2

The assessment of the osteogenic line (figures 19 and 20) exhibited numerous variances from both the neurogenic and parent ADSC cells however they retained a number of key profile patterns. Mapping and overlaying with PDQuest 2D brought some difficulties. This was due the osteogenic sample bias toward the acid end of the pH strip chiefly seen in the pH 3-10 gel (figure 19). Migration differences prevented an alignment without excessive warping of the gel images which would indeed produced further misalignments. The osteogenic pI partiality was experienced in technical and biological replicates (data not shown), however not as substantial in the pH 4-7. The closest profile alignment achieved between the ADSCs and the osteogenic gels were between the gels shown in figure 16 (ADSCs) and figure 20 (Osteogenic). The visual comparison between these gels revealed a number of differentially regulated proteins which could not be quantified via this method. The cells were however selected for further investigation by 1D PAGE and LC-MS/MS due to the range of change seen in the 2D gel as well as the positive results obtained from alizarin red stain and ALP assay.

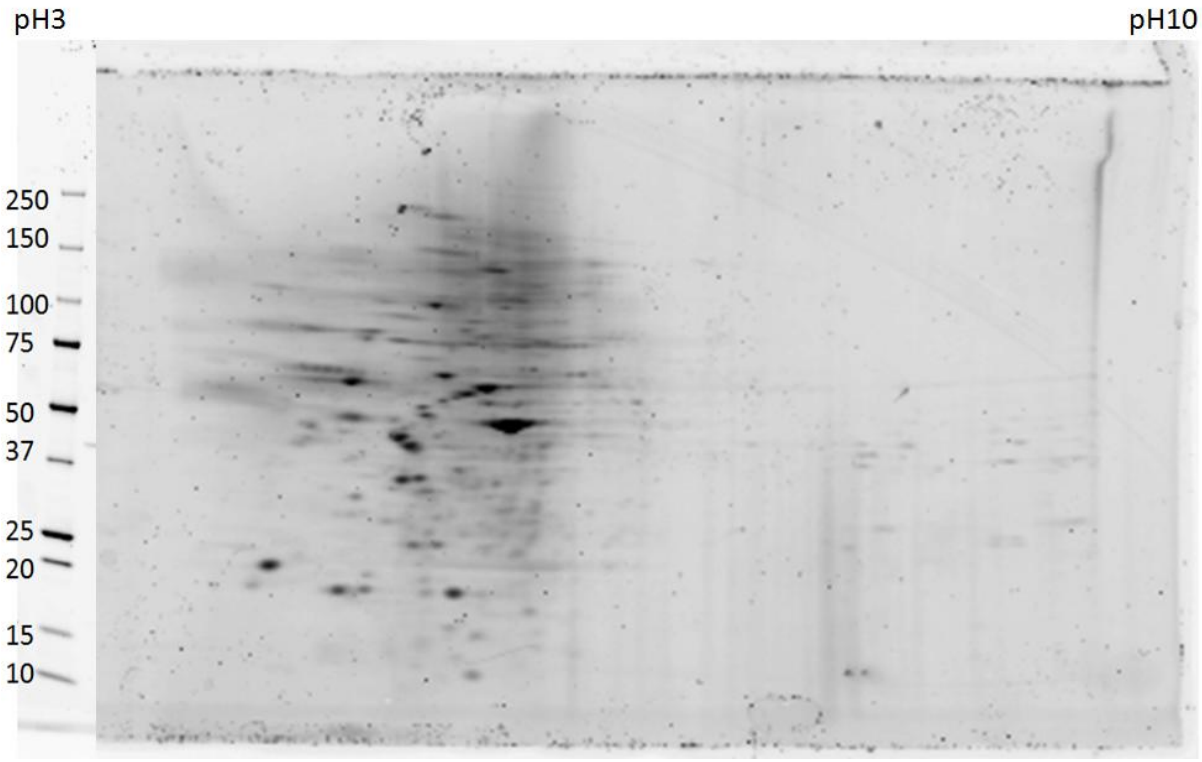

Figure 19 Osteogenic ADSCs 2D SDS-PAGE run in a 3-10 pH IPG strip for the first dimension and a 4-20% Bis-Tris second dimension

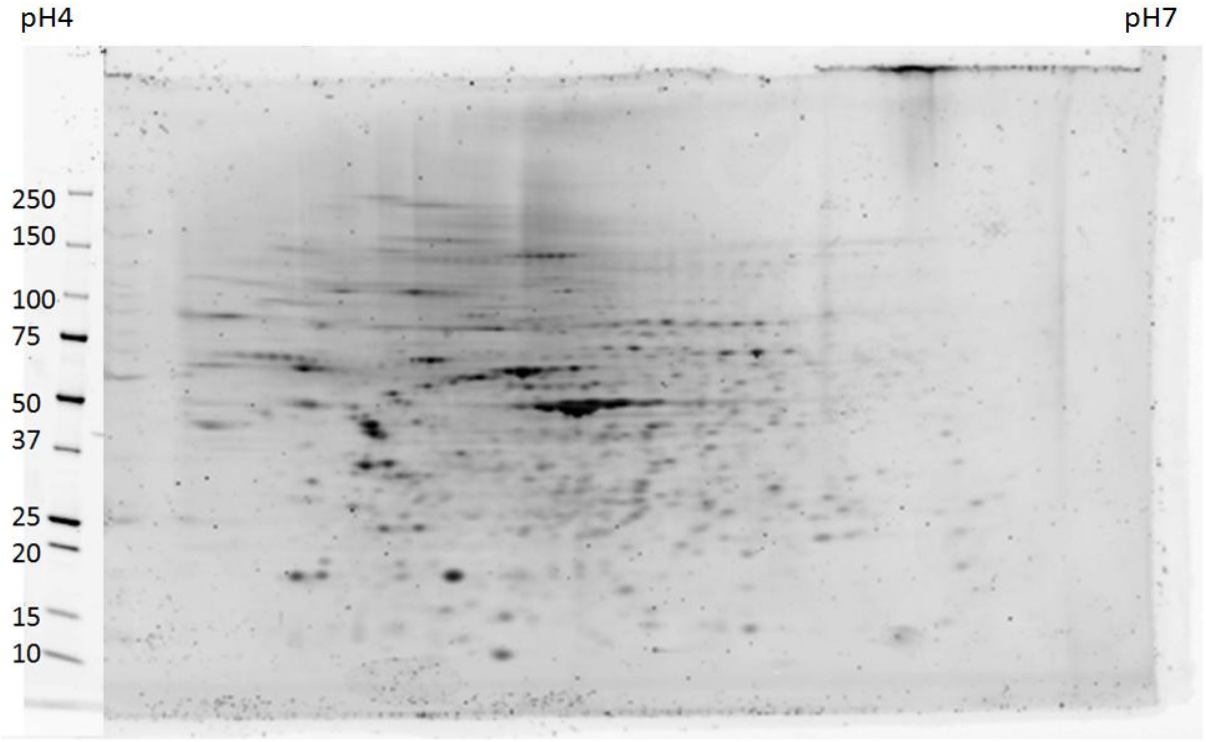

Figure 20 Osteogenic ADSCs 2D SDS-PAGE run in a 4-7 pH IPG strip for the first dimension and a 4-20% Bis-Tris second dimension

The largest variances in profiles were observed in the myogenic and adipogenic 2D gels which could still be aligned however would not be clear (fig 21 and 22). In the comparison of the myogenic differentiation sample to ADSCs, PDQuest identified up to 82 different spots of which 38 from the ADSCs were excised and 16 from the myogenic line. However, visual inspection of the myogenic gel (figure 21) revealed three considerably intense and large protein spots that are sizeable enough to mask numerous other proteins in its local vicinity. This posed a problem for the analysis software as isoforms and different proteins engulfed in this area would be considered as a single spot due to the mass up regulation of what could potentially be dozens of proteins.

The adipogenic cell line, whilst prepared in the exact same methodology in parallel to all other samples, produced gels of a quality that was unusable for gel to gel comparisons with PDQuest. The extent of horizontal streaking seen in figure 20 was considered to be due to the accumulated lipid within the cells which is a positive indication for adipogenic differentiation. The amount streaking makes this differentiation line difficult to continue proteomic analysis on using either 1D or 2D gel platforms without a more efficientlipid removal step. No spots were excised from this gel for further analysis.

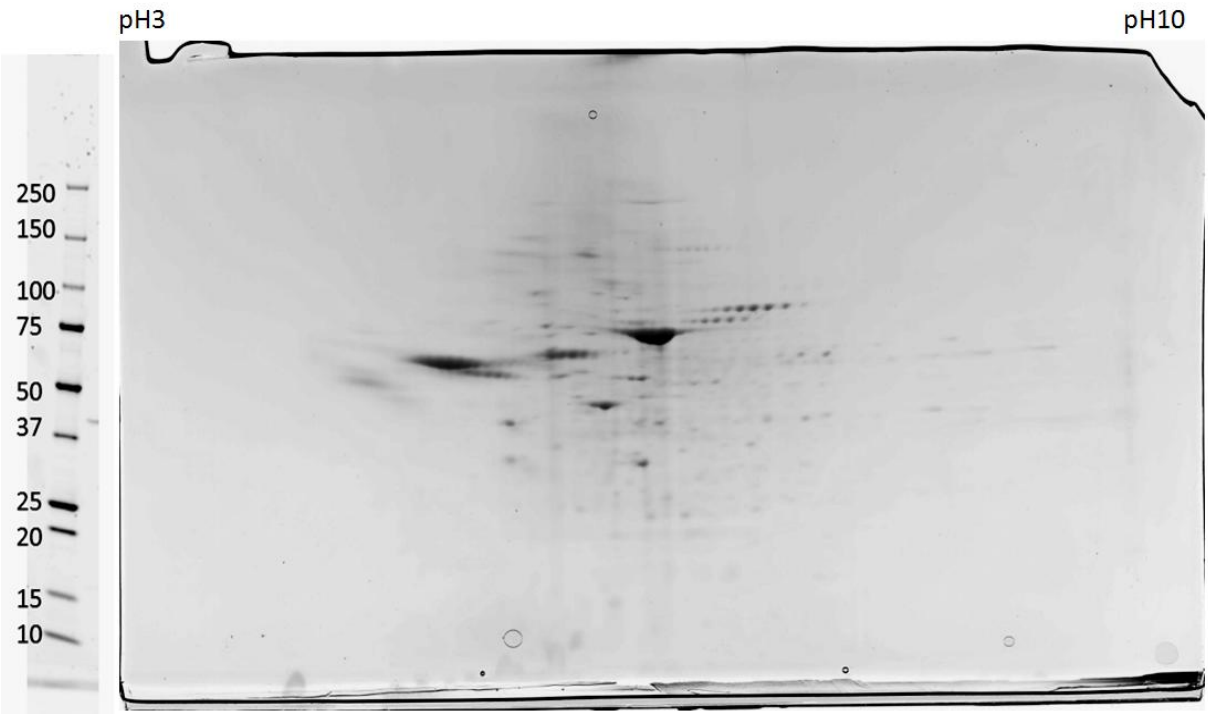

Figure 21 Myogenic ADCs 2D SDS-PAGE run in a 3-10 pH IPG strip for the first dimension and a 4-20% Bis-Tris second dimension

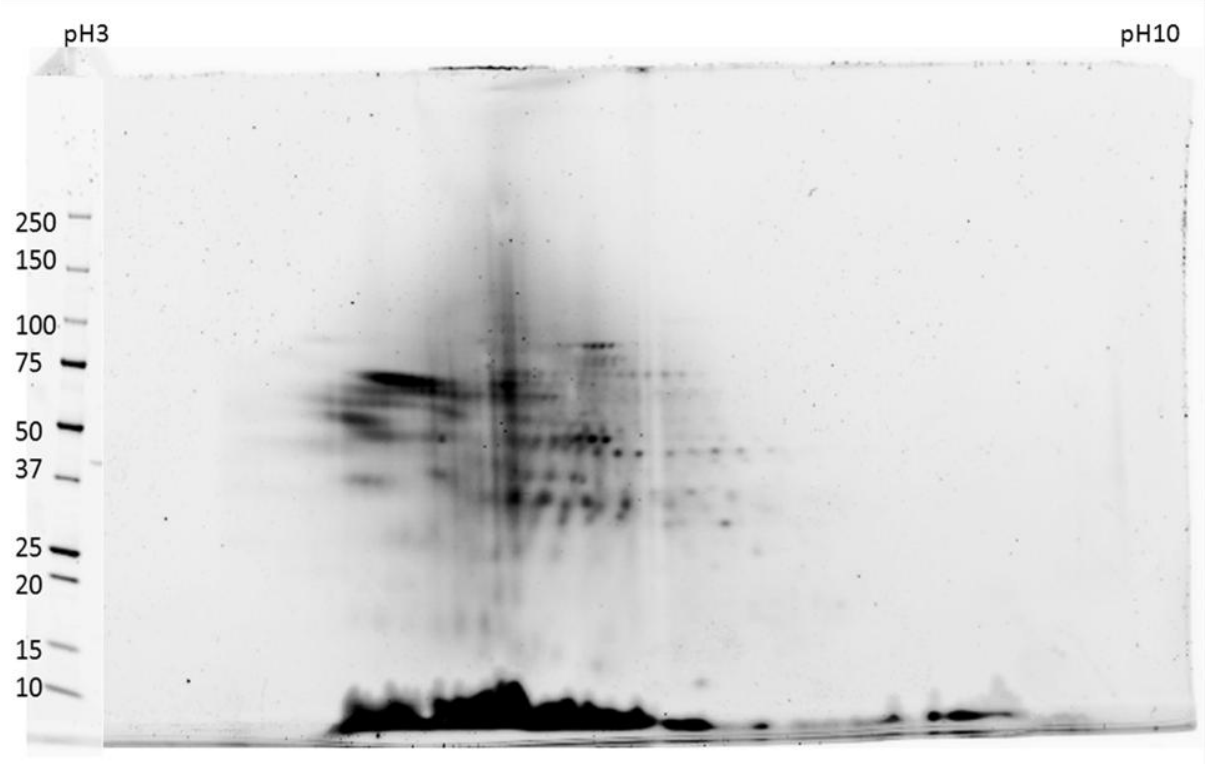

Figure 22 Adipogenic ADCs 2D SDS-PAGE run in a 3-10 pH IPG strip for the first dimension and a 4-20% Bis-Tris second dimension

2.3.4 One-Dimensional SDS-PAGE and liquid chromatography - tandem mass spectrometry

1-D SDS-PAGE and MS/MS were used to in an attempt to identify a greater number of proteins from each differentiation and subsequently utilise bioinformatic analyses to identify a protein's presence or absence between differentiated and basal stem cells, as well as measuring the fold change for proteins. The limitation of this technique is that a difference in protein isoforms is difficult to address. However for the broader view of the preliminary data set for basal and differentiated cell characterisation outweighs the minor limitations.

Basal ADSCs and three differentiation lines, neurongenic, osteogenic and chondrogenic were chosen for LC-MS/MS due to the range of changes displayed in the reasonably short differentiation time frame of 24 hours, 14 days and 21 days respectively. Each cell line was prepared in technical replicate and analysed using an AB Sciex QSTAR Elite mass spectrometer system and protein identification was carried out using Mascot (Matrix Science) to search the LudwigNR database. The neurogenic protein identification cohort was compared only to the basal ADSCs. The osteogenic and chondrogenic were both compared to the basal ADSCs as well as their primary derived counterparts (PDCs) (osteoblasts and chondrocytes). The following Venn diagrams (figure 23) present the unique and shared proteins between the ADSCs, differentiated and PDCs. The advantage of this analysis is the categorizing of uniquely expressed proteins which are specific for that differentiation. The Venn diagrams indicate a high number of shared proteins in all differentiations and a very small difference of uniquely expressed proteins in the osteogenic and chondrogenic differentiations. Whereas the neurogenic line presents the highest differences in unique proteins expressed which will be expanded on the discussion section. A full list of protein identifications is available in appendix 1A-D.

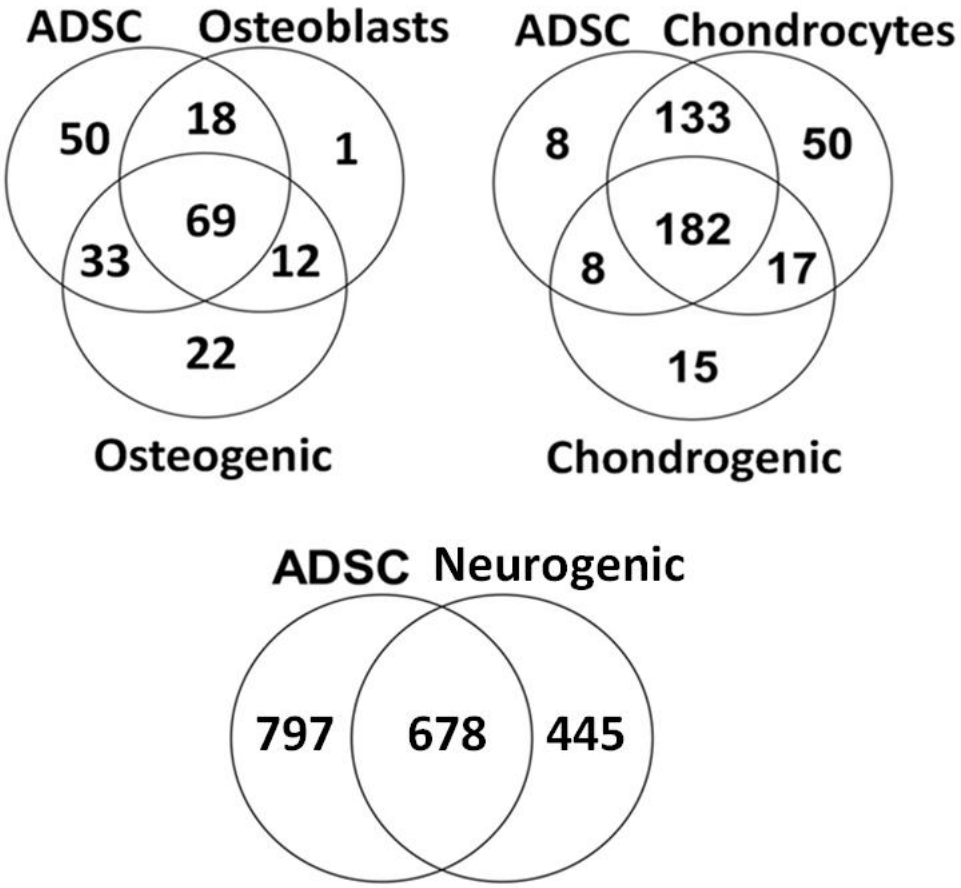

Figure 23 Three separate Venn diagrams of identified proteins from LC-MS/MS and database search using Mascot. The diagrams show the number of unique and shared proteins between three different comparisons, ADSC/Osteoblast/Osteogenic, ADSC/Chondrocytes/Chondrogenic and ADSC and Neurogenic.

2.3.5 Bioplex

The collected secretions from all *in vitro* samples were run in a Bioplex assay specific for 27 rat cytokines and chemokines. The results reveal that 24 out of the 27 cytokines were detected in varying levels, displaying unique expression profiles for each cell line. Due to the large variances between concentrations, the values were presented in a log graph layout and broken into four separate figures (figures 24-27) for relative comparisons. The secretion profiles in the $\log_{10}$ form exhibits trends which can be compared between cell lines. This is useful for the assessment of ADSCs, differentiated cells and the primary counterparts. Overall the ADSCs secrete low levels of most cytokines with a minimum detectable concentration of 4.18 pg/ml for IL-17, and a maximum of 636.34 pg/ml for IL-10 with an average of 91.52 pg/ml for all cytokines.

The first comparison of ADSCs, chondrogenic, primary chondrocytes, and chondrogenic blank media presents a stark difference in profiles. The blank chondrogenic media was utilised in the comparison profiles as it was the only media with unknown concentrations of supplemented cytokines from a proprietary commercial product. The ADSCs profile comprises of expression of the 24 targeted cytokines while the chondrogenic and chondrocytes are entirely divergent from these basal levels. Figure 24 shows the most disparity between the displayed cytokine levels; all except IL-2 and IL-4 in the chondrocytes and IL-5 in the chondrogenic blank media have concentrations above 1 pg/ml. The figure 25 cohort of cytokines exhibits a closer profile similarity between the chondrogenic and chondrocytes with only IL-10 been expressed in concentrations above 1 pg/ml, the chondrocytes are however 10-fold higher than the chondrogenic. Figure 26 reveals the levels of G-CSF are the lowest expressed cytokines in this study and is minimally secreted in both the chondrogenic and chondrocytes alike. Conversely the chondrocytes expression of IFN-γ was at least 10-fold higher than in the chondrogenic cells. Further to this the molecules Gro/KC and M-CSF were also detected at approximately 60-fold higher concentration than the chondrogenic cells. The final cohort (figure 27) of cytokines was relatively similar with only an approximately 4-fold increase in the chondrocytes of MIP-2 and MIP-3a levels. The only exception in this group is the enormous ~10000-fold (9413.27 pg/ml) difference in vEGF in the chondrocytes and the 100-fold higher levels in ADSCs compared to the barely detectable levels in the chondrogenic cells. This evidence indicates the ADSCs have differentiated into something resembling a chondrocytes. This profile is not indicative of *in vitro* chondrogenesis as there was no detection IL-1, IL-6, TNF-a and IFN-g which have been previously annotated for roles in chondrogenesis [289].

The relative fold changes between ADSCs, osteogenic and osteoblasts revealed an interesting profile assembly. The trends between all three cell lines are very similar with minor variations in a few molecules. Firstly the trend and concentration values for ADSCs compared to osteoblasts are almost identical with the only exclusion of IL-18, which is marginally elevated at a concentration of 18.87 pg/ml in ASDCs as opposed to 6.84 pg/ml in osteoblasts. Conversely GRO/KC is 25-fold higher and

vEGF is 100-fold higher in osteoblasts than ADSCs. vEGF in osteoblasts is the highest expressed molecule detected in this experiment, seconded by vEGF expression in chondrocytes at similar levels.

The cytokine assessment of osteodifferentiation alongside osteoblasts also presents a unique concentration trend. The patterns are exceptionally similar, only varying in the elevated concentrations in osteodifferentiation cells, with an average of ~8-fold higher concentration than osteoblasts for the majority of cytokines investigated with the exception of vEGF.

The cytokines measured in the neurogenic differentiation mirrored a similar trend and to the concentration levels seen in the osteogenic cells when compared to the basal ADSCs. The only disparity pertained to a 10-fold higher concentration of vEGF in neurogenic than ADSCs. The high expression level of vEGF has been annotated as playing a role in osteochondral ossification, which is the laying down of bone and cartilage material [290]. The peculiar similarities cannot be due to the media additives as these two differentiation medias were completely different, sharing only DMEM/F12 which has no added cytokines. The intriguing results of varying and similar cytokine levels of different cell lines require further investigation and discussion later in this chapter.

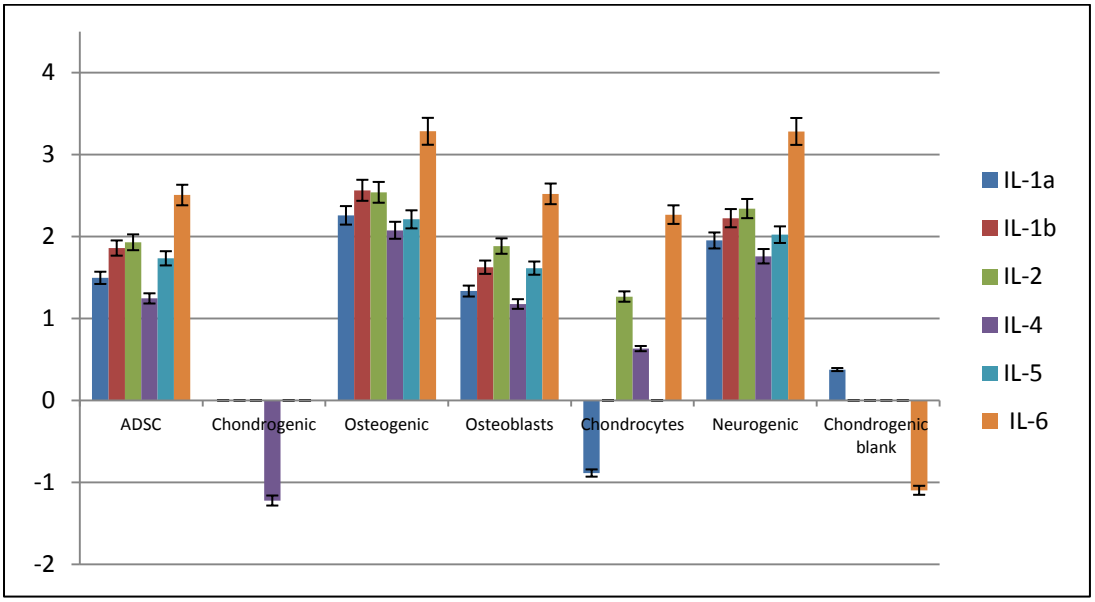

Figure 24 Bioplex results presented as Log_{10} Concentration for Interleukins Il-1a, Il-1b, Il-2, Il-4, Il-5 and Il-6 for ADSCs, Differentiated and Primary derived cells.

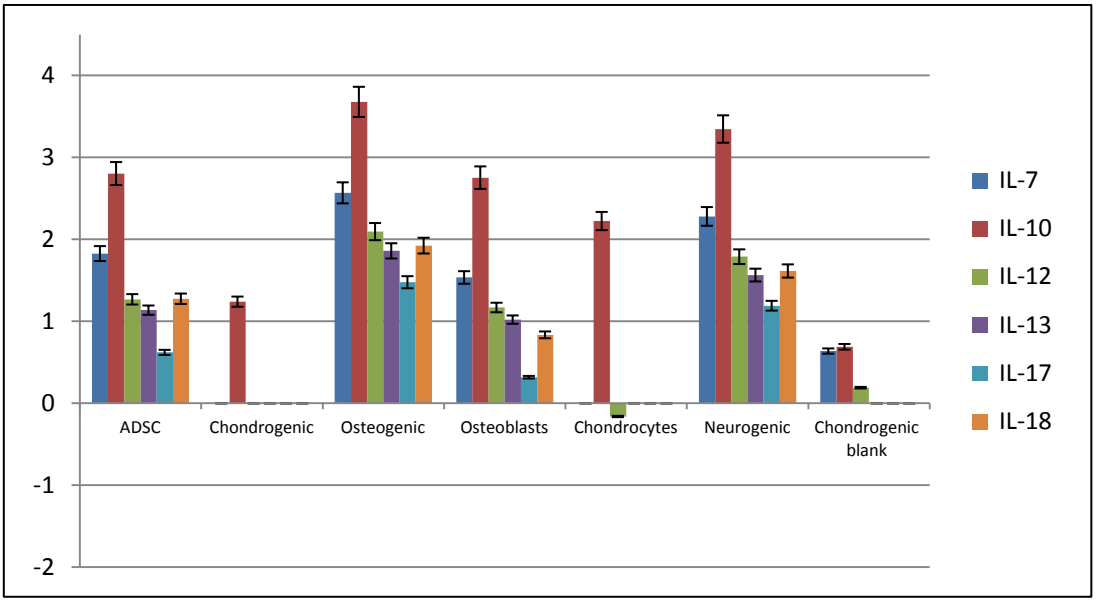

Figure 25 Bioplex results presented as Log_{10} Concentration for Interleukins Il-7, Il-10, Il-12, Il-13, Il-17 and Il-18 for ADSCs, Differentiated and Primary derived cells.

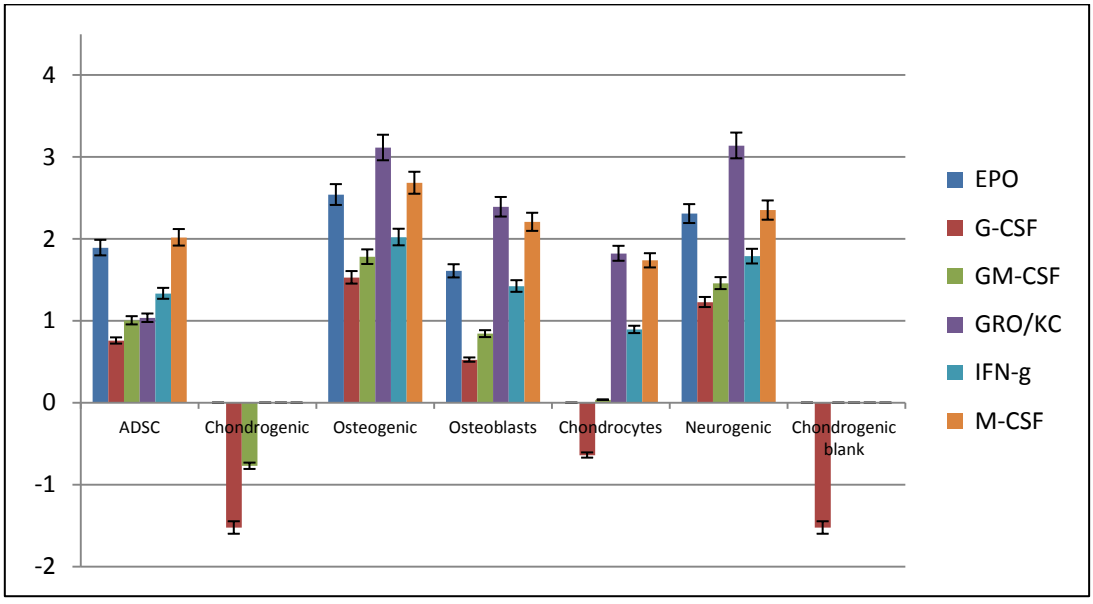

Figure 26 Bioplex results presented as Log_{10} Concentration for EPO, G-CSF, GM-CSF, GRO/KC, IFN-g and M-CSF for ADSCs, Differentiated and Primary derived cells.

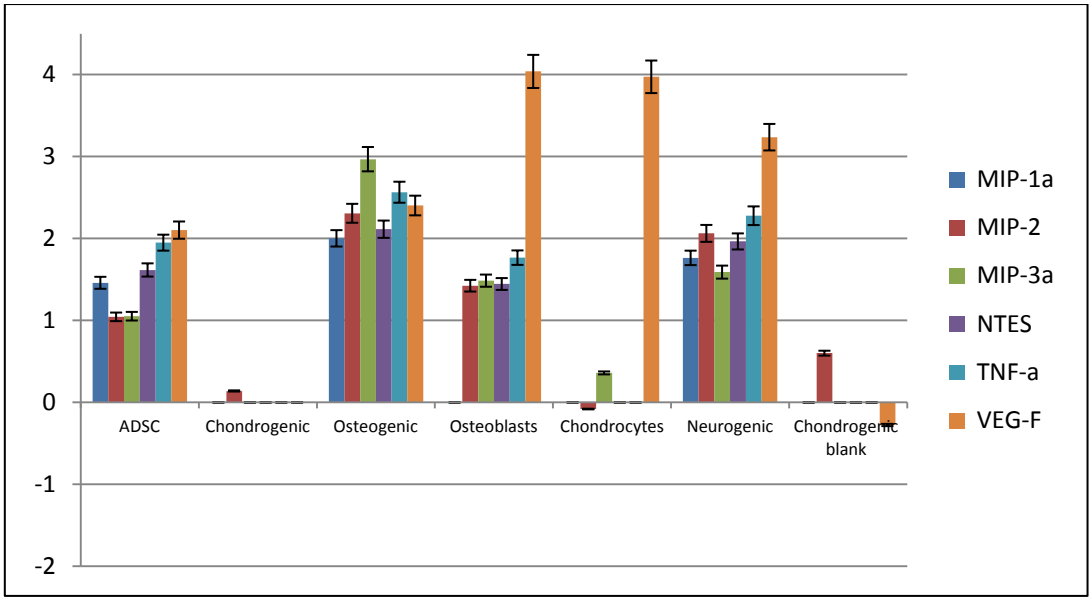

Figure 27 Bioplex results presented as Log_{10} Concentration for MIP-1a, MIP-2, MIP-3a, NTES, TNF-a and VEGF for ADSCs, Differentiated and Primary derived cells.

2.4.0 DISCUSSION

The principal initiative of this research was the examination and characterisation of ADSCs and their differentiated progenies by analysing the extent of molecular and morphological changes utilising alternative methods such as a proteomic analysis driven by LC-MS/MS and Bioplex analyses to those classically utilised surface marker immuneofluorescence and flow cytometric procedures to characterise cells.

This preliminary study is the first to utilise a range of proteomics techniques to compare rat ADSCs, their various differentiated progenies and mature primary derived cells to expand current knowledge about the extent of differentiation of these cells and determine the proteomic similarity to the mature actual counterparts. This is important as numerous previous studies have classified the ADSC progenies as being close to the mature counterparts based on confirmation of relatively few surface markers compared to the abundance of proteins which could be utilised [28, 104, 140, 194, 291-294]. An example is the use of the five widely sought after markers Nestin, Neurofilament 200, Beta Tubulin 3, Neuron Specific Enolase and Glial fibril associated protein in the determination of neurogenesis from MSCs seen in various differentiation studies employing diverse range of induction media [28, 46, 104, 193, 196, 265, 295, 296]. These minimal classification methodologies are usually observed in antibody based detection processes such as western blot, flow cytometry and immunofluorescence microscopy of certain surface markers [73, 78, 86, 136, 265, 288, 297, 298]. The analyses of markers is limited to the quality and specificity of the antibody produced, while a further limitation is the exorbitant price attached to each individual antibody and the limited multiplexing ability of Western blot and Flow Cytometry. While the utilised makers may not be incorrect in characterising cell types, the importance lays in the relevance of the produced cells at the therapeutic level. Essentially, we require a broader understanding of the extent of differentiation that the ADSCs are capable of, before we assume the produced cells will achieve their induced and directed purpose based solely on the positive identification of relatively few markers

from the copious available possibilities. Proteomics allows the exploration and examination of the diverse abundance of proteins.

The analysis with the proteomic techniques of 1D and 2D PAGE, LC-MS/MS and Bioplex assays of ADSCs differentiated down five separate lineages revealed unique proteomic and cytokine profiles as well as identified a score of proteins unique to each differentiation. The 2D-PAGE comparisons exhibited vast changes in the proteome of the differentiated ADSCs with a trend revealing the range of change was directly proportional to the length of time the cells remained in culture. The extent of change documented from these experiments showed the variety in proteome variation, which was the difference in the visualised proteome profiles by 1D and 2D PAGE, followed ADSC < Neurogenic < Osteogenic < Chondrogenic < Adipogenic < Myogenic, with ADSCs being the basal and Myogenic the most varied profile.

Multiple factors were considered prior to the selection of neurogenic, osteogenic and chondrogenic lineages for further investigation. The choice was based on the morphological changes, variation and similarity in 2D profiles, histological stains, length of time in culture, the acquirement and ease of *in vitro* culture of primary cells for comparison and the possible future clinical applications for the product cells.

As such, the selected cells; chondrogenic, osteogenic and neurogenic; morphological changes were most varied and producing an abundant monolayer of *in vitro* cells for further investigation. Even though the Adipogenic cells were cultured for a week less than the chondrogenic, the lipid accumulation was anticipated to be problematic, as seen in the 2D image of figure 20, for a number of techniques without further sample preparation. The chondrogenic cells were also selected moreover for their clinical relevance.

The delineation of the extent of differentiation will be covered in subsequent differentiation specific subsections. While the neurogenic, myogenic and adipogenic lineages produced diverse cell

populations, their proteomic comparison to their relative mature counterparts was limited due to the amount of primary material available. Although the neurogenic differentiations had the shortest turnover time in producing cells with the least 2D profile difference, further investigation was warranted due to the broader utility of those cells in neuronal repair and regenerative therapies which is a subject of subsequent chapters.

2.4.1 Chondrogenic Differentiation of ADSCs

Articular hyaline cartilage degenerative diseases and injuries still pose a significant challenge for orthopaedic surgeons as the sites of defect often have a limited capability for natural repair [164, 299]. As such there is an expanding effort in the use of stem cell transplants as regenerative therapies to assist in the restoration of structure and function. Adult stem cells (SCs) have garnered clinical interest due to their innate ability for self-renewal and potential for multipotent differentiation [57]. Bone marrow was a well established as a source of SCs used in a variety of applications however the yield of derived cells are often low and the harvesting procedure can be traumatic for many patients [41, 43, 166]. As previously mentioned, ADSCs have become an abundant source due to the high yield of derived stem cells as well as relative ease in harvesting, processing and preparation of cells for potential treatments [39]. Previous *in vitro* studies have shown that MSCs have a high capacity for chondrogenic differentiation with cells presenting a number of cartilage specific phenotypic markers subsequent to chondrogenic induction *in vitro* and *in vivo* [112, 156, 157, 166, 184, 185, 300, 301]. A number of health agencies that have surveyed autologous chondrocytes implantation recommend the method remains to be perfected [302]. The complex development and maturation of chondrocytes from stem cells requires definition. As part of this study we proteomically examine and compared ADSCs, the chondrogenic cells produced and their primary derived counterpart chondrocytes.

The identification of cartilage exploits a widely adopted histological stain; Alcian blue, which is utilised to identify the presence and cellular location of GAGs, a key constituent of connective tissue

like cartilage. Chondrocytes express high quantities of hyaluronan which is an α-D-N-acetylglucosamine (GlcNAc) GAG. Hyaluronan is the only GAG which is completely non-sulfated and its role in the extracellular matrix of chondrocytes is essential for cell-to-cell cross bridging for cell aggregation prior to cartilagous formation [303, 304]. The expression of hyaluronan was not detected in basal undifferentiated ADSCs when compared to the high abundance detected in chondrocytes (Figure 7). Subsequent to chondrogenic induction the hyaluronan content increased over time (data not shown), with greater than 95% of cells staining positively for hyaluronan content by the final differentiation time point at 21 days. Numerous studies utilise the morphology and hyaluronan detection by alcian blue as a positive indicator for chondrogenesis [54, 171, 268]. A further assessment prior to proteomic profiling was an ALP activity assay, which very rapidly allows the distinguishing between differentiating cells of the chondrogenic and the osteogenic lineage, as AlP activity is a widely used marker for the latter [172, 281, 305]. chondrogenic and chondrocytes cells did not express ALP as levels detected were nominal and equivalent to basal ADSCs.

The proteomic analysis revealed several interesting results from the MS identification of fractionated proteins and from the Bioplex assay of secreted cytokines. Firstly, from the 413 protein identifications from the three cell lines, only 15 were found to be uniquely expressed in the chondrogenic cells and with a further 17 proteins were shared with the primary chondrocytes cells. The fascinating result is that the chondrocytes shared a higher number of proteins, 133, with the ADSCs and a further 182 proteins with both the ADSCs and chondrogenic cells. While this is a significantly large number, the level of similarity was however not unexpected due to the shared mesodermal lineage. The unexpected outcome was the diminutive number of proteins unique to the chondrogenic cells as well as the equally small number shared with the chondrocytes. The small number of detected proteins is only a fraction of the estimated total proteins; the possibility for changes to be occurring below the limit of detection is plausible. As such, the use of a more sensitive method and instrument such as iTRAQ and the ABSciex 5600 may allow for a further depth of

protein identification. Table 3 and 4 below summarises the both the unique proteins in chondrogenic and chondrocytes as well as their shared molecules.

Table 3 Protein identification from tandem MS/MS unique to chondrogenic ADSCs

Protein	Accession number	Mass (kDa)	Peptide matches
Susd2	B5DEX6	77	2
Amine oxidase [flavin-containing] A	D3ZFS8	60	2
Aldehyde dehydrogenase	D3ZIM4	55	6
Protein Col6a1	D3ZUL3	109	19
Protein Pgm5	D3ZVR9	62	6
Protein Col6a3	D4A115	288	53
Lactadherin	D4A6C7	51	8
sorbin and SH3 domain containing 1	ENSRNOP00000021114	104	3
Carboxylesterase 1D	G3V822	62	7
Galectin-3	P08699	27	5
Corticosteroid 11-beta-dehydrogenase isozyme 1	P16232	32	5
Dipeptidase 1	P31430	46	6
Pyruvate dehydrogenase E1 component subunit beta	P49432	39	2
Fatty acid-binding protein	P70623	15	2
Complement component receptor 1-like protein	Q63135	62	4

Table 4 Protein identification from tandem MS/MS of proteins shared between chondrogenic ADSCs and mature chondrocytes.

Protein	Accession number	Mass (kDa)	Peptide matches
Hydroxyacyl-Coenzyme A dehydrogenase type II	B0BMW2	27	4
SH3 domain-binding glutamic acid-rich-like protein	B5DFD8	13	4
Cathepsin D	D3ZGP8	48	3
Voltage-dependent anion-selective channel protein 3	D3ZP84	31	4
Beta-galactosidase	D3ZUM4	73	10
Alpha-N-acetylgalactosaminidase	D4A3N3	47	4
LOC100362685 Uncharacterized protein	D4A786	6	5
Protein Myof	D4AB02	208	1
collagen, type VI, alpha 2 precursor	ENSRNOP00000001695	109	13
Protein Sptbn1	G3V6S0	247	14

Acetyl-CoA acetyltransferase	P17764	45	7
Enoyl-CoA delta isomerase 1	P23965	32	4
Biglycan	P47853	42	7
Hadha Trifunctional enzyme subunit alpha	Q64428	83	7
Guanine deaminase	Q9JKB7	51	21
Barrier-to-autointegration factor	Q9R1T1	10	3
Peroxiredoxin-4	Q9Z0V5	31	4

Although a small number of unique proteins from the chondrogenic differentiation and shared chondrocytes line were identified, some have also been previously investigated as supporting markers for chondrogenic development and maturation. From the fifteen unique proteins identified in the chondrogenic sample, three have involvment in cartilage development, aldehyde dehydrogenase (ALDH), Protein Col6a1 and Protein Col6a3. ALDH has been previously used as a marker based on its activity to purify ADSCs from adipose tissue. A study by Estes *et al*., 2006 [306], investigated the potential of increasing ALDH concentration and activity has on ADSCs chondrogenic potential and furthermore if it could be utilised as a marker for chondrogenesis. They found that while chondrogenesis increased with passage number and ALDH activity could not be adequately used as a marker for chondrogenesis as it was expressed in similar proportions in other cell types as well being found to influence early neurogenesis [306-308]. The expression of the remaining two unique proteins, collagen, type6, alpha 1 (Col6a1) and collagen, type6, alpha 3 (Col6a3) are not much more promising as cartilage specific markers as they both are integral constituents of ECM in most connective tissues in adults [309, 310]. Therefore their utility as a chondrogenesis specific marker is questionable; however their use as a marker of ECM development is a possibility.

The proteins identified and shared between chondrogenesis and chondrocytes have a much higher probability for practical use as the mutuality between only those two cell lines conveys a closer affiliation between them. Two key identifiers, collagen, type 4, alpha 2 (Col4a2) and biglycan, both play significant roles in ECM development as well. Col4a2 is however not specific to cartilage and is

also expressed in mesengial ECM [311]. Biglycan however has been linked to the GAG attachment in ECM of mature osteochondral cells especially articular cartilage [28, 312, 313].

The role of the identified proteins unique to chondrogenesis has the potential be applied in the characterisation of differentiating chondrogenic ADSCs. The high similarity between the three cell lines leave little to be explored by difference in presence and absence of uniquely expressed proteins in the limited context offered by 2DE. A much more sensitive assay investigating proteins with a low copy number may be useful within a temporal differentiation experiment. Due to the similarity of the three cell types a method such as iTRAQ for relative quantitation would be ideal to examine these expression level differences. Alternatively a Selective Reaction Monitoring (SRM) assay directed at a specific assemblage of the chondrocyte specific proteins would be valuable in the identification of their expression in chondrogenic cells over time.

2.4.2 Osteogenic differentiation of ADSCs

The development of osteogenic therapies for bone degenerative conditions, structural defects and musculoskeletal injuries are in vogue due to the widespread afflictions. Musculoskeletal damage is the most common cause of severe long-term pain and physical disability affecting millions of people worldwide [22]. Diseases such as osteoporosis, osteoarthritis and rheumatoid arthritis are the world's leading causes of skeletal and joint damage and the fourth leading cause of disability and World Health Organisation (WHO) estimates it to effect approximately 6.3 million people by 2050 [135]. In light of this, the growing enthusiasm and number of cellular therapies for such afflictions have become popular in the last decade. For example, the guided bone regrowth for maxillofacial reconstructions utilises mesenchymal stem cells and osteoblastic promoting material which are directly implanted into a patient [314]. Similarly these applications have been applied to fractures, breaks and osteoarthritic patients [315]. However, the current dilemma encircling these clinical applications remains, which is that we still do not completely understand the normal processes of

bone healing. Many believe we are not at a stage where we can be entirely certain that stem cell transplant techniques will work [315], especially if we do not scrutinise the developments undergoing at the cellular level which can be investigated *in vitro*. Thus determining the extent of ADSC differentiation toward an osteogenic linage would be conducive in the future generation of suitable *in vivo* therapies.

Previous studies of osteogenic development from MSCs have utilised ECM embedded proteins of collagen, osteocalcin, osteopontin and bone sialoprotein as markers which are established alongside vast calcium deposition in the form of hydroxyapatite [116, 294, 316, 317]. The detection of these proteins as well as the high enzyme activity of ALP is characteristic of osteoblastic activity. This study agrees with the presence of such activity shown by the calcium detected in the produced osteogenic cells as well as the concurrent high abundance of calcium in primary osteoblasts by the histological stain alizarin red (figure 3-5) and the ALP activity (figure 12), which are robust and invariant detection methods. The proteomic interrogation and Bioplex assays present an interesting and broader view of the extent of ADSCs differentiation when compared to primary derived osteoblasts. The three cell lines, similarly to the chondrogenic comparisons, have a closer homology and overlapping protein catalogues due to a common dermal linage. However, the 22 unique proteins identified in the osteogenic line and the 12 shared between osteogenic and osteoblasts have relevance in the preliminary description of osteogenesis (Table 5 and 6).

Table 5 Protein identification from tandem MS/MS of proteins unique in osteogenic ADSCs

Protein	Accession number	Mass (kDa)	Peptide matches
Protein Col6a3	D4A115	288	38
Protein Col6a1	D3ZUL3	109	7
Lactadherin	D4A6C7		
Protein Col4a2 precursor	ENSRNOP00000001695	109	4
Guanine deaminase	Q9JKB7	51	4
Electron transfer flavoprotein subunit alpha	P13803	35	4
Laminin, gamma 1 (Protein Lamc1)	F1MAA7	177	4
Serine (Or cysteine) peptidase inhibitor, clade B,	Q6P9U0	43	3

member 6a			
Twinfilin-1	Q5RJR2	40	3
Procollagen, type VI, alpha 3	D4A111	240	2
F-actin-capping protein subunit alpha-1	B2GUZ5	33	2
Sideroflexin-3	D3ZHH2	32	2
galectin-3	NP_114020.1	27	2
Ornithine aminotransferase	P04182	48	2
Glutathione S-transferase alpha-3	P04904	25	2
Aquaporin-1	P29975	29	1
Cytochrome b-c1 complex subunit 2	P32551	48	1
RCG21039, isoform CRA_a	D3ZJ32	94	1
Retinoid-inducible serine carboxypeptidase	D4A9M8	45	1
annexin A3	NP_036955.1	36	1
Actin-related protein 2/3 complex subunit 5-like protein	A1L108	17	1
Redox-regulatory protein FAM213A	Q6AXX6	26	1

Table 6 Protein identification from tandem MS/MS of proteins shared between osteogenic ADSCs and mature osteoblasts

Protein	Accession number	Mass (kDa)	Peptide matches
Fructose-bisphosphate aldolase	G3V900	45	14
Malate dehydrogenase, mitochondrial	P04636	36	8
protein disulfide-isomerase A6 precursor	NP_001004442.1	49	12
Elongation factor 1-gamma	Q68FR6	36	7
integrin beta-1 precursor	NP_058718.2	88	5
Synaptic vesicle membrane protein VAT-1 homolog	Q3MIE4	43	8
Cathepsin D	D3ZGP8	48	4
Trifunctional enzyme subunit beta	Q60587	51	3
Annexin A4	P55260	36	3
Reticulocalbin 1	D3ZUB0	38	4
60S acidic ribosomal protein P0	P19945	34	4
Myosin regulatory light chain RLC-A	P13832	20	2

The predominant proteins unique to the osteogenic differentiated ADSCs are related to bone maturation as their expression increases and degeneration as their levels decrease. This is particularly relevant for the protein Laminin gamma 1, which when down regulated may have a role in the development of osteoporosis through its role in tissue morphogenesis [318, 319]. Laminin has also been found to initiate bone formation in *in vivo* trials of bone regeneration in the presence of hydroxyapatite in rats [320]. Yoshikawa *et* al findings also presented that the decrease of laminin coatings of bone implant materials decreased the percentage of bone formation as well as ALP activity [320]. In another study by Yang *et al* the gene encoding for laminin gamma was deleted from mouse embryos which was then found to affect a number of systems from the ECM and collagen density in basement membrane in kidneys to lowering structural integrity in skeletal system [321]. Furthermore, a structurally and functionally related molecule, laminin-5, has also been linked to the promotion of adhesion of osteogenic MSCs to each other and culture surfaces [322]. This has also been corroborated by the inclusion of laminin-1 in coated implant surfaces which promoted the adhesion of bone like structures while increasing ALP activity as well as expression of the classical osteogenic markers osteocalcin and collagen 1 [323]. While the up regulation of laminin gamma protein in the osteogenic cells may be significant for developing osteogenic cells, the noticeable lack of its presence in the primary osteoblasts cells is a factor that may limit its use as a marker for osteogenesis. However, not many studies have been conducted into the presence, absence or role of laminin in mature osteoblasts [324, 325]. While this protein holds some significance in osteogenesis, a determination of its usefulness will only advance once further analyses into its expression in other cell types is clear.

An associated protein of laminin is galectin-3 that has been solely identified in this study's osteogenic ADSCs [326]. Galectin-3's expression *in vitro* in RSF (rheumatoid synovial fibroblast) cultures has been directly linked to the synthetic glucocorticoid dexamethasone [327] which is a key component of the ADSC osteogenic induction media. Galectin-3 locality has also been established *in vivo* in osteoblasts as well *in vitro* in the maturation and ECM development phase of the

preosteoblastic MC3T3-E1 cell line [328]. Bruder's *et al* work on osteoblastic hybridomas suggested a refined model for the understanding of osteoblast maturation. This was based on a time dependant study of the presence and absence of cell specific molecules, which are only expressed on osteoblastic cells in this case, such as galectin-3 which can be used to define the position and extent of maturity of cells in an osteogenic lineage [329]. Aubin's *et al* data support that galectin-3 was a previously unrecognised product of osteoblastic cells and its expression coincides with the appearance of the prevalent osteogenic markers such as ALP activity, osteocalcin and bone sialoprotein [327]. The use of such a molecule, as a marker in osteogenesis, in conjunction with the partner laminins, as well as similar molecules, would allow a greater understanding of the maturation and ECM development occurring during ADSC differentiation toward an osteogenic cell line.

Equally the appearance and marker utility of molecules such as annexin A3 specifically for osteogenesis would also be valuable. Annexin A3 is a negative regulator of adipogenesis, thus its presence in the osteogenic induced linage of an adipose derived stem cells is a positive indicator that the maturation of the cell linage is progressing in the intended direction [330]. Annexin A3 and its interacting partners are not functionally linked to osteoblastic activity or maturation except in the inhibition of adipogenesis, a down regulation of these proteins increases the adipogenic potential at the expense of osteogenic differentiation [330].

The potential of proteins mutually presented in both osteogenic and osteoblasts to be utilised as markers may be beneficial as an unambiguous match between these cells conveys a qualitative evaluation of maturation in the osteogenic lineage. An enzyme reciprocally expressed in osteogenic cells and osteoblasts was cathepsinD which has the significance of degrading proteoglycans and GAGs during the maturation and calcification process of osteoblast-like cells [331]. A study by Xynos *et al*., investigating the production of osteogenic related proteins, like cathepsin D, in an *in vitro* environment in which osteoblasts cells were cultured on an osteoconductive bioglass material,

found an increased expression of cathepsin D by 310% above basal levels [332]. The evidence provided above reveals there are numerous proteins that are specific to osteogenic differentiation, albeit the limited detection level. This extends for a further investigation with a higher sensitivity method and instrument, for example the iTRAQ and ABSciex 5600. This would allow a further variety of uniquely expressed osteogenic proteins to be identified.

Cytokines have been noted to have a wide variety of roles in osteoblast proliferation and differentiation [333]. The established Bioplex cytokine profile comparisons between osteogenic ADSCs and osteoblasts have near identical trends however the osteogenic cells present values that are on average 10-fold higher than osteoblasts (figures 23-26). Cytokines annotated as having integral roles in osteogenesis are IL-1, IL-6, TNF-a, GRO/KC, vEGF, MIP-2 and, in a limited capacity, IL-10 [333-336]. Mesenchymal and osteoblastic cells can produce the mutlipotent cytokine IL-1 which is known to regulate osteoblast and osteoclast activity in formation and resorption of bone respectively [337, 338]. Varying studies have found opposing function for IL-1, some of which have shown an inhibition of osteoblast proliferation and enhancement of bone formation or *vice versa* [339-342]. An interesting assignment of function is that IL-1 has been found to stimulate osteoblasts to secrete IL-6 which has been annotated as playing a role in bone resorption and osteoblast proliferation, additionally increasing ALP activity [336, 343, 344]. The aforementioned three cytokines have vastly traceable trends with the osteogenic cells expressing 10-fold greater concentration than the osteoblasts. Moreover the osteogenic cells presented an appreciably higher ALP activity. The remaining cytokines TNF-a, GRO/KC, vEGF and MIP-2 are expressed in considerably in higher quantities relative to the other assayed cytokines. Correspondingly to the preceding cytokines, the remaining four have also conflicting data presented about the inhibitory or promotional effects of either osteoblastic proliferation or bone formation [335, 345].

The opposing findings in roles of cytokines have been postulated as being related to the differences in cells analysed from *in vivo* and *in vitro* sources [346, 347]. The main difference is due to the

environment of the harvested material. Cytokines analysed from *in vivo* sampling would be influenced by a three dimensional heterogeneous cell population whereas most *in vitro* studies examine samples from two-dimensional monolayers of homogenous cell cultures [347-349]. While extensive progress has been made in describing osteoblasts maturation, the differentiation potential of ADSCs is still relatively unknown. However drawing from previous data and studies, an overall pattern can be formulated in the regulatory signals and markers being presented in a temporal study during the differentiation cycle.

2.4.3 Neurogenic Differentiation of ADSCs

The investigation into transdermal differentiation potential of stem cells to identify the degree of neurogenic potential of the produced cells has been a goal for regenerative medicine due to the boundless opportunities for rehabilitation to those afflicted with neurodegenerative diseases, congenital defects or traumatic injury to the CNS or PNS. ADSCs have been shown to present morphological cues and several neuronal related marker molecules when treated with *in vitro* with simple chemicals such as β-mercaptoethanol [104]which has been part of this preliminary study.

A microscopy analysis of ADSCs induced toward a neurogenic linage revealed that the produced cells are in accord with previous studies, displaying morphological similarities with primary cultured neurons [104, 192, 196, 350-352]. In a similar circumstance to the chondrogenic and osteogenic cells, the investigation into the extent of differentiation was conducted via proteomic analysis and comparison of the expressed proteins at basal and the end time points. This analysis however was limited to the comparison between ADSCs and the neurogenic cells due to the inherent difficulties of culturing sufficient primary rat neural material for proteomic analysis.

The comparison of ADSCs and the neurogenic cells presented a marked difference in protein expression with 445 unique proteins identified in the neurogenic material LC-MS/MS. The analyses of the neurogenic cells compared with ADSCs presented a broad range of unique proteins in the former, of which the most interesting were annotated as the neurogenic promoting and stress

related proteins. A gene ontology (GO) categorisation by biological function shows the varying percentage breakdown of the identified proteins in the neurogenic ADSCs (figure 28). Interestingly the percentage of proteins involved in cell differentiation and response to stress were approximately 3.36% and 3.56% respectively. These sundry categories of proteins were not unexpected as the corresponding neuronal-like morphological changes were considered to be related to the neurospecific proteins where as the stress and shock induced proteins were postulated to be associated to the substantial cellular death which ensued subsequent to induction (table 7 and 8).

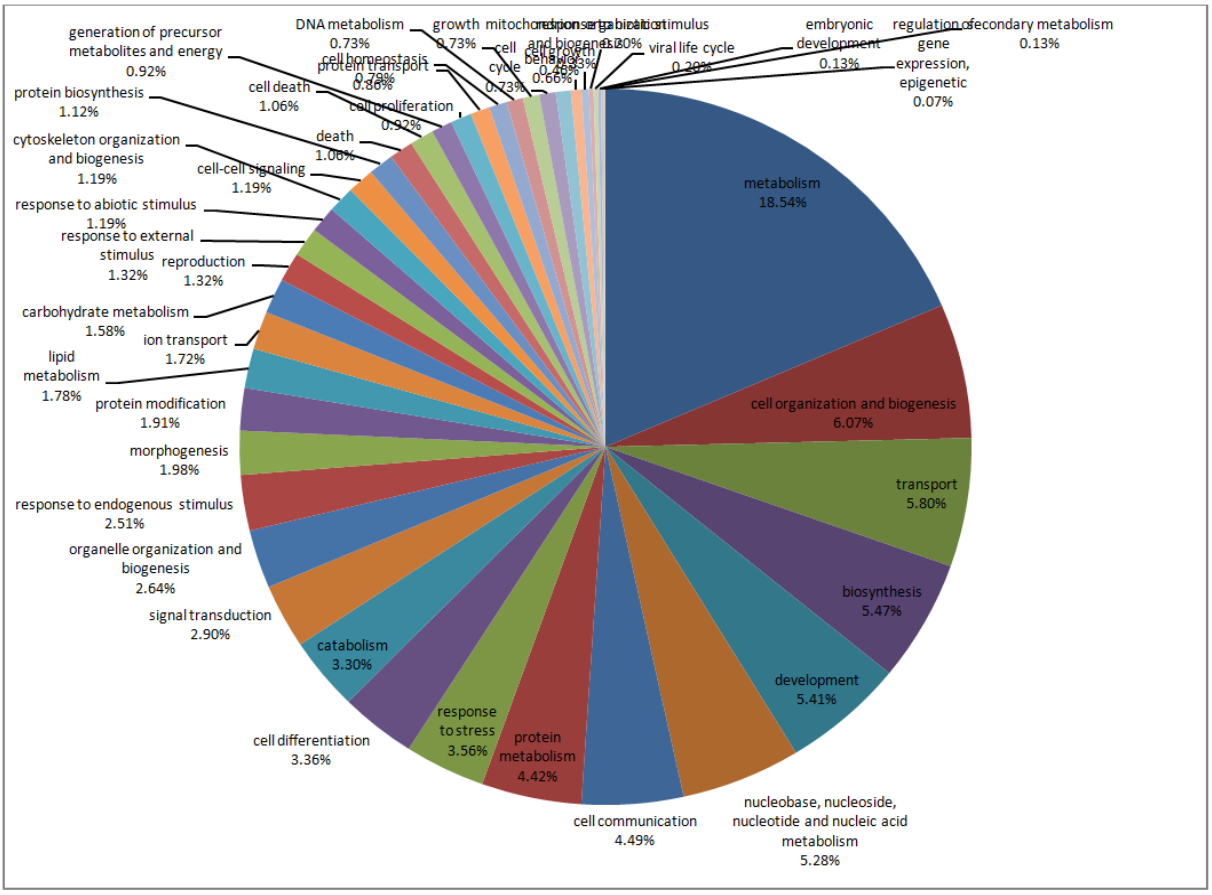

Figure 28. Gene Ontology designation of captured proteins from the neurogenic differentiation

Table 7 Proteins identified in neurogenic cells related to neurogenesis

Accession Number	GO ID	Protein Name	GO annotation
Q4QRB4	GO:0007411	Tubulin beta-3 chain	axon guidance
P70580	GO:0007411	Membrane-associated progesterone receptor component 1	axon guidance
Q3MID6	GO:0031103	Calumenin	axon regeneration
Q5U302	GO:0031103	Catenin alpha 1	axon regeneration
Q3MID6	GO:0007409	Calumenin	axonogenesis
O55012	GO:0007409	Phosphatidylinositol-binding clathrin assembly protein	axonogenesis
Q5U302	GO:0007409	Catenin	axonogenesis
Q63610	GO:0007420	Tropomyosin alpha-3 chain	brain development
P61751	GO:0007420	ADP-ribosylation factor 4	brain development
P31044	GO:0007420	Phosphatidylethanolamine-binding protein 1	brain development
P30904	GO:0007420	Macrophage migration inhibitory factor	brain development
O35264	GO:0007420	Platelet-activating factor acetylhydrolase IB subunit beta	brain development
P07335	GO:0007420	Creatine kinase B-type	brain development
P17764	GO:0007420	Acetyl-CoA acetyltransferase, mitochondrial	brain development
P13668	GO:0007420	Stathmin	brain development
O35263	GO:0007420	Platelet-activating factor acetylhydrolase IB subunit gamma	brain development
Q66HL0	GO:0007420	5' nucleotidase, ecto	brain development
Q6TXF3	GO:0007420	LRRGT00046	brain development
B2GV06	GO:0007420	Succinyl-CoA:3-ketoacid coenzyme A transferase 1, mitochondrial	brain development
P30904	GO:0002035	Macrophage migration inhibitory factor	brain renin-angiotensin system
O35567	GO:0003360	Bifunctional purine biosynthesis protein PURH	brainstem development
Q63610	GO:0007420	Tropomyosin alpha-3 chain	brain development
Q6P6V0	GO:0043524	Glucose-6-phosphate isomerase	negative regulation of neuron apoptosis
Q99J82	GO:0043524	Integrin-linked protein kinase	negative regulation of neuron apoptosis
P61589	GO:0045665	Transforming protein RhoA	negative regulation of neuron differentiation
F1LRG5	GO:0010977	Galectin-1	negative regulation of neuron projection development
P47875	GO:0007399	Cysteine and glycine-rich protein 1	nervous system development
Q9WTT7	GO:0007399	Basic leucine zipper and W2 domain-containing	nervous system development

		protein 2	
Q8K1M8	GO:0007399	Protein FAM5B	nervous system development
P82995	GO:0001764	Heat shock protein HSP 90-alpha	neuron migration
Q91Y81	GO:0031175	Septin-2	neuron projection development
Q9Z270	GO:0031175	Vesicle-associated membrane protein-associated protein A	neuron projection development
P62332	GO:0031175	ADP-ribosylation factor 6	neuron projection development
Q9ER24	GO:0031175	Ataxin-10	neuron projection development
Q3MID6	GO:0048812	Calumenin	neuron projection morphogenesis
P61589	GO:0048812	Transforming protein RhoA	neuron projection morphogenesis
O55012	GO:0048812	Glucose-6-phosphate isomerase	neuron projection morphogenesis
Q99J82	GO:0048812	Integrin-linked protein kinase	neuron projection morphogenesis
Q5U302	GO:0048812	Catenin	neuron projection morphogenesis
F1LPC3	GO:0007218	Cadherin EGF LAG seven-pass G-type receptor 3	neuropeptide signaling pathway
F1MAS4	GO:0007218	Uncharacterized protein	neuropeptide signaling pathway
D3ZF17	GO:0007218	Protein LOC689257	neuropeptide signaling pathway
D4A687	GO:0007218	Protein Bai2	neuropeptide signaling pathway
O88767	GO:0043526	Protein DJ-1	neuroprotection
P22734	GO:0042135	Catechol O-methyltransferase	neurotransmitter catabolic process
P47875	GO:0007399	Cysteine and glycine-rich protein 1	nervous system development
P61589	GO:0043525	Transforming protein RhoA	positive regulation of neuron apoptosis
P05982	GO:0043525	NAD(P)H dehydrogenase [quinone] 1	positive regulation of neuron apoptosis
P39069	GO:0014042	Adenylate kinase isoenzyme 1	positive regulation of neuron maturation
P19804	GO:0010976	Nucleoside diphosphate kinase B	positive regulation of neuron projection development
Q05982	GO:0010976	Nucleoside diphosphate kinase A	positive regulation of neuron projection development
P30904	GO:0010976	Macrophage migration inhibitory factor	positive regulation of neuron projection development
F1LRG5	GO:0045664	Galectin-1	regulation of neuron differentiation
P61983	GO:0045664	14-3-3 protein gamma	regulation of neuron differentiation
P19804	GO:0045664	Nucleoside diphosphate kinase B	regulation of neuron differentiation
Q05982	GO:0045664	Nucleoside diphosphate kinase A	regulation of neuron differentiation
P47942	GO:0045664	Dihydropyrimidinase-related protein 2	regulation of neuron differentiation
P30904	GO:0045664	Macrophage migration inhibitory factor	regulation of neuron differentiation
P61589	GO:0045664	Transforming protein RhoA	regulation of neuron differentiation
P01830	GO:0045664	Thy-1 membrane glycoprotein	regulation of neuron differentiation
Q62920	GO:0045664	PDZ and LIM domain protein 5	regulation of neuron differentiation

P39069	GO:0045664	Adenylate kinase isoenzyme 1	regulation of neuron differentiation
P62332	GO:0045664	ADP-ribosylation factor 6	regulation of neuron differentiation
Q99J82	GO:0045664	Integrin-linked protein kinase	regulation of neuron differentiation
Q62639	GO:0048168	GTP-binding protein Rheb	regulation of neuronal synaptic plasticity
P31044	GO:0001505	Phosphatidylethanolamine-binding protein 1	regulation of neurotransmitter levels
Q6P9Y4	GO:0001505	ADP/ATP translocase 1	regulation of neurotransmitter levels
P22734	GO:0001505	Catechol O-methyltransferase	regulation of neurotransmitter levels

Table 8 Proteins identified in neurogenic cells related to stress response

Accession Number	GO ID	Protein Name	GO annotation
P07150	GO:0034599	Annexin A1	cellular response to oxidative stress
P19804	GO:0034599	Nucleoside diphosphate kinase B	cellular response to oxidative stress
P30904	GO:0034599	Macrophage migration inhibitory factor	cellular response to oxidative stress
O35244	GO:0034599	Peroxiredoxin-6	cellular response to oxidative stress
O88767	GO:0034599	Protein DJ-1	cellular response to oxidative stress
Q6LDS4	GO:0034599	Superoxide dismutase [Cu-Zn]	cellular response to oxidative stress
P07895	GO:0034599	Superoxide dismutase [Mn], mitochondrial	cellular response to oxidative stress
F1LRG5	GO:0033555	Galectin-1	multicellular organismal response to stress
P22734	GO:0033555	Catechol O-methyltransferase	multicellular organismal response to stress
O55171	GO:0033555	Acyl-coenzyme A thioesterase 2, mitochondrial	multicellular organismal response to stress
P14600	GO:0033555	Substance-P receptor	multicellular organismal response to stress
P04906	GO:0032873	Glutathione S-transferase P	negative regulation of stress-activated MAPK cascade
P62963	GO:0051496	Profilin-1	positive regulation of stress fiber assembly
P63039	GO:0006979	60 kDa heat shock protein, mitochondrial	response to oxidative stress
P07150	GO:0006979	Annexin A1	response to oxidative stress
P04906	GO:0006979	Glutathione S-transferase P	response to oxidative stress
P23928	GO:0006979	Alpha-crystallin B chain	response to oxidative stress
P19804	GO:0006979	Nucleoside diphosphate kinase B	response to oxidative stress
P04642	GO:0006979	L-lactate dehydrogenase A	response to oxidative stress

		chain	
P31044	GO:0006979	Phosphatidylethanolamine-binding protein 1	response to oxidative stress
P30904	GO:0006979	Macrophage migration inhibitory factor	response to oxidative stress
O35244	GO:0006979	Peroxiredoxin-6	response to oxidative stress
O88767	GO:0006979	Protein DJ-1	response to oxidative stress
Q6LDS4	GO:0006979	Superoxide dismutase [Cu-Zn]	response to oxidative stress
P07895	GO:0006979	Superoxide dismutase [Mn], mitochondrial	response to oxidative stress
F1LM16	GO:0006979	Plasminogen activator inhibitor 1	response to oxidative stress
Q63716	GO:0006979	Peroxiredoxin-1	response to oxidative stress
Q9WUC4	GO:0006979	Copper transport protein ATOX1	response to oxidative stress
D3ZQI1	GO:0006979	Glutathione peroxidase	response to oxidative stress
P02454	GO:0006979	Collagen alpha-1(I) chain	response to oxidative stress
Q6AXM8	GO:0006979	Serum paraoxonase/arylesterase 2	response to oxidative stress
P04041	GO:0006979	Glutathione peroxidase 1	response to oxidative stress
P05982	GO:0006979	NAD(P)H dehydrogenase [quinone] 1	response to oxidative stress
Q9QXK0	GO:0006979	Signal transducer and activator of transcription 1	response to oxidative stress
Q924S5	GO:0006979	Lon protease homolog, mitochondrial	response to oxidative stress
P63039	GO:0006979	60 kDa heat shock protein, mitochondrial	response to oxidative stress
P34058	GO:0009651	Heat shock protein HSP 90-beta	response to salt stress
P82995	GO:0009651	Heat shock protein HSP 90-alpha	response to salt stress
Q9QXQ0	GO:0006950	Alpha-actinin-4	response to stress
F1LRG5	GO:0006950	Galectin-1	response to stress
P63039	GO:0006950	60 kDa heat shock protein, mitochondrial	response to stress
P01026	GO:0006950	Complement C3	response to stress
P55063	GO:0006950	Serum paraoxonase/arylesterase 2	response to stress
P07150	GO:0006950	Annexin A1	response to stress
Q66HD0	GO:0006950	Endoplasmin	response to stress
P34058	GO:0006950	Heat shock protein HSP 90-beta	response to stress
P82995	GO:0006950	Heat shock protein HSP 90-alpha	response to stress
P04906	GO:0006950	Glutathione S-transferase P	response to stress
P05065	GO:0006950	Fructose-bisphosphate aldolase A	response to stress
Q6IN22	GO:0006950	Cathepsin B	response to stress
P23928	GO:0006950	Alpha-crystallin B chain	response to stress
P19804	GO:0006950	Nucleoside diphosphate kinase B	response to stress
P61751	GO:0006950	ADP-ribosylation factor 4	response to stress

P04642	GO:0006950	L-lactate dehydrogenase A chain	response to stress
P31044	GO:0006950	Phosphatidylethanolamine-binding protein 1	response to stress
P26772	GO:0006950	10 kDa heat shock protein, mitochondrial	response to stress
P67779	GO:0006950	Prohibitin	response to stress
P11884	GO:0006950	Aldehyde dehydrogenase, mitochondrial	response to stress
P30904	GO:0006950	Macrophage migration inhibitory factor	response to stress
O35244	GO:0006950	Peroxiredoxin-6	response to stress
Q3MID6	GO:0006950	Calumenin	response to stress
O88767	GO:0006950	Protein DJ-1	response to stress
Q6LDS4	GO:0006950	Superoxide dismutase [Cu-Zn]	response to stress
P61589	GO:0006950	Transforming protein RhoA	response to stress
P80254	GO:0006950	D-dopachrome decarboxylase	response to stress
P07895	GO:0006950	Superoxide dismutase [Mn], mitochondrial	response to stress
P07943	GO:0006950	Aldose reductase	response to stress
P52944	GO:0006950	PDZ and LIM domain protein 1	response to stress
P08699	GO:0006950	Galectin-3	response to stress
Q63617	GO:0006950	Hypoxia up-regulated protein 1	response to stress
P13084	GO:0006950	Nucleophosmin	response to stress
F1LM16	GO:0006950	Plasminogen activator inhibitor 1	response to stress
O88600	GO:0006950	Heat shock 70 kDa protein 4	response to stress
Q63321	GO:0006950	Procollagen-lysine,2-oxoglutarate 5-dioxygenase 1	response to stress
P11232	GO:0006950	Thioredoxin	response to stress
D3ZQR7	GO:0006950	Procollagen-lysine,2-oxoglutarate 5-dioxygenase 2	response to stress
P97519	GO:0006950	Hydroxymethylglutaryl-CoA lyase, mitochondrial	response to stress
Q00238	GO:0006950	Intercellular adhesion molecule 1	response to stress
Q63716	GO:0006950	Peroxiredoxin-1	response to stress
Q9EQX9	GO:0006950	Ubiquitin-conjugating enzyme E2 N	response to stress
Q9WUC4	GO:0006950	Copper transport protein ATOX1	response to stress
D3ZQI1	GO:0006950	Glutathione peroxidase	response to stress
Q5FVM4	GO:0006950	Non-POU domain-containing octamer-binding protein	response to stress
P0C5H9	GO:0006950	Mesencephalic astrocyte-derived neurotrophic factor	response to stress
P11608	GO:0006950	ATP synthase protein 8	response to stress
P02454	GO:0006950	Collagen alpha-1(I) chain	response to stress
P17764	GO:0006950	Acetyl-CoA acetyltransferase, mitochondrial	response to stress
Q6NT88	GO:0006950	Cold inducible RNA binding protein	response to stress

Q07009	GO:0006950	Calpain-2 catalytic subunit	response to stress
Q6AXM8	GO:0006950	Serum paraoxonase/arylesterase 2	response to stress
P04041	GO:0006950	Glutathione peroxidase 1	response to stress
P22734	GO:0006950	Catechol O-methyltransferase	response to stress
P05982	GO:0006950	NAD(P)H dehydrogenase [quinone] 1	response to stress
O55171	GO:0006950	Acyl-coenzyme A thioesterase 2, mitochondrial	response to stress
Q9QXK0	GO:0006950	Signal transducer and activator of transcription 1	response to stress
P16975	GO:0006950	SPARC	response to stress
Q5U302	GO:0006950	Catenin (Cadherin associated protein), alpha 1	response to stress
P23928	GO:0051403	Alpha-crystallin B chain	stress-activated MAPK cascade
P23928	GO:0031098	Alpha-crystallin B chain	stress-activated protein kinase signaling cascade
P61589	GO:0031098	Transforming protein RhoA	stress-activated protein kinase signaling cascade
P07943	GO:0031098	Aldose reductase	stress-activated protein kinase signaling cascade

A number of interesting neuronal related proteins were identified some of which have been annotated as neurotrophic factors for example fibronectin, vimentin, vinculin, peroxiredoxin, astrocytic phosphoprotein, mesencephaolic astrocyte-derived neurotrophic factor, brain acid soluble protein, β-Tubulin 3, gamma-enolase and neudesin of which the final three are widely used neurogenic markers [28, 44, 104, 195, 196, 274, 301, 353, 354]. The appearances of the above proteins are noteworthy bringing further evidence of the neurogenic potential of ADSCs and have deemed the neurogenic differentiation laudable for further investigation. On the other hand the range of shock and stress related proteins were deemed reasonably significant which also warrants further investigation. The expression and variation of stress related proteins and neurotrophic proteins are an important study that will be required in the assessment of the produced cells clinical value. This can only be determined by evaluation of all the captured and identified proteins being actively expressed during the differentiation.

This differentiation has been previously utilised by a number of researches that have presented valuable insights to some of the markers presented as well as some electrophysiological data. There

is still a varying amount of conjecture surrounding the extent of differentiation that the ADSCs are capable of in the presence of BME containing differentiating conditions

2.5.0 CONCLUSION

This preliminary research into the characterisation of differentiated ADSCs by proteomic methodologies has presented ADSCs are indeed capable of differentiating into a variety of cell types of osteogenic, chondrogenic, neurogenic, myogenic and adipogenic. All of which present unique 2DE proteomic profiles. In terms of the methodologies utilised, whilst a visual inspection is useful for identifying uniquely expressed proteins in gels that have qualitative and to a certain degree quantitative differences in protein expression, without the use of expensive robotics it becomes difficult and vastly time consuming to analyse every protein spot for identification over such a vast array of differentiation samples. As such, the whole captured proteome was then fractionated by 1D SDS-PAGE, extracted and tryptically digested for investigation by LC-MS/MS. From the utilised methods, a variety of alternate differentiation specific molecules were identified. The major limitation of this analysis is the high percentage of similarity between ADSCs, osteogenic and osteoblasts. The differences may only be noted with a higher sensitivity methodology or instrument such as iTRAQ, SRM, targeted immunofluoresence microscopy. As such the iTRAQ method was employed however the results combined were of no use due to a non-specific precipitation of proteins. The exorbitant price and time required to repeat and prepare the cell lines for iTRAQ analysis was far too high and as such the remainder of the project focused on the neurogenic potential of ADSCs.

The morphological and histological analyses of the produced cells are within current standing knowledge; the advancement in the field comes from the identification by LC-MS/MS of unique and shared molecules expressed by differentiated ADSCs and their primary counterparts such as osteoblasts and chondrocytes. Furthermore proteins identified as having conjunction roles in the

development of mature differentiated cells, for example neuronal, are also beneficial for the identification of the extent of differentiation.

For future studies the detection limitation can be overcome by utilising advanced methods such as iTRAQ and instruments with a higher sensitivity to detect the further changes occurring below the QSTAR Elite capabilities. Furthermore the for the further significance for the detected molecules in differentiated ADSCs a switch to human cells would be beneficial to relate the produced cells for a clinical setting.

Chapter 3

Proteomic analysis of human adipose derived stem cells during *in vitro* neuronal differentiation with β-mercaptoethanol

3.1.0 INTRODUCTION

Regenerative and translational medicine is a rapidly expanding area made possible by the availability of an abundant source of adipose derived stem cells (ADSCs) from lipoaspirates, and the less abundant bone marrow derived stem cells (BMSCs) and induced pluripotent stem cells (iPSCs). The mounting understanding of regenerative therapies in osteogenesis and chondrogenesis has increased interest in transdifferentiation of the various sources of stem cells for autologous transplants and therapy development [355-357]. Not surprisingly, neuronal regeneration and repair therapies has accumulated great interest because of its potential to reverse injuries that have severe effects on quality of life and is thus a broadly investigated area [202, 351, 358, 359].

The generation of differentiated neuronal cells from progenitor stem cells has been attempted by a number of researchers over the last decade [28, 104, 296, 360]. Several have reported the successful passage of ADSCs and BMSCs, *in vitro* and *in vivo*, in the presence of simple chemicals and/or growth factors to rapidly differentiate morphologically toward a neuronal linage. The resultant cell populations have been shown to express morphological and protein surface marker identities consistent with that seen in primary derived neuronal tissue and cultured neuronal cell lines.

ADSCs and BMSCs have been treated with a number of simple chemicals such has BME [28, 104, 196], retinoic acid (RA) [204] , DMSO [350, 351] and BHA. Each chemical induced similar morphological changes over time in the MSCs, which ultimately present varying degrees of similarity to primary astrocytic and oligodendritic neuronal-like cells.

BME is a reducing agent and has been shown to be toxic to certain cell types when presented in concentrations higher than the µmolar range [361]. The potential for BME to be used as an inducing agent for neuronal differentiation has been studied in a limited capacity [28, 104] and shown to rapidly cause differentiation into cells presenting neuronal morphologies within 24 hours of induction [28, 104, 196, 257]. Consistent with these morphological changes, BME induced MSCs

have been noted to express neuronal specific markers such as NSE, β-βT3, GFAP, S-100 and Neudesin (NENF) [28, 104, 196, 257].

However, determining the functionality of the produced cells has proved to be much more difficult. The function of BME transdifferentiated cells or the ability of the produced cells to conduct an action potential is of great significance. This functionality would invariably prove the cells produced are terminally differentiated neurons. Barnabé *et al* [196] conducted patch clamping to detect the Na^+ and K^+ currents to determine electrophysiological potential. The assays revealed that the produced cells did not show evidence of Na^+ or K^+ currents nor the ability to fire action potentials. Furthermore they claim that a disruption of the redox circuitry affects the biochemical pathways resulting in cellular damage which manifests as cytoskeletal modifications and the loss of ion-gate function that ultimately causes cell death [196]. If the cells are extensively damaged and do not express the appropriate mechanisms, in terms of the numerous functional proteins, to conduct action potentials at the final differentiation time point, the cells will not be clinically useful. While the extended exposure to such chemicals may damage the MSCs, a time-limited treatment may be sufficient to initiate the differentiation process. Therein remains a void in the field regarding the proteomic characterisation of the produced cells relative to their mature counterparts. Whilst the cells have been noted and published to produce a range neuronal proteins and markers by chemical and growth factor induction, the extent of their differentiation has not been characterised. Examining the proteomic profiles will allow a complete comparative measurement of the extent of biological change through the differentiation process. Although the cells have produced a subset of desired physical and limited surface markers determined by IFM [362, 363], there is a lack of evidence of the extent of differentiation of MSCs toward neuronal cells. The examination these cells at the proteome level to investigate the complex fluctuation of proteins of differentiating MSCs in the presence of the somewhat toxic chemical cocktail must be performed.

In this study, we found that human ADSCs, when treated with BME, could be induced toward a neuronal-like lineage within 24 hours, presenting the morphological and surface chemistries as per previous publications. We also found the total acquired soluble proteome of ADSCs differentiated for 12 hours and 24 hours to be quite different from basal ADSCs and control Glioblastoma cells (GBCs), expressing a number of remodelling, neuroprotective and neuroproliferative proteins. However there are also a number of stress and shock related proteins that have also been up regulated and a large down regulation of structural proteins. The cytokine profiles furthermore present evidence of a large cellular remodelling shift as well cellular distress. However the vast loss of cell population, drastically decreased cytokine profiles and stress proteins reveal that this chemical induction may not be suitable for a clinical application as a number of the mechanisms and stress proteins convey that the cells are in trauma whilst producing neuronal morphologies.

3.2.0 Materials and Methods

3.2.1 Cell culture

3.2.1.1 Human adipose derived stem cells harvest and cell culture

This research was approved by the Macquarie University human research ethics committee (Ref #: 5201100385). Adult ADSCs were derived from lipoaspirates and subsequent steps were conducted under sterile conditions in a class II laminar flow hood (Clyde-Apac BH2000 series). Lipoaspirates were rinsed twice in Dulbecco's Modified Eagle's Medium (D-MEM, Gibco). The sample was then minced with a pair of scissors briefly till a fine slurry was formed and the connective tissue digested with collagenase type 1 (Gibco) for 45 minutes at 37 ^{o}C. The suspension was then centrifuged at 1600 x g for 10 minutes at 4^{o} C to separate adipocytes from the SVF. Three layers are seen above the pellet. The upper most layer is the free lipid and appears as a clear/white colour, the middle layer is a very small portion of undigested adipose, and the lower layer a red digestion solution. These layers were carefully decanted to leave the pellet containing a variety of cell types. The pellet was resuspended in 3 ml of D-MEM and layered on top of 3 ml of Ficoll Paque PLUS (Sigma-Aldrich).

Centrifugation at 1600 x g for 20 minutes was performed to remove red blood cells from the SVF. The ADSCs were then removed from the interface between the Ficoll and D-MEM. 8ml of D-MEM was then added to dilute residual Ficoll. The cells were washed twice in D-MEM and centrifuged at 1000 x g for 10 minutes. Upon completion of the final wash, the pellet is resuspended in D-MEM Glutmax/F12 (Gibco) with 10% FBS (Invitrogen) and 1% ABAM (Invitrogen). 2 mL of the suspension was then aliquoted into a T25 culture flask (Nunc) and incubated at 37^{o} C at 5% CO_2 for 48 hours until ADSCs adhered to the culture flask. Non-adherent cells are eliminated by replacing the media. ADSCs were passaged 3-5 times by stripping cells with TrypLE Express (12604 Gibco) before utilised in differentiation experiments.

3.2.1.2 Chemical induction for differentiation

Subconfluent ADSCs were washed twice in pre-warmed sterile D-MEM/F12 (Invitrogen). The cells were then cultured for a further 24 hours in a serum-free pre-induction medium consisting of D-MEM/F12 (Invitrogen), ABAM (Invitrogen) and 1mM β-mercaptoethanol (Sigma). The media was then replaced after 24 hrs with the neural inducing media consisting of D-MEM/F12 (Invitrogen), ABAM (Invitrogen) and 10mM β-mercaptoethanol (Sigma) as per Woodbury *et al*., (2000).

3.2.1.3 Glioblastoma Cell culture

GBCs line (NCH612 Cell Line Service, Germany) were cultured in Neurobasal media supplemented with B27 and 0.5 mM Glutamine (Gibco). The cells were grown to 90% confluence prior to passaging or harvesting for proteomics.

3.2.2 Microscopy

3.2.2.1 Cell counts

In vitro cell counts were carried out utilising a novel procedure to determine the approximate colony forming units per square millimetre of cells adherent to the culture flask which were induced for differentiation and subsequently utilised for proteomics. A grid of squares 2.5 mm x 2.5 mm was printed on a transparent laminate and cut to fit outer bottom side of a T175 culture flask (BD Falcon). Spanning the temporal differentiation ten squares were chosen and cells counted at the

objective of 100X on an Olympus CK40 inverted microscope the cell counts from the ten squares were averaged for each flask to find a mean total cfu/mm^2. The cell numbers from the ten squares were averaged and then multiplied by 28000 (16*10*175) to find the total cell population in the T175 culture flask. To find cfu/mm^2 the average cell number from the ten squares were divided by 2.5 mm. At the final time point cells were removed from the culture flask and an aliquot was stained with trypan blue to determine live/dead ratio using a Neubauer chamber. The total cell number data was also utilised in the Bioplex analysis to determine the amount of cytokines secreted per cell. This was calculated by multiplying the concentration by the total volume of the flask and dividing by the total cell number at the respective time point.

3.2.2.2 Histological stains

Haematoxylin is basic stain that stains basophilic structures and is generally used as nuclei stain, producing a deep purple to blue colour. In conjunction with haematoxylin, eosin is used as a membrane counter stain which stains acidophilic structures red. Following general fixation in 4% formaldehyde slides with cells were flooded with haematoxylin [Sigma, H3136 haematoxylin 6 g, absolute alcohol 300 ml, distilled water 300 ml, glycerol 300 ml, glacial acetic acid 30 ml, ammonium or potassium aluminium sulphate 30 g and sodium iodate 0.9 g] for 5 minutes, rinsed in water for 30 seconds and the slide submerged in acid alcohol for 15 seconds to remove excess stain. This was followed by a 30 second rinse in water, submersion in Harris bluing agent [0.5% w/v sodium acetate in distilled water] for 2 minutes another rinse in water before counterstaining with Eosin Y (2% v/v in distilled water) for 30 seconds. The slide was then dehydrated by 30 second submersions in 75%, 95% and then 100% ethanol before the slide was sealed with clear xylene for 5 minutes followed by the addition of a coverslip. Stained cells were visualised on an Olympus IX51 inverted microscope and images captured with the attached Olympus DP70 camera.

3.2.3 Protein extraction

Culture media was decanted and the cells washed 2-3 times with sterile 1X PBS. Cells were harvested by treating cells with 3 ml TrypLE Express (12604 Gibco) for 10-15 minutes at 37^{o} C. Detached cells were rinsed and collected in 11 ml of sterile 1x PBS in a 15 ml falcon tube. Cells were centrifuged at 1000 rcf for 10 minutes to pellet. Supernatant was decanted and the cell pellet was resuspended in 100 µl of 1%SDS and transferred to 0.65 ml eppendorf tube and boiled for 10 minutes to lyse cell pellets. Lysates were centrifuged at 16000 rcf for 10 minutes to pellet debris. Supernatent was then buffer exchanged into 0.1% SDS with SCC Micro-Biospin columns (BioRad).

3.2.4 1D Electrophoresis

Samples were diluted 1:1 with LDS loading buffer (Invitrogen), heated at 95^{o} C for 10 minutes then centrifuged. Samples were then loaded into 4-12% Bis-Tris Criterion gel (BioRad) in XT-MES (BioRad) running buffer then electrophoresed according to the standard product protocol of 160 V for 50 minutes (BioRad). Upon completion of electrophoresis, unless required for western blot (see section 2.5), gels were placed in fix solution (40% methanol and 10% acetic acid) and incubated on a gentle rocker at room temperature for 60 minutes. Gels were then placed in Flamingo fluorescent protein stain (Biorad) and incubated for a further 60 minutes. Gels were imaged using a PharosFX Plus (Biorad) imager and Quantity One software (BioRad). The gel was then placed in Coomassie Blue G stain overnight, post staining a solution of 1% acetic acid to remove background stain. The gel was then scanned with an Epson Perfection 4800 document scanner.

3.2.5 Western blot

The Western blot method as adapted from Jobbins *et al*., 2010 [284], buffers were prepared as follows: 2 blot papers (BioRad) soaked in Buffer 1 [40mL 10X stock (400mM amino-caproic acid, 250mM Tris), 40mL methanol, 1mL 20% SDS, 400mL dH2O], 2 blot papers were soaked in Buffer 2 [20 mL 10X stock (250 mM Tris), 40mL methanol, 200mL dH2O] and 1 blot paper was soaked in Buffer 3 [10mL 10X stock (3 M Tris), 100mL dH2O]. Post 1D-SDS-PAGE of whole cell lysates as prepared in section 2.3, the gel was rinsed for 1 min in deionised water then equilibrated in buffer 1

for 5min. A piece of Polyvinylidene fluroride (PVDF) membrane (BioRad) was cut to the same dimensions as the gel and placed in methanol for 2min prior to equilibration in Buffer 2. The Western blot stack was assembled within an Owl HEP-1 Semi dry electroblotting cassette (Thermo Fisher Scientific) with Buffer 1 soaked papers at the cathode base, then the gel, PVDF membrane, Buffer 2 soaked papers, and lastly Buffer 3 soaked paper under the anode top. The stack was rolled to remove excess buffer and any potential air bubbles and run at 300mA for 30min. Once the gel was electrophoretically transferred, the membrane was washed in PBS with 0.1% Tween [BioRad, USA] for 20 minutes and then blocked with PBS, 0.1% Tween and 5% skim milk powder for 1hour to prevent non-specific antibody binding. The membrane was then placed in a solution containing the one of the following primary monoclonal antibodies: mouse anti-human NeuN/Fox3 (M377100 Biosensis 1:5000), mouse anti-human NF200 (M988100 Biosensis 1:500), rabbit anti-human ϐ-TUBBIII (ab18207 Abcam 1:1000) or rabbit anti-human GFAP (ab7260 Abcam 1:50000) diluted in PBS respectively and incubated overnight at 4^{o}C on a gentle rocker. Subsequently washed 3 times with PBS and probed with a secondary antibody either and anti-mouse IgG (A4416 Sigma) or anti-rabbit IgG (A4312 Sigma) dependant on the primary probe. Both secondary antibodies were alkaline phosphatase conjugated for development with 5-bromo-4-chloro-3-indolyl phosphate/nitro blue tetrazolium chloride (BCIP/NBT) (Sigma).

3.2.6 Bioplex

ADSCs and differentiation secretion samples were collected at time 0min as a control and at 30min, 1hr, 3hrs, 5hrs, 20hrs and 24hrs subsequent to adding the differentiation media for assay. Concentrations of IL-1ra, IL-1b, IL-2, IL-4, IL-5, IL-6, IL-7, IL-8, IL-9, IL-10, IL-12(p70), IL-13, IL-15, IL-17, Eotaxin, FGF basic, G-CSF, GM-CSF, IFN-γ, MCP-1, MIP-1a, MIP-1b, PDGF-bb, RANTES, TNF-α and vEGF were simultaneously evaluated using a commercially available multiplex bead-based sandwich immunoassay kits (Bioplex human 27-plex, M50-0KCAF0Y BioRad Laboratories). Assays were performed according to the manufacturer's instructions. Briefly, 27 distinct sets of fluorescently dyed beads loaded with capture monoclonal antibodies specific for each cytokine to be tested, were

used. Secretion samples (50 µl/well) or standards (50 µl/well) were incubated with 50 µl of pre-mixed bead sets into the wells of a pre-wet 96 well microtitre plate. After incubation and washing, 25 µl of fluorescent detection antibody mixture were added for 30 min and then the samples were washed and resuspended in assay buffer. High standard curves for each soluble factor were used, ranging from 2.00 to 32,000.00 pg/ml and the minimum detectable dose was <10 pg/ml. The formation of different sandwich immunocomplexes on distinct bead sets was measured and quantified using the Bioplex Protein Array System (BioRad Laboratories). A 50 µl volume was sampled from each well and the fluorescent signal of a minimum of 100 beads per region (chemokine/cytokine) was evaluated and recorded. Values presenting a coefficient of variation beyond 10% were discarded before the final data analysis [285].

3.2.7 iTRAQ

After cell lysis and protein extraction (Section 2.3) the total of 4 samples for iTRAQ labelling (1 – ADSCs, 2 - 12hr BME Differentiation hADSC, 3 - 24hr BME Differentiation hADSC and 4 - Glioblastoma control (GBCs)) were buffer exchanged in 0.1% SDS using a Tris free Micro Bio-Spin Chromatography Columns (BioRad) and made up to a final concentration of 60ug/100uL each. The labelling method and MS/MS run parameters are outlined below.

Instrument

Mass spectrometer: TripleTOF 5600 (AB Sciex). Nanoflow Liquid Chromatography system: Eksigent Ultra nanoLC system (Eksigent). Analytical column: SGE ProteCol C18, 300Å, 3µm, 150µm x 10 cm. Strong Cation eXchange (SCX) HPLC: Agilent 1100 quaternary HPLC system with Polysulfoethyl A 100mmx2.1mm 5um 200Å column.

Sample preparation

300 uL of 0.25M TEAB was added to each sample. The samples were then reduced with tris(2-carboxyethyl)phosphine (TCEP), alkylated with Methyl methanethiosulfonate (MMTS) and digested with trypsin. The digested samples were labelled according to the list below:

Sample name iTRAQ label

1 - 114 Basal hADSC

2 - 115 12hr BME Differentiation hADSC

3 - 116 24hr BME Differentiation hADSC

4 - 117 Glioblastoma control (GBCs)

Strong cation exchange HPLC

The labelled samples were fractionated by SCX HPLC. The buffer A was 5mM Phosphate 25% Acetonitrile, pH 2.7 and buffer B was 5mM Phosphate 350mM KCl 25% Acetonitrile, pH 2.7. The dried iTRAQ labelled sample was resuspended in buffer A. After sample loading and washing with buffer A, buffer B concentration increased from 10% to 45% in 70 minutes and then increased to 100% and remained at 100% for 10 minutes at a flow rate of 300 ul/min. The eluent was collected every 2 minutes at the beginning of the gradient and at precisely every 4 minutes interval thereafter.

NanoLC ESI MS/MS data acquisition

The SCX fractions were resuspended in 100 µL of loading/desalting solution (0.1% trifluoroacetic acid and 2% acetonitrile 97.9% water). Sample (40µL) was injected onto a peptide trap (Michrom peptide Captrap) for pre-concentration and desalted with 0.1% formic acid, 2% ACN, at 5 µL/min for 10 minutes. The peptide trap was then switched into line with the analytical column. Peptides were eluted from the column using a linear solvent gradient, with steps, from mobile phase A: mobile phase B (98:2) to mobile phase A:mobile phase B (65:35) where mobile phase A is 0.1% formic acid and mobile phase B is 90% ACN/0.1% formic acid at 600 nL/min over a 100 minute period. After peptide elution, the column was cleaned with 95% buffer B for 15 minutes and then equilibrated with buffer A for 25 minutes before the next sample injection. The reverse phase nanoLC eluent was subject to positive ion nanoflow electrospray analysis in an information dependant acquisition mode (IDA). In IDA mode a TOFMS survey scan was acquired (m/z 400 - 1500, 0.25 second), with the ten

most intense multiply charged ions (counts >150) in the survey scan sequentially subjected to MS/MS analysis. MS/MS spectra were accumulated for 200 milliseconds in the mass range m/z 100 – 1500 with the total cycle time 2.3 seconds.

3.2.8 Data processing

The experimental nanoLC ESI MS/MS data were submitted to ProteinPilot V4.0 (AB Sciex) for data processing using *Homo sapiens* species. Bias correction was selected. The detected protein threshold (unused ProtScore) was set as larger than 1.3 (better than 95% confidence). FDR (False discovery rate) Analysis was selected. Volcano plots, Gene ontology and Bioplex heat maps were generated using DanteR.

3.3.0 RESULTS

3.3.1 Microscopy

Human ADSCs (hADSCs) were cultured in a monolayer and passaged three times producing a morphologically homogenous culture with cells exhibiting the spindle-fibroblastic form consistent with current literature. The cells were maintained at sub-confluency prior to addition of differentiation media containing BME as per Woodbury *et al*., [104]. Figure 1 A-D shows the rate of cellular remodelling over a 24 hour period after the addition of the differentiation media. Basal ADSCs (Figure 1A) generally grow in a flat, large fibroblastic configuration. Within 3 hours (Figure 1B) of neuronal induction the morphological changes became evident with a number of cells showing signs of cytoplasmic retraction toward the nucleus of the cell. The now elongated membrane produced a firm and contracted bipolar or multi-polar configuration. At the 12 hour time point (Figure 1C) the cells morphological changes are ubiquitous across the cultured population with a majority of the cells presenting the retracted cytoplasm and multi-polar shape with evidence of extensions and processes reaching between cells. The cell bodies appear condensed and light refractive compared to the basal hADSCs. At the 24hour time point prior to harvesting, the cells have

a unique morphology compared to the basal state hADSCs with the majority of adherent cells producing polar extensions and processes reaching between cells with some evidence of detachment [109, 202]. In summary these cells morphologically appear to resemble neuronal cells.

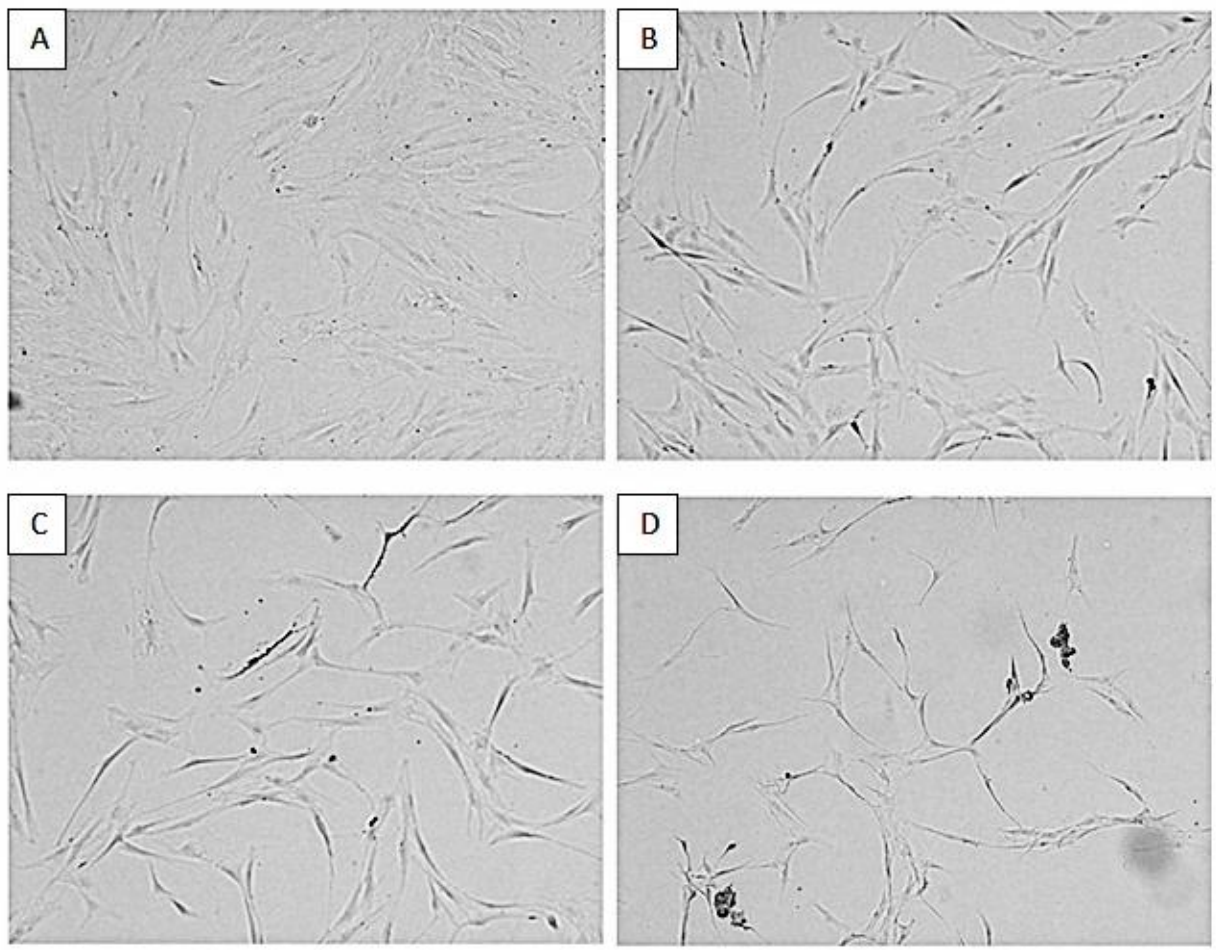

Figure 1 A: Basal human ADSCs cultured as a control prior to differentiation. B-D: hADSCs 3 hours, 12 hours and 24 hours after induction with neurodifferentiation media with the progressive structural remodelling over the 24 hour time period from large flat fibroblastic cells to long, multipolar highly refractive cells producing extensions and processes reaching between cells.

3.3.1.1 Cell Counts

The cell numbers from the ten squares were averaged and calculated to find the total cell population in the T175 culture flask. To find cfu/mm^2 the average cell number from the ten squares were divided by 2.5mm. The total cell count and average cfu/mm^2 trends are identical presenting no change in cell population in the triplicate flasks from basal cells up to 1hr post induction. The basal population counts averaged at 77 cfu/mm^2 or total population of 5.42E+06 cells. Subsequent to the BME treatment the population decreases by approximately 18% to 63cfu/mm^2 by the 5 hour time

point. After 20 hours the cell population decreases by 46%, to 35 cfu/mm^2, relative to the basal cells (Figures 2 and 3). Upon harvest of the final time point the total dead/live ratio was 1:9 i.e. an average of 10% of cells were stained blue with trypan.

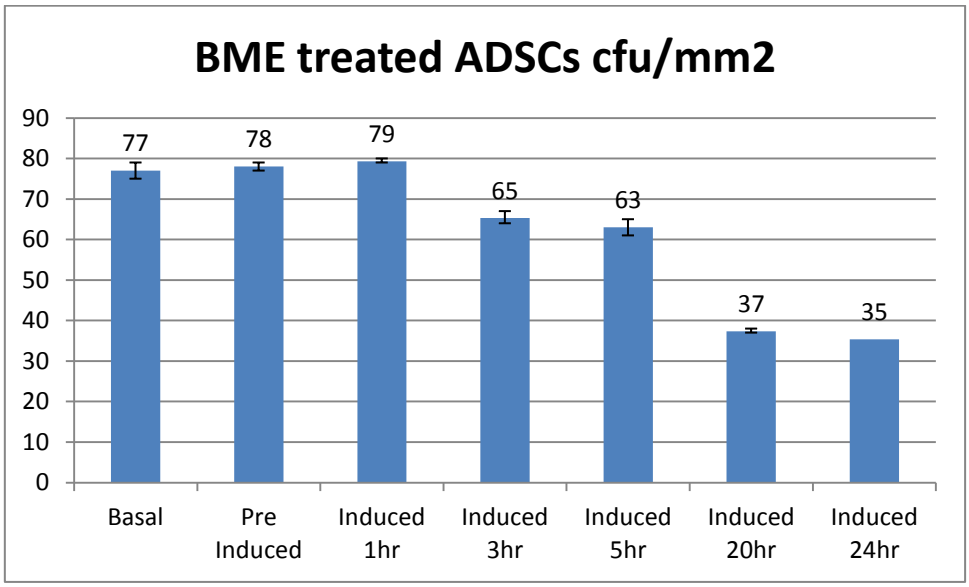

Figure 2 Average colony forming units per square millimetre of basal ADSCs and ADSCs treated with BME over 24 hours

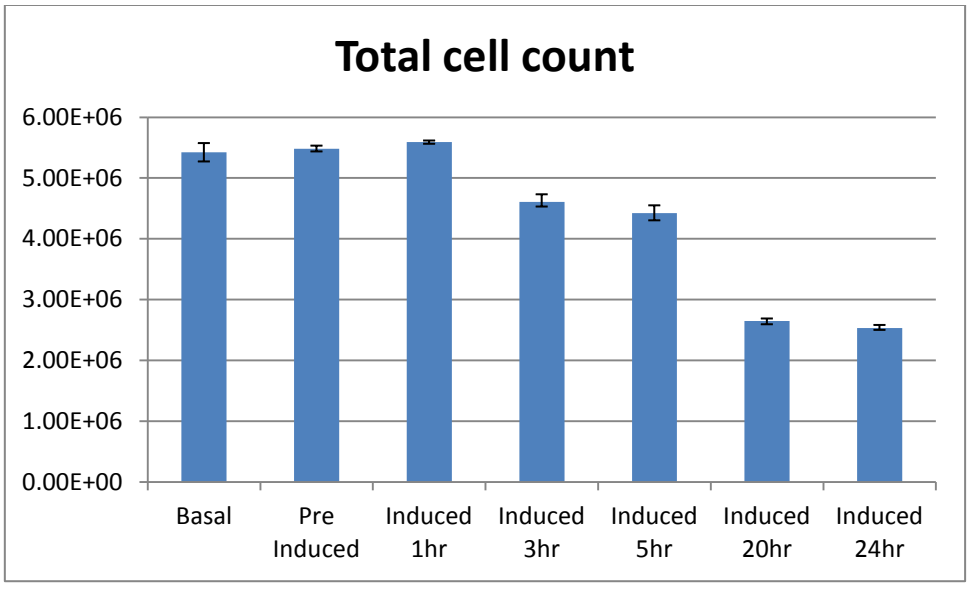

Figure 3 Average total cell count at each time point over the BME treatment of ADSCs

3.3.2 iTRAQ proteome comparisons of hADSCs, 12 hour, 24 hour differentiated and GBCs control

The digested proteins from each cell line were labelled with the iTRAQ isobaric tags as follows: hADSCs, 12 hour differentiated hADSCs, 24 hour differentiated hADSCs and GBCs labelled with 114, 115, 116 and 117 isobaric tags respectively. The protein fold changes between samples were done comparatively and are relative to a base denominator. The base denominator chosen for the majority of the analysis was the basal hADSCs -114, all comparisons were made relative to this, i.e. 115 vs 114, 116 vs 114 and 117 vs 114. This was done to elucidate the relative protein fold changes across the captured and labelled proteome of the differentiating cells, determining the up or down regulation of protein species over time during differentiation.

Table 1 summarises the iTRAQ results of basal hADSCs, hADSCs differentiated for 12 hours, hADSCs differentiated for 24 hours and a control GBCs cell line. The summary table shows the upper 99%, 95% and 66% cut off for detected proteins. The upper 95% range was chosen for all data analysis and, within that cutoff, a total of 2,568 proteins consisting 38,786 distinct peptides were identified from 171,862 spectra (appendix 2A). An average of 5.89 peptides was matched per protein with an average of 13.88% sequence coverage from the total cohort of the detected proteins. The total number of proteins identified by a single peptide match was 980 proteins from the 2,568 identified which is approximately 37% of identified proteins. The analysis cut off removed proteins with below the average peptides matched (i.e. 5 peptides/protein) to increase the robustness of the dataset and the conclusions drawn. The subsequent cut offs utilised were based on p-value (<0.05) and fold change ($\log_2$ <-0.2 or 0.2 >). These partitions refine the later analyses to statistically significant proteins which have an average of 20 matched peptides per protein. The ProteinPilot group file, the protein summaries and peptide summary (without background corrections) were exported to XML format for further analysis with specified denominators for inter-sample comparisons through the generation of volcano plots and gene ontology graphs.

Table 1 iTRAQ of ADSCs, ADSCs differentiated for 12hours and 24hours and Glioblastoma cells Protein Pilot results

Unused (conf) Cutoff	Proteins Detected	Proteins Before Grouping	Distinct Peptides	Spectra Identified	% total Spectra
>2.0 (99)	2203	2948	37370	169630	66.8
>1.3 (95)	2568	3505	38786	171862	67.7
>0.47 (66)	2886	5410	40209	173935	68.5
Cutoff applied: >0.05 (10%)	3760	16315	43347	178197	70.2

To visualise the up/down regulated proteins, volcano plots were generated showing P-values versus the $\log_2$ protein fold change of each experimental cell line vs. Basal hADSCs of all 2,568 proteins. The quantitation criteria cut off of significant protein fold changes were completed statistically with the students t-test at P-values of <0.05 and $\log_2$ fold change cut off of <-0.2 or >0.2. This found 2,418 proteins were directly comparable between any two sample types at a time (appendix 2D). The blue nodes outside the horizontal and vertical asymptotes represent the statistically significant changed proteins above > 0.2 log fold change up-regulated proteins and the below <0.2 fold change down-regulated proteins. The grey nodes represent the non-significantly changed proteins with a P-value >0.05 and within the cut off for fold change.

The number of statistically significant up and down regulated proteins from each fold comparisons between 12 hr differentiated vs ADSCs (115v114) revealed 81 up regulated and 171 down regulated (appendix 2A and 2F) proteins, comparisons between 24hr differentiated vs ADSCs (116v114) revealed 85 up regulated and 138 down regulated proteins, and comparisons between GBCs vs ADSCs (117v114) revealed 429 up regulated and 504 down regulated proteins (See volcano graphs in appendix 2D). A table of all of the above proteins is available in appendix 2A.

Figure 4 exhibits the ratio of statistically changed proteins across all samples compared to basal ADSCs in the form of a bar graph. The blue bar presents non-statistically significant changed proteins, red bar is the statistically significant up regulated proteins and green is the statistically significant down regulated proteins. The GBC line was utilised in place of human derived hippocampal neurons or Pheochromocytoma (PC12) cell line which are rare in comparison to the rat

counterparts that are routinely utilised in rodent based neuronal studies [354, 364]. The recommendations to use GBCs were due to their relative ease to culture *in vitro* compared to primary neuronal cells, furthermore the GBCs were considered to have adequate quantities of neuronal proteins for a comparison of differentiated stem cells with a neuronal phenotype. The relative quantitation shows that the ADSCs, the neurogenic induced and the GBCs share the same proteins but at varying regulations. While there are a very large percentage of proteins that remain statistically unchanged between the four cell types, the largest variance is seen in the comparison between the neurogenic and the GBCs, with approximately four times as many proteins up/down regulated in the latter. This has been suggested to be due to the maturity of the GBCs over the induced neurogenic cells.

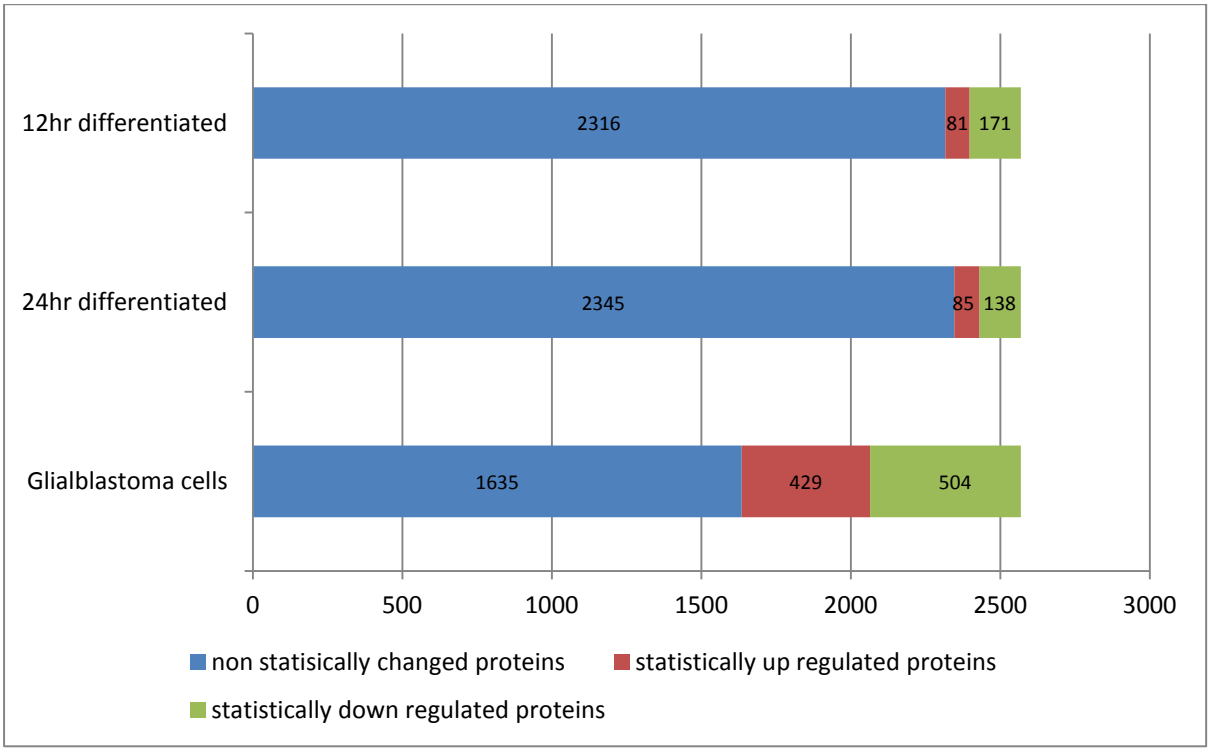

Figure 4. Bar graph shows the ratio of statistically changed proteins across all samples compared to basal ADSCs. Blue bar presents non-statistically significant changed proteins, red bar is the statistically significant up regulated proteins and green is the statistically significant down regulated proteins

The identified proteins in each treatment were grouped using GO annotation and categorised on the basis of molecular function and partitioned by up and down regulation into separate pie graphs

(figure 5A-F). The major categories of molecular functions of up regulated proteins identified in both 12 hour differentiation and 24 hour differentiation were metabolism, nucleobase metabolism, biosynthesis, cell organization and biogenesis, transport, development, cell organization, development and response to stress. The minor groups appearing as the partitioned section “other” contains functionally important proteins related to differentiation such as cell proliferation, morphogenesis, cell differentiation, cytoskeleton organization and biogenesis (appendix 2E).

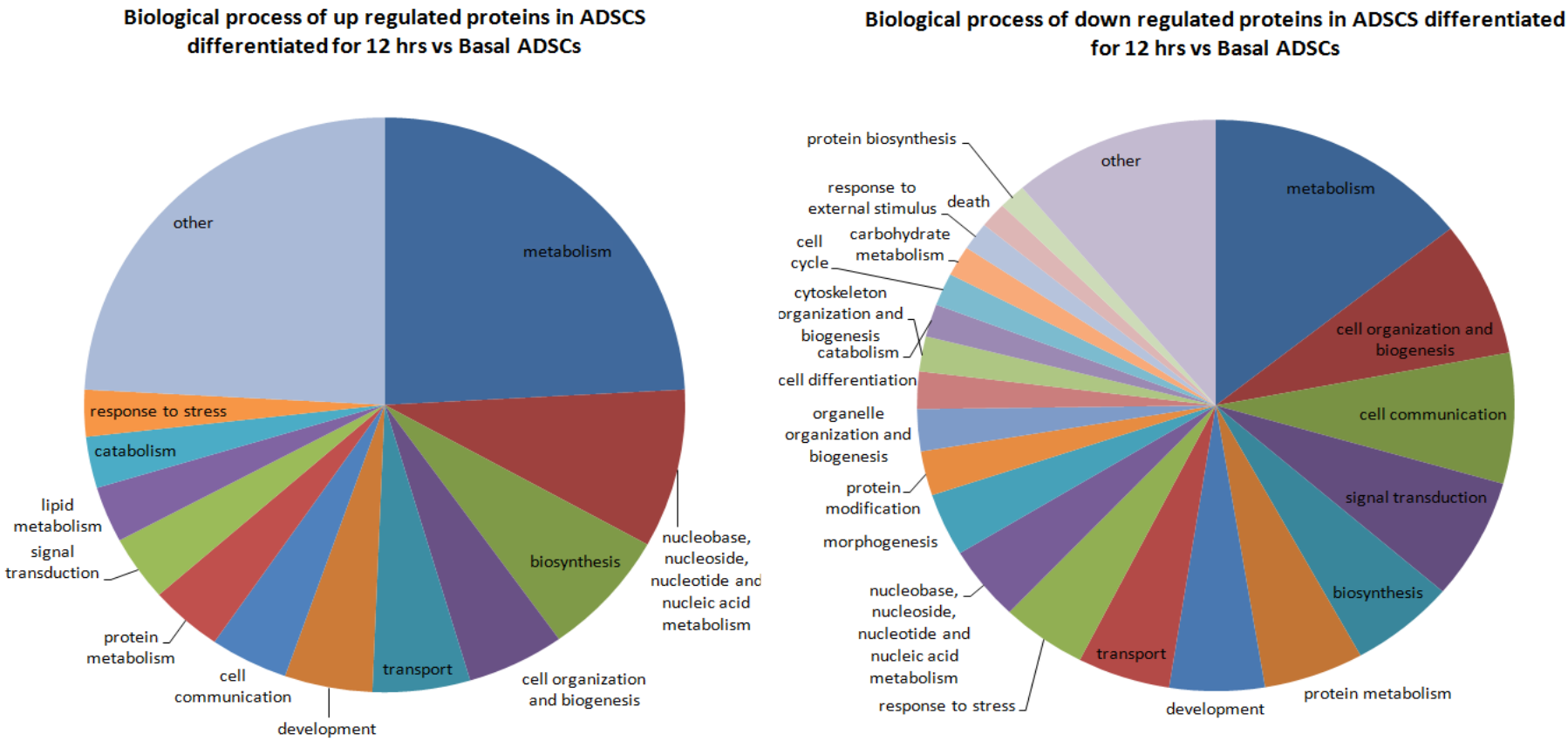

Figure 5 A and B Gene Ontology of biological process of A) up regulated proteins and B) down regulated proteins in ADSCs differentiated for 12 hrs vs Basal ADSCs.

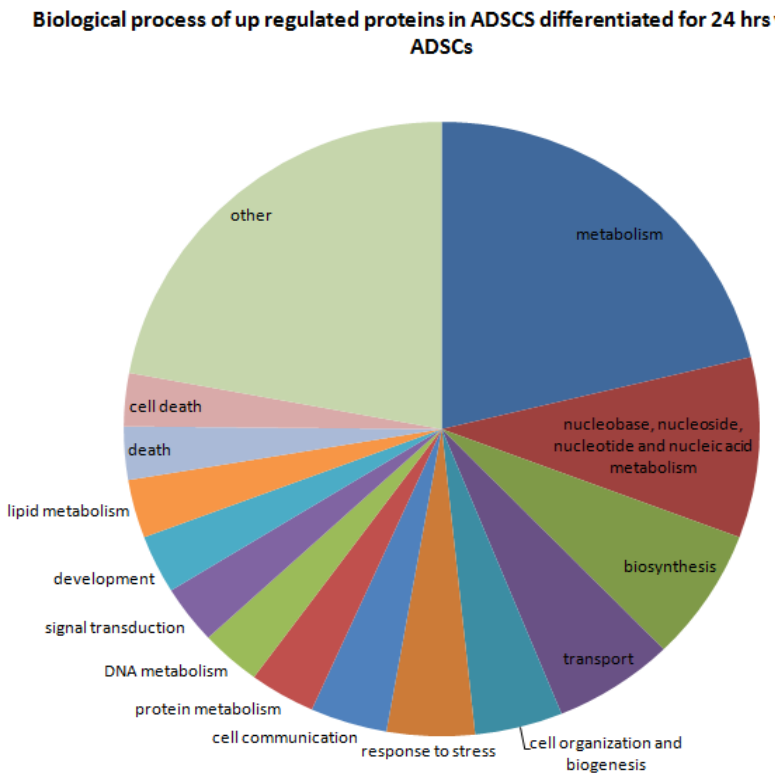

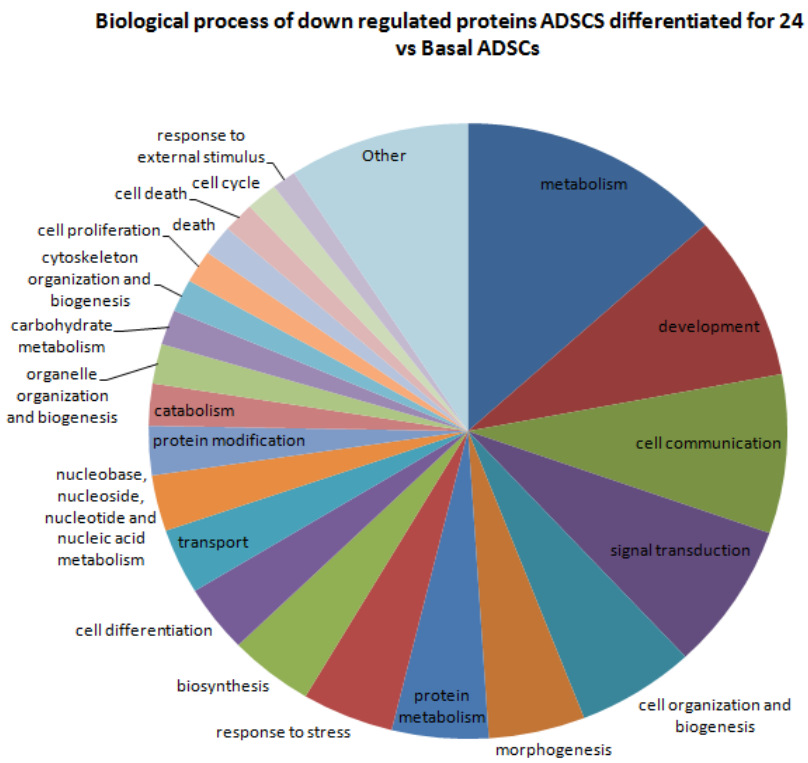

Figure 5 C and D Gene Ontology of biological process of C) up regulated proteins and D) down regulated proteins in ADSCs differentiated for 24 hrs vs Basal ADSCs.

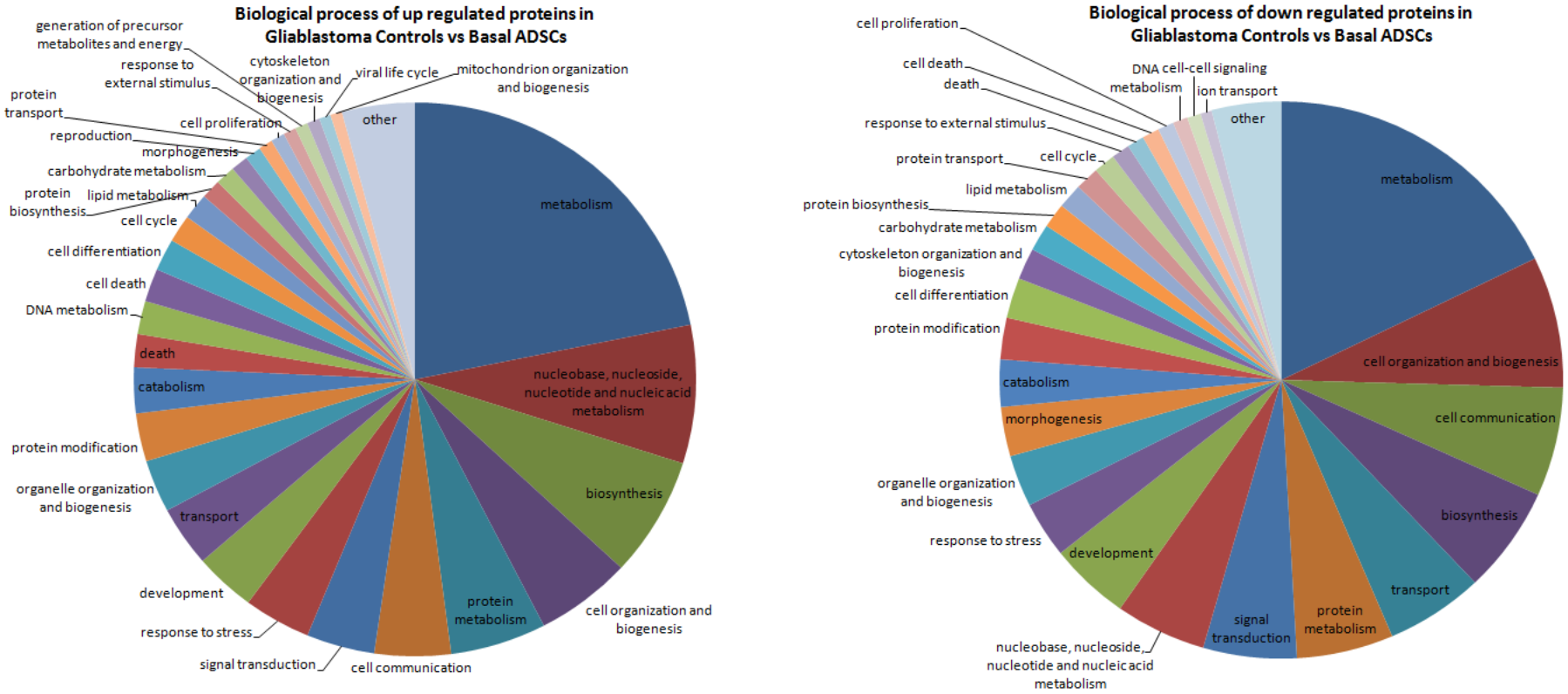

Figure 5 E and F Gene Ontology of biological process of E) up regulated proteins and F) down regulated proteins in Gliablastoma controls vs Basal ADSCs.

The statistically relevant identified proteins at the 12 hour differentiation time point comparison relative to ADSCs showed that 29 unique proteins were up regulated and 36 unique proteins were down regulated. At the 24 hour differentiation time point, 26 different unique proteins were identified in both the up and down regulated proteins respectively. The largest numbers of unique proteins were observable between the GBCs control with 357 up regulated proteins and 364 down regulated proteins. A subset of shared proteins between time points were also observed between the 12hr differentiated, 24 hr differentiated and the GBCs control; with 11, 32 and 25 proteins up regulated and 19, 27 and 50 down regulated respectively. Furthermore a group of 16 up regulated proteins were common to both differentiated time points and the GBC control and a group of 66 down regulated proteins were common to all three groups (Figure6). The Venn diagrams below show that the compared cells are different from the basal ADSCs. The statistically significant up and down regulated proteins are highlighted in appendix 2A which presents a data subset summary of 139 statistically significant up regulated proteins that were identified as unique or common between the 12 hour, 24 hour differentiation and GBC control from Venn diagrams (Figure 6).

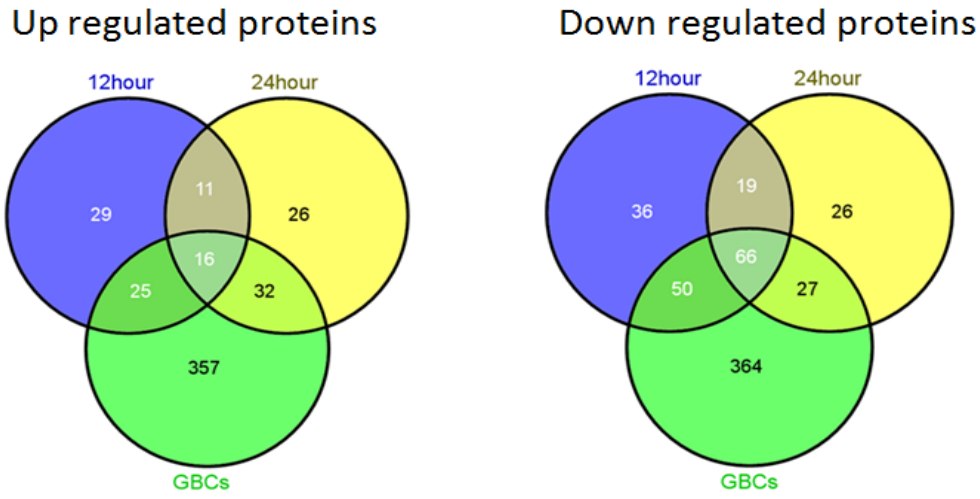

Figure 6. Three way Venn diagrams of up and down regulated proteins in the 12 hour differentiated, 24 hour differentiated hADSCs and the GBCs showing unique and shared proteins. 'A' shows up regulated proteins revealing there are 29, 26, 357 unique proteins with 11, 32 and 25 shared proteins between each of the corresponding tested cell lines as well as 16 shared proteins between all three relative to basal hADSCs. 'B' shows down regulated proteins revealing there are 36, 26, 364 unique proteins with 19, 27 and 50 shared proteins between each of the corresponding tested cell lines as well as 66 shared proteins between all three relative to basal hADSCs.

Table 2 presents the statistically significant proteins unique to each differentiation time point related to neurogenesis by cell proliferation, cell differentiation, morphogenesis, cytoskeleton remodelling or response to stress or shock by function according to GO biological processes. The mutual expression of neurogenic and stress related proteins indicates the cells are experiencing a directed push toward a phenotype expressing neuronal proteins however the stress proteins indicate that the chemical differentiation is traumatic to the cells and is damaging them throughout the process.

Table 2 Statistically significant neuronal and stress proteins expressed by induced stem cells at 12 and 24 hrs.

	Accession number	**Name**		**Accession number**	**Name**
	Neurogenic related proteins			Stress and Shock related proteins	
12 hour Unique proteins	Q09666	Neuroblast differentiation-associated protein		P09601	Heme oxygenase
	O94925	Glutaminase		P48507	Glutamate--cysteine ligase regulatory subunit
	P12111	Collagen alpha-3(VI) chain		P11413	Glucose-6-phosphate 1-dehydrogenase
	A1X283	SH3 and PX domain-containing protein 2B			
24 hour unique proteins	P23219	Prostaglandin G/H synthase 1		P23219	Prostaglandin G/H synthase 1
	P50402	Emerin (wnt pathway)		Q9Y547	Heat shock protein beta-11
12 and 24 hour common proteins				GRP75	Stress-70 protein
12 hours and GBC common proteins	P14136	Glial fibrillary acidic protein			
	P15559	NAD(P)H dehydrogenase [quinone] 1			
	Q2M2I8	AP2-associated protein kinase 1			
24 hours and GBC common proteins	Q06830	Peroxiredoxin-1		P04264	Keratin, type II cytoskeletal 1
	P09429	High mobility group protein B1		P04792	Heat shock protein beta-1
	P30048	Thioredoxin-dependent peroxide reductase		P61604	10 kDa heat shock protein, mitochondrial
	P15121	Aldose reductase			

Interestingly, while not appearing as statistically significant, a number of up regulated neuronal specific proteins were detected as well as previously known markers in both 12 hour and 24 hour

ADSC differentiation time point data sets. The array of these neuronal specific proteins are; mesencephalic astrocyte-derived neurotrophic factor, spectrin brain form, glycogen phosphorylase brain form, brain acid soluble protein, V-type proton ATPase subunit B brain isoform, protein kinase C and casein kinase substrate in neurons protein 2, neuroplastin, N-acylneuraminate cytidylyltransferase, cell cycle exit and neuronal differentiation protein 1, activity-dependent neuroprotector homeobox protein, neurogenic locus notch homolog protein 2, neuron navigator 1, neurolysin and optineurin.

The majority of the aforementioned have more than 5 unique positively matched peptides (see appendix 2A). This larger list of neuronal related proteins were deemed to be important and required further investigation as three out of the four most widely used markers for neurogenic differentiation [28, 46, 104, 105, 193, 194, 279, 293, 296], Neuron specific enolase (NSE), Neudesin (NENF) and Beta- tubulin III (βT3) fell within this statistically non-significant, up regulated neuronal related protein cut off group. The fulfilment of the 5 peptides or greater cut-off suggests that these molecules are changing but not statistically significantly. Moreover, βT3 has been annotated as a neurospecific protein however it has also been detected in the basal ADSCs at higher levels than in the neurogenic cells and the GBCs, a result which is confirmed in a western blot in section 3.3. Due to the relative low abundance of NSE and NENF, the use of a single reaction monitoring (SRM) assay would allow a targeted capture and quantitiation of the above low abundance proteins from the background. The mutual presence of these proteins in the neurogenic and the ADSCs leads us to the conclusion that these proteins are not well suited for the use as neurospecific markers for neurogenesis.

Identification of the down regulated proteins was accomplished by clustering and sorting the statistically significant proteins by p-value (<0.05) and partitioning them by uniqueness or commonality with proteins from each differentiation time point. The data subset acquired identified a collective of 224 down regulated proteins in the ADSCs treated with BME for 12 and 24 hours.

Constituting this group are 36 unique proteins from the 12 hour time point and 26 unique proteins from the 24 hour time point. The remaining 162 proteins are common proteins shared between the 12 hour, 24 hour differentiation and the GBC control (figure 6). The major categories, from the combined down regulated proteins sorted by functional groups, showed that of the 224 statistically significant down regulated proteins, 54 were enzymes, 25 were ribosomal proteins, 17 were collagen and cytoskeletal related, 8 were myosin/muscle related and 4 were shock related proteins.

The down regulation of significant numbers and types of cytoskeletal related proteins, such as actin and tubulin proteins, in the 12 and 24 hr differentiated ADSCs to levels consistent with the GBCs indicates a large morphological restructuring of the cell as identified during microscopy or damage. The relatively large decrease in myosin related proteins in both differentiation time points indicates that the differentiating cells have shifted away from a mesodermal linage. This trend is further supported by the mass down regulation of pro-collagen and collagen related structural proteins which, when in high abundance, play a pivotal role in connective tissue, adipose, cartilage and bone formation. Conversely a down regulation of similar structural support proteins is also an indication of cellular damage and stress which has been noted to occur in acute epithelial cell injury [365].

Interestingly a decrease in the enzyme alpha enolase and the relative increase in gamma enolase/ NSE levels are consistent with the development of neuronal tissue seen in rats and humans [366]. A switch from alpha enolase, which is mesodermal specific, to gamma enolase which is ectodermal/neuronal specific is often used as an enzymatic biomarker for neuronal development [367]. The levels of alpha enolase detected in the differentiation time points are equivalent to the GBC cell line. However, the detected levels of up regulated NSE within the differentiated and GBCs lies in the non-statistically significant identified proteins.

3.3.3 Western Blots

Western blots to detect commonly used neuronal markers βT3, GFAP, NF200 and NeuN [28, 104, 194, 196, 274, 293] were carried out to compare these protein's expression in the BME treated

ADSCs with GBC whole cell lysates in this study and previous literature. βT3 is a 55 kDa protein which is positively detected in the basal ADSCs, the BME differentiated ADSCs and the GBCs (figure 7A). The GFAP molecule is only detected at the 48 kDa mark in the GBC lane at a normal exposure (figure 7B). By decreasing the contrast by 20% the GFAP is just detectable in the BME differentiated cells. The NF200 protein is detected in both the BME differentiated and with a slightly stronger presence in the GBC at 200 kDa and there is no trace present in the ADSC lane (figure 7C). The NeuN however was not detected in the BME differentiated cells but very faintly in the ADSC and GBCs (figure 7D). The major deficiencies in the literature are that these "neurospecific" markers have been annotated as not solely expressed in neuronal cells [368-371]. βT3 has been used to characterise primitive neuroepithelium and catalogued as being solely expressed on neuronal cells [372-374] however βT3 has been found to be expressed in the ADSCs within this study. Similarly the presence of NeuN in the ADSCs confounds the use of this protein as a neuronal specific marker. Thus the identification and quantitatation of the extent of differentiation with relatively few markers is insufficient.

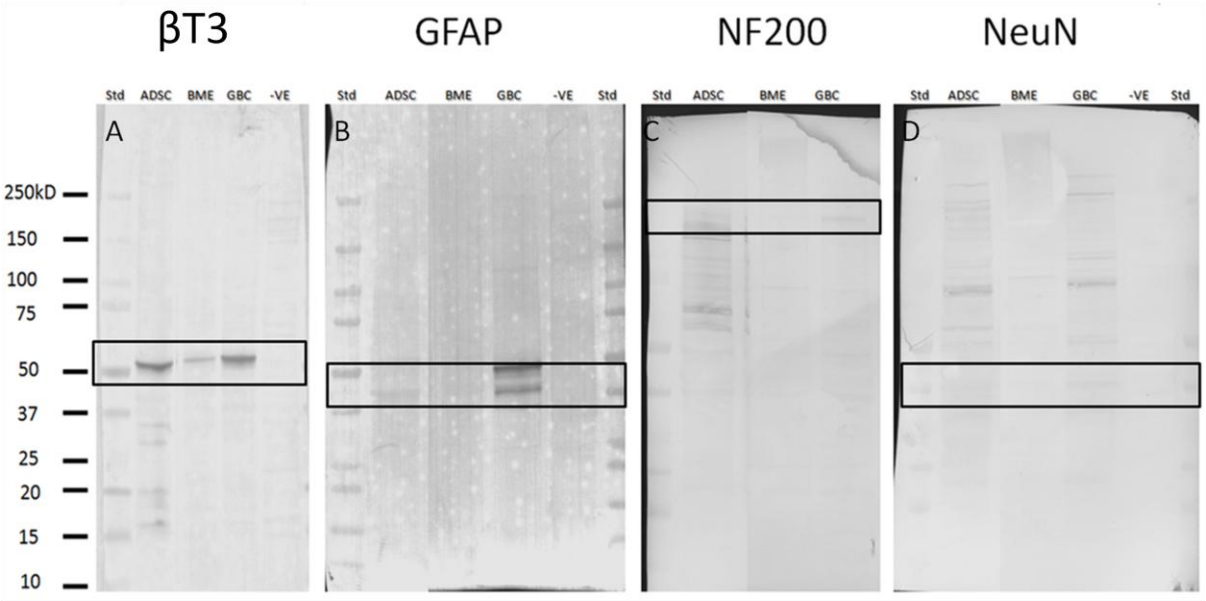

Figure 7 A-Western blot of βT3 positive in ADSCs, BME differentiated and GBCs seen at 55 kDa. B-GFAP positively detected in GBCs at 48 kDa. C-NF200 positively identified at 200 kDa in GBCs and very weakly in BME differentiated. D-NeuN a very low positive in ADSCs and GBCs only.

3.3.4 Bioplex

The Bioplex assay is an efficient system for examining up to 27 cytokines across multiple sample types simultaneously, revealing quantitative changes and relative concentrations of these secreted molecules. Aliquots of the media the cells were growing in were collected and analysed from the differentiation time points 0, 1, 3, 5, 20 and 24 hours. A hierarchical clustering and Euclidean test in the DanteR software were used to cluster the multiple data points in a heat map configuration where red represents expression above median; green: expression below the median and Black: median expression across all samples (figure 5a). The hierarchical clustering (figure 5b) presents the cytokines with similar concentration trends over the differentiation time points. Due to the decrease in cell population during the differentiation, a cell number normalisation across all samples and time points was utilised to assemble a relative and comparable cytokine concentration profile per cell. Table 3 summaries the temporal analysis of each cytokine's concentration secreted per cell.

Table 3 Cytokine concentration normalisation per cell for temporal BME induction.

Cytokines	Basal 0hr	pg/ml/cell	1hr	pg/ml/cell	3hrs	pg/ml/cell	5hrs	pg/ml/cell	20hrs	pg/ml/cell	24hrs	pg/ml/cell
IL-1ra	79.28	1.46E-05	23.83	4.26E-06	25.56	5.55E-06	38.8	8.77E-06	20.39	7.71E-06	29.04	1.15E-05
IL-2	11.2	2.07E-06	4.62	8.26E-07	5.91	1.28E-06	7.91	1.79E-06	5.52	2.09E-06	5.65	2.23E-06
IL-4	2.29	4.22E-07	0	0.00E+00	0.18	3.91E-08	0.18	4.07E-08	0.18	6.80E-08	0.27	1.07E-07
IL-5	1.75	3.23E-07	0.47	8.41E-08	0.52	1.13E-07	0.52	1.18E-07	0.52	1.97E-07	0.52	2.06E-07
IL-6	0	0.00E+00	30.1	5.38E-06	36.71	7.97E-06	64.71	1.46E-05	205.3	7.76E-05	165.21	6.53E-05
IL-7	16.11	2.97E-06	0.28	5.01E-08	0.61	1.32E-07	0.78	1.76E-07	0.78	2.95E-07	0.94	3.72E-07
IL-8	28591.59	5.27E-03	10.84	1.94E-06	4.22	9.16E-07	10.38	2.35E-06	333	1.26E-04	337.13	1.33E-04
IL-9	40.66	7.50E-06	3.72	6.65E-07	3.72	8.07E-07	7.83	1.77E-06	4.4	1.66E-06	6.45	2.55E-06
IL-10	25.96	4.79E-06	0	0.00E+00	0.05	1.09E-08	0.23	5.20E-08	0.42	1.59E-07	0.32	1.27E-07
IL-12(p70)	237.18	4.37E-05	1.85	3.31E-07	2.18	4.73E-07	2.45	5.54E-07	2.86	1.08E-06	3.96	1.57E-06
IL-13	13.22	2.44E-06	0.61	1.09E-07	0.75	1.63E-07	0.82	1.85E-07	0.79	2.99E-07	0.98	3.87E-07
IL-15	4.49	8.28E-07	4.27	7.64E-07	5.66	1.23E-06	5.06	1.14E-06	3.34	1.26E-06	3.03	1.20E-06
IL-17	8.66	1.60E-06	5.81	1.04E-06	6.93	1.50E-06	8.97	2.03E-06	5.81	2.20E-06	6.77	2.68E-06
Eotaxin	74.14	1.37E-05	42.18	7.54E-06	51.58	1.12E-05	74.92	1.69E-05	45.21	1.71E-05	49.05	1.94E-05

FGF basic	43.2	7.97E-06	11.44	2.05E-06	14.95	3.24E-06	19.27	4.36E-06	17.17	6.49E-06	30.06	1.19E-05
G-CSF	61.12	1.13E-05	0.42	7.51E-08	0.42	9.11E-08	1.4	3.17E-07	0.42	1.59E-07	0	0.00E+00
GM-CSF	50.28	9.27E-06	71.17	1.27E-05	88.97	1.93E-05	88.11	1.99E-05	67.92	2.57E-05	64.87	2.56E-05
IFN-g	265.87	4.90E-05	11.15	1.99E-06	13.37	2.90E-06	15.64	3.54E-06	15.64	5.91E-06	15.64	6.18E-06
MCP-1(MCAF)	1174.32	2.17E-04	19.62	3.51E-06	20.56	4.46E-06	46.14	1.04E-05	94.82	3.58E-05	99.45	3.93E-05
MIP-1a	2.08	3.84E-07	0.64	1.14E-07	0.66	1.43E-07	0.75	1.70E-07	0.66	2.49E-07	0.66	2.61E-07
MIP-1b	6.77	1.25E-06	0.92	1.65E-07	0.92	2.00E-07	2.39	5.40E-07	2.18	8.24E-07	2.18	8.62E-07
PDGF-bb	7.5	1.38E-06	0	0.00E+00	0	0.00E+00	1.25	2.83E-07	0	0.00E+00	0.25	9.88E-08
RANTES	9.4	1.73E-06	1.15	2.06E-07	0.47	1.02E-07	3	6.78E-07	2.47	9.33E-07	2.83	1.12E-06
TNF-a	16.31	3.01E-06	0	0.00E+00	0.5	1.09E-07	1.4	3.17E-07	0.5	1.89E-07	1.1	4.35E-07
VEGF	5546.75	1.02E-03	22.79	4.08E-06	25.6	5.56E-06	27.62	6.24E-06	39.63	1.50E-05	38.8	1.53E-05
Total cell count	5.42E+06		5.59E+06		4.61E+06		4.42E+06		2.65E+06		2.53E+06	

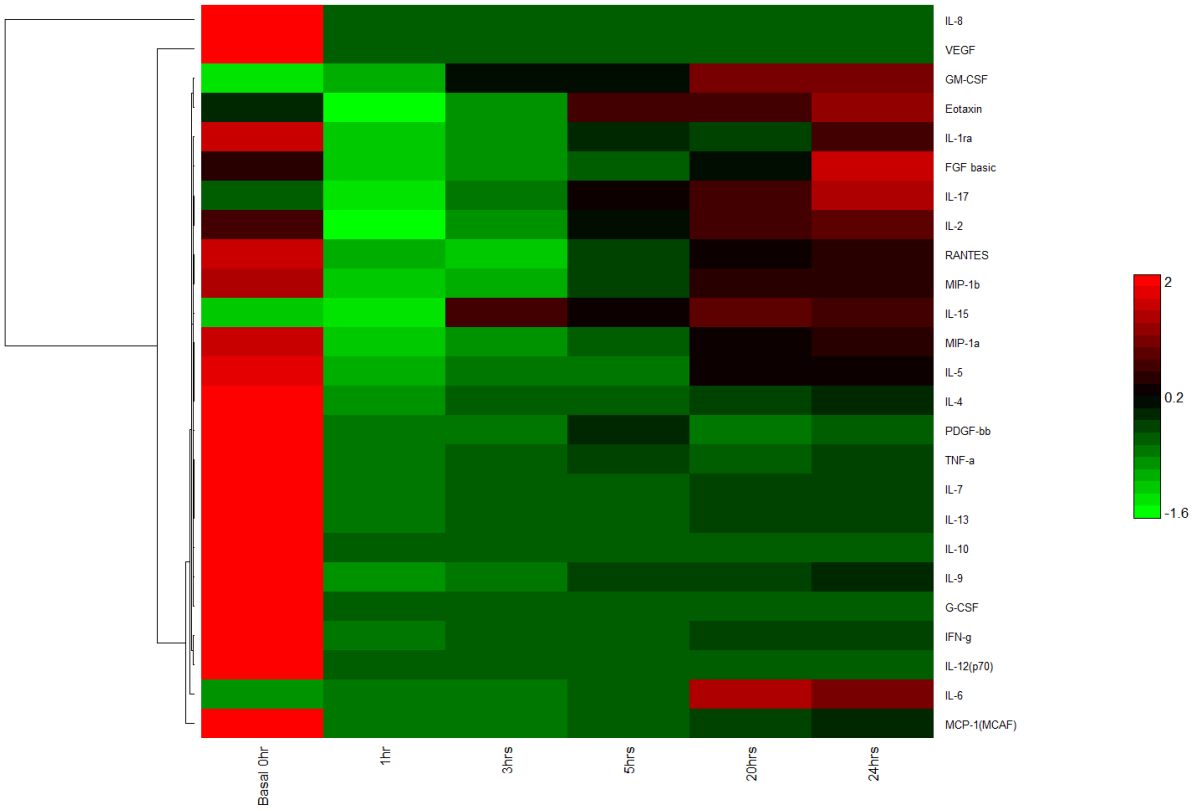

Figure 8A Bioplex comparisons of interleukins and cytokine secretions from basal ADSCs and temporal differentiation with BME neuronal differentiation media. Hierarchical clustering software and Euclidean test Red: expression above median; Green: expression below the median; Black: median expression across all samples.

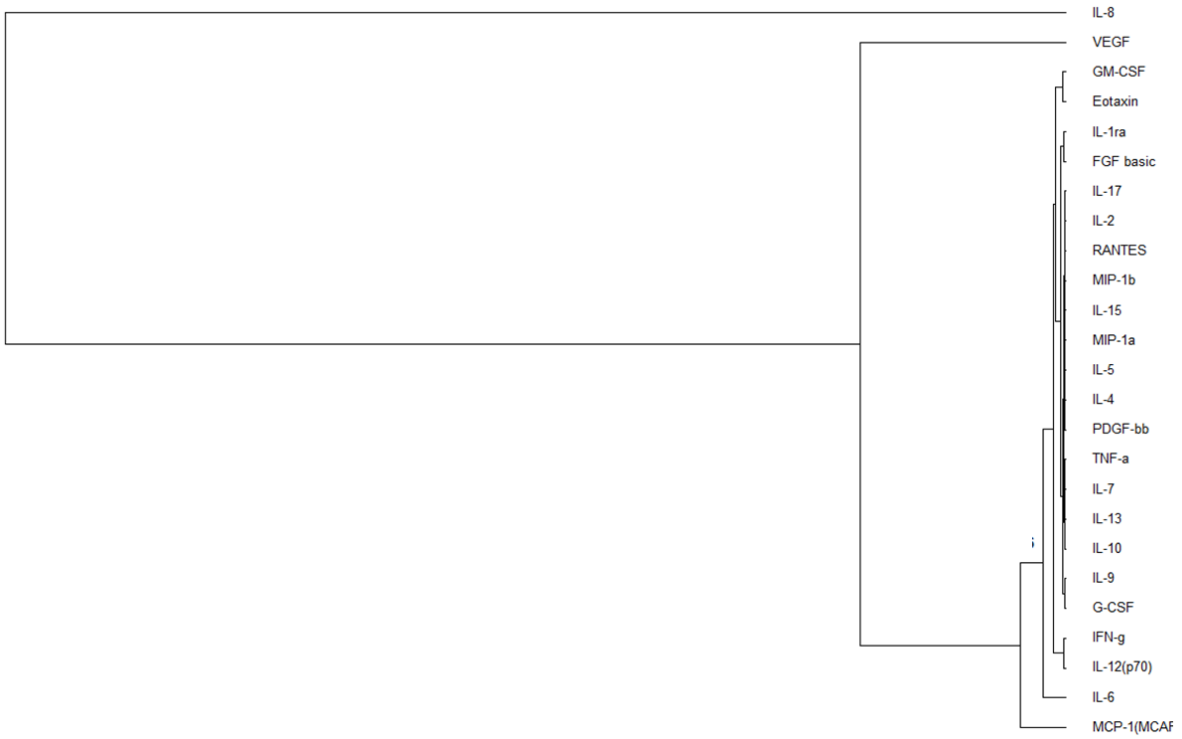

Figure 8B Bioplex comparisons of secretions from basal ADSCs and temporal differentiation with BME neuronal differentiation media Hierarchical clustering of interleukins and cytokines.

Cytokines, while having their unique roles in metabolic and cellular processes, can often be regulated in synchrony or regulate the expression of other cytokines in MSCs [375]. Individually and collectively their relative concentrations can be related to particular cellular events. As such a number of trends occur within the Bioplex temporal differentiation data set. The molecules IL-1ra, Eotaxin, IL-2 and Rantes share a uniform trend in this dataset with similar concentration fluctuations between IL-1ra and Eotaxin which are comparable to IL-2 and Rantes. The trend reveals the highest concentration of the respective molecules is present at the 0hr time point, with a uniform decrease to the lowest concentrations at the 1 hr time point. This is followed by a slight recovery at the 3rd through the 5th hr. The concentration decreases fractionally again at the 20th hr for IL-1ra and Eotaxin then stabilises at the final time point (Fig 9A).

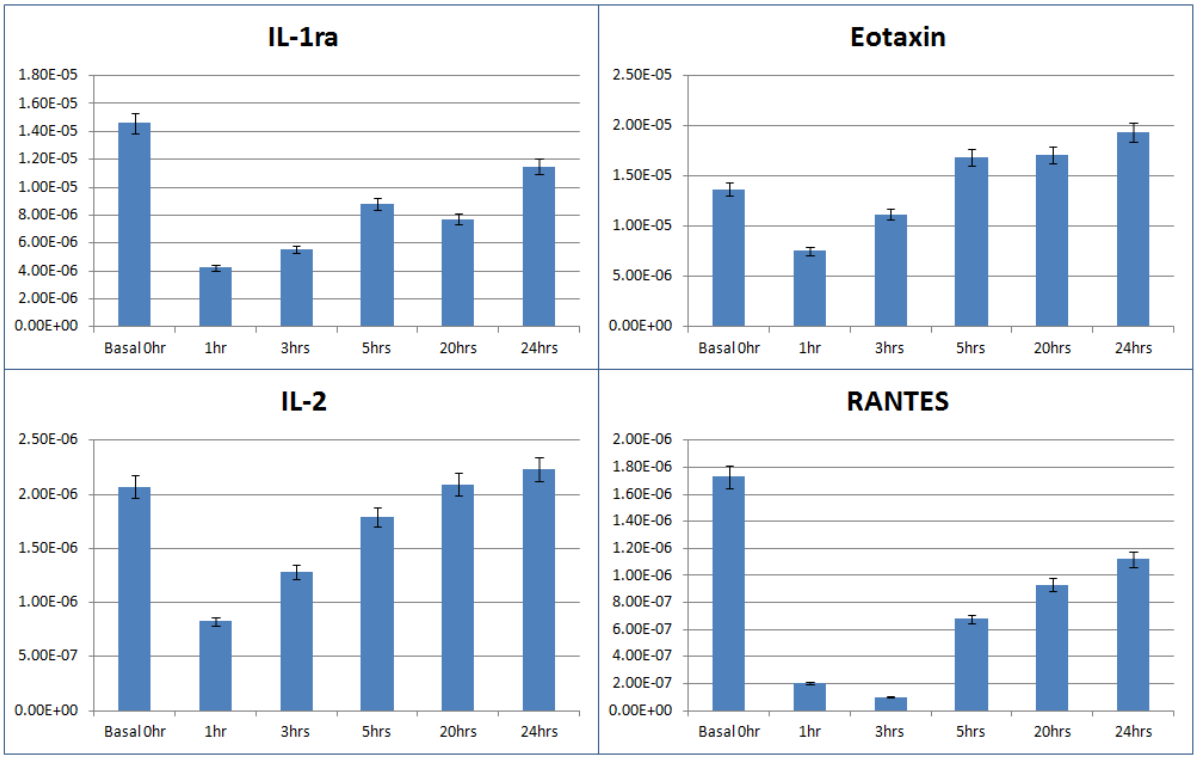

Figure 9A. Group 1 Bioplex trend related secreted cytokines IL-1ra, Eotaxin, IL-2 and Rantes over a temporal differentiation normalised as pg/ml/cell

The grouping consisting of IL-15, IL-17 and GM-CSF followed a trend with relatively lower levels at the basal non-treated ADSCs at time point 0hrs; followed by a decrease of IL-15 and IL-17 below basal levels 1hour post induction. A recovery period occurs during 3-5hours followed by a steady increase in concentration from 20 to 24hours. The highest concentration occurred at 20 hrs for IL-15 and GM-CSF, with a slight variation with IL-17 which had a slightly increased concentration at 24 hrs (fig 9B).

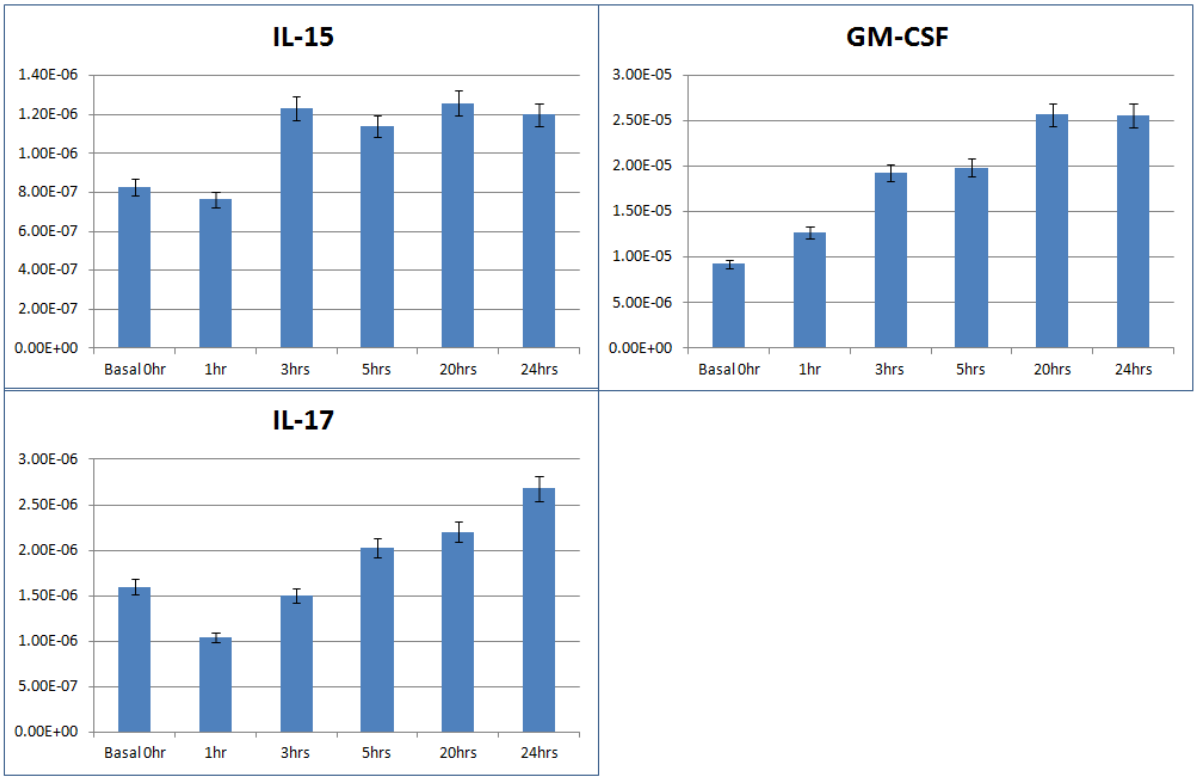

Figure 9B Group 2 Bioplex trend related secreted cytokines IL-15, IL-17 and GM-CSF over a temporal differentiation normalised as pg/ml/cell

The next group of trend related cytokines were composed of IL-4, IL5, IL-9, MIP-1a and MIP-1b which followed a fairly simple and distinct trend. The highest concentration occurs at time point 0hrs which then decreases approximately by 75% for all five cytokines thereafter and remains comparatively at the similar concentrations for all time points, with a minor recovery at 3 hrs post induction (fig 9C). The group consisting of IL-7, IL-13, PDGF-bb, TNF-a, MCP, IFN-g have a somewhat similar trend to the previous group, in that the highest concentrations occur at time point 0hrs, the major defining trend for this series is the significant decrease in concentration to less than 10% in

the next time point which is maintained over the course of the differentiation time showing a marginal increase at the 24 hour mark (fig 9D). The following group: IL-8, IL-10, IL-12, G-CSF and VEG-F also share some common features with the previous two groups in that the highest concentration is observable at time point 0 hrs. The difference is the substantial decrease to near non-detectable concentrations for the entirety of the differentiation (figure 9E). Conversely the two remaining cytokines IL-6 and FGF were grouped together due to their unique trends that appear to be somewhat related. The main difference between these trends in these two cytokines is that IL-6 appears to have a concentration below the detectable level at time point 0 hrs where as FGF has approximately 42 pg/ml at the same time point. The trends display a somewhat similar trait after 1 hour with increasing concentrations in both cytokines with the highest levels at the final two time points (fig 9F).

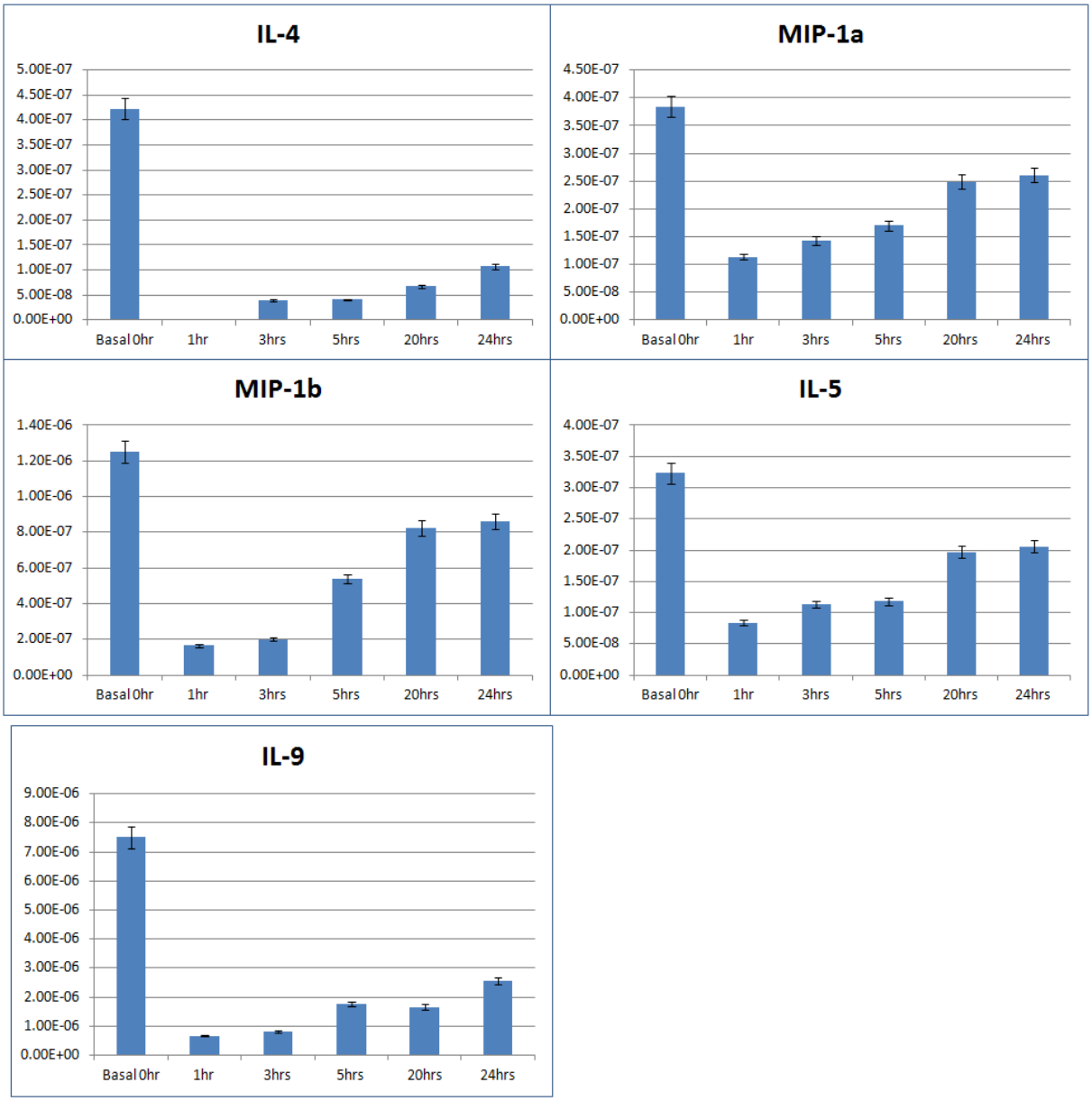

Figure 9C Group 3 Bioplex trend related secreted cytokines IL-4, MIP-1a, MIP-1b, IL-5 and IL-9 over a temporal differentiation normalised as pg/ml/cell

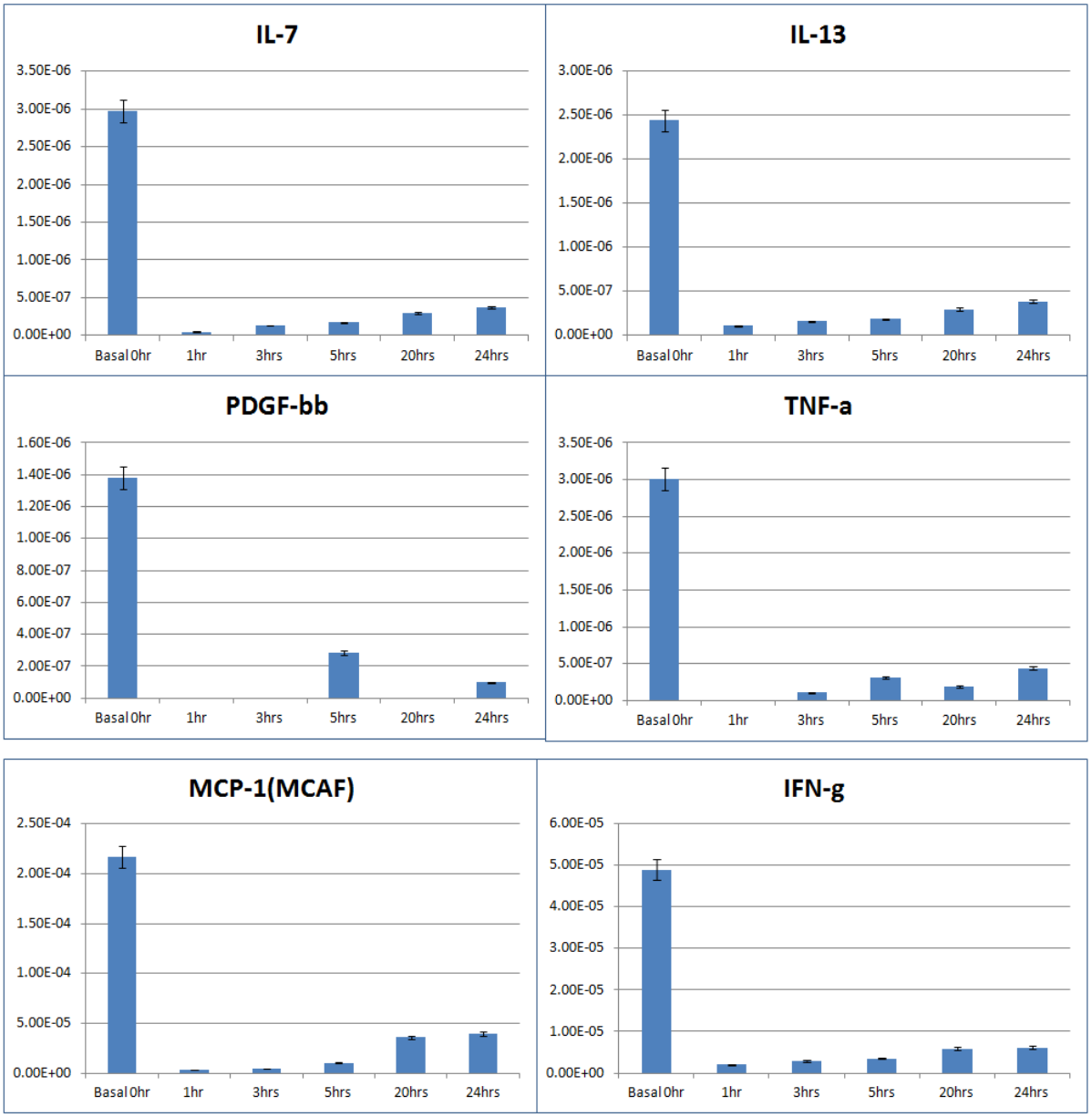

Figure 9D Group 4 Bioplex trend related secreted cytokines IL-7, IL-13, PDGF-bb, TNF-a, MCP-1 and IFN-g over a temporal differentiation normalised as pg/ml/cell

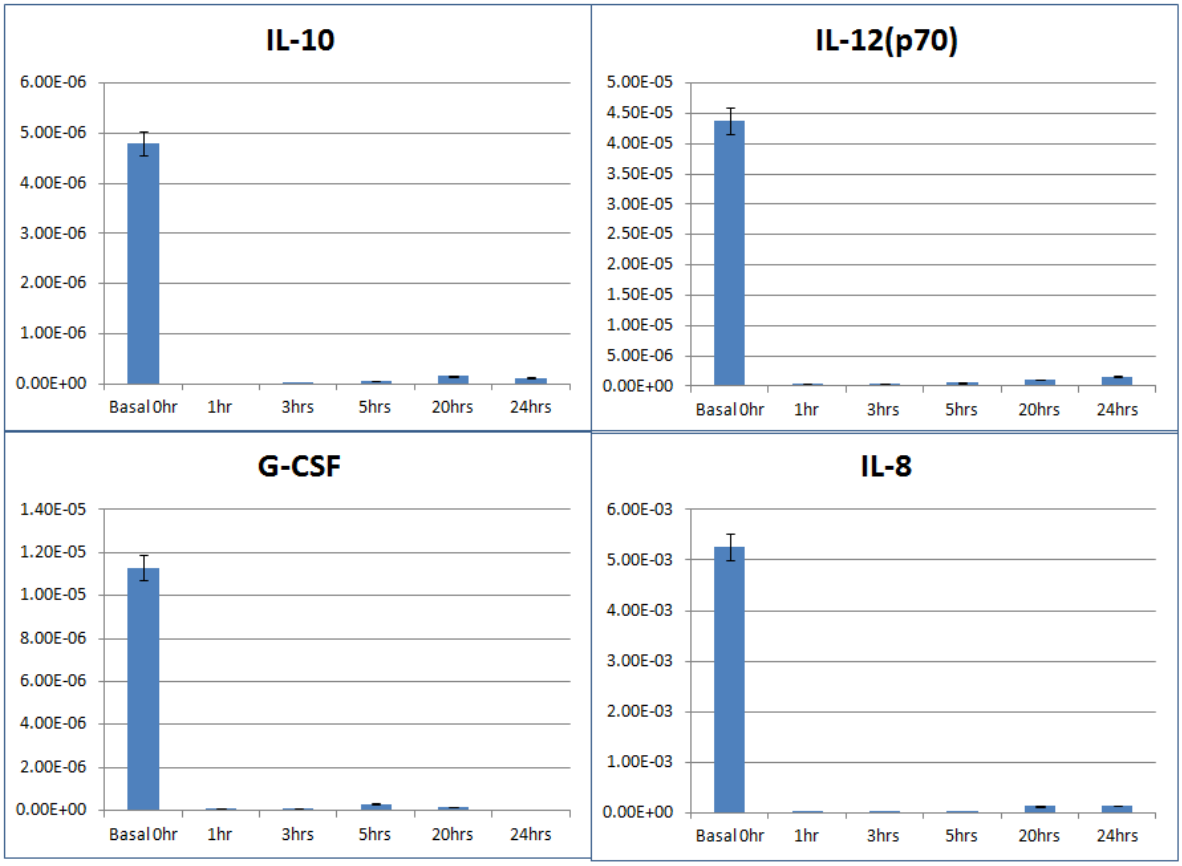

Figure 9E Group 5 Bioplex trend related secreted cytokines IL-10, IL-12. G-CSF and IL-8 over a temporal differentiation normalised as pg/ml/cell

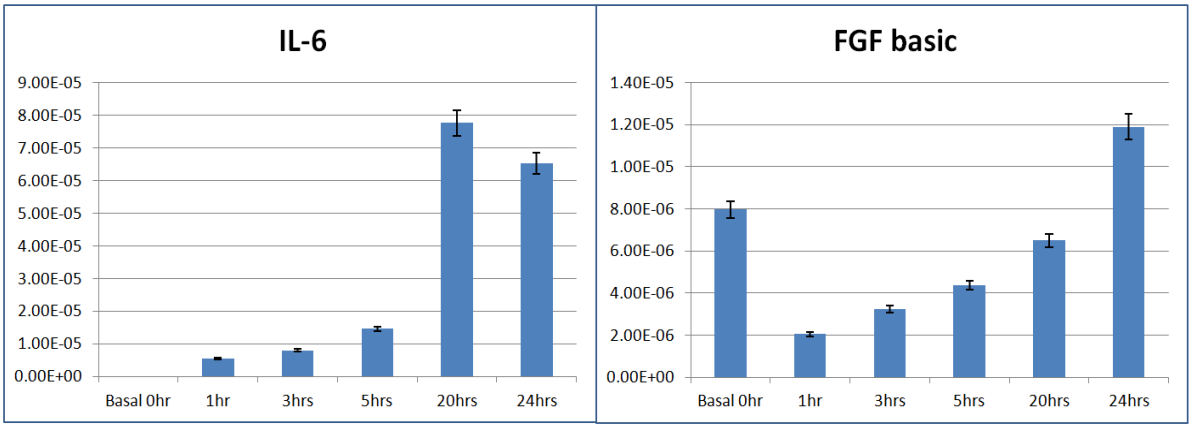

Figure 9F Group 6 Bioplex trend related secreted cytokines IL-6 and FGF over a temporal differentiation normalised as pg/ml/cell

3.4.0 DISCUSSION

In this study, we investigated hADSCs ability to transdifferentiate toward a neuronal-like lineage within 12 and 24 hours, as well as the changes in the proteome occurring during the differentiation process. It was found that the cells responded to BME differentiation media with similar morphological and marker profiles as previously reported [28, 104, 195, 376] and several groups of proteins involved in neural growth and protection were identified by MS/MS analysis. We also found the acquired soluble proteome of hADSCs differentiated for 12 hours and 24 hours to be noticeably different from basal ADSCs and GBCs, presenting a number of fold changes in neuronal related differentiation, cytoskeletal remodelling as well as an array of stress response proteins. Furthermore Bioplex cytokine profiles present evidence of a large cellular remodelling shift and stress response activity during the induced differentiation process which is reflected in the proteomic data sets. This study reveals that the BME treatment of ADSCs toward a neurogenic lineage is initiating the differentiation presenting a wide array of neuronally related proteins and morphology however the extended exposure of BME to the cells does induce a stress response as well.

3.4.1 Western blot marker analysis

Numerous studies investigating neurogenesis of MSCs have widely employed the presence or absence of markers such as GFAP, βT3, NeuN and NF200 as indicators of neuronal-like differentiation of MSCs [104, 190, 192-195, 377]. One of the more interesting proteins up regulated in the 12 hour differentiation time point identified was GFAP. The difference in abundance of GFAP between the basal ADSCs, 12 hour differentiation and GBCs varied substantially; the ratio of GFAP in the 12 hour and GBC samples relative to ADSCs were 1.15 and 55.99 fold higher respectively in the iTRAQ data. A western blot (figure 7) analysis of the above samples for GFAP shows consistent levels of the protein identified by iTRAQ LC-MS/MS, where the 1.15 fold increase is barely detectable when compared to the 55.99 fold increase. The GBC control stained positively for GFAP however, due to

the relative abundance being approximately 56 fold higher than the basal and BME treated ADSCs, the GBC signal overshadows the small up regulation of GFAP in the neuronally induced ADSCs.

GFAP is an intermediate filament found primarily in cells found in the central nervous system and is commonly used as a cell specific marker for the identification of neuronal development and distinguishing astrocytes from other glial cells. Identifying GFAPs presence in differentiated MSCs has been previously utilised as evidence of neuronal differentiation [293]. Functionally GFAP is involved in a number of important processes forming junctures for cell to cell signalling and maintaining the blood-brain barrier [378]. Its role in cell to cell signalling, differentiation and maturation is of particular interest. A study by Wislet-Gendebien *et al*., [379] found that the expression of GFAP in BMSCs was often regulated by a number of other neuronal related proteins such as nestin, which is also a membrane bound filament responsible for axonal growth and is usually present in immature or developing neurons and is replaced by GFAP during neurogenesis in mature neuronal cells [380]. Three annotated interacting partners of GFAP were also identified in the iTRAQ datasets; solute carrier family 1 (glial high affinity glutamate transporter), epidermal growth factor receptor and signal transducer and activator of transcription 3. However none were statistically significant in either iTRAQ analyses of the BME treated ADSCs. There was however a noticeable and significant increase in all of the above proteins in the GBC cells when compared to the ADSC with each presenting approximately a two fold increase in the GBCs. Functionally each of the three identified GFAP-interacting partners are involved in, to some extent, neuronal development, survival and repair [381-385]. While the role of GFAP may be intergral to the development and maturation of neuronal cells, especially glial cells, its detection by Western blot or iTRAQ is limited by its time of expression within the differentiating cells. The rapid differentiation of the ADSCs toward a neuronal morphology, within 24 hours, may in fact be a too early time point to detect GFAP due to its later stage expression and replacement of Nestin [379]. The lack of GFAP from the BME treated ASDCs is further evidence the produced cells are not mature neuronal cells.

βT3 belongs to a family of globular proteins making up microtublues which are known to be prominently expressed in neuronal cells and thus βT3 use in the identification of primitive neuron epithelium development has been extensively reported [372]. Within this study, βT3 was detected by Western blot in approximately similar levels in all neuronally differentiated ADSCs as well as the control GBC and unexpectedly in the basal ADSCs as well. Comparatively the iTRAQ results reflect an analogous trend of minute variance in βT3 levels found in basal ADSCs compared to differentiated cells. Conversely, Barnabé *et al* [196] found little to no βT3 expression in any of the Western blot results of similarly induced MSCs. However by applying immunohistochemical staining of monolayers they detected the same marker sparsely across all samples in a small fraction of cells [196]. The above findings are confirmed by another study investigating a chemical induction of BMSCs toward neuronal cells, where Deng *et al* [274] identified that MSCs spontaneously express neuronal proteins in culture. Their finding holds true in non-induced cells for several markers used to identify neuronal differentiation such as nestin, NFM, PSA-NCAM, S100-β [274]. Our Western blot and iTRAQ results support this observation for ADSCs, where the expression levels of βT3, NeuN, and NF200 were not significantly differentially expressed in our non-induced and induced ADSCs. The reliance on a few internal protein markers to determine the extent of neuronal differentiation is confounded by the results of this study as well as the aforementioned previous studies. As such pursuing a proteomic capture of the breadth of acquired soluble proteins may offers a comprehensible biological context of the proteins being expressed during neuronal differentiation process.

3.4.2 Proteomic analysis by iTRAQ

Investigating the soluble protein fractions from the four different cell types using an iTRAQ labelling strategy allowed for the simultaneous and relative quantitative comparison of the expressed proteomes. This enabled the assessment of large groups of proteins revealing the respective expression levels in each sample type and how they may correlate to the differentiation process. As

such, expression levels for all proteins were evaluated according to the fold change relative to the basal hADSCs sample, thus each ratio could be directly compared. Comparing the ratios and biological roles of the largely statistically relevant proteins in each time point, has revealed and quantified a number of them with neurogenic and stress properties related to cytoskeleton organisation, growth and structure. As such, the proteins identified uniquely or shared in each time point will be elaborated on in context of the proteins within that time point and to demonstrate any relevant extending affects in the role of differentiation or stress.

3.4.2.1 Neurogenic related roles of identified proteins

The fold change datasets of induced neuronal differentiations were compared relative to the basal ADSCs. Coincidently, the protein with the highest coverage in this study is aptly annotated as Neuroblast differentiation-associated protein (AHNAK) with coverage of 88% of the neuronal specific protein, reflecting its high abundance in the differentiation samples. Due to its high abundance and being the top identification in all the differentiation samples it was imperative further investigate its biological relevance in neuronal differentiation.

Despite its name, the exact biological function of AHNAK is largely unknown, although several putative interacting proteins have been identified [386]. The role of this protein in the neurogenic process is still under investigation. According to the GO classification, the AHNAK protein is involved in nervous system development (GO0007399). At the cellular level, in the presence of high calcium concentrations, it is present near the plasma membrane and is known to interact with the annexin2/S100-A10 complex which regulates actin cytoskeleton organisation, cell membrane architecture and cell-cell junction formation [386-389]. Borgonovo *et al* [390] found that AHNAK is part of a subcellular vesicle called the *enlargosome* which is shuttled to the plasma membrane in high cellular calcium concentrations and have been proposed to play a role in cell membrane differentiation and repair [390]. There are a number of publications that indicate AHNAK has a

number of functional roles in conjunction with or as part of other protein complexes. The presence of the AHNAK interacting partner annexin in this study was noted to have levels similar after 12 hour and 24 hour BME differentiation and in the GBC samples and at levels at least 40% lower relative to hADSCs. The complementary interacting complex partner, the S100-A10 is present at marginally lower levels in the 12 and 24 hour BME differentiation time points compared to the basal hADSCs, whereas the levels in GBCs it is approximately 60% higher. S100-A10 has been previously identified as a transport mechanism for the neurotransmitter, serotonin, and intercedes in the interaction between annexin2 and AHNAK [386, 391]. Although the levels of annexin2 and S100-A10 varied between cell types, their fold changes were not marked as statistically significant. An interesting report on the down regulation of annexin2/S100-A10 by Benaud *et al* saw a decrease of the AHNAK association with the plasma membrane however does not affect its expression levels [386].

The non-membrane bound AHNAK is also free to interact with a several other putative partners. Lee *et al*., [387] reported that AHNAK is phosphorylated by PKC and activates phospholipase C (PLC), both of which are involved in the activation of inositol metabolism. In this work, a number of PKC's identified were marginally up regulated in both differentiation time points, with similar levels present in the GBCs. Inositol metabolism is essential in cytoskeleton assembly, nerve guidance, serotonin modulation and the control of intracellular calcium concentration [392]. It is well established that PKC's have a broad variety of roles in the regulation of differentiation and proliferation of numerous cell types. In particular, PKC has a role in the phosphorylation of Endophilin I, a calcium binding and shuttling protein, in actin cytoskeleton organization as well as the activation of serotonin and acetylcholine receptors in neurons in the central nervous system and autonomic ganglia [393, 394]. Further to this, phospholipase C has also been associated with the activation of several neurotransmitter receptors and maintaining intracellular calcium concentrations [395]. This may indicate that a feedback mechanism may exist between AHNAK activation of PKC, PLC and their effect on intracellular calcium concentrations, which in turn

determines if AHNAK is localised in the nucleus in low calcium concentrations or shuttled near the plasma membrane in high concentrations. This leads us to the view that the AHNAK protein, dependant on its localisation, is an intermediary functional protein in a number of early neurogenic developmental and cellular restructuring processes. This protein may indeed be a useful marker for the identification of the neurogenesis. A super resolution microscope and fluorescently conjugated monoclonal antibodies would be useful to further investigate the cellular localisation of AHNAK.

It can be assumed a number of enzymes are important in the process of transdifferentiaiton and therefore in neurogenesis as well, catalysing reactions and controlling expression and movement of proteins and other molecules in response to the differentiating media. Enzymes that have specific roles in brain and CNS tissues identified in the differentiating cells may be used as an indicator for the development of neuronal-like cells depending on their activities. For example, the enzyme glutaminase is an aminohydrolase which generates glutamate from glutamine. Glutaminase is primarily found in glial cells, regulating the concentration of the neurotransmitter glutamate in the brain.

Glutaminase is not limited to the brain as there are three tissue specific isoforms. Isoform 1 is detected in the brain cortex as well as numerous other tissues. Isoform 3, which was identified in this study, is detected in both the brain and kidney and is more commonly known as a neurotransmitter secretion [396-399]. The expression levels of glutaminase found in the 12 hour differentiation is approximately 16% higher than basal hADSCs and 50% higher than the control GBCs. The levels detected in the 24 hour time point are 20% higher than the control GBCs. The trend indicates the glutaminase decreases over the differentiation process to approximate levels seen in glial cells. The effect of metabolic acidosis on the synthesis and turnover glutaminase is an essential component in the control of acid-base balance which can significantly affect the amount of the glutamine present [400]. Thus the increase in detected glutaminase can be directly related to the concentration of glutamine accumulated in cells.

Some studies have shown that if the concentration of glutamine accumulates to excessively high levels it can often become toxic and cause neuropathies especially seen in glial and astrocytic cells [398, 401]. As one of many metabolic countermeasures, glutaminase converts glutamine to glutamate[401]. Thus the steady decrease in glutaminase can be attributed to the intracellular control of glutamine and subsequent conversion to glutamate. Alternatively the role of glutaminase could also play a role in the promotion and formation of the synapse. Sulzer *et al* found *in vitro* cultured cholinergic neurons were able to synthesise and secrete two different neurotransmitters such as dopamine and glutamate and concentrate them and terminals allowing the formation of both dopaminergic and glutamatergic synapses [402]. The ability to produce glutamate, initiated the correct chemotaxin conditions to form glutamatergic synapses in cells that did not usually require it. The presence of higher concentrations of glutaminase is also present in glutamatergic neurons compared to glial cells [403] which is similar to the findings between the early differentiated ADSCs and the control GBCs. The precise role of the glutaminase as well as other metabolites in the differentiating ADSCs toward neuronal-like cells requires further investigation with a metabolomics approach as a complimentary method. The functionality of glutaminase is undoubtedly involved in numerous neuronal cell growth events making it ideal for the use as a marker of differentiation.

A number of proteins act as cell-binding mechanisms and are intricately involved in the chemotaxis processes. Collagen alpha-3(VI) (CO6A3) chain is a protein known to assist with cell-binding and directs the migration of an axon growth cone between cells. It has also been noted to be involved in the interaction between neuroectodermal cells and the ECM of the normal brain is important in several developmental processes such as differentiation, proliferation and migration [404]. CO6A3 has a number of interacting partners similarly linked to the structural guidance and growth of ECM, in this study it was identified that COL6A3 was similarly up regulated along with another major interacting partner, CD44.

CD44 mediates a number of functions, especially cell-cell interaction, mainly through collagens and matrix metalloprotineases. Su *et al* identified that CD44 plays an important role in neuronal maturation in primary derived neural progenitor cells from the adult mouse hippocampus cells via a regulation through an ECM dependant mechanisms. CD44 has a several direct interactions with a several growth factors of neuronal functionality and developmental related proteins such as fibroblast growth factor, fibronectin 1 and IL2 that are covered in the subsequent Bioplex sections. In the acquired iTRAQ dataset, CD44 protein has been found to act as an interacting protein for three other concurrently up regulated proteins with roles in neurogenesis, these proteins are COL6A3, Serine Hydroxymethyltransferase (SHMT) and matrix metallopeptidase 14 (MMP14). SHMT reversibly catalyses the conversion of L-serine into glycine, which serves as both an inhibitory or excitatory neurotransmitter in the CNS [405]. SHMT has been shown to promote normal neural tube growth, and single polymorphisms in the encoding gene can cause a dysfunctional mutant protein having a downstream effect that produces neural tube defects in mammals especially during developmental stages [406]. The third interacting enzyme identified, MMP14, which is a matrix metalloproteinase class protein. MMP14 has been implicated in astrocyte migration and ECM remodelling. These enzymes are becoming increasingly recognised as having a regulatory action on neural plasticity and in neurogenesis, myelin formation and axonal growth and are secreted in abundance by neuronal and glial cells [407, 408]. The mutual functionality of the discussed cluster of proteins is directly related to the ECM remodelling process which is usually a concerted effort via the action of several proteins in unison. Both neurons and glial cells contribute to the production of ECM which plays an important role in proliferation, migration and differentiation of neuronal cells especially axonal guidance and dendrite structure growth [409]. These early developmental initiating factors prove to be essential in primary developing brain and CNS, their up regulation in this study of ADSCs differentiating toward neuronal-like cells are a promising indicator that a simple chemical cocktail can apply a sufficient stimulus to direct the cells toward a neuronal-like progeny.

Up regulated proteins commonly identified between the 12 hour differentiated time point and the GBCs revealed a number of neuronal functionally linked molecules including previously well known and widely used neuronal markers. The array of proteins include NADPH dehydrogenase [quinone] 1 (NQO1), AP2-associated protein kinase 1 (AAK1) and GFAP. NADPH dehydrogenase has been implicated in cholinergic synaptic transmission and positive regulation of neuron apoptotic process [410]. AAK1 is a protein involved in the interaction of metalloproteinases, like the previously mentioned MMP14, and has also been identified as having an integral role in the Notch signalling pathway which determines if maturing neuronal cells will adopt a neuron or glial fate [411]. The mutual presence of these molecules in GBCs and differentiating ADSCs indicates that the ADSCs are in the process of expressing shared neuronal related enzymes that are not just aberrant expression events.

3.4.2.2 Stress related roles of identified proteins

The use of chemical inducers to initiate neurogenesis has become well accepted because of its simplicity and due to its relatively rapid outcome of producing morphologically neuronal-like differentiated cells compared to the alternative growth factor induction methods. It is important that the choice of chemical inducer is not toxic to the cells to the extent that major cell death is apparent. While the use of BME produces interesting results in the induction of neurogenesis in ADSCs, it is quite toxic to cells and therefore would not be useful in a clinical setting. This is reflected in the figures 2 and 3 which reveal a 46% decrease in total cell population within the 24 hours of induction. The high death rate in the BME neurogenic induction would not be permissive for *in vivo* treatments, especially since the extent of damage or stress to the surviving cells has not been well characterised. A catalogue of stress proteins and potential markers can be useful in identifying the biological processes initiated during induced neurogenesis when utilising alternative chemicals to BME.

As demonstrated in this work, the secreted material can be analysed via iTRAQ proteomics or Bioplex cytokine analysis for definitive profiling. Several stress and shock related proteins were identified and presented in the results section 3.2 in table 2. The proteins Heme oxygenase, Glutamate--cysteine ligase regulatory subunit (GCLM), Glucose-6-phosphate 1-dehydrogenase (G6PD), Prostaglandin G/H synthase 1 (PTGS1), Heat shock protein beta-11,(HSPB11) Stress-70 protein (HSP-70), Keratin, type II cytoskeletal 1, Heat shock protein beta-1 (HSPB1) and 10 kDa heat shock protein (HSPE1), mitochondrial were all investigated to ascertain their role during induction as they were statistically significantly up regulated stress related proteins at the various time points.

The expression of Heme oxygenase (HO) in neurogenic induced ADSCs is an interesting finding since its primary function is the degradation of heme producing biliverdin, iron and carbon monoxide [412]. The expression of HO has been found in lung epithelial and liver cell types experiencing oxidative stress [413-415]. Furthermore HO has annotated roles in the response to the action of the oxidative stress linked proinflammitory cytokines IL-1B and TNF-α in astroglial cells [416, 417]. It has also been found that HO and the proinflammatory cytokines play a protective role in neuronal cells experiencing oxidative stress as neurons over expressing HO are resistant to oxidative stress mediated cell death [416, 418, 419]. The Bioplex results exhibited the expression of IL-1B and TNF-α was far too low for a discernible concentration to be calculated for the former and very low concentrations for the latter to elicit a proinflammatory affect [420, 421]. The expression of HO in neurogenic induced ADSCs is undoubtedly due to oxidative stress however the prevention of cell death was not apparent (Figures 2 and 3). Its use as a potential marker indicating cellular distress and protection against oxidative induced death is useful in future studies to indicate stress in chemical inductions [419, 422].

The expression of GCLM has also been linked to a response to oxidative stress; however it has also been detected in high concentrations in muscle cells and lung epithelium undergoing hypoxic or oxidative stress [423, 424]. Some studies have linked GCLM to improving the antioxidative defence

in astroglial cells by enhancing hydrogen peroxide scavenging ability however this was also in the presence of a thyroid hormone [425], and modulation of the survival of astrocytes and neurons in the presence of reducing agents [426].

Similarly, the high expression of G6PD, like many of the other proteins in this cohort, has been linked to the oxidative stress response by maintaining a redox imbalance-induced apoptosis in a number of cell types [427, 428]. Studies in Parkinson's disease relating oxidative damage to neuronal cells in transgenic mice have shown a moderate increase in G6PD activity and an over expression and neuroprotective activity in aged animals [429].

Equally PTGS1 has been annotated by gene ontology to promote neuronal development and be induced due to oxidative stress. The mechanisms of which PTGS1 is expressed as a neuronal support protein or stress related protein are in response to different signals. The link PTGS1 has to neuronal development is directly associated with the moderate expression of the proinflammatory cytokines IL-1B and TNF-α [430, 431], which in this study has been previously mentioned to have near undetectable concentrations. Studies into the expression during oxidative stress has shown a high expression of PTGS1 from various cell types in the presence of DMSO [432, 433] which incidentally has also been used as an analogous neurogenic induction chemical [104, 196, 350, 351].

Chemically induced oxidative stress to cells has been linked to inhibiting the COX-1 and Cox-2 gene which directly affects the proliferation of cells and the high expression of PTGS1 [434]. Our findings and the supportive literature indicates that the ADSCs treated with BME neurogenic induction media are responding in a similar manner to other cells types experiencing an overexposure to chemicals which cause an imbalance to the redox state in cells.

Further, to the detected oxidative stress proteins, a variety of additional stress and shock related proteins were noteworthy to this study. HSPB11, which has been linked to an inflammatory response in certain diseases [435], was found to be uniquely and highly expressed in the 24 hour induced

ADSCs with none of its ten annotated interacting partners detected in our datasets. Minimal literature is available on the investigation of HSPB11's role in the stress response. Its presence in the induced ASDCs cannot be accounted for except in response to inflammatory cytokines or due to the oxidative stress experienced by the cells.

HSP-70 is a widely studied heat shock protein and has been found to be ubiquitously expressed in all organisms, linked to the control of cellular proliferation and maintenance during aging [436, 437]. One study into homologous stress related proteins in *Mytilus edulis* have shown a differential in temperature determines the level and sites of expression of stress-70-like proteins in tissue [438]. The over expression of HSP-70 has also been linked to the cell's response to toxic chemicals and the development of cancerous growth [439-441]. The purpose of HSP-70 is postulated to be involved in the protection of cells under thermal or oxidative stress by inhibiting the aggregation of damaged and unfolded proteins [442].

Similarly, HSPB1 and HSPE1 expression is increased when cells are in distress which includes thermal, physical and chemical stressors [443] (table 2). They are functionally similar to the HSP-70, also annotated in the inhibition aggregating damaged or stressed proteins [444]. Thus the high expression of heat shock proteins reveals that the ADSCs are being exposed to a prolonged period in traumatic, stress inducing conditions.

Numerous of the above stress related proteins have been linked to the maintenance or protection of neuronal cells experiencing oxidative stress, the remaining shock induced proteins are not related to neuronal cells and are dually expressed due to the extensive stress. While these proteins functions are to preserve the cells in this environment, the loss of approximately 50% of the cell population is alarming and indicates that the surviving cells expressing the detected proteins may in fact be damaged by the induction process.

A shorter treatment may initiate the induction toward a neurogenic differentiation, as an exposure of more than 12 hours to the BME containing media is a stress inducing environment. Our findings essentially indicate that the produced cells may have had the potential for neurogenic differentiation due to the wide variety of neuronal related proteins expressed and detected. However the high abundance of up regulated stress related proteins and high cell death indicates the cells are being damaged. This suggests the culture conditions for inducing ADSCs toward a neurogenic linage with BME is not conducive to producing complete neuronal cells. Nonetheless, the process and mechanisms which drives the cells to differentiate is the most important result acquired as this could be mimicked with much milder and non-toxic chemical cocktails.

3.4.3 Bioplex analysis and roles of cytokines in BME induced ADSCs

This study aimed to investigate the roles of the most significant expressed proteins in differentiating ADSCs which were treated with a published neurogenic differentiation media. The acquired soluble proteins from the treated cells were compared to basal ADSCs and a control glial cell, and the functional roles that the selected proteins have in the cells during crucial time points was explored. Through investigating the up regulated proteins whose role includes neuroprotection cellular remodelling, response to oxidative stress and shock and the down regulation of other functional proteins, the altered pathways and mechanisms involved in chemically induced neurogenesis could be elucidated. Two complimentary methods were utilised ITRAQ which was covered in previous sections and the Bioplex method which analyses the expressed cytokines in each sample.

Cytokines have a diverse range of roles in all cell types including neural development. Cytokines are functional at all development stages from the generation of the neuroepithelium to the controlled apoptosis in non-functional cells as well as functioning as neurotrophic factors for the repair and regeneration of cells [445]. Furthermore certain groups of cytokines, such as chemokines, regulate the directed growth and communication between radially migrating neuronal cells which give rise to mature neurons, glial, astrocytes and oligodedricytes [445]. Due to their relatively low abundance and the dynamic range of a proteome making their analysis by LC/MS challenging, isolating and

analysing these molecules was achieved utilising a Bioplex cytokine, chemokine and growth factor assay.

The Bioplex assay allows the relative quantitation and comparison of 27 secreted cytokines. Group clustering was carried out to identify the cytokines which responded with similar trends during the differentiation process. The clustering allowed the subdivision of the cytokines by trends into 6 distinct groups (Figure 6A-F).

Each cytokine group cluster was investigated in terms of their role in neurogenic differentiation, response to stress and concurrent functionality with other proteins. Group 1 consisted of IL-1ra, IL-2, Eotaxin and Rantes. The general trend observed in secreted concentrations for this group saw a decrease by approximately 75% within the first hour of induction. A recovery phase then followed 5 hours post-induction with concentration levels stabilised to below 50% of the basal levels over the remaining time points to the 24 hour end point. IL-1ra has not been widely studied in the area of neural repair as it is associated with anti-inflammatory and immune responses. It is broadly secreted from immune, epithelial cells and adipocytes and has been established as an inhibitor of hippocampal neurogenesis and CNS IL-1β activity [446, 447]. Hitherto, recent studies propose that IL-1ra functions synergistically between neural stem cells and immune cells in support of neurogenesis, functioning as a potent signal that induces neural stem cell proliferation and migration in the CNS [448]. Thus may play a role in transdermal differentiation of ADSCs to a neuronal like lineage. Its incremental increase in concentration in the context of this study may be beneficial to neurogenesis of ADSCs.

Animal studies have shown that decreased levels of IL-2 and Eotaxin can have a positive effect on neurogenesis in the hippocampus [449]. The chemokine Rantes has been linked to the neuronal protection and recovery from neuronal loss as a result of inflammatory conditions [450]. IL-2 knockout mice displayed an increase in neurogenesis in the PNS [451]. Furthermore the deletion of IL-2 caused a dysregulation of cytokines; such as IL-15, MCP-1, IL-6 and MIP-1α; produced by the CNS

which induced an increase in neurogenesis in the hippocampus [451]. The relative increase of IL-15, MCP-1, IL-6 and MIP-1α observed by Beck Jr *et al* [451] corresponds to a similar concentration increase, especially for IL-15 and IL-6, within our *in vitro* differentiation study.

The second group comprised of IL-15, IL-17 and GM-CSF presents a unique trend whereby the concentration levels decrease for the first 3 hrs subsequent to induction then were raised beyond the levels seen in the basal ADSCs. The levels increase gradually throughout the temporal analysis, surpassing the basal levels after 5 hours.

The role of IL-15 in neurogenesis has been linked to decreased levels of IL-2 [452]. Interestingly the two molecules, IL-2 and IL-15, are structurally similar and are able to bind to the same receptor, however the response elicited downstream is quite different in neurogenesis, where IL-2 is inhibitory and IL-15 promotes neurogenesis [451]. IL-15 has also been linked to neuroprotection in stroke cases, increasing the migration of glial cells to the site of damage due to oxidative stress [453].

IL-17 is a proinflammitory cytokine that acts synergistically with TNF-α and IL-1 [454, 455]. The role of IL-17 in the nervous system has not been explored in great detail. Recently a study by Chisholm *et al* [456] provided the first evidence that *in vitro* neurons treated with IL-17 showed neurite outgrowth independent of glial cell interaction. Furthermore the studies have shown that inflammation is vital in the regulation of neural stem cell maturation [452]. There is also now substantial evidence that GM-CSF functions as a neurotrophic factor and can induce differentiation and maturation of neural stem cells (NSCs) in a dose dependant manner *in vitro* [457, 458]. There is further evidence of *in vivo* neuronal repair and functional recovery as well as differentiation with induced NSCs and bone marrow derived stem cells (BMSCs) [459, 460].

All three cytokines within this group have direct links to neuronal growth, development and differentiation. The intriguing detail that these molecules are all secreted from cells that have been

directed toward a neuronal-like provides further evidence that neuronal differentiation by chemical stimulation may elicit a neurogenic response with the cell's experiencing increased oxidative stress.

The following three collections of cytokines; Group 3 (IL4, IL5, IL9, MIP-1a and MIP-1b), Group 4 (IL-7, IL13, PDGF, TNFα, MCP-1 and IFN-γ) and Group 5 (IL-8, IL-10, IL-12, and vEGF) share similar trends with slight variances that make each trend cluster unique. Generally all three groups share a similar fate whereby the concentration of the cytokines are highest in the basal non-induced ADSCs followed by a substantial decrease for the remainder of the temporal study. Group 3's identity is attributable to the decrease of cytokine concentration to a quarter of the basal levels from induction and incrementally increases over successive time points to approximately half the basal levels. Group 4's cytokines are the most extensively and uniformly depleted to minute fractions relative to their basal levels. Group 5 shares an analogous outcome with a slight resurgence to 1% of the basal levels at the final time point.

IL-4 and IFN-γ have been postulated to show signs of activation of microglia cells which may assist in the induction of NSCs, however no direct effect on neuronal differentiation has been recorded [461, 462]. Moreover, IL-4 has been linked to inducing oxidative stress in cells [463]. Further to this, IL-9 exacerbates brain lesions in mice and causes neuronal damage [464]. None of the remaining cytokines within Group 3 have been identified to have roles in neither neurogenesis nor response to cellular oxidative stress and thus it is unsurprising that their abundance declines. The slight increase in concentration in the later time points has been attributed to the massive cell death in which we suggest the lysed cells have lost their cytosolic contents to the assayed media.

The role of Group 4 in neuronal cells is reported to be exceptionally limited. Negative effects from cytokines such as IL-13 decreases the induction of COX-2 which plays an important role in neurogenesis [465]. It has also been established that TNF-α is a negative regulator of neurogenesis in the hippocampus [466]. The very single link in group 4 to neuronal development is MCP-1 which has one report of influencing adult NSC migration in a Boyden chamber [467] however there are no

other annotated effects on neurogenesis nor any protective roles in response to stress, which is reflected by the low concentrations over the entirety of the assayed time points.

The main role of cytokines in Group 5 is reported as neurogenic inflammation and cellular death [468-470]. The only member within this group with a somewhat positive function is VEGF which may play a protective and regulatory role in damaged mature neurons due to oxidative stress [471]. There has also been some links to neuronal development whereby VEGF, TGFβ and FGF introduced into *in vitro* cultures have induced axonal outgrowth in maturing neurons [471-474].

The final group consists of two molecules, IL-6 and FGF-basic, whose concentration levels are quite low at induction however at each time point thereafter a significant increase is observable (figure 6F). Both molecules have garnered wide attention due to their effects on neuronal differentiation and the maturation of stem cells [475]. IL-6 has been shown to induce neuronal differentiation in a variety of cells including neural stem cells, PC12 cells and neuroepithelial cells [476-479]. The presence of the IL-6 receptor complexed to IL-6 is a system that drives neurite outgrowth and survival and has been thought to induce nerve maturation and myelin sheath formation. Furthermore, the inflammation response and increased oxidative stress that occurs subsequent to brain injury that has been shown in IL-6-defiecent mice supports the link between IL-6 expression and a decrease in oxidative stress, assisting in cellular protection [480]. The role of FGF has been noted to direct oligodendricyte maturation [481]. Furthermore it is able to induce neuronal differentiation comparable to cells treated with nerve growth factor (NGF). The inclusion of FGF in ADSC-neuronal differentiation studies has also been carried out with cells exhibiting neuronal morphologies and up-regulation of neural-specific genes [292]. The relatively high abundance of IL-6 and FGF secreted by the treated ADSCs can play a supportive role in neuronal differentiation.

3.5.0 CONCLUSION

In conclusion the analysis of the proteome of BME treated ADCSs presents evidence of a directed differentiation toward a neuronal-like lineage cell type where the produced cells display an

extensive array of neuronal developmental proteins and mechanisms as well as a large cohort of stress and shock induced proteins. An extended exposure of any mammalian cells to high concentrations of reducing agents for extended periods of time will damage the cells, exemplified by the extensive cell death that occurs and the up-regulation of stress and protective proteins. Also, the unused excess chemical will non-preferentially reduce any protein it comes into contact with, leading to cellular stress events and eventually to apoptosis as seen in other cell types treated with reducing agents [197, 198].

The complementary results from the iTRAQ and Bioplex indicate the cells are producing a number of molecules which are involved in processes of neurogenesis and response to stress. However the molecules involved in neurogenesis are more in line with the neuroprotection and maintenance of cells under oxidative stress and subjected to inflammatory conditions. However these expressed proteins are considered to be early event levels and are producing cells that have a closer morphology and proteome to premature neuronal cells which await further stimulation to complete the differentiation process. This is supported by the identification of the some of the most abundant and statistically significant proteins identified, such as AHNAK neuronal specific protein which has been proposed, dependant on its localisation, to be an intermediary functional protein in a number of early neurogenic developmental and cellular restructuring processes [386-388, 390, 395]. Furthermore, the highly expressed brain isoform of the enzyme glutaminase is annotated as an early neuronal development protein which was found to be higher in the BME treated cells than the control GBCs.

The notion of an early neuronal-like cell is supported by the low amounts of GFAP in the BME treated cells; GFAP is only present in developed neurons. Cells in the process of neuronal development are predominately supported by Nestin instead of GFAP. The presence of stress and shock induced proteins however revealed the cells are indeed in a stressful environment that is

damaging the produced cells. This is evident by the expression of numerous oxidative stress response proteins such as G6PD, PTGS1, HSPB11, HSP-70, HSPB1, and HSPE1.

Furthermore the high cell death and presence of cytokines that are expressed in inflammatory and oxidative stressed environments indicate the BME treated cells are in being damaged by the long exposure in the chemical induction media. Therefore this suggests the culture conditions for inducing ADSCs toward a neurogenic linage with BME is not conducive to producing complete, fully functional neuronal cells. Nonetheless, the process and mechanisms which drives the cells to differentiate is the most important result acquired as this could be mimicked with much milder and non-toxic chemical cocktails yielding a higher population of neurongenic differentiated cells.

The future directions from this study, leads toward investigating chemical inducers that are non-toxic, biologically stable and have the capability of producing a high population of cells that resemble neuronal-like cells morphologically as well as presenting an array of neuronal proteins that support the development and growth in that lineage. The chemical treatment of the ADSCs would be evaluated in a similar fashion to this study, utilising the proteomics platforms of iTRAQ and Bioplex for an in depth view of the proteome changes of the induced cells. The knowledge accrued from this study will allow for the identification of numerous neurogenic and/or stress proteins to be quickly recognized.

Chapter 4

Proteomic analysis of human adipose derived stem cells during novel *in vitro* neuronal differentiation with cyclic ketamines

4.1.0 Introduction

Stem cell sciences have advanced to the point where it is now possible to provide a range of tissues and cell types to be used in transplantation for regenerative therapies for a wide variety of tissue and organ types [20, 21, 57, 122, 124, 174, 356, 482-485]. However and as previously mentioned, the production of neurons from stem cells has been more difficult, and therefore the application of stem cell technology to minimise impairments in neuronal function or the discovery of compounds capable of the same has been more limited [28, 193, 196, 295, 296, 350, 351, 377, 486].

To date, a range of stem cells including those found in cord blood, bone marrow and adipose tissue have been selected as starting materials from which differentiation along the neuronal lineage has been induced [104, 202, 293, 351, 487, 488]. Further, a range of factors and differentiation agents have been utilised including growth factors such asEGF, TGF-β), neurotrophin, neudesin or simple chemical additives such as;BME, DMSO and BHA [104, 350].

Numerous publications have attempted to show that stem cells can be differentiated into neurons. Sanchez-Ramos *et al* (2001) discusses the generation of neuron-like cells from human umbilical cord blood cells treated with retinoic acid and nerve growth factor [293]. Choi *et al*. 2001 discusses the generation of cells of neuronal phenotype from human cord blood cells using BME [193] and US patent no 7078230 [489] discusses the generation of neuronal cells from adipose tissue-derived stromal cells using retinoic acid. Each of the above mentioned differentiation techniques are associated with problems. Chapter 3 details the extent of proteomic changes occurring during the BME treatment of ADSCs. First, most of the techniques result in the production of cells that resemble neurons morphologically with only a few surface markers confirmed but no indication of whether the cells are functional, such as being able to transmit an action potential. Second, some of the listed agents used for differentiation are toxic and cannot be used clinically as seen with chapter 3 analysis of the effect of BME on ADSCs and their considerable stress response after 24 hours of

treatment. Third, many of the techniques utilising growth factor additives require extensive and complex culture over a period of weeks which produced cells that are not suitable for clinical applications. Furthermore, the growth factor additive techniques have shown a low success rate in terms of the amount of neuronal cells produced [100, 195, 490].

It would be advantageous to be able to provide cells that are highly similar to neurons using a technique that does not involve toxic chemicals, nor xenogenic growth additives, that enables relatively simple induction and culture with a reasonably high production rate of relevant cells as compared to glial cells.

This study aims to at least minimise one or more of the above mentioned problems or limitations, or to provide an alternative approach to the formation of cells having neuron-like properties. UtilisingADSCs this work aims for the production of a cell population that is morphologically and phenotypically similar to a neuronal cell. The produced cells will be analysed in comparison to the BME ADSCs by investigating the current literature neuronal cell markers for consistency and since a global proteome analysis will be conducted numerous pieces of evidence that neuronal cells are being produced is also anticipated.

Prior studies of inducing stem cells toward a neuronal phenotype most commonly utilised sulphur containing reducing agents or strong antioxidants such as BME, DMSO and BHA or similar compounds. The work in the previous chapter shows these chemicals as having a strong effect on reduction pathways and decreasing oxidative stress, thus acting as the instigating factor driving the shift from stem cells toward a neuronal-like phenotype.

In the work presented in this chapter, biologically stable and non-toxic chemicals with analogous effects on MSCs to the above mentioned chemicals have been examined for their potential to drive ADSCs towards a neuronal phenotypic differentiation were investigated. Numerous chemical cocktails were trialled and the optimum cocktail concentration was then selected as it eventuated

cells with a neuronal visage determined by microscopy. The derived cyclic ketamines (CK) additives; lanthionine ketamine (LK), lanthionine ketamine ethyl ester (LKEE) and S- aminoethyl-L-cysteine ketamine (AECK) established the optimal results with cells that resembled neuronal cells morphologically. The rationale behind testing these chemicals is that they are reducing agents like BME however are non-toxic at the tested concentrations.

Briefly, CKs are cyclic sulphur-containing reducing agents that are naturally found in the brain and CNS and have been reported with possessing pro-neuronal growth properties [491-493]. CKs basic chemical structure resembles a modified version of the amino acid proline as shown in figure 1 as LK and AECK. The two R-groups allow for a wide variety of synthetic and semi-synthetic side chain additions for example branched-chain alkyl groups and cycloalkyl (alicyclic) groups. The groups, $–CH_3$, $–CH_2CH_3$, $–CH_2CH_2CH_3$, $–CH(CH_3)_2$, $–CH(CH_2)_2$, $–CH_2CH_2CH_2CH_3$, $–CH(CH_3)CH_2CH_3$, $–CH_2CH(CH_3)_2$, $–C(CH_3)_3$, $–CH_2C(CH_3)_3$, cyclopentyl, and cyclohexyl, are all cases of heteroatom-unsubstituted alkyl groups.

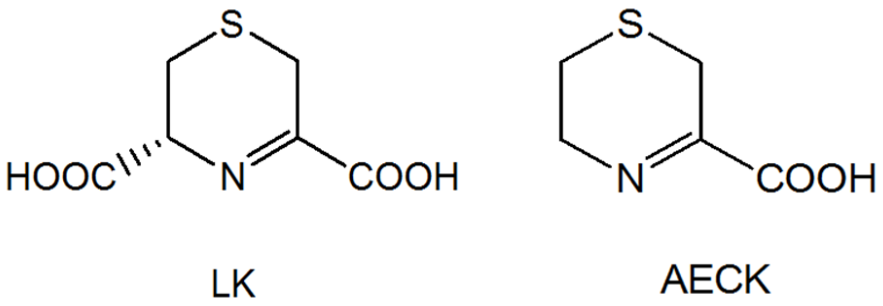

Figure 1: General structures of cyclic ketamine are sulphur-containing cyclic compounds. The CKs for use in the present investigation are the compounds above as chemical structure of Lanthionine Ketamine (LK) and structure of S- aminoethyl-L-cysteine ketamine (AECK).

The modification of R-groups is one aspect for improved delivery of CKs to target cells, to allow their delivery through cell membranes and/or cause enhanced permeability through the blood brain barrier (BBB). Previous work has accomplished improved delivery through the esterification or amidation of the carboxyl groups in compounds based on LK (fig 1) [494, 495]. These ester- and

amide-containing compounds provide an optimal balance of hydrophobic/hydrophilic character, allowing these compounds to penetrate cell membranes and to reach the intracellular targets of action. In some incarnations, ester- and amide-containing compounds have an improved ability to pass through the BBB, which is required for the treatment of most CNS disorders [496, 497]. In some of these embodiments, the ester- and amide-functionalised compounds have functional groups in the R_l and/or R_2 positions that interact with BBB-specific transport mechanisms. For example, an ascorbyl derivative of the compounds can be expected to take advantage of BBB ascorbyl transporters. Also, certain amino acid ester- or amide-containing compounds are expected to be readily transported across the BBB by means of BBB transport enzymes.

Previous studies with LK and LKEE have had some to links to neurotrophic activity, promoting process extension from neurons *in vitro* and have been indicated to protect neurons against oxidative stress [498]. While lanthionine-related compounds have been used for treatment of inflammatory disease [499] and display antioxidant, neurotrophic, neuroprotective and neuritigenic activity [500], the capacity of these molecules to cause formation of neuronal cells is unknown. The neurogenic effect on adult stem cells has not been investigated. This is the first study detailing a novel application of CKs in developing neuronal-like cells from patient acquired adipose derived stem cells and the effect of which is being measured using a comprehensive global proteome wide approach.

This study investigates the proteomic changes of treating stem cells with a CK and CKR under conditions permitting the formation of a cell having neuronal-like morphological appearance consistent with previous studies. As demonstrated in the previous chapter, analysis of the proteome of the differentiated cells will give a deeper insight into whether these cells are neuronal or simply neuron-like with a significant stress response.

4.2.0 Materials and Methods

4.2.1 Cell Culture

4.2.1.1 Human adipose derived stem cells harvest and cell culture

This research was approved by the Macquarie University human research ethics committee (Ref #: 5201100385). Adult ADSCs were derived from lipoaspirates and subsequent steps were conducted under sterile conditions in a class II laminar flow hood (Clyde-Apac BH2000 series). Lipoaspirates were rinsed twice in D-MEM (Gibco. The sample was then minced with a pair of scissors briefly till a fine slurry was formed and the connective tissue digested with collagenase type 1 (Gibco) for 45 minutes at 37 ^{o}C. The suspension was then centrifuged at 1600g for 10min at 4^{o}C to separate adipocytes from the SVF. Three layers are seen above the pellet. The upper most layer is the free lipid and appears as a clear/white colour, the middle layer is a very small portion of undigested adipose, and the lower layer a red digestion solution. These layers were carefully decanted to leave the pellet containing a variety of cell types. The pellet was resuspended in 3ml of D-MEM and layered on top of 3ml of Ficoll Paque PLUS (Sigma-Aldrich). Centrifugation at 1600g for 20min was performed to remove red blood cells from the SVF. The ADSCs were then removed from the interface between the Ficoll and D-MEM. 8ml of D-MEM was then added to dilute residual Ficoll. The cells were washed twice in D-MEM and centrifuged at 1000g for 10min. Upon completion of the final wash, the pellet is resuspended in D-MEM Glutmax/F12 (Gibco) with 10% Foetal Bovine Serum (FBS, Invitrogen) and 1% Antibiotics/Antimycotics (ABAM, Invitrogen). 2mL of the suspension was then aliquoted into a T25 culture flask (Nunc) and incubated at 37^{o}C at 5% CO_2 for 2 days until ADSCs adhered to the culture flask. Non-adherent cells are eliminated by replacing the media. ADSCs were passaged 3-5 times by stripping cells with TrypLE Express (12604 Gibco) before utilised in differentiation experiments.

4.2.1.2 Chemical induction for differentiation

Subconfluent ADSCs were washed twice in pre-warmed sterile D-MEM/F12 (Invitrogen). The cells were then cultured for a further 24 hours in a serum-free pre-induction medium consisting of D-MEM/F12 (Invitrogen), ABAM (Invitrogen) and 10% of the final concentration of the added Ketamine. The media was then replaced after 24hrs with the neuronal inducing media consisting of D-MEM/F12 (Invitrogen), ABAM (Invitrogen) and 0.5 mM AECK, or 0.6 mM LK, or 0.3 mM LKEE or 10 mM β-mercaptoethanol (Sigma) as per Woodbury *et al*., (2000).

4.2.1.3 Glialblastoma Cell culture

GBC line was cultured in neurobasal media supplemented with B27 and 0.5 mM Glutamine (Gibco). The cells were grown to 90% confluence prior to passaging or harvesting for proteomics.

4.2.2 Microscopy

4.2.2.1 Cell counts

In vitro cell counts were carried out utilising a novel procedure to determine the approximate colony forming units per square millimetre of cells adherent to the culture flask which were induced for differentiation and subsequently utilised for proteomics. A grid of squares 2.5 mm x 2.5 mm was printed on a transparent laminate and cut to fit outer bottom side of a T175 culture flask (BD Falcon). Spanning the temporal differentiation ten squares were chosen and cells counted at the objective of 100X on an Olympus CK40 inverted microscope the cell counts from the ten squares were averaged for each flask to find a mean total cfu/mm^2. The cell numbers from the ten squares were averaged and then multiplied by 28000 (16*10*175) to find the total cell population in the

T175 culture flask. To find cfu/mm^2 the average cell number from the ten squares were divided by 2.5 mm. At the final time point cells were removed from the culture flask and an aliquot was stained with trypan blue to determine live/dead ratio using a Neubauer chamber. The total cell number data was also utilised in the Bioplex analysis to determine the amount of cytokines secreted per cell. This was calculated by multiplying the concentration by the total volume of the flask and dividing by the total cell number at the respective time point.

4.2.2.2 Histological stains

Haematoxylin is basic stain that stains basophilic structures and is generally used as nuclei stain, producing a deep purple to blue colour. In conjunction with haematoxylin, eosin is used as a membrane counter stain which stains acidophilic structures red. Following general fixation in 4% formaldehyde slides with cells were flooded with haematoxylin [Sigma, H3136 haematoxylin 6 g, absolute alcohol 300 ml, distilled water 300 ml, glycerol 300 ml, glacial acetic acid 30 ml, ammonium or potassium aluminium sulphate 30 g and sodium iodate 0.9 g] for 5 minutes, rinsed in water for 30 seconds and the slide submerged in acid alcohol for 15 seconds to remove excess stain. This was followed by a 30 second rinse in water, submersion in Harris bluing agent [0.5% w/v sodium acetate in distilled water] for 2 minutes another rinse in water before counterstaining with Eosin Y (2% v/v in distilled water) for 30 seconds. The slide was then dehydrated by 30 second submersions in 75%, 95% and then 100% ethanol before the slide was sealed with clear xylene for 5min followed by the addition of a coverslip. Stained cells were visualised on an Olympus IX51 inverted microscope and images captured with the attached Olympus DP70 camera.

4.2.3 Protein extraction

Harvesting cells for proteomic analysis by LC-MS/MS or iTRAQ and Western blot were generally completed at the desired end time point as per the following. Aspiration and collection of expended media for Bioplex analysis was followed by rinsing the cells with excess pre-warmed DMEM/F12 to

dilute out and remove FBS components. The cells were then exposed to TrypLE Express (Invitrogen) for 10-15 minutes at 37 ^{o}C. Cells were then collected in 10 ml DPBS, gently inverted to rinse cells, then centrifuged at 1000 x g for 10 minutes. The DPBS washes were carefully decanted not to disturb the pellet. The cells were resuspended again gently in DPBS to rinse and centrifuged again at 1000 x g for 1 minutes. The DPBS was decanted and the cells were resuspended in 200 µl of 1% SDS and sonicated for 10 minutes for 1-DE SDS-PAGE or an extraction buffer (1% (w/v) C7bz0, 2 M Thiourea, 7 M Urea, and 40 mM Tris-HCl pH 8.8) for 2-DE electrophoresis . Lysates were centrifuged at 16000 x g for 10minutes to pellet cell wall debris. The lysed cell's proteins were then reduced and alkylated with 10 mM TBP (Sigma) and 20 mM Acrylamide (Sigma) for 90 minutes at room temperature [283]. Insoluble material was removed by centrifugation at 16000 x g for 10 minutes and the pellet was discarded. The supernatant was removed and the proteins were precipitated in five volumes of acetone for 30 minutes at room temperature. The precipitate was centrifuged at 4000 x g for 10 minutes, the acetone decanted and the pellet was left to air dry briefly prior to resuspending in 100µl of 1% SDS (1-DE) or extraction buffer without Tris-HCl (2-DE). All samples were assayed to determine protein concentration using 1-DE SDS-PAGE and densitometry. Protein concentrations were approximated against serial dilutions of 1 mg/mL BSA. BSA dilutions along with neat and 1:10 diluted samples underwent 1D SDS-PAGE though only electrophoresed for 5 minutes at 160 V, keeping all proteins stacked in a single band, before fixing the gel and staining with Flamingo (BioRad). Concentration was measured using densitometry available through QuantityOne software (BioRad). Each sample was diluted to 100 µg/100 µl. Samples were then frozen in liquid nitrogen and stored at minus 80 ^{o}C till required.

4.2.4 1D Electrophoresis

Samples were diluted 1:1 with LDS loading buffer (Invitrogen), heated at 95^{o}C for 10 minutes then centrifuged. Samples were then loaded into 4-12% Bis-Tris Criterion gel (BioRad) in XT-MES (BioRad)

running buffer then electrophoresed according to the standard product protocol of 160V for 50 minutes (BioRad). Upon completion of electrophoresis, unless required for western blot (see section 2.5), gels were placed in fix solution (40% methanol and 10% acetic acid) and incubated on a gentle rocker at room temperature for 60 minutes. Gels were then placed in Flamingo fluorescent protein stain (BioRad) and incubated for 60 minutes. Gels were imaged using a PharosFX Plus (Biorad) imager and Quantity One software (BioRad). The gel was then placed in Coomassie Blue G stain overnight, post staining a solution of 1% acetic acid to remove background stain. The gel was then scanned with an Epson Perfection 4800 document scanner.

4.2.5 Two -Dimensional SDS-PAGE (2-DE)

All protein extraction was performed in the procedure outlined in section 2.3 and isoelectric focusing performed using a modified method from Jobbins *et al* [284]. The whole cell lysates protein extract was separated in the first dimension on an IPG strip (11 cm, pH 4−7 or pH 3−10, BioRad) for at least 100kVhours. The focused IPG strip was equilibrated in 2% (w/v) SDS, 6 M Urea, 250 mM Tris-HCl (pH 8.5) and then separated in the second dimension on a 4−12% Bis-Tris gel using the MES buffer system at 160 V. Following separation and fixation, gels were visualized by staining with either Flamingo Fluorescent Gel Stain (BioRad, Australia) or Coomassie Blue G-250 [284]. A differential display analysis utilising PDQuest (BioRad) software was utilised to identify difference in 2D-gel profiles.

4.2.6 Protein band excision and extraction for in-gel trypsin digestion and LC-MS/MS

Gel bands (1D) or spots (2D) stained with Coomassie Blue G250 were excised and destained with 50% acetonitrile (ACN) in 50 mM ammonium bicarbonate until the blue colour was no longer visible. Gel pieces were then dehydrated with 100% ACN for 5 minutes before removing ACN. Reduction and

alkylation was then carried out by incubating the gel pieces with 100 µL 5 mM TBP and 20 mM acrylamide in 100 mM Am for 90 minutes. The solution was discarded and gel pieces washed first with 100 µL 100 mM ammonium bicarbonate and then twice with 50% ACN in 50 mM ammonium bicarbonate followed by dehydration with 100 µL ACN. Once the gel pieces had shrunk and turned noticeably white, Trypsin Gold, MS grade [Promega USA] in 100 mM ammonium bicarbonate (12.5 ng/µL) was added and left to incubate for 30 minutes at 4^0C. The sample was spun briefly and more 100 mM NH4HCO3 added to cover the pieces before digestion overnight at 37^0C. Peptides were extracted by sonicating briefly and transferring the digestion solution into a new tube. To the gel pieces 50% ACN and 2% formic acid was added and incubated for 20 minutes before sonicating again and removing the liquid to combine with initial digest solution. This last step was repeated before the digestion solution was concentrated to approximately 15 µL using a VacufugeTM Concentrator 5301 [Eppendorf Germany] and then centrifuged at 14,000 xg for 10 minutes. The solution was then transferred to an autosampler vial for LC-MS/MS analysis.

Once samples were prepared for analysis, all subsequent MS operations were performed by Dr Matt Padula from the Proteomics Core Facility at UTS using the Tempo/QSTAR Elite system and standardized automated methods. Samples were placed onto the autosampler of a TEMPO^{TM} nanoLC system [Eksigent USA] and loaded at a rate of 20 µL per minute onto a Michrom reverse phase trapping cartridge before eluting onto a 75 µmID X 150 mm PicoFrit column [New Objective, USA] packed with Magic C18AQ chromatography resin [Bruker-Michrom, USA]. Peptides were separated using an increasing gradient of ACN at 300 nL/minute and ionised at 2300 V by the Microlonspray II head into the source for the QSTAR EliteTM Quadrupole TOF MS [Applied Biosystems/MDS Sciex]. The QSTAR performs IDA to analyse ions transmitted through the first quadrupole to the TOF analyser. If a multiply charged ion (2-5+) was detected at greater than 30 counts per scan, the ion was selected and transmitted to the second quadrupole collision cell to be fragmented and the fragment masses measured by the TOF analyser.

The MS/MS data files produced by the QSTAR were searched using Mascot Daemon (version 2.3.02, provided by the Walter and Elisa Hall Institute, Parkville, Vic. Perkins, D.N. 1999) and searched against the LudwigNR database (comprised of the UniProt, plasmoDB and Ensembl databases (vQ212. 19375804 sequences, 6797271065 residues) with the following parameter settings: Fixed modifications: none; Variable modifications: propionamide, oxidised methionine, deamidated asparagine and glutamine; Enzyme: semitrypsin; Number of allowed missed cleavages: 3; Peptide mass tolerance: 100 ppm; MS/MS mass tolerance: 0.2 Da; Charge state: 2+ and 3+. The results of the search were then filtered by including only protein hits with at least one unique peptide and excluding proteins identified by a single peptide hit with a p-value > 0.05.

4.2.7 Western blot

The Western blot method as adapted from Jobbins *et al*., 2010 [284], buffers were prepared as follows: 2 blot papers (BioRad) soaked in Buffer 1 [40 mL 10X stock (400 mM amino-caproic acid, 250 mM Tris), 40mL methanol, 1 mL 20% SDS, 400 mL dH2O], 2 blot papers were soaked in Buffer 2 [20 mL 10X stock (250 mM Tris), 40mL methanol, 200 mL dH2O] and 1 blot paper was soaked in Buffer 3 [10 mL 10X stock (3 M Tris), 100 mL dH2O]. Post 1D-SDS-PAGE of whole cell lysates as prepared in section 2.3, the gel was rinsed for 1 minute in deionised water then equilibrated in buffer 1 for 5 minutes. A piece of PVDF membrane (Bio-Rad) was cut to the same dimensions as the gel and placed in methanol for 2 minutes prior to equilibration in Buffer 2. The Western blot stack was assembled within an Owl HEP-1 Semi dry electroblotting cassette (Thermo Fisher Scientific) with Buffer 1 soaked papers at the cathode base, then the gel, PVDF membrane, Buffer 2 soaked papers, and lastly Buffer 3 soaked paper under the anode top. The stack was rolled to remove excess buffer and any potential air bubbles and run at 300 mA for 30 minutes. Once the gel was electrophoretically transferred, the membrane was washed in PBS with 0.1% Tween [Bio-Rad, USA] for 20 minutes and then blocked with PBS, 0.1% Tween and 5% skim milk powder for 60 minutes to prevent non-

specific antibody binding. The membrane was then placed in a solution containing the one of the following primary monoclonal antibodies: mouse anti-human NeuN/Fox3 (M377100 Biosensis 1:5000), mouse anti-human NF200 (M988100 Biosensis 1:500), rabbit anti-human ϐ-TB3 (ab18207 Abcam 1:1000) or rabbit anti-human GFAP (ab7260 Abcam 1:50000) diluted in PBS respectively and incubated overnight at 4^{o}C on a gentle rocker. Subsequently washed 3 times with PBS and probed with a secondary antibody either and anti-mouse IgG (A4416 Sigma) or anti-rabbit IgG (A4312 Sigma) dependant on the primary probe. Both secondary antibodies were alkaline phosphatase conjugated for development with BCIP/NBT (Sigma).

4.2.8 Bioplex

ADSCs and differentiation secretion samples were collected at time 0 minute as a control and at 30 minutes, 60 minutes, 3 hourrs, 5 hours, 20 hours and 24 hours subsequent to adding the differentiation media for assay. Concentrations of IL-1ra, IL-1b, IL-2, IL-4, IL-5, IL-6, IL-7, IL-8, IL-9, IL-10, IL-12(p70), IL-13, IL-15, IL-17, Eotaxin, FGF basic, G-CSF, GM-CSF, IFN-γ, MCP-1, MIP-1a, MIP-1b, PDGF-bb, RANTES, TNF-α and VEGF were simultaneously evaluated using a commercially available multiplex bead-based sandwich immunoassay kits (Bioplex human 27-plex, M50-0KCAF0Y Bio-Rad Laboratories). Assays were performed according to the manufacturer's instructions. Briefly, 27 distinct sets of fluorescently dyed beads loaded with capture monoclonal antibodies specific for each cytokine to be tested, were used. Secretion samples (50 µl/well) or standards (50 µl/well) were incubated with 50 µl of pre-mixed bead sets into the wells of a pre-wet 96 well microtitre plate. After incubation and washing, 25 µl of fluorescent detection antibody mixture were added for 30 min and then the samples were washed and resuspended in assay buffer. High standard curves for each soluble factor were used, ranging from 2.00 to 32,000.00 pg/ml and the minimum detectable dose was <10 pg/ml. The formation of different sandwich immunocomplexes on distinct bead sets was measured and quantified using the Bioplex Protein Array System (Bio-Rad Laboratories). A 50 µl

volume was sampled from each well and the fluorescent signal of a minimum of 100 beads per region (chemokine/cytokine) was evaluated and recorded. Values presenting a coefficient of variation beyond 10% were discarded before the final data analysis [285].

4.2.9 iTRAQ

After cell lysis and protein extraction (Section 2.3) the total of 8 samples for iTRAQ labelling (1 – ADSCs, 2 – AECK treated hADSC, 3 – LK treated hADSC and 4 - Glioblastoma control (GBCs) in duplicate runs **B** and **C** were buffer exchanged in 0.1% SDS using a Tris free Micro Bio-Spin Chromatography Columns (BioRad) and made up to a final concentration of 60ug/100uL each. The labelling method and MS/MS run parameters are outlined below.

Instrument

Mass spectrometer: TripleTOF 5600 (AB Sciex). NanoLC system: Eksigent Ultra nanoLC system (Eksigent). Analytical column: SGE ProteCol C18, 300Å, 3µm, 150µm x 10 cm. SCX HPLC: Agilent 1100 quaternary HPLC system with Polysulfoethyl A 100mmx2.1mm 5um 200Å column.

Sample preparation

300uL of 0.25M TEAB was added to each sample. The samples were then reduced with TCEP), alkylated with Methyl methanethiosulfonate (MMTS) and digested with trypsin. The digested samples were labelled according to the list below:

Sample name iTRAQ label

Run B

1 - 114 Basal hADSC

2 - 115 AECK Differentiated ADSCs

3 - 116 LK Differentiated ADSCs

4 - 117 Glialblastoma control (GBCs)

Run C

1 - 114 Basal hADSC

2 - 115 AECK Differentiated ADSCs

3 - 116 LK Differentiated ADSCs

4 - 117 BME Differentiated ADSCs

Strong cation exchange HPLC

The labelled samples were fractionated by SCX HPLC. The buffer A was 5 mM Phosphate 25% Acetonitrile, pH 2.7 and buffer B was 5 mM Phosphate 350mM KCl 25% Acetonitrile, pH 2.7. The dried iTRAQ labelled sample was resuspended in buffer A. After sample loading and washing with buffer A, buffer B concentration increased from 10% to 45% in 70 minutes and then increased to 100% and remained at 100% for 10 minutes at a flow rate of 300 ul/min. The eluent was collected every 2 minutes at the beginning of the gradient and at precisely every 4 minutes interval thereafter.

NanoLC ESI MS/MS data acquisition

The SCX fractions were resuspended in 100 µL of loading/desalting solution (0.1% trifluoroacetic acid and 2% acetonitrile 97.9% water). Sample (40µL) was injected onto a peptide trap (Michrom peptide Captrap) for pre-concentration and desalted with 0.1% formic acid, 2% ACN, at 5 µL/min for 10 minutes. The peptide trap was then switched into line with the analytical column. Peptides were eluted from the column using a linear solvent gradient, with steps, from mobile phase A: mobile phase B (98:2) to mobile phase A:mobile phase B (65:35) where mobile phase A is 0.1% formic acid and mobile phase B is 90% ACN/0.1% formic acid at 600 nL/min over a 100 min period. After peptide elution, the column was cleaned with 95% buffer B for 15 minutes and then equilibrated with buffer A for 25 minutes before the next sample injection. The reverse phase nanoLC eluent was subject to positive ion nanoflow electrospray analysis in an information dependant acquisition mode (IDA). In IDA mode a TOFMS survey scan was acquired (m/z 400 - 1500, 0.25 second), with the ten most intense multiply charged ions (counts >150) in the survey scan sequentially subjected to MS/MS

analysis. MS/MS spectra were accumulated for 200 milliseconds in the mass range m/z 100 – 1500 with the total cycle time 2.3 seconds.

4.2.10 Data processing

The experimental nanoLC ESI MS/MS data were submitted to ProteinPilot V4.0 (AB Sciex) for data processing using *Homo sapiens* species. Bias correction was selected. The detected protein threshold (unused ProtScore) was set as larger than 1.3 (better than 95% confidence). FDR (False discovery rate) Analysis was selected. Volcano plots, Gene ontology and Bioplex heat maps were generated using DanteR.

4.3.0 RESULTS

4.3.1.1 Microscopy

The treatment of ADSCs with the CK and CK derivatives was conducted with the intention of producing cells that morphologically and phenotypically resemble neuronal cells. A microscopy analysis allowed for the evaluation of the morphological changes produced during the induction. Initially multiple flasks of human ADSCs were cultured and maintained in a monolayer until 85-90% confluence. These were then were sub-cultured up to three times producing a morphologically homogenous culture with cells exhibiting the spindle-fibroblastic form consistent with current literature [28, 104].

All culture vessels were maintained at sub-confluency prior to addition of differentiation media containing either AECK, LK, LKEE or BME as per Woodbury *et al*., [104]. Figure 2 A-D and Figure 2 A-D shows the rate of cellular response over a 24 hour period subsequent to the addition of the novel neurogenic differentiation media. Time points imaged for the AECK and the LK treatments were 0 hours, 3 hours, 5 hours and 24 hours. Figure 2A and 3A are the same basal image of non-treated

basal ADSCs presenting the general growth pattern and morphology appearing in a flat and fibroblastic arrangement. Figures 2B-D are the time points 3 hours, 5 hours and 24 hours respectively of AECK treated ADSCs. The cells display minimal changes at 3 and 5 hours with minor cytoskeletal shifts and retractions. The cells appear to be marginally more slender than the basal cells whilst also producing a condensed nucleus. The final time point extended marked changes with a majority of cells assuming a bipolar contouring with a smaller population of approximately 20% showing evidence of process growth and neurite extension.

The BME treated cells in parallel for comparison presented the same features as seen in chapter 3. In summary the BME treated cells showed morphological changes were evident within 3 hours with signs of cytoplasmic retraction toward the nucleus of the cell. At 12 hours the cells morphological changes are ubiquitous across the cultured population with a majority of the cells presenting the retracted cytoplasm and multi-polar shape with evidence of extensions and processes reaching between cells. At the 24 hour time point the cells exhibit polar extensions and processes reaching between cells with some evidence of detachment [109, 202].

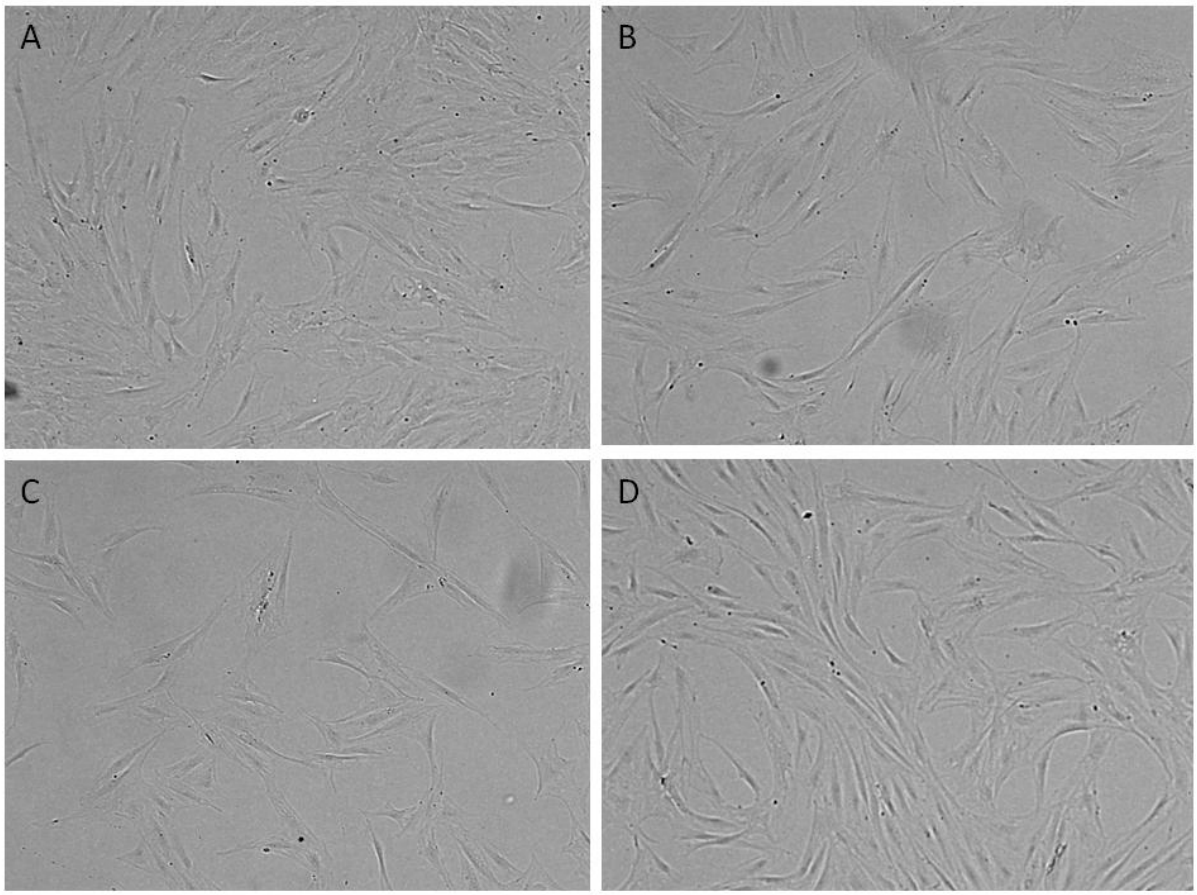

Figure 2 A. Basal human ADSCs *in vitro* culture (non-induced). B-D human ADSCs induced with 0.5 µM AECK time points captured at 3 hrs, 5 hrs and 24 hrs respectively. Time course shows minimal structural changes and some cellular contraction producing cells in D which are marginally more slender than those in A.

The LK treatment produced visually significant morphological changes over time. At the 3 hour time point, the cells are indistinguishable from the AECK treatment with minor cytoskeletal retractions toward the nuclei. Beyond the 5 hour time point (figure 3C) the strongest morphological changes from all trailed chemicals is visualised. The LK induced ADSCs are morphologically distinct and bear minimal to no resemblance to the parent basal ADSCs. Cells exhibit elongated membranes and are contracted displaying a bipolar architecture with multipolar extensions reaching between cells producing visible junctures as seen in Figure 3C. The final time point shows of the most expansive and uniform morphological differentiation within this study (figure 3D). Nearly 95% of cells appear to share the multipolar and dendrite extension character in a near network formation. A notable complimentary result is that cell death and detachment is almost undetectable in comparison to the BME treatments (Chapter 3).

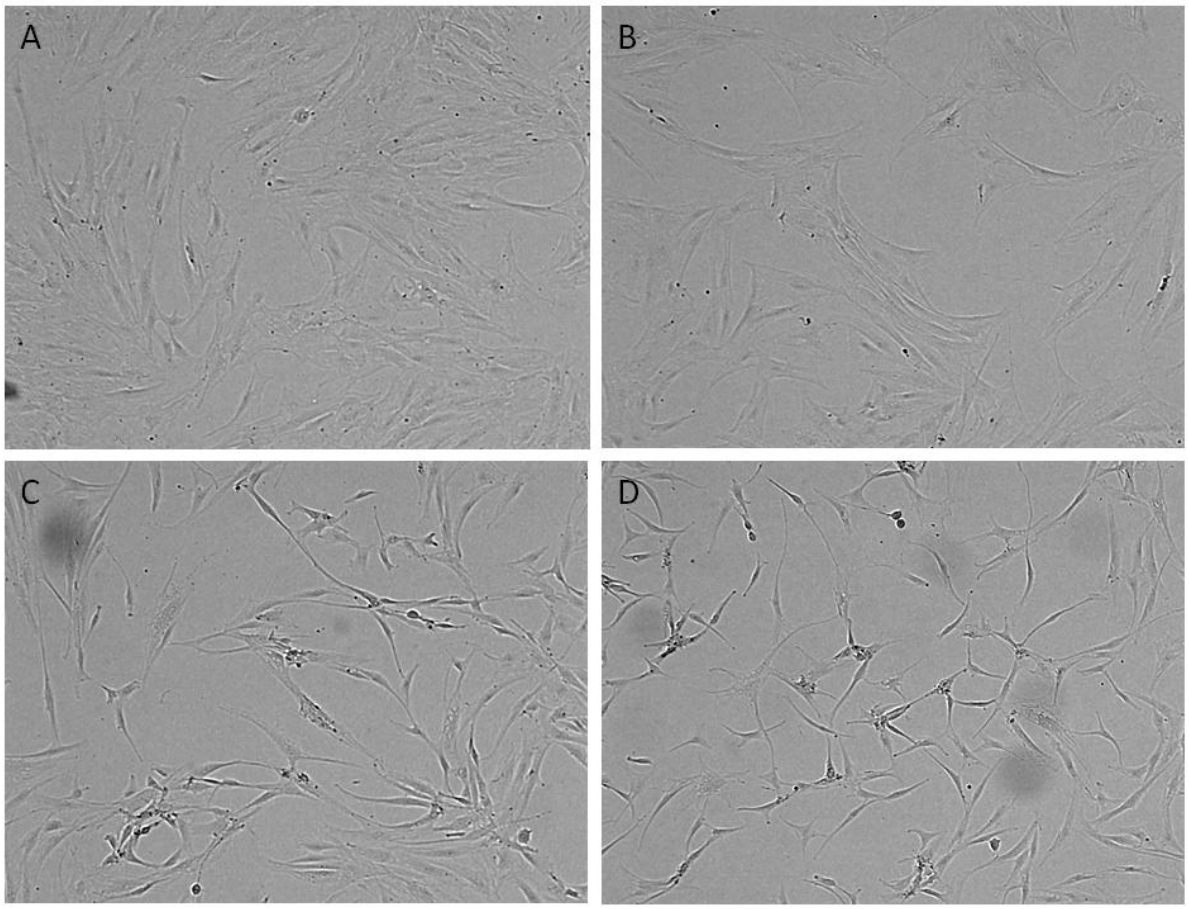

Figure 3A Basal human ADSCs *in vitro* culture (non-induced). B-D human ADSCs induced with 0.6μM LK time points captured at 3hrs, 5hrs and 24hrs respectively. Time course adequately exhibits large structural reconfiguration of ADSCs during differentiation. Cells display bipolar elongation, process and spindle formation.

4.3.1.2 Cell counts

The cell numbers from the ten squares were averaged and calculated to find the total cell population in the T175 culture flask. To find cfu/mm^2 the average cell number from the ten squares were divided by 2.5 mm. The total cell count and average cfu/mm^2 trends are identical presenting no change in cell population in the triplicate flasks from basal cells up to 60 minutes post induction.

The basal population counts averaged at 77 cfu/mm^2 or total population of 5.42E+06 cells. Subsequent to the AECK treatment, the population remained relatively unchanged in numbers within the AECK treatment with the population decreasing by approximately 5% overall in the final

time point (figure 4 and 5). At the final time point the total dead/live ratio was 1:116 i.e. an average of 0.10% of cells were stained blue with trypan.

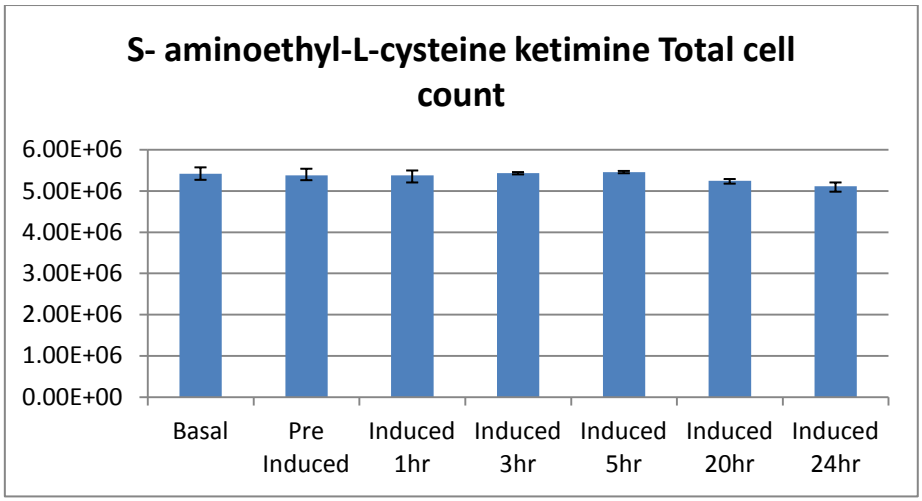

Figure 4 Average colony forming units per square millimetre of basal ADSCs and ADSCs treated with AECK over 24 hours

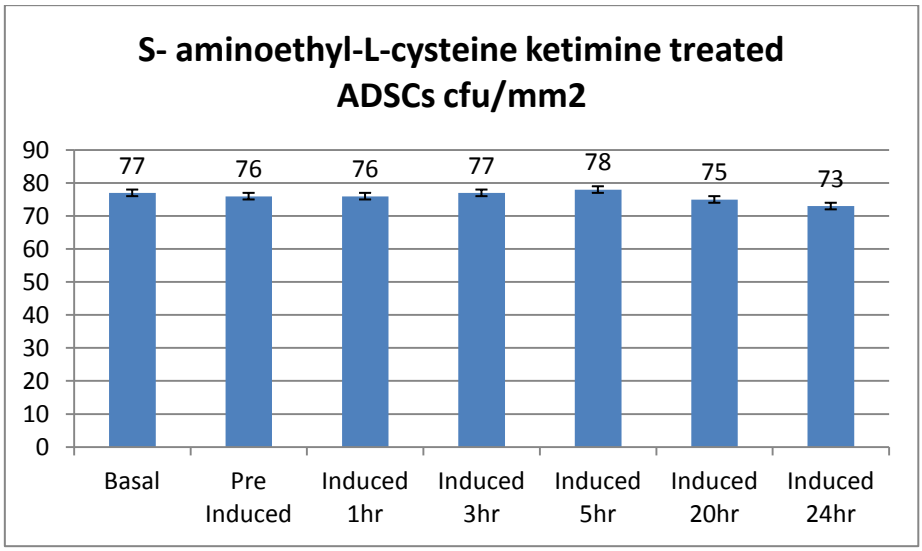

Figure 5 Average total cell count at each time point over the AECK treatment of ADSCs

Following treatment with LK, the population numbers were very similar to that of the AECK treatments up to 3 hours post induction. Successive time points after 3 hours exhibited minor decreases in the population averaging at 66 cfu/mm^2 or total population of 4.63E+06 cells (figure 6 and 7). This shows an approximate loss of 14% of cells over the differentiation period which is less

than the BME treated cells (Chapter 3). The harvested cells at the final time point presented a total dead/live ratio of 1:85 i.e. an average of 1.17% of cells stained blue with trypan which is 10-fold less than the BME treated cells in chapter 3.

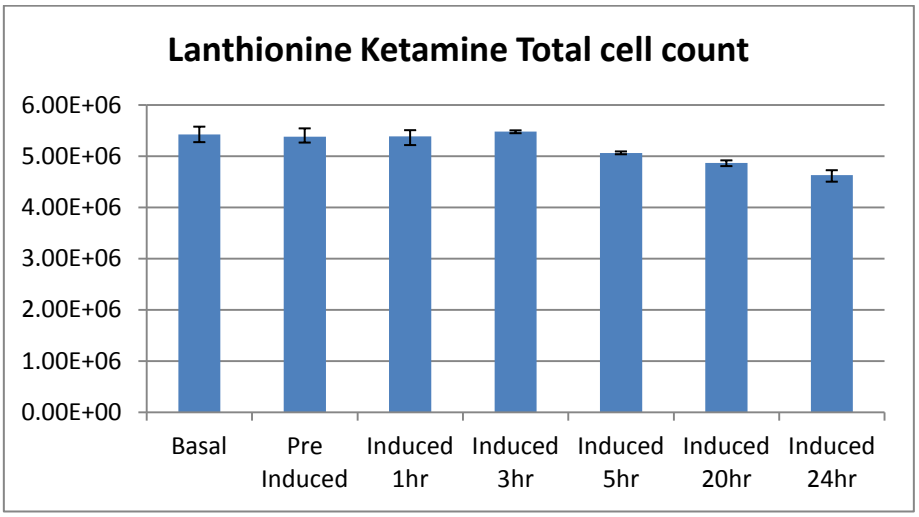

Figure 6 Average colony forming units per square millimetre of basal ADSCs and ADSCs treated with LK over 24 hours

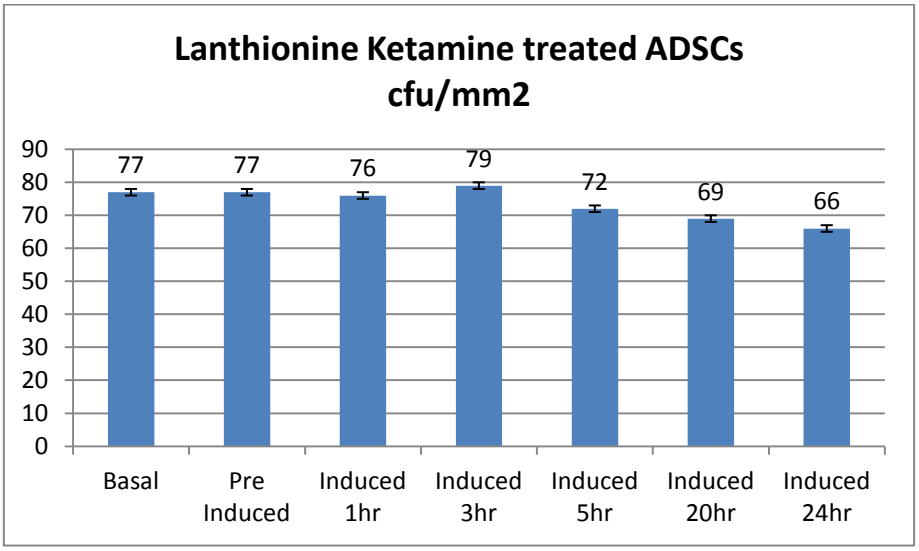

Figure 7 Average total cell count at each time point over the LK treatment of ADSCs

4.3.2 iTRAQ proteome comparisons of chemically induced hADSCs toward neuronal lineage

The digested proteins from each cell line were labelled with the iTRAQ isobaric tags as follows for Run B: hADSCs, AECK differentiated hADSCs, LK differentiated hADSCs and GBCs labelled with 114, 115, 116 and 117 isobaric tags respectively. Run C has hADSCs, AECK differentiated hADSCs, LK differentiated hADSCs and BME differentiated hADSCs labelled with 114, 115, 116 and 117 isobaric tags respectively.

The protein fold changes between samples were done comparatively and are relative to a base denominator. The base denominator chosen for the majority of the analysis was the basal hADSCs - 114, all comparisons were made relative to this, i.e. 115 vs 114, 116 vs 114 and 117 vs 114. This was done to elucidate the relative protein fold changes across the captured and labelled proteome of the differentiating cells, determining the up or down regulation of protein species over time during differentiation.

Table 1 summarises the iTRAQ results of the two iTRAQ runs B and C. The summary table shows the upper 99%, 95% and 66% cut off for detected proteins. The upper 95% range was chosen for all data analysis and, within that cutoff, Run B had a total of 2,430 proteins consisting 36,993 distinct peptides were identified from 178,574 spectra (appendix 2B). An average of 6.38 peptides was matched per protein with an average of 17.75% sequence coverage from the total cohort of the detected proteins. Run C had a total of 2,449 proteins consisting 32,613 distinct peptides were identified from 107,298 spectra (appendix 2C). An average of 8.61 peptides was matched per protein with an average of 17.06% sequence coverage from the total cohort of the detected proteins. The analysis cut off removed proteins with below the average peptides matched (i.e. 5 peptides/protein) to increase the robustness of the dataset and the conclusions drawn. The subsequent cut offs utilised were based on p-value (<0.05) and fold change ($\log_2$ <-0.2 or 0.2 >). These partitions refine

the later analyses to statistically significant proteins which have an average of 20 matched peptides per protein. The ProteinPilot group file, the protein summaries and peptide summary (without background corrections) were exported to XML format for further analysis with specified denominators for inter-sample comparisons through the generation of box and whisker plots, volcano plots and gene ontology graphs.

Table 1 iTRAQ of Run B hADSCs, AECK differentiated, LK differentiated and Glioblastoma cells Protein Pilot results. Run C hADSCs, AECK differentiated, LK differentiated and BME differentiated Protein Pilot results

	Unused (conf) Cutoff	**Proteins Detected**	**Proteins Before Grouping**	**Distinct Peptides**	**Spectra Identified**	**% total Spectra**
RUN B	**>2.0 (99)**	2108	2774	35891	176734	67.3
	>1.3 (95)	2430	3204	36993	178574	68.0
	>0.47 (66)	2741	5246	38381	180467	68.8
	Cutoff applied: >0.05 (10%)	3491	15271	41011	184078	70.1
	Unused (conf) Cutoff	Proteins Detected	Proteins Before Grouping	Distinct Peptides	Spectra Identified	% total Spectra
RUN C	**>2.0 (99)**	1916	2863	30725	104662	60.9
	>1.3 (95)	2449	3393	32613	107298	62.4
	>0.47 (66)	2540	3860	32916	107668	62.6
	Cutoff applied: >0.05 (10%)	2712	7600	33375	108222	62.9

4.3.2.1 Box and wisker plots of three separate iTRAQ experiments

The iTRAQ method allows for the isobaric labelling of all proteins in a sample for the relative quantification of single proteins across multiple sample types pooled together in a mass spectrometric global proteomic analysis. Figure 8 displays a non-parametric distribution of the identified data population of all labelled proteins from three separate iTRAQ experiments to compare datasets between separate runs. The division of the three experiments into A, B and C groups the cells types within that experiment. Experiment A is representative of the data collected from Chapter 3 in which the treatment of ADSCs with BME was investigated at two different time points along with a control GBC cell line. The experiments B and C include data collected specifically for this study with two biological replicates. Experiment B includes an internal control and biological

replicate of the GBCs for inter-iTRAQ run comparison and a similar scenario occurs in experiment C which includes ADSCs treated with BME for 24 hours acting as an internal control and a biological replicate. The dispersion and shape of the graphs boxes shows the similarity of the data sets, the importance of which is that similar shaped graphs are directly comparable. The data distribution for the ADSCs treated with BME, AECK or LK has a similar dispersion, while only the GBCs and the final BME treated ADSCs in experiment C has a larger skew. For the former it is expected due to the difference in cell lineage, as described in detail in chapter three, however the later, GBC and BME skew cannot be determined directly from this graph. The outliers in each plot are of particular significance since these are the most quantitatively changed proteins in the differentiation relative to the basal ADSCs.

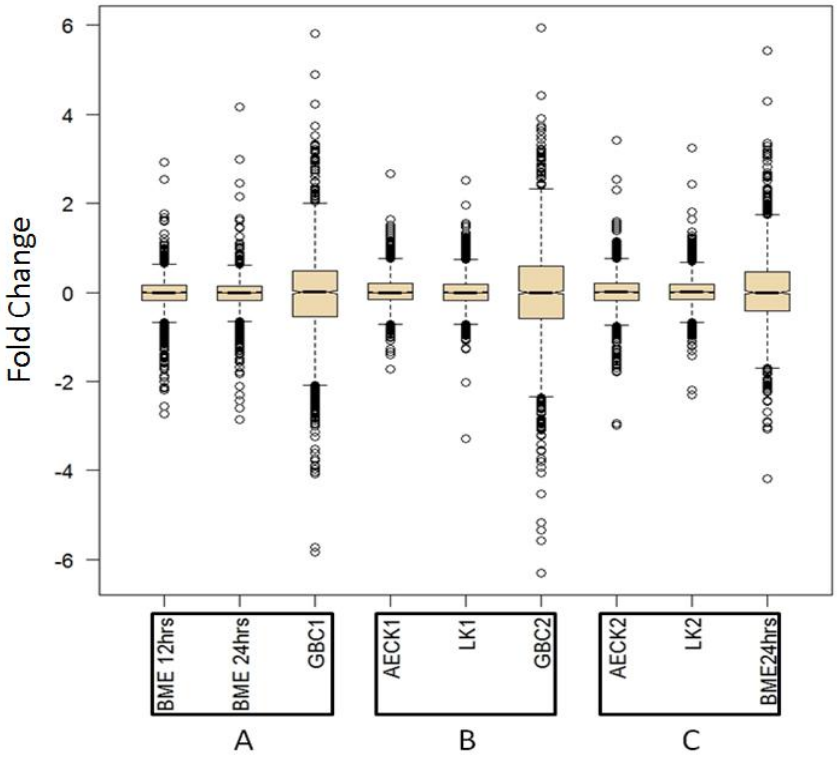

Figure 8 Box and whisker distribution and fold differential of three separate iTRAQ runs of ADSCs captured soluble proteomes subsequent to chemical induction toward neurogenic differentiation relative to basal non-induced ADSCs. A. ADSCs treated with BME for 12, 24 hours and control GBCs (from *Chapter 3)*. B. ADSCs induced with AECK or LK as experimental neurogenic differentiation and GBCs control for cross iTRAQ run comparison. C. Biological replicate of ADSCs treated with AECK or LK including a replicate of BME treated ADSCs for 24hrs for cross run comparisons.

4.3.2.2 Volcano plots, Venn diagrams and Gene Ontology graphs

Figure 9 and 10 are the comparative volcano plot layouts of the protein identifications of each iTRAQ replicate of ADSCs treated with either AECK or LK. The graphs show the expression differences by fold change (x-axis) and statistical significance by p-value (y-axis) of all captured and identified proteins compared to the basal ADSCs. The blue nodes represent the above > 0 log fold change up-regulated proteins and the below <0 fold change down-regulated proteins. The grey nodes represent the not significantly changed proteins with a P-value >0.05 and within the cut off for fold change. The representation of this data in this format is relevant to assess the range and extent of fold changes and statistical significance occurring across the entire global analysis in a single figure as well as trend comparisons between figures. This also allows for the selection of the most changed proteins in each plot and simultaneous comparison and position selection of the same protein in neighbouring plots, thus streamlining comparisons for large iTRAQ datasets.

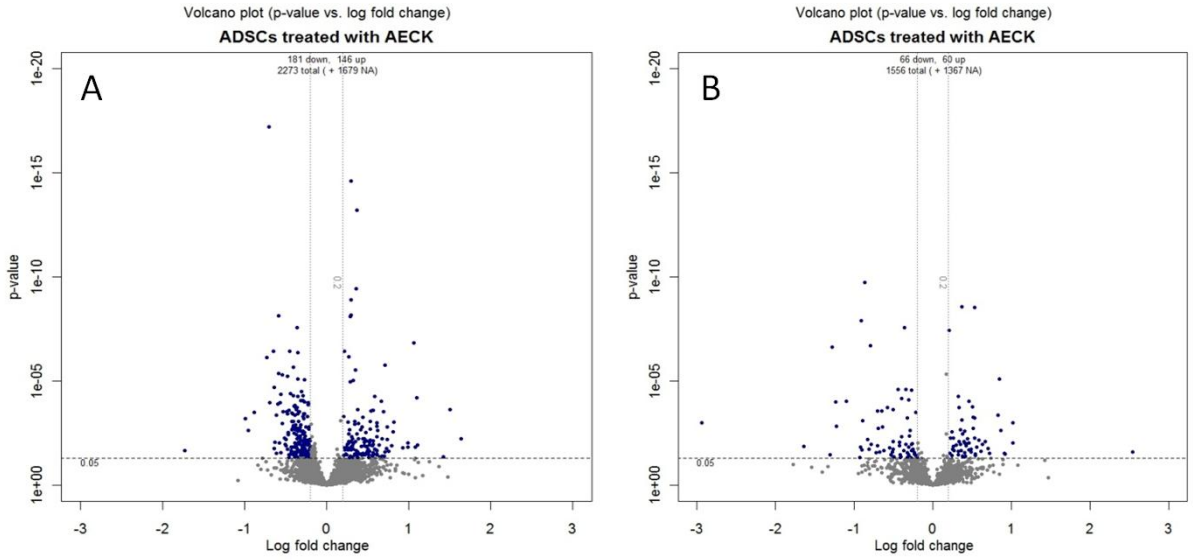

Figure 9 A and B Volcano plots iTRAQ biological replicates of ADSCs treated with AECK. Showing P-values versus protein fold change (log_2) of ADSCs differentiated for 24hours vs. Basal ADSCs proteins fulfilling strict quantitation criteria cutoff of statistically significant P-values <0.05 and log_2fold change cutoff of <-0.2 or >0.2. The blue nodes represent the above > 0 log fold change up-regulated proteins and the below <0 fold change down-regulated proteins. The grey nodes represent the not significantly changed proteins with a P-value >0.05 and within the cut off for fold change

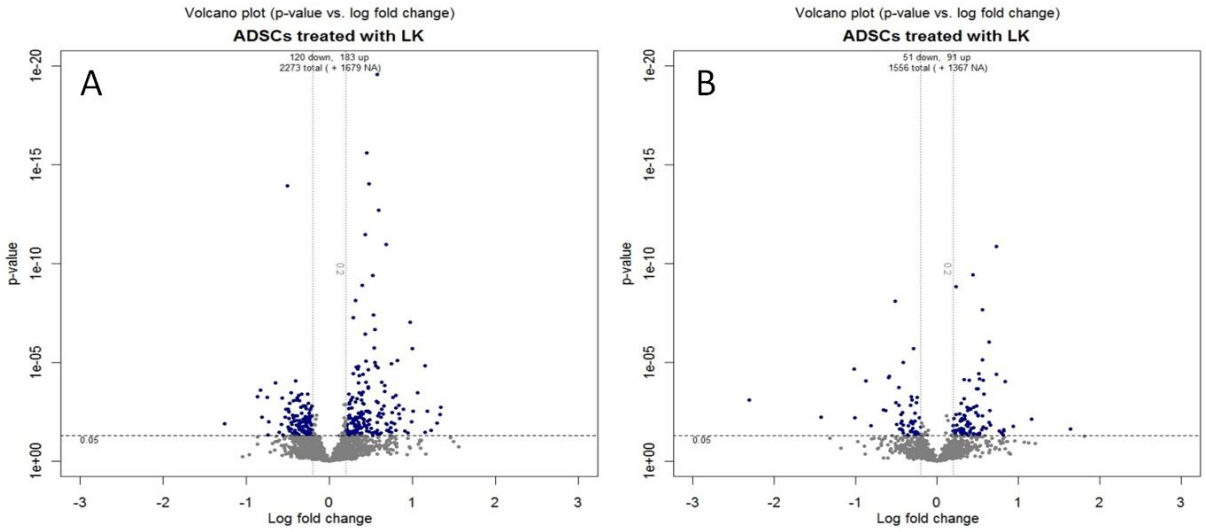

Figure 10 A and B Volcano plots iTRAQ biological replicates of ADSCs treated with LK. Showing P-values versus protein fold change (log_2) of ADSCs differentiated for 24hours vs. Basal ADSCs proteins fulfilling strict quantitation criteria cutoff of statistically significant P-values <0.05 and log_2fold change cutoff of <-0.2 or >0.2. The blue nodes represent the above > 0 log fold change up-regulated proteins and the below <0 fold change down-regulated proteins. The grey nodes represent the not significantly changed proteins with a P-value >0.05 and within the cut off for fold change.

From the above volcano plots (figure 9 and 10), the following Venn diagrams were constructed (figure 11) representing the number of proteins unique and shared between both replicates for each chemical treatment of the ADSCs. In the first biological replicate there are 46 and 82 unique proteins respectively for the AECK and LK compared to basal ADSCs, also sharing 85 proteins which have all been up regulated. The second replicate contained less protein identifications that were up regulated protein identifications, presenting 14 and 38 unique to AECK and LK respectively and 34 proteins shared. The total decrease in all metrics is attributable to technical variation between the two runs which were separated by 6 months. The second Venn diagram trend reveals there are a larger number of proteins down regulated in AECK replicates compared to the LK replicates. All the statistically significant proteins are highlighted and available in the appendix 2B and 2C. The GO pie graphs presented in figures 12-15 show the associated biological roles of each annotated protein to identify roles in neurogenesis or a stress response. The comparison of GO graphs between the CK treated cells and the BME treated cells are quite different. A noteworthy difference is the decrease of cell death and death related proteins from the BME treated cells which constitute approximately

6% of proteins detected. Whereas the CK treated cells present an average of 2.6% of death related proteins. Furthermore the percentage of stress related proteins has decreased by an average of 1% of total detected proteins from the BME to the CK treated ADSCs.

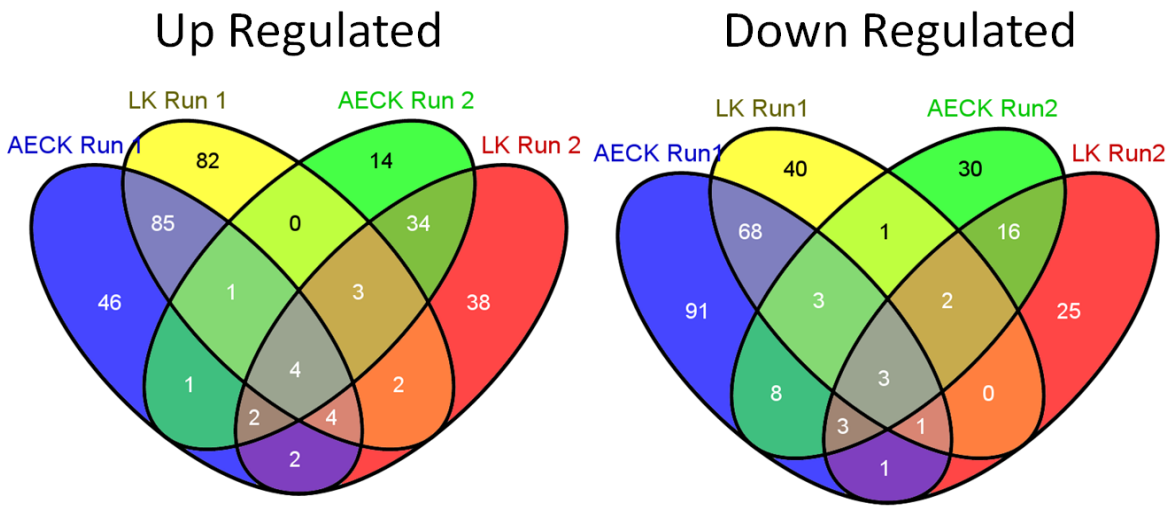

Figure 11 Four way cross sectional Venn diagrams displaying all up and down regulated proteins (P-values <0.05 and log_2fold change cutoff of <-0.2 or >0.2) from both biological replicates to identify unique and shared proteins in each treatment.

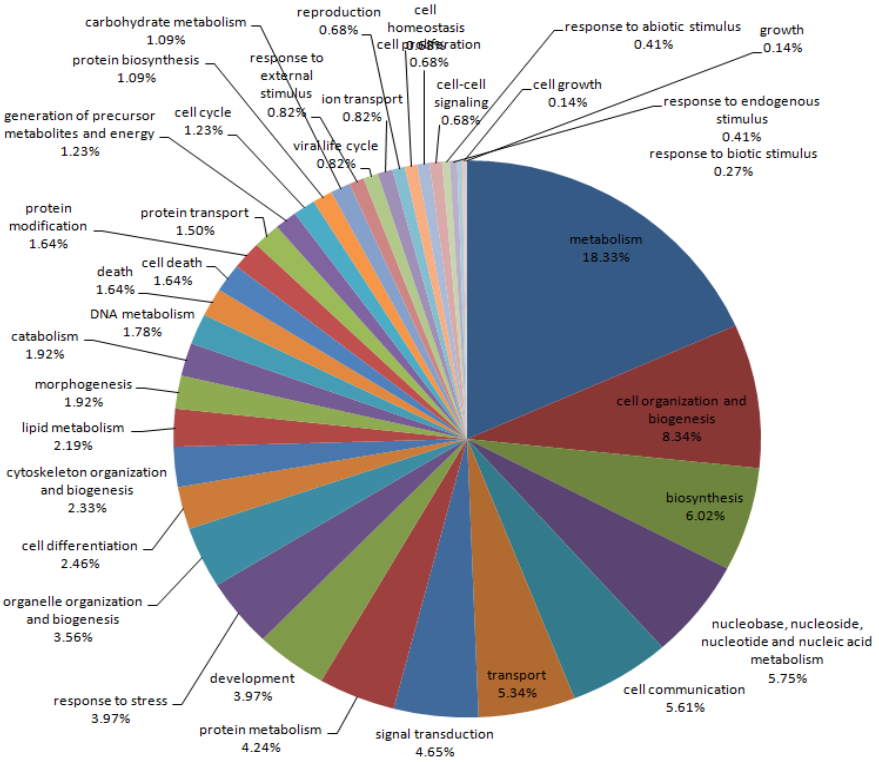

Figure 12 Gene ontology of statistically significant up regulated iTRAQ identified proteins for the ACEK treated ADSCs

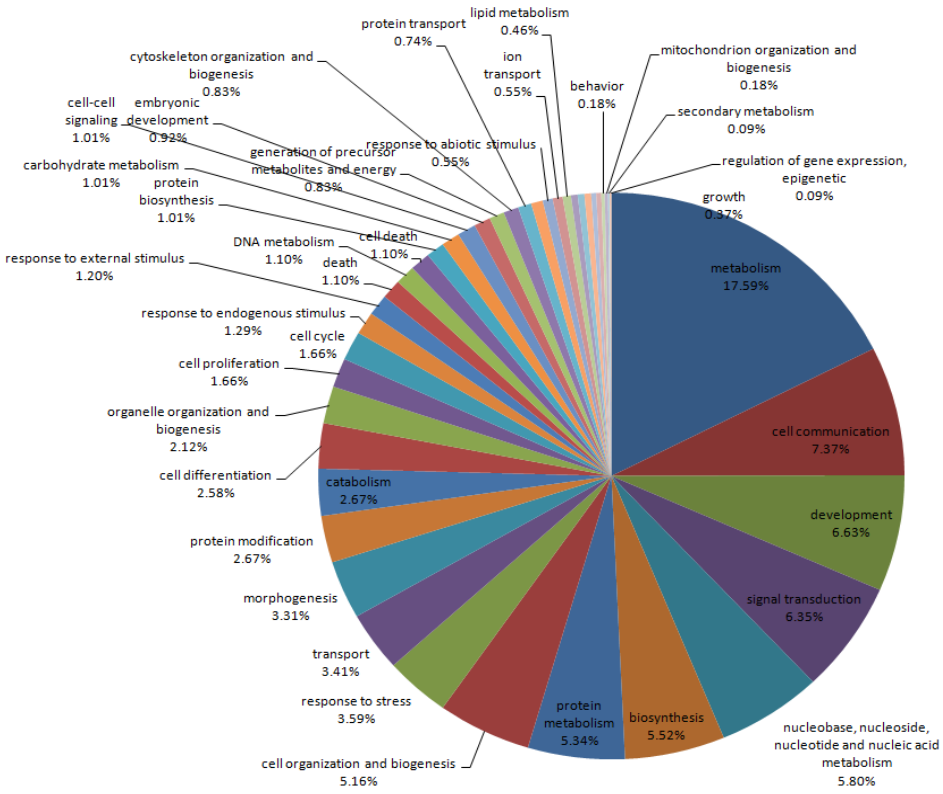

Figure 13 Gene Ontology of statistically significant down regulated iTRAQ identified proteins for the ACEK treated ADSCs

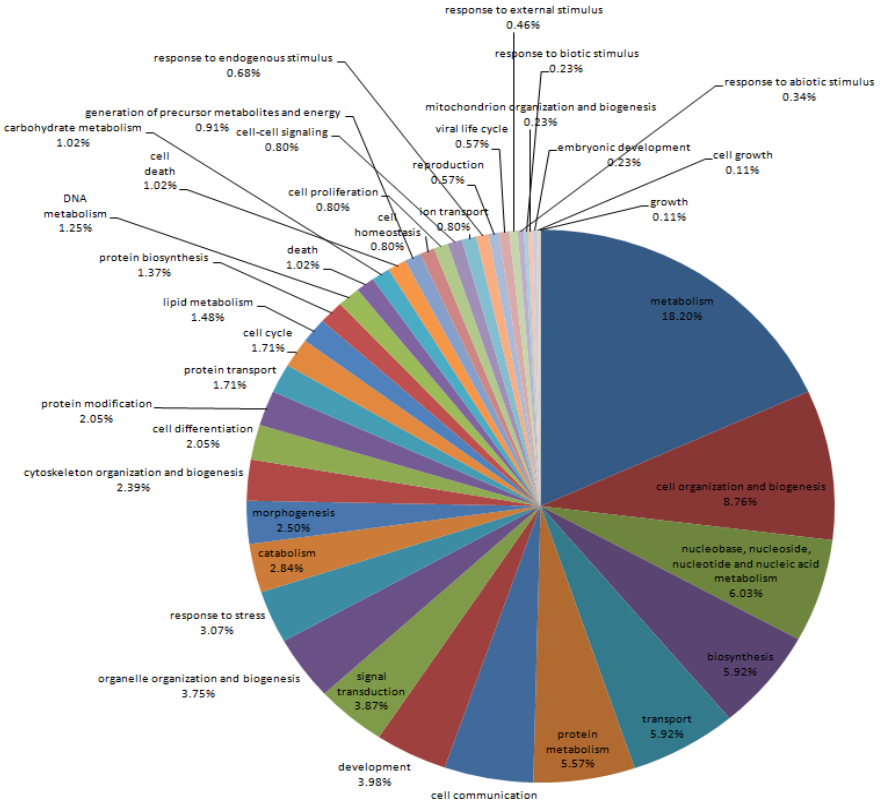

Figure 14 Gene Ontology of statistically significant up regulated iTRAQ identified proteins for the LK treated ADSCs

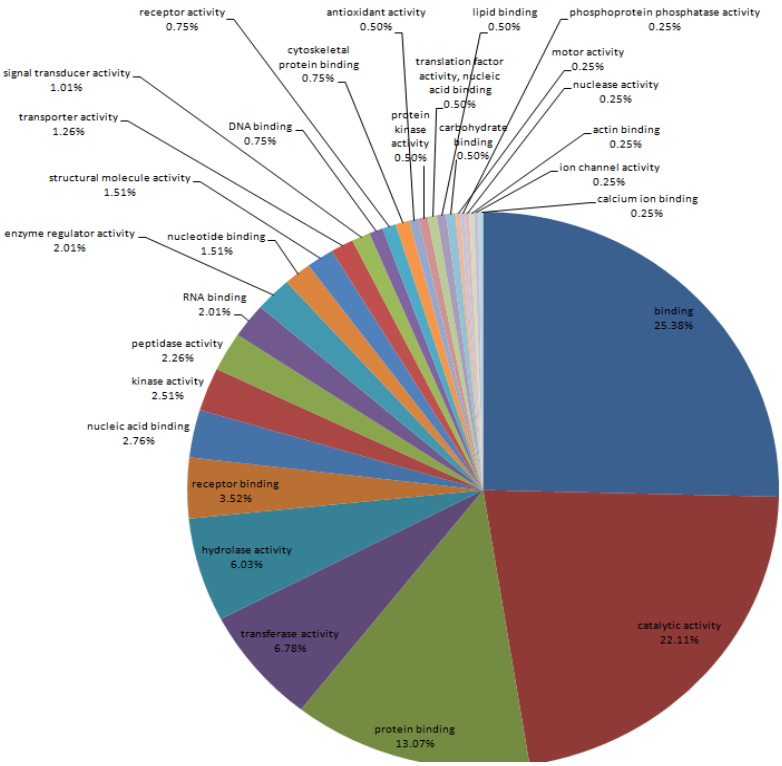

Figure 15 Gene Ontology of statistically significant down regulated iTRAQ identified proteins for the LK treated ADSCs

4.3.3 Western blots

Similarly to the Western blots carried out in chapter 3, the commonly used neuronal markers βTB3, GFAP, NF200 and NeuN were examined within this study as well to compare the expression in the AECK and LK treated ADSCs with GBC whole cell lysates (Figure 16). The results of the AECK and LK treated cells are varied from the BME treated cells (Chapter 3 section 3.3). The βT3 55 kDa protein is strongly detected across all chemically treated ADSCs as well as the positive GBC control. Similarly to the BME treated cells, the AECK and LK treated ADSCs have a similar low level of expression detected. The detection of the NF200 protein in the AECK and LK treated cells is a departure from the previous results from BME treated cells. The AECK samples presents an equivalent detected level to that seen in the GBCs, while the LK samples show significantly lower intensity and at a comparable level to that seen in the ADSCs. Coincidently, the ADSCs should not be expressing a 'neurospecific' marker. This has been previously stated in chapter 3 as a discrepancy in the literature, whereby certain neuronal markers have now been annotated as being expressed in a variety of cells [368-371]. Correspondingly, the discovery of the neuroepithelium specific marker βT3 [372-374] and the minor appearance of NeuN in the ADSCs, AECK and LK samples at a concentration comparatively lower than in the GBCs, contradicts the reported usefulness of these neurospecific markers. This reinforces the value of a proteomic characterisation of cells that have been directed toward a neuronal phenotype with a novel chemical stimulation.

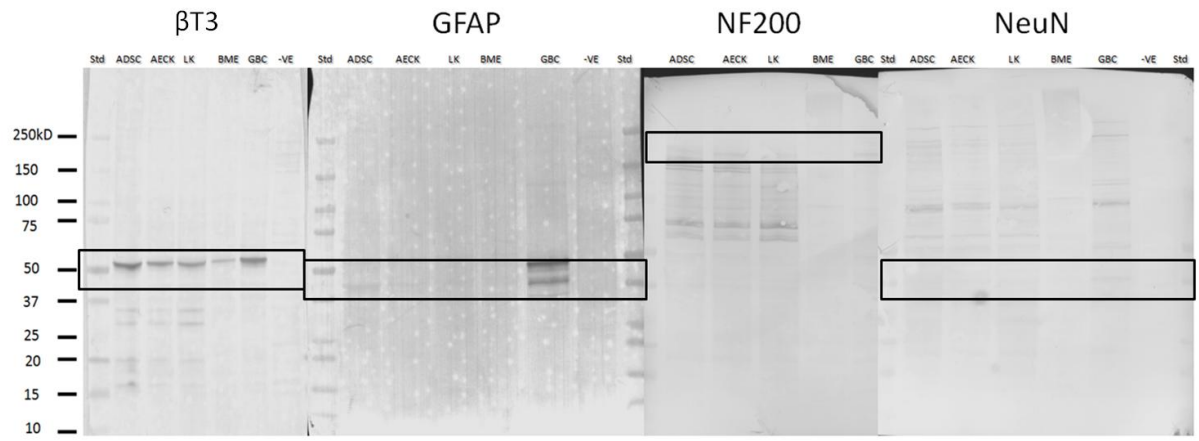

Figure 16 Western blot of βT3 positive in ADSCs, AECK, LK, BME differentiated and GBCs seen at 55 kDa. GFAP positively detected in GBCs at 48 kDa and very faintly in chemically treated cells. NF200 positively identified at 200 kDa in GBCs and very weakly in chemically differentiated. NeuN a very low positive in ADSCs, AECK, LK and GBCs only at 46 and 48 kDa.

4.3.4 Bioplex

4.3.4.1 Bioplex cell number normalisation and trend clustering

The Bioplex assay is a multiplex system for investigating the relative quantitative changes of 27 cytokines across multiple sample types simultaneously. Aliquots of the differentiation media supplemented with either AECK or LK were collected at time points 0, 1, 3, 5, 20 and 24 hours and the 27 cytokines measured. A hierarchical clustering and Euclidean test in the DanteR software were used to cluster the multiple data points in a heat map configuration where red represents expression above median, green represents expression below the median and Black represents median expression across all samples. The hierarchical clustering (figure 17 and 18) presents the cytokines with similar concentration trends over the differentiation time points. A concentration per cell normalisation was completed (table 2 and 3) to adjust for any discrepancies due to cell death which was apparent in previous BME differentiation studies (chapter 3) and in a limited extent in the LK samples.

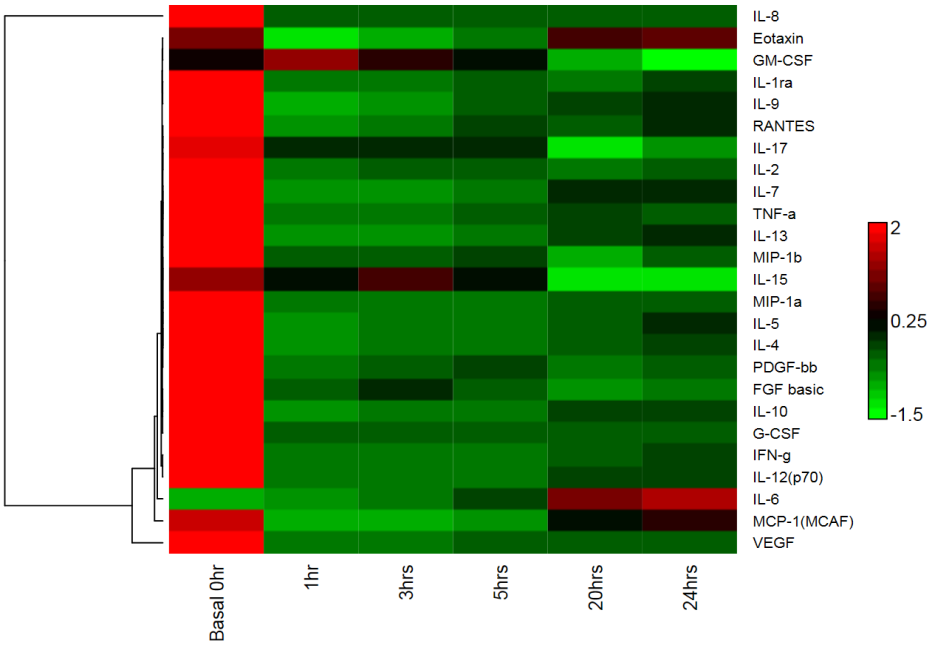

Figure 6 Bioplex comparisons of interleukins and cytokine secretions from basal ADSCs and temporal differentiation with AECK neuronal differentiation media. Hierarchical clustering software and Euclidean test Red: expression above median; Green: expression below the median; Black: median expression across all samples.

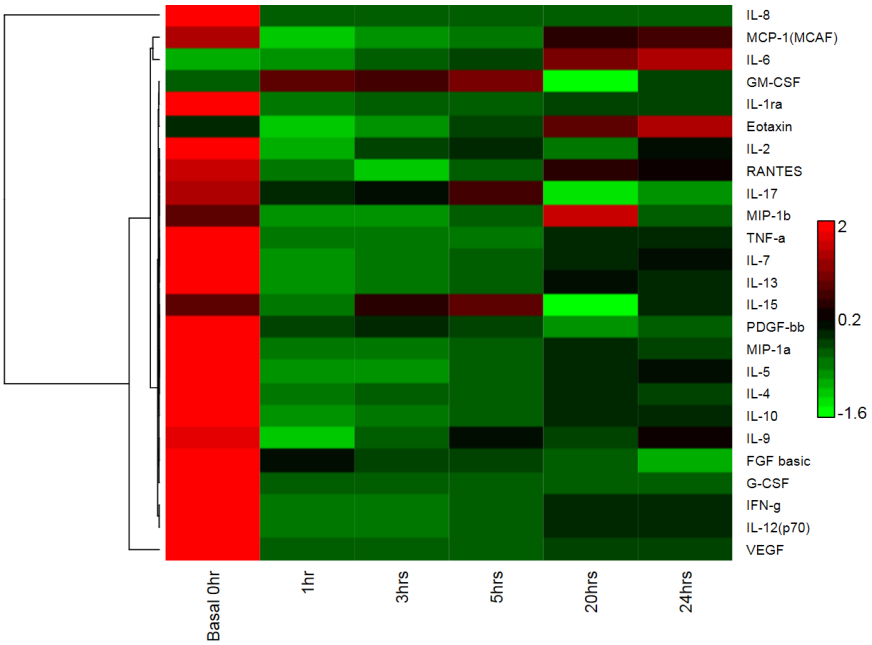

Figure 7 Bioplex comparisons of interleukins and cytokine secretions from basal ADSCs and temporal differentiation with LK neuronal differentiation media. Hierarchical clustering software and Euclidean test Red: expression above median; Green: expression below the median; Black: median expression across all samples.

Table 2 Cytokine concentration normalisation per cell for temporal AECK induction

Cytokines	Basal 0hr	pg/ml/cell	1hr	pg/ml/cell	3hrs	pg/ml/cell	5hrs	pg/ml/cell	20hrs	pg/ml/cell	24hrs	pg/ml/cell
IL-1ra	79.28	1.46E-05	23.83	4.43E-06	25.56	4.70E-06	27.29	5.00E-06	25.56	4.87E-06	31.69	6.20E-06
IL-2	11.2	2.07E-06	5.27	9.80E-07	5.65	1.04E-06	5.91	1.08E-06	5.14	9.79E-07	5.39	1.05E-06
IL-4	2.29	4.23E-07	0.07	1.30E-08	0.13	2.39E-08	0.18	3.30E-08	0.36	6.86E-08	0.49	9.49E-08
IL-5	1.75	3.23E-07	0.52	9.67E-08	0.57	1.05E-07	0.62	1.14E-07	0.67	1.28E-07	0.80	1.56E-07
IL-6	0	0.00E+00	68.75	1.28E-05	117.34	2.16E-05	215.21	3.94E-05	580.79	1.11E-04	679.65	1.33E-04
IL-7	16.11	2.97E-06	1.11	2.06E-07	1.77	3.25E-07	2.94	5.38E-07	4.79	9.12E-07	4.83	9.44E-07
IL-8	28591.59	5.28E-03	26.7	4.96E-06	12.69	2.33E-06	58.08	1.06E-05	179.17	3.41E-05	209.71	4.10E-05
IL-9	40.66	7.50E-06	17.95	3.34E-06	19.36	3.56E-06	22.2	4.07E-06	22.56	4.30E-06	23.99	4.69E-06
IL-10	25.96	4.79E-06	1.91	3.55E-07	2.67	4.91E-07	3.99	7.31E-07	6.38	1.22E-06	6.22	1.22E-06
IL-12(p70)	237.18	4.38E-05	7.86	1.46E-06	11.33	2.08E-06	20.34	3.73E-06	40.54	7.72E-06	42.52	8.32E-06
IL-13	13.22	2.44E-06	1.5	2.79E-07	1.84	3.38E-07	2.47	4.52E-07	3.83	7.30E-07	4.06	7.94E-07
IL-15	4.49	8.28E-07	3.43	6.38E-07	3.98	7.32E-07	3.55	6.50E-07	2.3	4.38E-07	2.26	4.42E-07
IL-17	8.66	1.60E-06	5.15	9.57E-07	5.15	9.47E-07	5.15	9.43E-07	2.39	4.55E-07	3.44	6.72E-07
Eotaxin	74.14	1.37E-05	34.14	6.35E-06	41.3	7.59E-06	48.2	8.83E-06	63.86	1.22E-05	65.74	1.29E-05
FGF basic	43.2	7.97E-06	8.14	1.51E-06	13.83	2.54E-06	9.17	1.68E-06	3.8	7.24E-07	4.68	9.15E-07
G-CSF	61.12	1.13E-05	0.93	1.73E-07	0.42	7.72E-08	0	0.00E+00	0	0.00E+00	0.62	1.21E-07
GM-CSF	50.28	9.28E-06	56.74	1.05E-05	51.8	9.52E-06	50.05	9.17E-06	41.1	7.83E-06	35.61	6.97E-06
IFN-g	265.87	4.91E-05	15.64	2.91E-06	17.97	3.30E-06	27.76	5.08E-06	43.53	8.29E-06	47.67	9.33E-06
MCP-1(MCAF)	1174.32	2.17E-04	38.08	7.08E-06	75.99	1.40E-05	144.12	2.64E-05	539.13	1.03E-04	639.55	1.25E-04
MIP-1a	2.08	3.84E-07	0.66	1.23E-07	0.68	1.25E-07	0.7	1.28E-07	0.73	1.39E-07	0.75	1.46E-07
MIP-1b	6.77	1.25E-06	3	5.58E-07	3	5.51E-07	3.19	5.84E-07	1.95	3.71E-07	2.65	5.18E-07
PDGF-bb	7.5	1.38E-06	0.25	4.65E-08	0.76	1.40E-07	1.25	2.29E-07	0.25	4.76E-08	0.63	1.22E-07
RANTES	9.4	1.73E-06	3.48	6.47E-07	4.07	7.48E-07	4.63	8.48E-07	4.07	7.75E-07	4.76	9.31E-07
TNF-a	16.31	3.01E-06	1.71	3.18E-07	2.03	3.73E-07	2.98	5.46E-07	3.63	6.91E-07	3.39	6.63E-07
VEGF	5546.75	1.02E-03	56.39	1.05E-05	68.06	1.25E-05	122.12	2.24E-05	262.23	4.99E-05	332.22	6.50E-05
Total cell count	5.42E+06		5.38E+06		5.44E+06		5.46E+06		5.25E+06		5.11E+06	

Table 3 Cytokine concentration normalisation per cell for temporal LK induction

Cytokines	Basal 0hr	pg/ml/cell	1hr	pg/ml/cell	3hrs	pg/ml/cell	5hrs	pg/ml/cell	20hrs	pg/ml/cell	24hrs	pg/ml/cell
IL-1ra	79.28	1.46E-05	30.8	5.71E-06	36.11	6.59E-06	32.56	6.43E-06	32.56	6.69E-06	31.24	6.75E-06
IL-2	11.2	2.07E-06	4.75	8.81E-07	6.29	1.15E-06	6.42	1.27E-06	4.88	1.00E-06	5.975	1.29E-06
IL-4	2.29	4.22E-07	0.07	1.30E-08	0.18	3.28E-08	0.27	5.34E-08	0.44	9.03E-08	0.375	8.10E-08
IL-5	1.75	3.23E-07	0.52	9.65E-08	0.57	1.04E-07	0.67	1.32E-07	0.77	1.58E-07	0.82	1.77E-07
IL-6	0	0.00E+00	48.39	8.98E-06	185.29	3.38E-05	268.54	5.31E-05	682.2	1.40E-04	737.765	1.59E-04
IL-7	16.11	2.97E-06	0.94	1.74E-07	1.77	3.23E-07	2.77	5.47E-07	4.87	1.00E-06	5.12	1.11E-06
IL-8	28591.59	5.27E-03	18.46	3.42E-06	50.75	9.26E-06	106.59	2.11E-05	231.49	4.75E-05	200.06	4.32E-05
IL-9	40.66	7.50E-06	18.83	3.49E-06	24.34	4.44E-06	26.85	5.31E-06	23.27	4.78E-06	25.42	5.49E-06
IL-10	25.96	4.79E-06	1.44	2.67E-07	2.29	4.18E-07	3.71	7.33E-07	6.5	1.33E-06	6.62	1.43E-06
IL-12(p70)	237.18	4.37E-05	5.09	9.44E-07	9.88	1.80E-06	16.17	3.20E-06	42.57	8.74E-06	45.575	9.84E-06
IL-13	13.22	2.44E-06	1.36	2.52E-07	1.79	3.27E-07	2.23	4.41E-07	4.59	9.43E-07	4.105	8.87E-07
IL-15	4.49	8.28E-07	2.25	4.17E-07	3.96	7.23E-07	4.14	8.18E-07	0.65	1.33E-07	2.47	5.33E-07
IL-17	8.66	1.60E-06	5.81	1.08E-06	6.45	1.18E-06	6.77	1.34E-06	3.46	7.10E-07	3.97	8.57E-07
Eotaxin	74.14	1.37E-05	39.54	7.34E-06	46.93	8.56E-06	64.26	1.27E-05	96.18	1.97E-05	108.65	2.35E-05
FGF basic	43.2	7.97E-06	18.43	3.42E-06	15.47	2.82E-06	13.13	2.59E-06	11.08	2.28E-06	5.63	1.22E-06
G-CSF	61.12	1.13E-05	0.93	1.73E-07	1.4	2.55E-07	0.42	8.30E-08	0.93	1.91E-07	0.42	9.07E-08
GM-CSF	50.28	9.27E-06	59.46	1.10E-05	59.34	1.08E-05	57.57	1.14E-05	36.14	7.42E-06	43.395	9.37E-06
IFN-g	265.87	4.90E-05	15.64	2.90E-06	20.35	3.71E-06	27.76	5.49E-06	54.61	1.12E-05	53.275	1.15E-05
MCP-1(MCAF)	1174.32	2.17E-04	52.05	9.66E-06	173.72	3.17E-05	252.19	4.98E-05	668.05	1.37E-04	702.33	1.52E-04
MIP-1a	2.08	3.84E-07	0.73	1.35E-07	0.7	1.28E-07	0.77	1.52E-07	0.88	1.81E-07	0.815	1.76E-07
MIP-1b	6.77	1.25E-06	4.1	7.61E-07	4.1	7.48E-07	4.44	8.77E-07	7.05	1.45E-06	4.095	8.84E-07
PDGF-bb	7.5	1.38E-06	2.23	4.14E-07	2.72	4.96E-07	1.99	3.93E-07	0.76	1.56E-07	1.74	3.76E-07
RANTES	9.4	1.73E-06	5.15	9.55E-07	4.36	7.96E-07	5.15	1.02E-06	6.57	1.35E-06	6.11	1.32E-06
TNF-a	16.31	3.01E-06	2.66	4.94E-07	2.66	4.85E-07	2.66	5.26E-07	4.61	9.47E-07	4.61	9.96E-07
VEGF	5546.75	1.02E-03	39.63	7.35E-06	63.73	1.16E-05	104.78	2.07E-05	275.52	5.66E-05	320.195	6.92E-05
Total cell count	5.42E+06		5.39E+06		5.48E+06		5.06E+06		4.87E+06		4.63E+06	

4.3.4.2 Bioplex trend graphs

Cytokines have a variety of functions in cellular processes and are often expressed in response to a change in a system which in turn can also regulate the expression of other molecules [375]. Individually and collectively their relative concentrations can be related to particular cellular events or response mechanisms. With this in mind, a number of trends can be observed within the Bioplex temporal ADSC differentiation data set. The comparison of the Bioplex results between AECK and LK treated ADSCs present similar trends with variations within the trend groups. The trends can be subcategorised into seven subsidiary groups of which the AECK Bioplex graphs appear blue and the LK Bioplex graphs appear red. The trend graph grouping utilised in this chapter are unique compared to those appearing in chapter three with the BME treated ADSCs. This is due to the unique trends formed in this study's treatment of the ADSCs with CKs.

Group 1 (figure 19) comprises of IL-1ra, IL-2, MIP-1a, MIP-1b and Rantes which generally follows the trend where the highest concentration occurs in the basal cells, the concentration then decreases by approximately 50% post induction and remains at that level for the remainder of the time points. The variation of the group trend is identified between the comparison of the AECK and LK MIP-1b and Rantes levels. The MIP-1b in the LK treatment increases above the basal ADSC concentration at the 20 hr time point. Similarly at the same time point in the LK treatment, the Rantes concentration increases breaking trend with the rest of the cohort relative to the AECK samples. The trends for this group of cytokines is vastly different from the chapter 3 BME treated ADSCs. The main difference is the types of cytokines present, which the BME treated cells lack the MIP-1a and MIP-1b however has Eotaxin. Additionally the concentration variation over the time course is another differentiating factor where the BME group presents the large decrease 1hr after induction and a continuous increase in concentration of the cytokines till the final time point (chapter 3, figure 9A).

Figure 19 Group 1 Bioplex trend related secreted cytokines IL-1ra, IL-2, MIP-1b, Rantes and MIP-1 over a temporal differentiation normalised as pg/ml/cell (AECK - Blue, LK - Red)

Group 2 (TNF-α, IL-10, IL-7, IL-4, IL-12 and IL-13) (figure 20) presents a similar trend to group 1 wherein the highest concentration is present in the basal untreated ADSCs which then decreases to less than a quarter of the basal levels with a minor recovery across all cytokines after the 20 hr time point. This group draws parallels with a number of the cytokine presented in the BME treated cells which also present a large concentration decrease subsequent to induction with a minimal recovery.

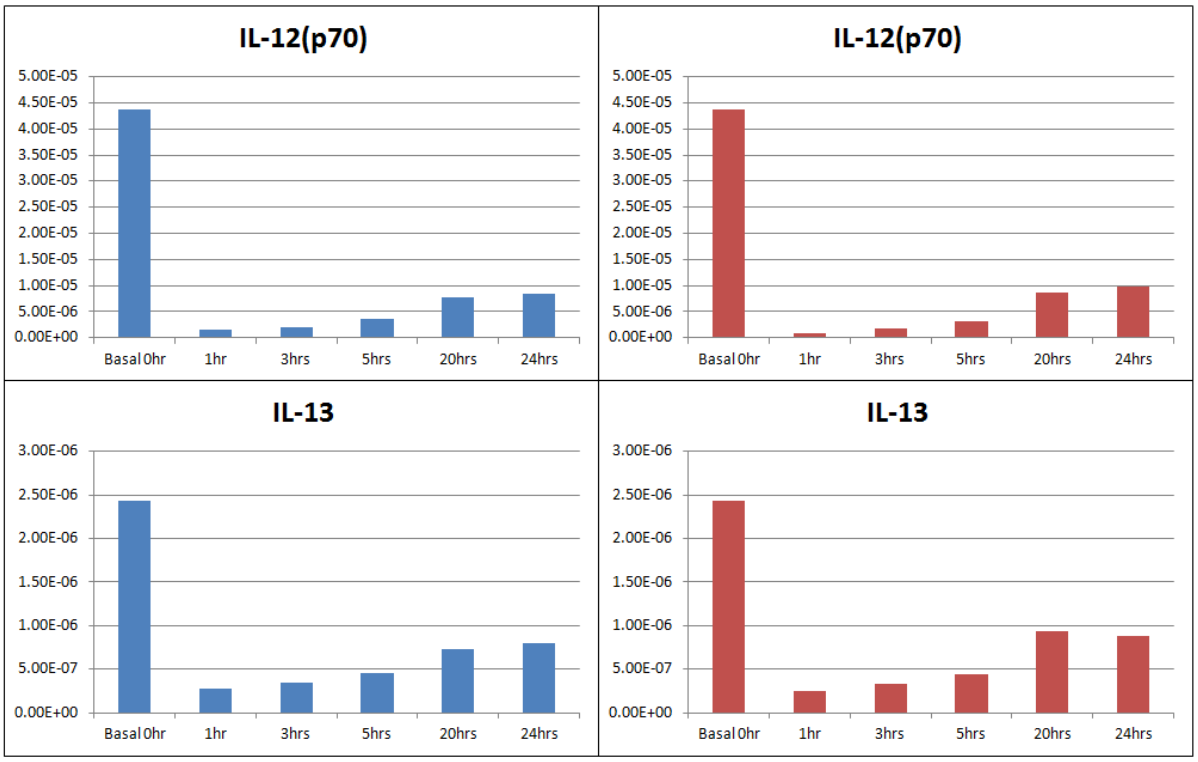

Figure 20 Group 2 Bioplex trend related secreted cytokines IL-7, IL-4, TNFα, IL-10, IL-12 and IL-13 over a temporal differentiation normalised as pg/ml/cell (AECK - Blue, LK - Red)

Group 3 (figure 21), comprised of PDGF-bb, IFN-γ and MCP-1 also shares the high basal concentrations in common with group 1 and 2 where a substantial decrease within the first hour is followed by minor recover for every time point thereafter. The differences in cytokine concentration between the AECK and LK samples are infinitisimal within this group . An interesting trend variation within this group occurs for both the AECK and LK MCP-1 which assumes an approximately 50% concentration recovery by the 20th hr time point which increases again at the 24th hour time point. Interestingly the PDGF-bb displays a similar small recovery at 5 hours and at 24 hours as in the BME treated cells (chapter 3, figure 6D).

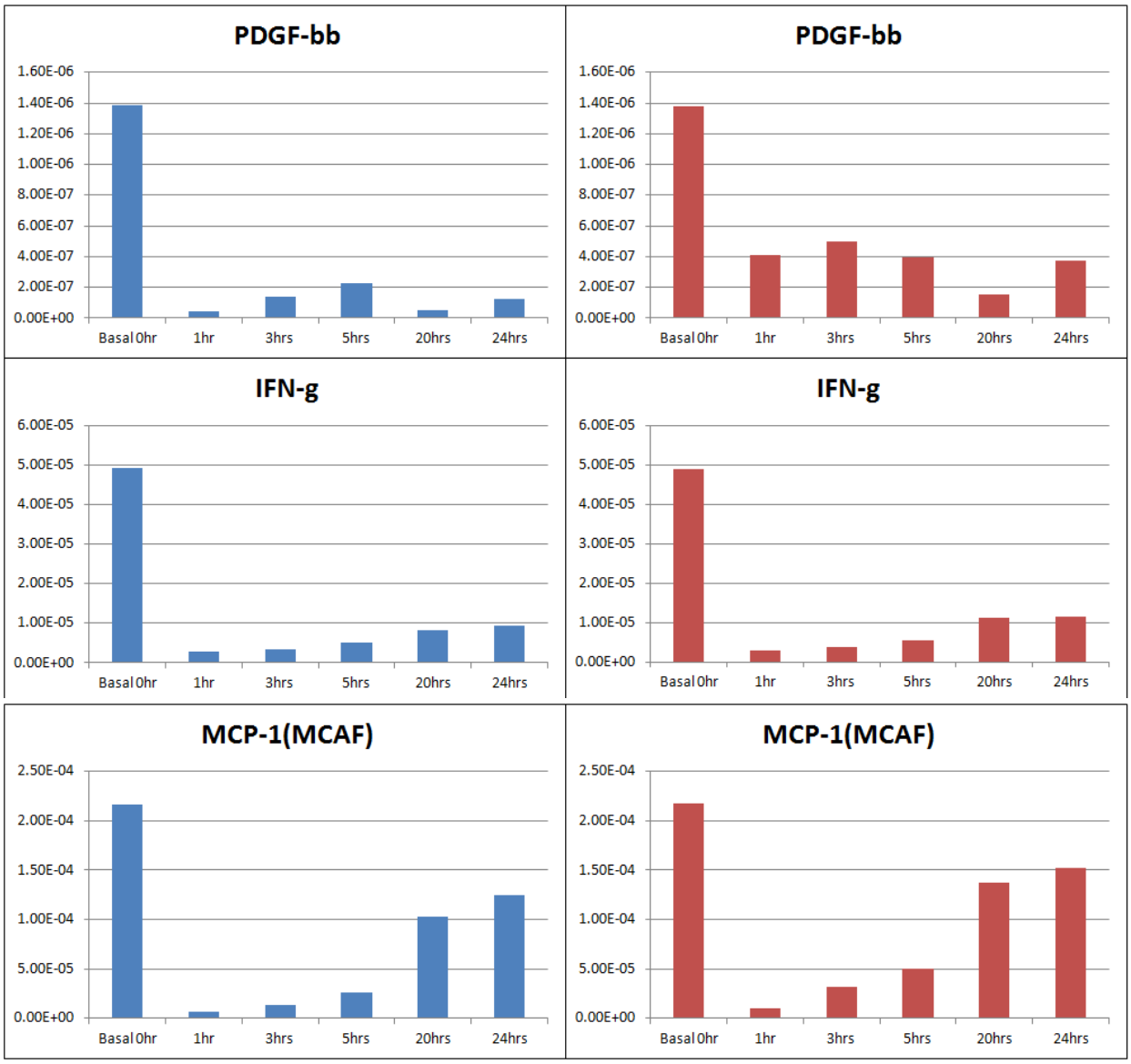

Figure 21 Group 3 Bioplex trend related secreted cytokines PDGF-bb, IFNγ and MCP-1 over a temporal differentiation normalised as pg/ml/cell (AECK - Blue, LK - Red)

Group 4 (figure 22) consisting of the three molecules, Eotaxin, IL-5 and IL-9, has a simple trend in which the large decrease in basal levels after 1 hour post induction is observed again as per previous groups. The unique feature of this group is the concentration recovery for every time point thereafter to at least 50% of the basal ADSC levels is seen for IL-5 and IL-9. Eotaxin however returns to basal levels for the AECK treatment and surpasses basal level in the LK treatment. The IL-5 and IL-9 concentration levels in the BME treated cells are decreased compared to the CK treated cells relative IL-5 and IL-9 concentrations.

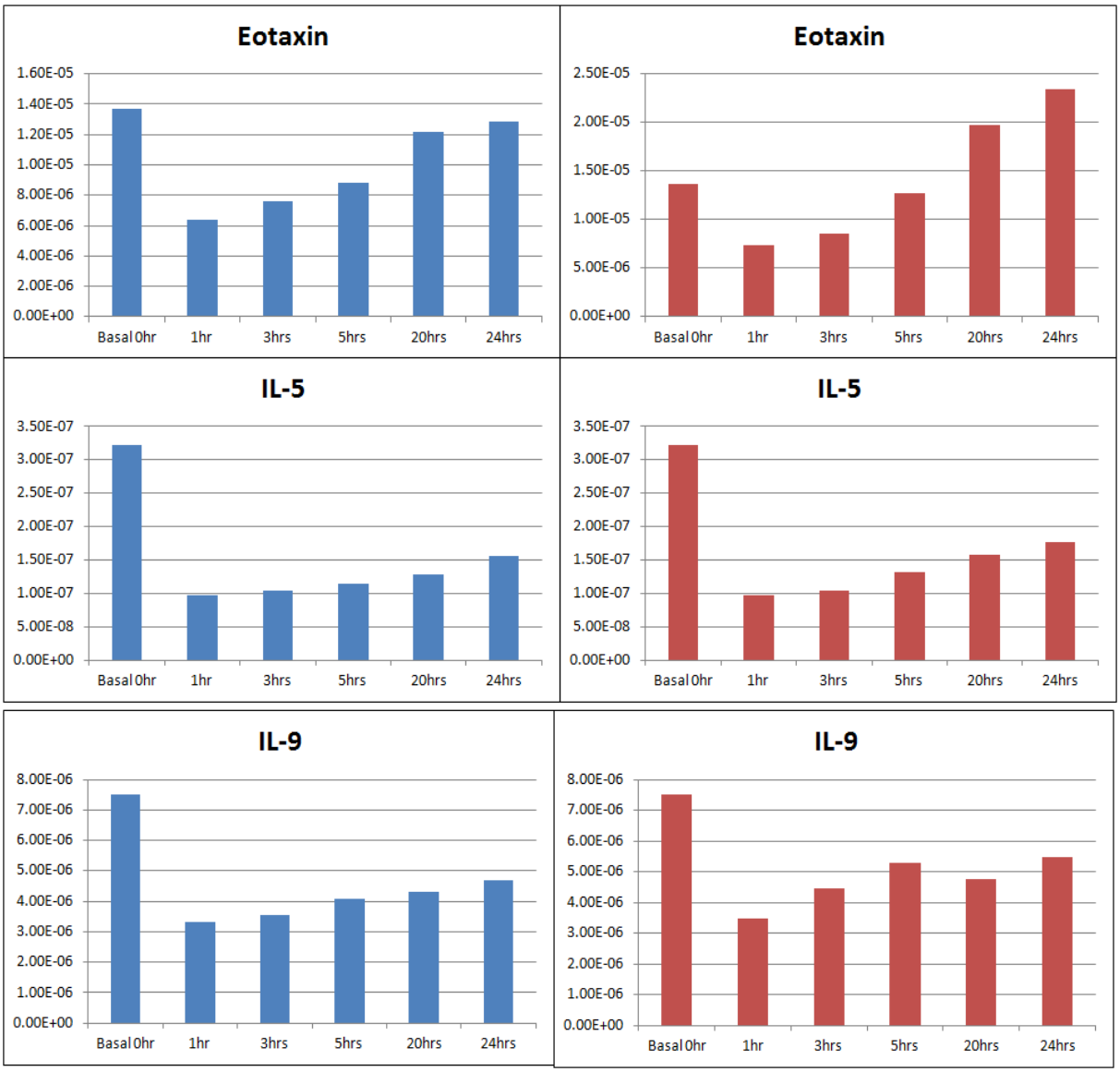

Figure 22 Group 4 Bioplex trend related secreted cytokines Eotaxin, IL-5 and IL-9 over a temporal differentiation normalised as pg/ml/cell (AECK - Blue, LK - Red)

Group 5's (figure 23) molecules present the greatest variation between AECK and LK treatments of ADSCs. The trends within this group are not as consistent as previous groups; the main factor clustering these molecules together is the overall relative similarity of their concentrations. The difference between the AECK and LK IL-15 is noteworthy, where each time point presents a variation in the concentration compared to the other. The most noteworthy variances are present at 1 hour and 20 hours post induction where the LK's IL-15 concentration is significantly lower than the AECKs. Conversely the concentration of IL-17 and GM-CSF in the LK sample is higher at all time points compared to the AECK sample. This group is clustered together in chapter 3 (figure 6b) however

displaying a very different trend which generally indicates a large increase in concentration over time, in which the highest concentrations appear in the final time points (chapter 3 figure 9B).

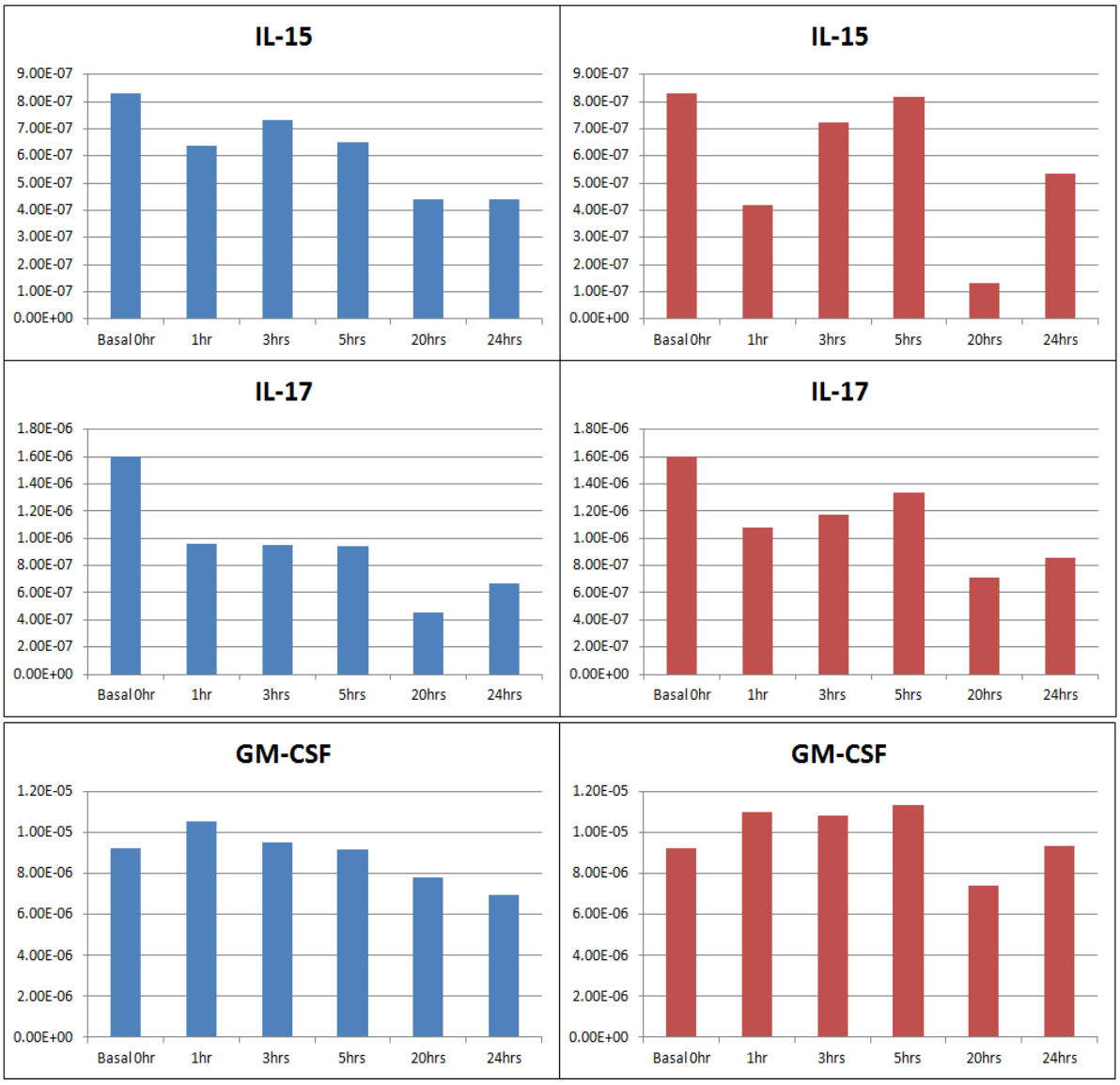

Figure 23 Group 5 Bioplex trend related secreted cytokines IL-15, IL-17 and GM-CSF over a temporal differentiation normalised as pg/ml/cell (AECK - Blue, LK - Red)

Group 6 (G-CSF, IL-8, VEGF) seen in figure 24 has the most basic trend of all subcategorised cytokines whereby the concentrations is depleted across the board at all time points with minor resurgences detected for VEGF post 5 hrs. This appears to be very similar to the trends in chapter 3 for the same cytokines.

Figure 24 Group 6 Bioplex trend related secreted cytokines IL-15, IL-17 and GM-CSF over a temporal differentiation normalised as pg/ml/cell (AECK - Blue, LK - Red)

Group 7 (figure 25) consists of FGF basic and IL-6 which trends are inverse of each other. The FGF basic concentration starts high and subsequently decreases over time whereas the IL-6 starts at undetectable concentrations in the basal cells and increases substantially till the highest concentration at the 24 hour time point. This group's trend matches the BME treated cells IL-6 and FGF basic group trend very closely.

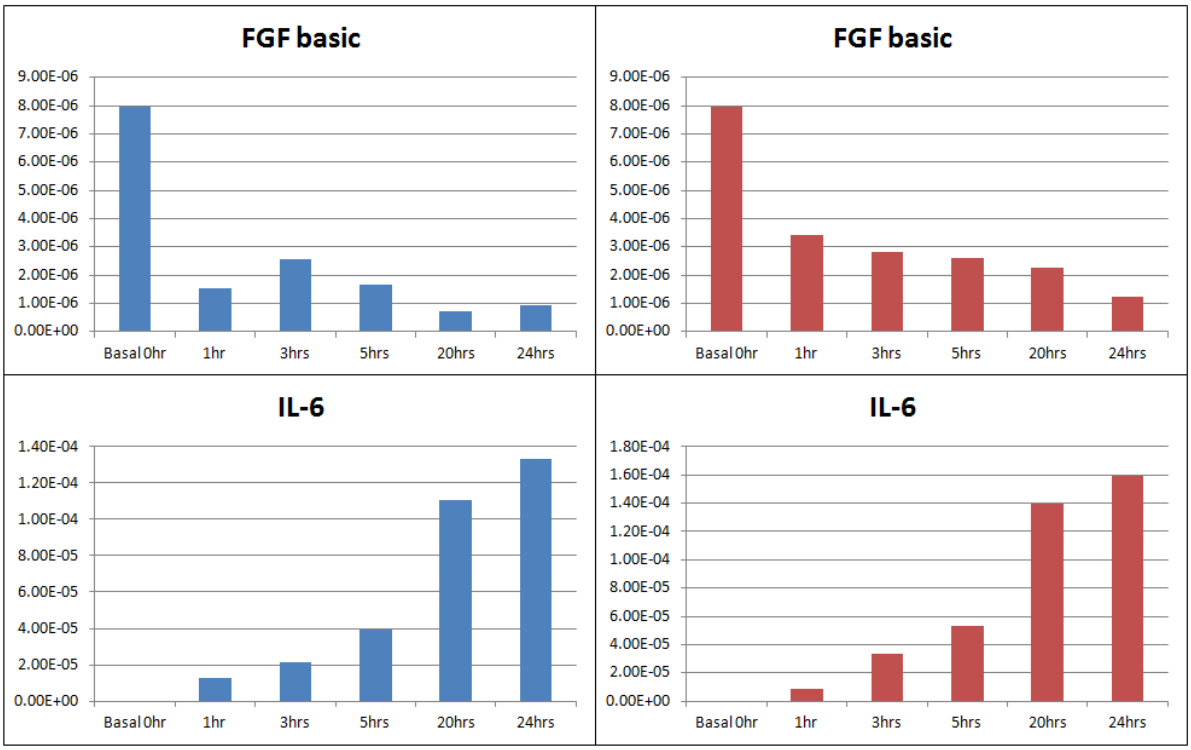

Figure 25 Group 7 Bioplex trend related secreted cytokines FGF-basic and IL-6 over a temporal differentiation normalised as pg/ml/cell (AECK - Blue, LK - Red)

4.4.0 DISCUSSION

The premise of utilising CK compounds in an attempt to induce ADSCs toward a neurogenic linage was based several factors pertaining to their chemical properties as well as biological implications. Firstly, based on the chemical properties, ketamines are a natural class of sulphur and nitrogen-containing cyclic compounds with reductive activity [501] which are key features of previously studied simple chemical neurogenic inducing agents, BME and DMSO [28, 104, 192, 196, 350, 351]. Furthermore CK is primarily found in the brain as a natural metabolic by product of transamination

of sulphur containing amino acids [493, 502]. LK and AECK have been purified from bovine brain to which binding and interaction studies have been successfully completed in the presence other brain specific imine reductases [503]. LK has also been observed to exhibit neuroprotective, neurotrophic and anti-inflammatory activities [491]. Additionally, the derivatised LKEE displayed a higher efficiency for membrane permeability and was revealed to protect *in vitro* motor neurons from oxidative stress as well as promote neurite outgrowth at nanomolar concentrations [491, 504]. The AECK molecule has been noted to react with a similar chemistry to the LK and LKEE and is thought to play similar physiological and biochemical roles [505]. The group has also been shown to prevent ischemic neuronal injury via the innate neuroprotective function [506]. CKs are now noted as novel neurotrophic small molecules that hold some promise for the treatment of neurodegenerative diseases [507]. Their use for promoting the growth of neurogenic cells from ADSCs was required, as a number of the criteria for a stable, non-toxic and naturally occurring chemical for directed neurogenesis were fulfilled.

In this study, ADSCs were treated for up to 24 hours with a novel differentiation media containing the CK compounds LK and AECK for the purpose of a directed neurogenic induction. The extent of differentiation was investigated by the changes in the proteome occurring during the process. The treatments indicated the ADSCs responded favourably to the neurogenic induction media by presenting a number of morphological cues previously seen [28, 104, 195, 376] and a higher cell population post induction compared to previous studies with BME (chapter 3).

Furthermore a variety of proteins were identified by mass spectrometric analyses that are annotated as being involved in neurogenic development. Complementing the iTRAQ proteomic data sets, the Bioplex cytokine profiles present evidence of cellular response to external stimuli and structural rearrangement as well as an altered panel of stress response cytokines relative to the BME treated ADSCs.

4.4.1 Cellular morphology and preliminary testing of CKs

Prior to the treatment of human ADSCs, varying concentrations of LK, AECK and their ethyl ester derivatives were trialled against rat ADSCs to investigate the extent of a morphological response that may indicate neurogenic-like growth. The optimal concentrations tested which elicited a cellular response in which the produced cell's morphology resembled neuronal like outgrowth within 24 hours were 0.5 mM AECK, 0.6 mM LK and 0.3 mM LKEE. In terms of morphological appearance, the AECK and LK produced the most cells with neuronal-like appearance which presented neurite-like out growth (figure 26 A and B). The ethyl ester produced fewer morphologically differentiated cells that presented neurite outgrowth at the final time point however it did produce a large number of spheroid, semi-detached cells (figure 26 C). The downfall of the ethyl ester derivates was a low cell population at the final time point which was thought to be due to the increased membrane permeability which may have induced a toxic intracellular environment evidenced by the higher proportion of lysed cells. Concentrations lower than the above stated did not yield a response at the given time point.

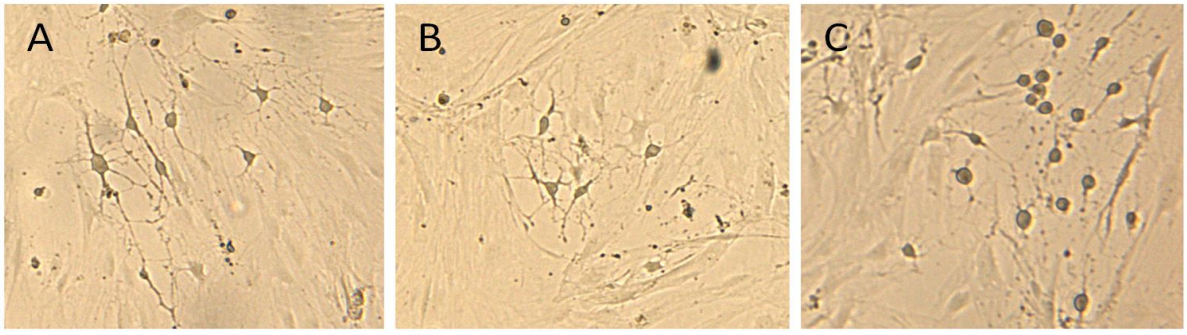

Figure 26 Rat ADSCs treated with AECK (A), LK (B) and LKEE (C) for 24 hours. Cells appear morphologically distinct with neurite-like extensions produced from cells compared to surrounding non-differentiated ADSCs.

The treated cells were also investigated by 2D SDS-PAGE as per methodologies chapter 2 to establish any broad proteome differences between the basal ADSCs and the CK treated (figure 27 A-D). While the profiles appear to retain a number of similarities, the outstanding differences appear in expression levels variances in a number of the marked areas. The protein preparations were

fractionated by 1D-PAGE and tryptically digested for LC-MS/MS analysis as per chapter 2. This identified a wide variety of proteins including a number of neurogenic related proteins unique to the CK treated rADSCs (appendix 2G). Based on the higher yields of cells presenting morphological cues as well as a number of neuronal markers, the AECK and LK molecules were selected for testing on human ADSCs to be analysed via iTRAQ and Bioplex.

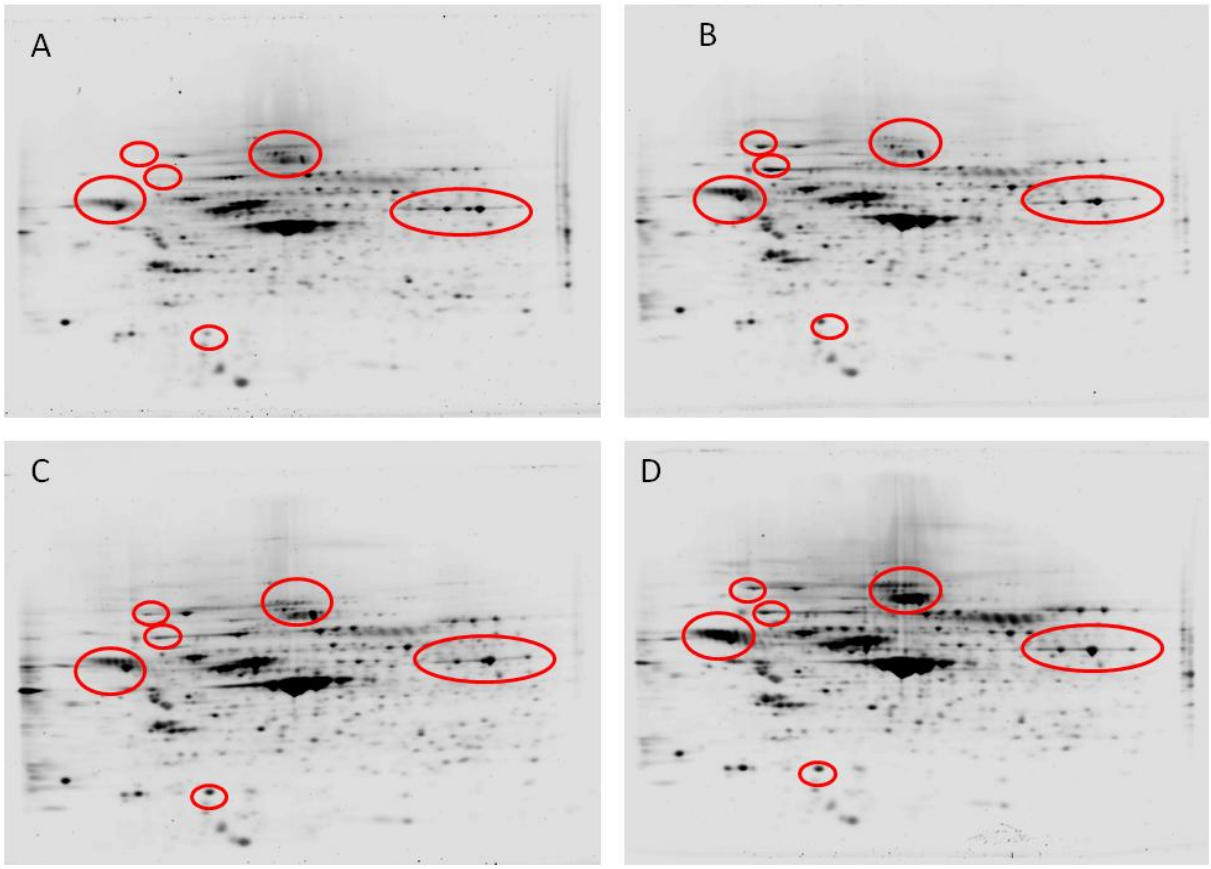

Figure 27 2D-PAGE of rat ADSCs treated with AECK (A), LK (B) and LKEE (C) with basal rADSCs (D) for proteome change comparisons which some examples are generally marked in red circles

4.4.2 Proteomic analysis

4.4.2.1 Western Blot analysis

Western blot analyses is a widely utilised tool to identify the presence, absence and, to a certain extent, the relative quantitation of a certain protein in a sample. A plethora of studies investigating

neuronal tissue or neurogenesis from MSCs have widely employed the presence or absence of markers such as GFAP, βT3, NeuN and NF200 as indicators of neuronal-like differentiation of MSCs [104, 190, 192-195, 377]. These markers were previously investigated in chapter 3 with the BME treated ADSCs for neurogenic induction. Briefly recapping the results from this study, the βT3 and NF200 were identified in all CK treatments as well as the basal ADSCs and the control GBCs. The GFAP was at the highest concentration in the GBCs with barely detectable levels in any of the other cell types. NeuN as well had a weak positive however equivalent levels in basal ADSCs, CK treated ADSCs and the GBC control. The positive identification of three out four markers is a promising result for most. However the appearance of equivalent band intensities in the untreated ADSCs shows how problematic the utility of "neuronal" specific markers is. The presence of these proteins in untreated ADSCs contradicts their use as a definitive neuron-specific maker. Thus the broader proteomic investigation into further markers unique to cells treated at specific time points may assist in the elucidation of the extent of differentiation occurring.

4.4.2.2 Neurogenic related roles of identified proteins by iTRAQ

Gene ontology sorting of the iTRAQ datasets by biological process filtering only for neuronal-related functions enabled the assessment of large data sets for relevant proteins. The comparison of identified proteins unique and shared between the CK treated and basal ADSCs expression levels in each sample assisted in their correlation to the differentiation process. Comparing the ratios and biological roles of the statistically relevant proteins in each treatment, has revealed and quantified a number of them annotated to have neurogenic and stress properties. As such, the proteins identified uniquely or shared in each category will be elaborated on in the context of the proteins within the same treatment to demonstrate any relevant affects during differentiation or stress. Table 4 summarises significant proteins identified in the AECK and LK treated ADSCs with a neuronal-

related biological process. The investigation of the up regulated neuronally related proteins roles is important to comprehend the biological context of their expression.

Filamin-B was identified in both chemically treated ADSCs with a statistically significant up regulation in each respective differentiated produced cell. Filamin-B is an actin-binding protein which is highly expressed in the CNS displaying roles in cellular migration and differentiation [508]. The relevance of Filamin-B in neurogenic differentiating ADSCs stems from its annotated role in neuroblast migration in the developing brain from the ventricular zone to the outer cortical plate [508]. The migratory roles are linked to the interaction between Filamin-B and its 70% homologous interacting partner Filamin-A which promotes the development and maintenance of the cells bipolar shape [509]. The up regulation of Filamin-B in treated ADSCs is significant since the morphological shape of the treated cells appear elongated and bipolar prior to the development of neurite outgrowth. An interesting binding partner was also identified within the statistically relevant proteins of both treatments. The partner; Ras-related C3 botulinum toxin substrate 1 (Rac1) is annotated with the biological process of nerve growth factor receptor signalling pathway. Rac1 is a pleitropic regulator of a variety of cellular processes including the proliferation, differentiation and neuronal maturation during embryonic and adult hippocampal development [510, 511]. The assistance in the migration and axonal and dendritic development is directed via its signalling interaction with similarly functional proteins to initiate the spatial reorganisation of the cytoskeleton for neuronal development [512, 513]. The identification of Rac1 in neuronal differentiating ADSCs indicates the morphological changes observed are maintained and directed through a number of control mechanisms that are widely seen in the development of *in* vivo neuronal tissue. Rac1 has the potential to be utilised as a novel marker for neurogenesis of ADSCs. The identification of Rac1 in neuronal differentiating ADSCs has the potential to be utilised as a novel marker for neurogenesis.

Thioredoxin and Peroxiredoxin-1 are abundantly expressed in both chemical treated ADSCs. Each protein is found ubiquitously in mammalian cells [514] thus they would not be suitable as a

neurospecific marker. Their function however is of great importance especially within the context of this study's focus on chemical induction. All Peroxiredoxins contain a conserved cysteine residue which undergoes a cycle of peroxide-dependent oxidation and thiol-dependent reduction [515, 516]. This is particularly relevant since it regulates the intracellular redox state, effectively protecting the cells from oxidative stress. This may occur, to a certain extent, based on the oxidative-stress response proteins seen up regulated with BME treatment (chapter 3). A study by Simzar *et al*., [517] found that the overexpression of peroxiredoxin in PC12 neuronal cells *in vitro* increased the presence of reactive oxygen species, essentially creating an oxidative stress inducing environment. This does not seem to be the case in this study as the cell population is maintained at sufficiently high numbers compared to the immense loss in the BME treated cells. The activity of Peroxiredoxin-1 is regulated by thioredoxin which reduces the cysteine in peroxiredoxin [518-520]. The regulatory mechanisms maintaining the levels of peroxiredoxin and thioredoxin levels are essential in preserving cells in distress. However if thioredoxin is overexpressed in damaged neuronal cells, neuronal degeneration can occur as a secondary injury [521]. The importance of expression and regulation of these two molecules in sustaining cells for proliferation is essential; furthermore it can be used as a marker of the level of stress experienced by neurogenic induced cells. In comparison with the BME treated ADSCs in chapter 3, both peroxiredoxin and thioredoxin expression levels were significantly up regulated, which reinforces the notion of the oxidative stress induced environment the ADSCs were exposed to in the presence of BME.

The only other shared neuronal-related protein identified was the broadly covered Neuroblast differentiation-associated protein (AHNAK) from chapter 3. AHNAK expression in AECK and LK treated ADSCs was found to be expressed at higher levels than in the BME treated cells. Furthermore the binding partner's annexin2 and S100-A10 were also identified with at least a two-fold increase over basal levels. The established GO classification for AHNAK is its involvement in nervous system development. It has also been recognized to have multiple roles in neuronal development dependent on its cellular localisation and calcium concentrations which regulates actin cytoskeleton

organisation, cell membrane architecture and cell-cell junction formation [386-390]. Moreover the non-membrane bound AHNAK promiscuously interacts with several reported partners such as protein kinase C and phospholipase C which are involved in the activation of inositol metabolism [392-394]. Protein kinase C and phospholipase C were both found to be statistically significantly up regulated in both the AECK and LK treated ADSCs. Inositol metabolism is vital in nerve guidance, serotonin modulation and the control of intracellular calcium concentration [392, 395]. As previously discussed there is mounting evidence for the usefulness of AHNAK as a marker for neurogenesis especially in the co-expression and up regulation of neuronal development related binding partners. This is further evidence that the CKs are more suitable for inducing neurogenesis of ADSCs.

An associated multifunctional-actin binding protein uniquely identified in the LK treated ADSCs is Gelsolin. Gelsolin localisation and expression has been determined to be highest in the CNS and PNS and it has been found to be involved in a number of growth promoting and neuroprotective functions [522, 523]. Its role in actin remodelling in the nervous system is calcium dependant, with the protein initiating actin polymerisation or disassembly [524]. Since the highest expression has been determined to be in the oligodendrocytes and Schwann cells myelin sheaths, Tanaka *et al*., [522] proposed the role of gelsolin to be involved in the maturation of the myelin sheath forming cells. The neuroprotective capability is noted dually to its anti-oxidative and anti-apoptotic functions in high oxidative-stress induced environments [525]. Interestingly the down regulation or proteolytic cleavage of gelsolin has been linked to the development of Alzheimer's disease [526, 527]. The expression levels of Gelsolin in the BME treated ADSCs in chapter 3 do not show any notable change in expression levels compared to the basal ADSCs.

The up regulation of Gelsolin in the CK treated ADSCs and value as a neuronal marker is apparent, since the presence of a neuronally related cytoskeletal remodelling protein with neuroprotective capabilities is an appealing find in the array of up regulated proteins of neurogenic differentiating

ADSCs. This is further evidence that the CK chemicals are better suited for inducing neurogenesis in ADSCs.

Clathrin heavy chain 1 has been statistically significantly up regulated in only the AECK samples and has been annotated by biological function as an axon guiding molecule also involved in the nerve growth factor receptor signalling pathway. However the amount of research into these systems is very limited and studied in the neurogenesis of *Drosophila* [528] and the role of this molecule remains to be elucidated. Spectrin alpha and beta chain however has been widely studied and are known to be major cytoskeletal components in the brain and distributed in the cytoplasm of neural cells [529-531]. There is now evidence that spectrin regulates the surface chemistry and morphology of neuronal cells and large modifications or degradation would produce major modifications to synapses [532]. Spectrin has also been implicated in the calcium regulated release of neurotransmitters between developing synapses [533]. The regulation of spectrin is derived from the calcium modulated calpain proteolytic enzyme [532]. The levels of calpain in both chemical treatments in this study are negligible. Here the presence of a heterodimer of the brain isoforms of spectrin alpha and beta chain is well noted in the prospect of utility as a neuronal marker for further studies.

Lastly Galectin-3 expression has been detected in the LK treated ADSCs. Recent studies have shown that galectin-3 is expressed in a variety of neuronal tissues, especially glial cells in the CNS in which it directs oligodendrocyte differentiation to control myelin sheath formation [534]. Furthermore, the control of neuroblast migration in brain development was proposed by Comte *et al*., [535]. A function that is more suited to the development of neuronal like cells was found by Pesheva *et al*., in which galectin-3 was found to stimulate neural cell adhesion and moreover, neurite outgrowth in developing cells [536, 537]. This also provides further evidence the ADSCs are responding favourably to the CK treatment, expressing neuronal-related proteins known to be functionally and structurally useful.

Table 4 Summary of significant up-regulated neuronal-related proteins identified in iTRAQ of hADSCs treated with AECK and LK.

AECK	Accession	Name	GO	Biological process	Peptides(95%)	fold change	Pvalue
	O75369	Filamin-B	GO:0030154	cell differentiation	129	1.230453968	2.44E-15
	P00367	Glutamate dehydrogenase 1, mitochondrial	GO:0006537	glutamate biosynthetic process	12	1.339429975	0.01273619
	P09429	High mobility group protein B1	GO:0031175	neuron projection development	16	1.15634203	0.03726548
	P10599	Thioredoxin	GO:0008283	cell proliferation	7	1.57030201	0.04286075
	P15144	Aminopeptidase N	GO:0030154	cell differentiation	32	1.223500967	1.10E-05
	P15559	NAD(P)H dehydrogenase [quinone] 1	GO:0007271	synaptic transmission, cholinergic	9	1.816967964	0.002394901
	Q00610	Clathrin heavy chain 1	GO:0048011	nerve growth factor receptor signalling pathway	69	1.205008984	7.17E-07
	Q01082	Spectrin beta chain, brain 1	GO:0007411	axon guidance	54	1.284289956	3.63E-10
	Q06830	Peroxiredoxin-1	GO:0008283	cell proliferation	25	1.434638977	0.008896183
	Q09666	Transforming protein RhoA	GO:0007399	nervous system development	16	1.167513967	0.019935589
	Q09666	Neuroblast differentiation-associated protein AHNAK	GO:0007399	nervous system development	285	1.527696013	1.40E-45
	Q13813	Spectrin alpha chain, brain	GO:0007411	axon guidance	71	1.29076004	6.27E-14
	P63000	Ras-related C3 botulinum toxin substrate 1	GO:0048011	nerve growth factor receptor signaling pathway	7	1.664183	0.006588
	Q9P0L0	Vesicle-associated membrane protein-associated protein A	GO:0031175	neuron projection development	10	1.441416979	0.006864889
LK	**Accession**	**Name**	**GO**	**Biological process**	**Peptides(95%)**	**fold change**	**Pvalue**
	O75369	Filamin-B	GO:0030154	cell differentiation	129	1.372761965	0.0149013
	P06396	Gelsolin	GO:0060271	cilium morphogenesis	23	1.32772994	0.001008915
	P10599	Thioredoxin	GO:0008283	cell proliferation	4	1.76563704	0.02659229
	P11142	Heat shock cognate 71 kDa protein	GO:0007269	neurotransmitter secretion	73	1.381860971	0.00224432
	P11413	Glucose-6-phosphate 1-dehydrogenase	GO:0001816	cytokine production	23	1.242061019	0.00224432
	P15144	Aminopeptidase N	GO:0030154	cell differentiation	32	1.44699502	0.019935589
	P17931	Galectin-3	GO:0030154	cell differentiation	7	1.757151961	0.006587825
	Q01082	Spectrin beta chain, brain 1	GO:0007411	axon guidance	54	1.506716013	6.27E-14
	Q09666	Neuroblast differentiation-associated protein AHNAK	GO:0007399	nervous system development	285	1.659075022	2.00E-25
	Q13813	Spectrin alpha chain, brain	GO:0007411	axon guidance	71	1.395959973	6.27E-14
	Q92974	Rho guanine nucleotide exchange factor 2	GO:0048011	nerve growth factor receptor signaling pathway	9	1.163854957	0.033079
	P63000	Ras-related C3 botulinum toxin substrate 1	GO:0048011	nerve growth factor receptor signaling pathway	7	1.616315960	0.006153737
	Q9P0L0	Vesicle-associated membrane protein-associated protein A	GO:0031175	neuron projection development	10	1.531931043	0.039667

4.4.2.3 Stress related roles of identified proteins by iTRAQ

The primary role of the treatment of the ADSCs with the CK chemicals was to attempt to initiate the production of a neurogenic lineage with a simple chemical inducer that was non-toxic and promoted neurogenic differentiation. The CK fulfilled these criteria in this study, producing a high population of cells that morphologically resembled neuronal cells and expressed a variety of neuronal proteins, some of which have been previously implicated in neuronal protection processes [491]. The amount of cellular distress judged by morphological appearance was minimal amongst all trialled chemicals when compared to the BME treated cells when observed by microscopy, in which 50% of a cell population was lost due to the strong and lasting effect of the BME differentiation inducer. In exploring the up regulated proteins, stress-related proteins are of interest as they can reflect the state and outcome of the produced cell. The previous study (chapter 3) found a large proportion of oxidative-stress related proteins in the iTRAQ data set, which indicated the cells produced were not suitable for a clinical application. This was not the case for the AECK and LK treatments. A summary of the stress related proteins from the AECK and LK treatment are available in table 5.

A minimal number of three proteins, compared to the BME treated cells, related to oxidative-stress were statistically significantly up regulated collectively across both chemical treatments. The proteins in question are Keratin, type II cytoskeletal 1, G6PD and Lon protease homolog. Keratin, type II cytoskeletal 1 is a ubiquitous structural protein which plays a role in the structural support of a number of cells. The moderately elevated detected levels of keratin in this study are unlikely to be involved in a specific neurongenic process or the response to stress. This can be supported by the studies in keratin stress related overexpression which has been related to a gene defect or in due to a malignant growth [538-540]. As such the slight fold increase is proposed as due to the rearrangement of the cytoskeleton during the differentiation process, which is visually apparent in the morphological changes visualised by microscopy.

The second protein annotated as a response mechanism to oxidative stress is G6PD which is seen to have 29% and 24% increase in the respective AECK and LK treated cells compared to basal ADSCs. G6PD has been implicated in the response to oxidative stress due to a mutation causing a G6PD deficiency [541] which is not the case in this study. Conversely in neuronal damage, Parkinson's and inflammation the redox system may be destabilised, G6PD may be overexpressed to increase its activity in the axon terminals in neurons for a cytoprotective role [429]. This seems to be the case in the BME treated cells which express a higher percentage of G6PD at 12 hours post induction than that of both the CK treated ADSCs. The over expression of G6PD in the BME treated cells indicates that those cells were indeed experiencing an increased oxidative stress environment caused by the BME.

Finally the Lon proteases primary role is catalysing the degradation of oxidatively modified mitochondrial matrix proteins arising from oxidative-stress environments [542]. The elevated levels of expression are nominal, any down regulation of this protein deregulates the mitochondria and leads to apoptosis [542].

A large proportion of the remaining up regulated statistically significant proteins were annotated as being involved in cellular component disassembly during apoptosis. The proteins gelsolin and spectrin were previously discussed in section 4.2.2 for their roles in the rearrangement of the cytoskeleton. The appearance of the protein plectin is significant, as this protein is a 500 kDa protein which is ubiquitous in mammalian tissue acting as the interacting support bridge between actins, microtubules and intermediate filaments maintaining cytoarchitechture [543]. This protein effectively connects junctures between individual cells [544]. A high expression of plectin is found in maturing neurons and ganglion in developing CNS [545] thus the higher expression of plectin in neurogenic differentiating ADSCs indicates a level or cytoskeletal reorganisation is occurring. Two of The interacting partners of plectin were also identified concurrently; vimentin and spectrin; also

have a role in cytoskeletal organisation function in developing neuronal cells as previously discussed in section 4.4.2.2.

The role of vimentin in cellular stress response has also been investigated, the protein being found to be vulnerable to heat shock, shear stress or stress induced by hypotonic environments [546-548] . Under these conditions, the protein will typically unfold in an effort to maintain the structural integrity of a cell however will not return completely to its native form [549] and the expression levels in a stress induced situation would usually increase to replace the physically altered proteins allowing a cytoskeletal reorganisation [550, 551]. Completing the cohort of responsive proteins involved in cellular disassembly are Prelamin-A/C and Alpha Adducin which, like several of the previous proteins, are expressed in numerous tissue types and are responsible for maintaining cytoskeletal architecture or rearrangement during the development of interceding tissues [552, 553]. The modulation of these 'stress' induced cytoskeletal proteins are thought to be up-regulated due to the reorganisation and the development of extending neurite outgrowth in the neurogenic induced ADSCs.

Table 5 Summary of significant up-regulated stress-related proteins identified in iTRAQ of hADSCs treated with AECK and LK

AECK Stress	Accession	Name	GO	biological process	Peptides (95%)	fold change	Pvalue
	P01892	HLA class I histocompatibility antigen, A-2 alpha chain	GO:0060333	interferon-gamma-mediated signalling pathway	4	1.4692	0.01600371
	P04083	Annexin A1	GO:0006954	inflammatory response	45	1.3066	0.00108737
	P04264	Keratin, type II cytoskeletal 1	GO:0006979	response to oxidative stress	13	2.0287	0.00100892
	P06396	Gelsolin	GO:0006921	cellular component disassembly involved in apoptosis	25	1.3732	2.05E-13
	P09429	High mobility group protein B1	GO:0002437	inflammatory response to antigenic stimulus positive regulation of apoptosis	16	1.1563	0.00754318
	P11413	Glucose-6-phosphate 1-dehydrogenase	GO:0034599	cellular response to oxidative stress	23	1.2994	0.00129321
	P15121	Aldose reductase	GO:0006950	response to stress	9	1.3973	0.00414161
	P16070	CD44 antigen	GO:0060333	interferon-gamma-mediated signalling pathway	15	1.3484	8.89E-05
	P30044	Peroxiredoxin-5, mitochondrial	GO:0034614	cellular response to reactive oxygen species inflammatory response	9	1.3299	0.00063648
	P35611	Alpha-adducin	GO:0006921	cellular component disassembly involved in apoptosis	12	1.5308	4.06E-12
	P51572	B-cell receptor-associated protein 31	GO:0006921	cellular component disassembly involved in apoptosis	7	1.4834	0.00252419
	P61586	Transforming protein RhoA	GO:0050772	positive regulation of axonogenesis	16	1.1675	0.00013793
	P63000	Ras-related C3 botulinum toxin substrate 1	GO:0008624	induction of apoptosis by extracellular signals	7	1.6642	3.48E-06
	P63000	Ras-related C3 botulinum toxin substrate 1	GO:0006954	inflammatory response	7	1.6642	0.00016355
	P63241	Eukaryotic translation initiation factor 5A-1	GO:0006917	induction of apoptosis	20	1.4873	6.36E-12
	Q02952	A-kinase anchor protein 12	GO:0030819	positive regulation of cAMP biosynthetic process	17	1.3261	0.0067851
	Q03135	Caveolin-1	GO:0009267	cellular response to starvation inactivation of MAPK activity positive regulation of calcium ion transport into cytosol positive regulation of canonical Wnt receptor signalling pathway response to hypoxia	7	3.1097	0.02121297
	Q13813	Spectrin alpha chain	GO:0006921	cellular component disassembly involved in apoptosis	71	1.2908	0.00131438
	Q15149	Plectin	GO:0006921	cellular component disassembly involved in apoptosis	174	1.3019	2.20E-09

	Q9NR28	Diablo homolog, mitochondrial	GO:0008625	induction of apoptosis via death domain receptors	6	1.2655	2.20E-09

LK Stress	Accession	Name	GO	biological process	Peptides(95%)	fold change	Pvalue
	P02545	Prelamin-A/C	GO:0006921	cellular component disassembly involved in apoptosis	63	1.4487	3.04E-09
	P06396	Gelsolin	GO:0006921	cellular component disassembly involved in apoptosis	23	1.3277	0.00031779
	P08670	Vimentin	GO:0006921	cellular component disassembly involved in apoptosis	199	1.2634	7.44E-05
	P11413	Glucose-6-phosphate 1-dehydrogenase	GO:0034599	cellular response to oxidative stress	23	1.2421	0.00100042
	P35611	Alpha-adducin	GO:0006921	cellular component disassembly involved in apoptosis	12	1.5308	0.02401391
	P36776	Lon protease homolog, mitochondrial	GO:0034599	cellular response to oxidative stress	17	1.4223	0.0050889
	P51572	B-cell receptor-associated protein 31	GO:0006921	cellular component disassembly involved in apoptosis	7	1.5205	0.00379271
	Q03135	Caveolin-1	GO:0009267	cellular response to starvation inactivation of MAPK activity	7	2.5188	0.00436605
	Q13813	Spectrin alpha chain, brain	GO:0006921	cellular component disassembly involved in apoptosis	71	1.396	9.24E-15
	Q15149	Plectin	GO:0006921	cellular component disassembly involved in apoptosis	174	1.569	2.06E-39

4.4.3 Bioplex analysis and roles of cytokines in AECK and LK induced ADSCs

Cytokines are pleotropic proteins that coordinate signalling across varied tissues and cell types including during neural development [445]. Cytokines display functional roles in a variety of development stages, acting as neurotrophic factors initiating the repair and regeneration of cells [445]. Furthermore certain groups of cytokines, such as chemokines, regulate the directed growth and communication between radially migrating neuronal cells which give rise to mature neurons, glial, astrocytes and oligodedricytes [445]. Due to their relatively low abundance and the dynamic range of a proteome, these molecules are extremely difficult to detect by MS and alternative detection methods such as the Bioplex cytokine, chemokine and growth factor assay system, allows the relative quantitation and comparison of 27 secreted cytokines.

As in the previous chapter, group clustering was carried out to identify the cytokines which responded with similar trends during the differentiation process. The clustering allowed the subdivision of the cytokines by trends into 7 distinct groups of which the most pertinent or outstanding fluctuation of a cytokine breaking trend will be expanded upon to discuss its possible role within the CK treated cells relative to neurogenesis.

The concentration change of molecules from group 1 was apparent with the out of trend large fluctuation of MIP-1b and RANTES in the LK treated ADSCs. MIP-1b is a pro-inflammatory protein which displayed a substantial increase at 20 hours in LK, indicating a significant pro-inflammatory affect. Interestingly, the increase in MIP-1b is mirrored by RANTES with a proceeding concentration increase at the same time point. The secretion of MIP-1b has been noted in a number of neuronal cells [554]. The developmental organisation of neuronal cells and CNS development have been linked to a synchronous regulation of MIP-1b alongside other chemokines [555]. Studies have shown that MIP-1b knockout mice soon die after birth due to brain formation abnormalities [555, 556].

Thus the role of MIP-1b in ADSCs has gained some interest especially with a number of co-regulations at the same time point in other cytokine groups. RANTES, also a pro-inflammatory cytokine, was found to initiate neuro-protective roles assisting in the survival of stressed hippocampal cell lines in the presence of a toxin [557, 558]. Interestingly a study conducted into investigating the effect of certain pain management drugs in patients with HIV, found that morphine treatment deregulated and decreased the expression of RANTES in the neuronal tissue. This progressive effect was implicated in the decrease in microglial cell migration due to the suppression of the chemotactic cytokine [559]. Furthermore another study into the affect of HIV glycoprotein120 on neuronal tissue presented a number up regulated secreted pro-inflammatory cytokines including RANTES which offered a neuroprotective role [560]. These responses all lead to the stimulation of the CX3CL1, CCL4 and CCL5 receptors of the above cytokines [555] which may also be regulated in the differentiating ADSCs.

Examining beyond group 1 with the consideration of the 20 hour time point, a number of similar variations in trends were identified amongst several cytokines in other groups. The decrease of IL-15 is a significant find as its expression and regulation, through an indirect neuroprotective mechanism, in astroglial cells has been found to be linked to RANTES, MIP-1a, MIP-1b and GM-CSF [561] . Interestingly IL-15, IL-17 and GM-CSF in LK's group 5 present a massive decrease in concentration per cell from the 5 hr to 20 hr time point. Elevated concentrations of IL-15 in neural stem cell (NSC) cultures have proven to reduce maturation and neurite out growth in differentiating neurons but not affect the proliferation [562]. Furthermore, IL-15-deficient mice exhibited defective JAK/STAT and ERK pathways which are key in the regulation of differentiation in NSCs. This substantiates the possible role for the decrease of IL-15 in LK treated ADSCs which presented greater morphological differentiation than the AECK treated cells [563]. The down regulation of IL-17 is also considered a beneficial decrease for cytokines in brain tissue, since elevated levels are usually present in a number of traumatic brain injuries or infarcts in which a large proportion of cells are damaged [564, 565]. No further interesting trend variations were seen in the other groups.

The Bioplex and iTRAQ data complement the findings that the AECK and LK treatments of ADSCs initiate the differentiation toward a neuronal lineage and the resultant cells, evidenced by the proteomic and microscopy are healthier than the BME treated cells. The results also indicate the ADSCs favour the treatment with LK over AECK for neuronal-like differentiation within the 24 hour treatment time. Notwithstanding the AECK did produce a slightly higher cell population at the end of the differentiation time and similar neurogenic-related proteins identified.

4.5.0 Conclusion and future directions

This study aimed to investigate the extent of proteomic change in ADSCs treated with two different CKs in an attempt to induce neurogenic differentiation. As demonstrated in this study a number of neurogenic and stress related proteins have been up-regulated, most of which are noted in the literature to have positive effects for neurogenic differentiation. A proportion of the statistically significant proteins were explored, investigating their known function in developing neurons and their probable role within the treated cells. Complementing the iTRAQ quantitative proteomic data, the Bioplex system allowed the investigation of a closed cohort of cytokines and interleukins allowing trends to be examined, allowing a closer look at the smaller and lower copy number proteins that have numerous profound affects in the immunogenicity and stress response of cells.

Here we have proven that the treatment of ADSCs with the CK compounds, AECK and LK, have the potential to induce ADSCs toward a neurogenic phenotype, producing similar morphological traits established in previous studies but with the added benefit of being seemingly non-toxic at the utilised concentrations as indicated by cell counts. The supporting evidence of the expression of neuronal-related proteins such as Spectrin brain isoform 1, Neuroblast differentiation-associated protein AHNAK and Gelsolin, which have not been previously utilised as neuronal markers but are known to play an integral role in the maturation and development of the CNS, further infers the CK's differentiation function. Thus the novel application of CK's to produce a neurogenic-like cell line

within 24 hours of induction holds some potential for further applications for neuroregeneration and in studies in the transdifferentiation of ADSCs.

The chief ensuing experimental procedures would be to investigate the range of changes that occur during the development of the treated cells in a temporal analysis as well as identifying changes occurring post 24 hours in a longer term *in vitro* culture. Furthermore, functionality tests to determine if the produced cells would propagate an action potential or express the supportive ion channel mechanisms need to be performed to give clear proof that these cells are indeed neurons.

Chapter 5

Final Summary, Concluding Remarks and Future Perspectives

This study presented the first investigation of its type, a broad proteomic investigation of differentiated ADSCs derived from both rat and human adipose tissue. These investigations revealed valuable insights into the cellular and secreted proteome changes of homogenous ADSC cultures directed toward various phenotypic lineages by means of induction media. The core chapters focused on an in depth analysis of neurogenic differentiation with the chemical inducers BME and a naturally occurring chemical alternative that was theorised to have a less toxic effect.

The conjecture summarised in chapter one indicated that the classical techniques, such as flow cytometry and immunohistochemistry, utilising relatively few cell surface markers is insufficient for the characterisation of ADSCs and their differentiated counterparts. Two main reasons point to this inference. Firstly there is an overabundance of literature which presents conflicting data about the presence and absence of the same set of surface markers on these cells all of which have been investigated by the same techniques. Secondly, a number of surface markers are now known to spontaneously change in expression levels *in vitro* [274] which causes quite the dilemma for using them as consistent characterisation markers for cells. Furthermore the minimal cluster of markers indicated by the literature does not elucidate the extent of differentiation achieved by the induced ADSCs. The lack of a full characterisation of the cell, let alone the proteome, and the lack of a comprehensive understanding of the biological context of the molecular changes is a large gap in the field. Thus the main aim of this thesis was to examine and profile the extent of changes occurring at the global level of the proteome of differentiating ADSCs.

The proteomic investigation in chapter two into the development of osteogenic, chondrogenic, myogenic, adipogenic and neurogenic cells with comparison to their primary derived counterparts (PDCs) aimed to expand on the current knowledge of the degree of differentiation attained by the induced ADSCs, which were differentiated using published methods. The analyses of the captured proteome by various proteomic toolsets attempted to investigate both high and low abundance proteins by utilising 1D and 2D SDS-PAGE both coupled with LC-MS/MS, and the Bioplex assay for

low abundance cytokines. This initial investigation is the first report to utilise a range of proteomics techniques to compare rat ADSCs, their various differentiated progenies and mature primary derived cells to explore the level of differentiation of these cells and determine the proteomic similarity to their mature counterparts. Furthermore it was also an evaluation of whether or not the currently employed markers are of any use and whether others should be considered in their place.

Proteomic profiling by 2D-PAGE exhibited that the differentiated cells displayed unique and varied proteome changes in comparison to the basal cells which followed a trend of least to most changed 2D-PAGE profiles as a function of differentiation relative to the basal ADSCs; ADSC < Neurogenic < Osteogenic < Chondrogenic < Adipogenic < Myogenic. From this trend the first three differentiated cell lines were chosen for further investigation by 1D-PAGE and LC-MS/MS. Coincidently the trend also indicated the length of time the cells spent in culture till their final time point. The first three where chosen due to their relatively shorter differentiation time as well as the interest into these areas that drove the research direction. The chondrogenic and osteogenic differentiation experiments were run in parallel with basal ADSCs and primary derived chondrocytes and osteoblasts. Similarities in the proteomic profiles were expected between the basal ADSCs and the differentiated cells as well as similarities between the differentiated cells and the PDCs which were considered to be useful in determining the extent of differentiation by the induced ADSCs. The trisecting comparisons between all three cell types revealed a high degree of similarity shared between the basal, treated and PDC cells by total unique and shared proteins identified. More than 50% of the identified proteins in this comparison are shared between the three cell types, indicating a large proportion of the shared proteins are present in the various mesodermal cells. This comparison is important as it allows some biological context of the expressed shared and unique proteins to be elucidated and how much their expression levels vary in each differentiation. While the qualitative differences in the presence or absence of unique proteins are useful in terms of markers, the complete quantitative differences of both shared and uniquely expressed proteins between the compared lines is equally important. For example, the shared proteins between the

chondrogenic cells and the primary chondrocytes, that are not present in the ADSCs, may be useful as targeted cartilage specific marker proteins. Examples of such proteins involved in cartilage development identified within this study were Aldehyde dehydrogenase, Protein Col6a1 and Protein Col6a3. These proteins are biologically important in the development of ECM in during cartilage maturation [309, 310]. The presence of these molecules in the chondrogenic and primary cartilage reveals that the ADSCs are expressing cartilage structural and functional proteins after induction. Complementary to this, the unique proteins expressed in the ADSCs not appearing in the other cell types would also be useful as ADSC specific markers. Furthermore this assists the comparisons as the percentage of shared proteins from the total number of identified proteins indicates the extent of differentiation achieved by the ADSCs. The shared proteins between the differentiated and the PDCs gained the most interest as these results would indicate the relative extent of differentiation and phenotypic closeness to its mature counterpart. The chondrogenic cells expressed a number of cartilage specific extracellular matrix basement proteins such as Biglycan, which were concurrently identified in the primary chondrocytes. Biglycan and various other chondrocyte specific proteins (see chapter 2 table 3) exhibit that the ADSCs are capable of expressing a diverse assortment of functional and structural cartilage proteins and not merely aberrant expressions in response to a changed media. This complemented the positive alcian blue histological staining of GAGs found predominantly in maturing chondrocytes.

Within the parallel osteogenic evaluation, a larger percentage overlap of shared proteins was identified between the osteogenic and osteoblastic cells. The relevance of critical maturation proteins such as laminin-1 and galectin-3 has been associated with the development of calcium rich ossified bone matrix [318, 320, 322, 326, 328]. Previous studies have exhibited the presence of such molecules in collusion with the up regulation of other osteogenic markers such as ALP activity, osteocalcin and bone sialoproteins [28, 330, 356, 566]. The up regulation of bone maturating proteins adds a greater depth of knowledge and a list of usable marker proteins which indicate osteogenesis. The proteins identified here have a higher probability for practical use as

unambiguous markers for osteochondral maturation which is in accord with PDC expression. Furthermore, a broader perspective of expressed proteins during differentiation allows for a greater comprehension of the biological context of ADSCs mesodermal differentiation capabilities.

Continuing in chapter two, the examination of a transdermal differentiation of rat ADSCs toward a neuronal-like lineage utilising a simple chemical additive, BME [104], was also included in the proteomic analysis. The large amount of unique proteins (445) identified by LC-MS/MS in the neurogenic samples was intriguing especially since a considerable portion were annotated with neuroprotective, neurotrophic and growth related processes. Supplementary to this list of neuronal related proteins, a number of stress and shock related proteins were also identified. The expression of proteins such as astrocytic phosphoprotein, mesencephaolic astrocyte-derived neurotrophic factor, brain acid soluble protein, βT3, gamma-enolase and neudesin of which the final three are widely used neurogenic markers [28, 44, 104, 195, 196, 274, 301, 353, 354] indicates a number of neuronal specific proteins and mechanisms for transdermal differentiation can be activated within 24 hours of treatment. The potential of using a simple chemical for initiating neuronal differentiation of ADSCs may retain some validity despite the nil results from some researchers investigating the propagation of action potential as though the produced cells were terminally differentiated neurons [196]. The potential was also confirmed by Kingham et al [191] work wherein ADSCs were seen to develop into Schwann cells. Rat ADSCs transdermal differentiation *in vitro* has a broad spectrum of neuronal related proteins. While the BME chemical may not be clinically applicable due to its relative toxicity to cells at the concentration utilised, the markers acquired from this study can be applied to further studies, utilising the array of proteins identified as further markers for neurogenesis (see chapter 3 table 2).

The Bioplex assay approach has not been used in the context of comparing basal, differentiated cells and PDCs before. This offered a greater detail about low abundance proteins that were otherwise masked due to the dynamic range of high abundance proteins or are secreted in such low copy

number that they are frequently below the limit of detection by mass spectrometry. The Bioplex system not only allowed the individual cytokines to be evaluated but also their group clustered trends were compared between the basal cells, differentiated cells and PDC secretions. The secreted cytokine profiles displayed were unique for each cell type however similarities were identified between the osteogenic and osteoblasts as well as the chondrogenic and chondrocytes. The trends indicated a close affiliation between the developing and mature cells. The trends indicate very similar mechanisms are being stimulated as the secreted cytokines only differ marginally in levels but their overall trend is very similar between differentiating and mature cells.

Investigating the extent of differentiation by comparison of differentiated cells to primary derived counterparts provided additional proteins to be added to the repertoire of known markers of chondrogenesis and osteogenesis, while the mechanisms that drive this differentiation process forward in ADSCs are slowly being unravelled. Through further research utilising instruments with greater sensitivity, such as the ABSciex TripleTOF 5600, to perform global proteomic analysis or using a targeted SRM approach will allow for the individual processes and biological mechanisms to be clarified further.

Exploring the neurogenic potential of human ADSCs treated with BME was continued in chapter three. The primary objective was to survey the changes occurring in the proteome and if these alterations would shed certain light for future clinical applications of a simple chemical neurogenic differentiation. Proteomic analysis was performed on much more sensitive instruments utilising the iTRAQ isobaric tagging system for absolute quantitiation to analyse protein expression differences between basal, differentiated and a gliablastoma cell line as a relative measure of expressed neuronal proteins. Furthermore, the analysis of cytokine expression levels and trend profiles were completed with the Bioplex system.

This arm of research indicated that neurogenic and stress proteins were produced as previously determined in the rat ADSC studies. Further investigation indicated the expressed neuronal related

molecules identified were annotated as neuroprotective and maintenance proteins of cells experiencing oxidative stress and inflammatory conditions. However the abundance of proteins such as Neuroblast differentiation-associated protein (AHNAK) [386-388, 395], Glutaminase [396, 398, 400] and their interacting partners, all found in this work show a significant up regulation in expression levels, have been directly linked to early neuronal development and cellular restructuring. This indicates that the differentiation process is stuck in the early stages, as though initiating the neurogenic process but being unable to support the continual neuronal development due to the persistence of the BME in the culture. This theory is supported by the increase in expression of oxidative stress and heat shock response proteins, the presence of cytokines due to inflammatory and oxidative stress conditions and the high level of cell death. The wealth of investigated proteins from this study can undoubtedly be used in the future to identify developmental or stress proteins during *in vitro* neurogenic studies.

Whilst the inclusion of BME as an initiating factor for inducing neurogenesis produced cells which resemble neuronal-like cells with a phenotypic expression of numerous neuronal specific proteins, the culture conditions may not be suitable for producing complete neuronal cells. It seems that the chemical properties of BME that initiates the process is invaluable and these properties may be mimicked by a variety of alternative compounds that are stable, non-toxic and biologically relevant.

Future work related to BME induced cells would include a short temporal proteomic investigation, between 1-12 hours, of ADSCs exposed to BME neurogenic media. Similar treated cells should subsequently be maintained in a continual cell culture in media supplemented with neurogenic growth factors which are formulated to maintain primary neuronal cells. This can then be coupled with the directed SRM investigation of the previously utilised marker proteins such as GFAP, Nestin, Neudesin, NF200 and Neuron Specific Enolase as well as further markers presented in this body of work which have shown much merit for further investigations. Furthermore, a metabolomics approach probing for the by-products of enzymes as glutaminase, which is directly related to the

glutamine present in neuronal cells [400], will supplement the expanding knowledge of neurogenesis. A targeted protein approach with high quality fluorescently labelled antibodies to AHNAK coupled with high resolution microscopy such as the OMX will provide detailed localisation and compartmentalisation of the protein during differentiation.

Chapter four continued the investigation of ADSCs transdermal differentiation potential with the single treatment with a non-toxic and biologically stable chemical to induce neurogenesis. This may allow the production of a group of cells that have the initiative or directive to mature into a variety of neuronal-like cells *in vitro* or *in vivo* dependant on the supplemental maintenance or usage. This chapter draws numerous comparisons to the BME induced ADSCs, from chapter 3, which presented a number of neuronal proteins during their differentiation and the expression of stress and shock proteins as well as the stress induced apoptosis that removed this differentiation process from a clinical application. The application of the cyclic ketamines, LK and AECK, produced a higher population of cells that were highly similar in morphology to neuronal cells compared the BME treated ADSCs. The importance of comparing the CK and BME treated data sets allows a number of biologically relevant links to be made between related responses that these simple chemicals impose on the basal ADSCs. Whilst the BME produced cells that may not be clinically applicable due to the oxidative stress experienced, the proteins expressed in response to that environment can be used as a point of reference and comparison for further simple chemical treatments as an indicator of similar stress events.

Through proteomic analyses, a range of neurospecific, supportive and restructuring proteins were identified in the CK treated cells. Importantly, this novel method also produced cells that did not express the stress proteins seen in the BME treated ADSC samples. The main outcomes from the proteomic analysis presented major neuronal functional proteins such as Filamin-B, Rac1, AHNAK, Annexin2, S100-A10 and Gelsolin of which the overarching relevance of these early developmental neuronal proteins has the potential be utilised as novel markers for neurogenesis of ADSCs.

The Bioplex results present a unique view at the low abundant secreted cytokine proteins complementing the mass spectrometric proteomic datasets. This analysis allows for a further biological context to be unfurled by relating and comparing these molecule's changes in expression levels and roles in the various differentiations. Figure 1 summarises the Bioplex data from chapter 3 and 4 of the $\log_{10}$ concentration of assayed cytokines from the basal ADSCs and the ADSCs treated with AECK, LK and BME 24-hours post induction. The data set has been sorted according to lowest to highest concentration by using the basal ADSCs as the baseline comparison, allowing a relative comparison of all the up/down regulated cytokines across all neurogenic inductions. Figure 1's Bioplex data cross reference ultimately infers that the AECK and LK differentiations are much gentler on the cells than the BME, as the overall trend in cytokine expression is not overtly different from that of the basal stem cells, at least in the mid range of the graph from IL-17 to MCP-1. There are only minor variations between the AECK and LK treated samples compared to the BME treated cells, an unsurprising and previously determined finding as BME is known to be quite toxic and stress inducing to the cells even though it is capable of inducing the expression of neurogenic support proteins.

In summary ADSCs treated with the CKs respond favourably and neuronal differentiation was initiated which was also deemed to be superior to the previous chemical induction additives by the higher total cell population which displays neuronal morphology and by the higher number of neuronal functional and developmental proteins identified, furthermore the decrease in cell death, stress and shock related proteins also indicates that this induction process in much more gentle and effective. The presence of the aforementioned proteins and high population of morphological neuronal-like cells has allowed a patent to be filed around this method for development into a clinical and pharmaceutical application (see appendix 3A patent number: AU2011903817).

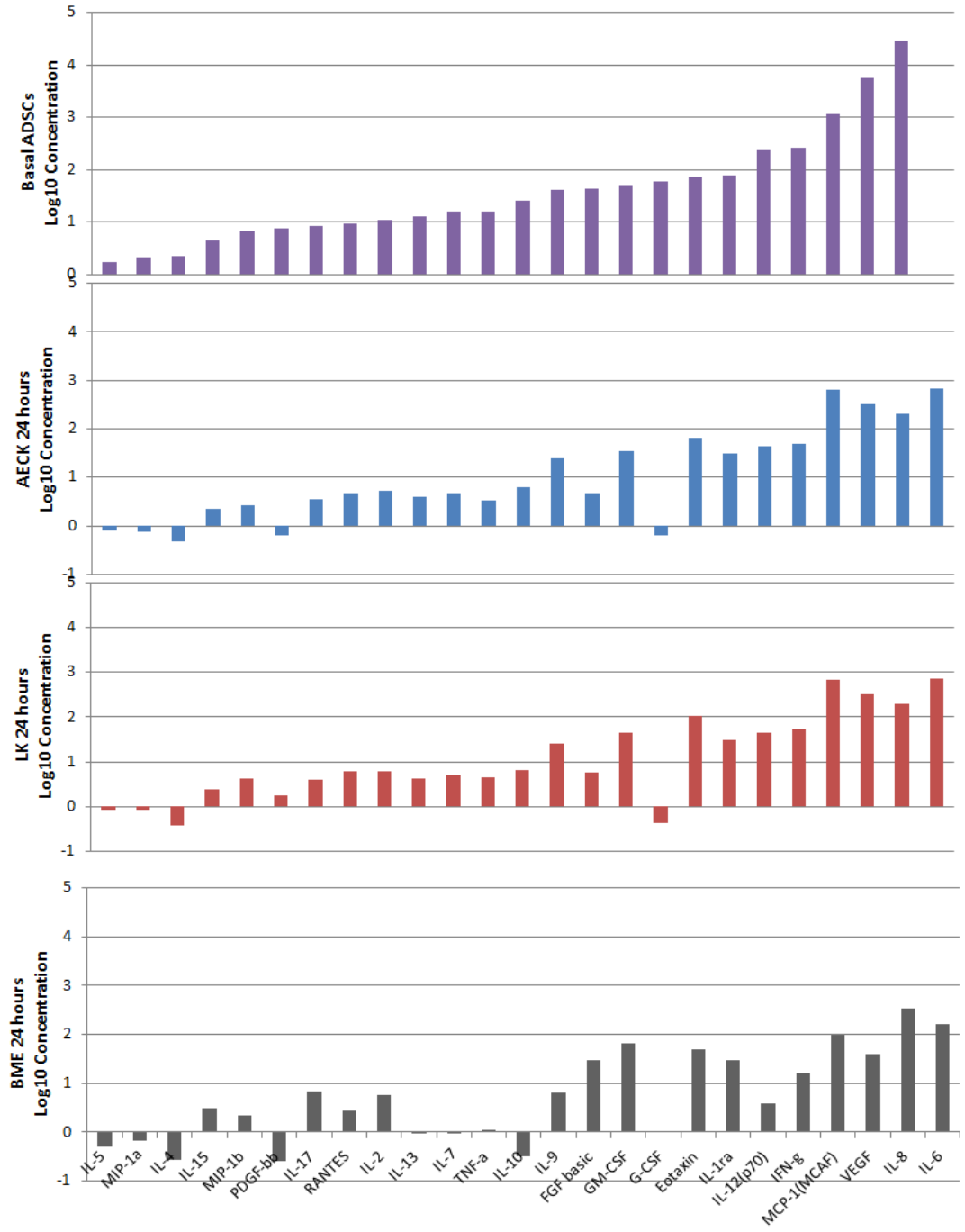

Figure 1 Comparative graph of the log10 concentration of all assayed cytokines from basal ADSCs (purple) and treated ADSCs 24 hours post induction with AECK (blue), LK (red) and BME (black) from top to bottom.

In conclusion, the proteomic investigation and analysis of differentiating ADSCs has indeed expanded the knowledge of the extent of change that these cells undergo in their respective culture conditions. The variety of proteins expressed, identified in the mass spectrometric and Bioplex assays, have exhibited the need for a broader characterisation than those previously used. This has allowed for a greater comprehension of the biological context of the cellular changes occurring rather than relying on a handful of markers and morphological distinctions.

Future directions include revisiting the chondrogenic and osteogenic differentiation with comparison to their primary derived counterparts utilising a combination of the iTRAQ and the recent high sensitivity proteome coverage LC-MS/MS methods from the Matthias Mann research group [235, 237] will be highly beneficial for a deeper comparative proteomic profile of the differentiating ADSCs. These methods will aid in the fractionation and identification of the mid to low range expressed proteins that were previously masked in earlier experiments. These expanded methodologies will allow a broader analysis into the up and down regulated proteins specific in each of these differentiations. Further techniques to complement the proteomic data sets would be a transcriptomic analysis investigating the correlation between mRNA levels and expressed proteins in a temporal study. The osteochondral differentiations should also be trialled by culturing on synthetic biomimetic scaffolds such as beta-tricalciumphosphate (β-TCP) spheres [567] or naturally occurring coralline scaffolds [568] and the resultant cells should then be subject to the proteomic analysis and comparisons.

The neurogenic differentiation work requires variable induction culture times and adjustments of the neurogenic support media prior to the *in vitro* functionality assays. The variable induction culture times would investigate the optimal time that neurogenesis is initiated by the chemical inducers. Subsequently the culture medium should then be replaced with the neuronal support media such as Neurobasal media (Invitrogen) supplemented with growth factor cocktails such as B27

or N2 (Invitrogen). These are commercially available media designed to support the growth of primary derived neuronal cells. The support by this media may allow the neurogenic induced ADSCs to mature into neuronal cells. The proteomic analysis of the resultant cells of this process would be invaluable as it would assist in defining if transdermal differentiation of ADSCs can produce terminally mature and functional neurons *in vitro*. Further to this the functionality assays such as patch clamping and action potential assays would then be necessary to demonstrate phenotype.

The SRM approach of targeting a range of now known neurogenic proteins and examining their expression levels can also be complemented by high quality fluorescently labelled antibodies and high resolution microscopy for cellular localisation. Further afield, the development of the patent innovation toward a clinical application requires an *in vivo* animal model study to be completed; specifically in peripheral nerve damage animal model to identify the effect the neurogenic ADSCs has on neuronal repair and regeneration *in situ*. Exploring the clinical significance of the ketamines for neurogenic regenerative medicine is the ultimate goal in the development of a translational therapy for the various neurological deficits. A large question that will need an answer is; is it possible to expand and differentiate stored autologous or allogenic ADSCs toward neuronal cells in culture and apply them to a patient as a regenerative therapy? In a similar manner which is currently conducted with bone regeneration by the company Mesoblast.

In summary this thesis covered the differentiation potential of ADSCs derived from both rat and human adipose tissue which was assessed with an in depth proteomic investigation. This thesis revealed important insights that cellular and secreted proteomes change of ADSCs when induced and directed toward chondrogenic, osteogenic and neurogenic phenotypic lineages. The neurogenic research focused on the analysis of neurogenic differentiation with the chemical inducers such as BME and the CK chemical alternative was identified as having a less toxic effect and a higher success rate of developing neuronal-like cells. Subsequent to this a patent was filed around the CK neurogenic-induction method. The extent of differentiation achieved was assessed by the

proteomic comparison to primary derived cells or equivalent control cells. The reliance on the 'classical' markers was also challenged by the comprehensive proteomic quantitation and a broader understanding of the expressed proteins biological context of differentiating stem cells. Proteomics as a toolset has become import part of cellular biology and will continue to grow and allow a greater comprehension of biological context of stem cell biology and regenerative medicine.

Bibliography

1. Ryan, J., et al., *Mesenchymal stem cells avoid allogeneic rejection.* Journal of Inflammation, 2005. **2**(1): p. 8.
2. Mason, C. and P. Dunnill, *A brief definition of regenerative medicine.* Regen Med, 2008. **3**(1): p. 1-5.
3. Devine, S.M. and R. Hoffman, *Role of mesenchymal stem cells in hematopoietic stem cell transplantation.* Curr Opin Hematol, 2000. **7**: p. 358 - 363.
4. Majumdar, M.K., E. Wang, and E.A. Morris, *BMP-2 and BMP-9 promotes chondrogenic differentiation of human multipotential mesenchymal cells and overcomes the inhibitory effect of IL-1.* Journal of Cellular Physiology, 2001. **189**(3): p. 275-284.
5. Reya, T., et al., *Stem cells, cancer, and cancer stem cells.* Nature, 2001. **414**(6859): p. 105-111.
6. Jiang, Y., et al., *Pluripotency of mesenchymal stem cells derived from adult marrow.* Nature, 2002. **418**: p. 41 - 49.
7. Cancedda, R., et al., *Tissue engineering and cell therapy of cartilage and bone.* Matrix Biology, 2003. **22**(1): p. 81-91.
8. Bonilla, S., et al., *Functional neural stem cells derived from adult bone marrow.* Neuroscience, 2005. **133**(1): p. 85-95.
9. Gomillion, C.T. and K.J.L. Burg, *Stem cells and adipose tissue engineering.* Biomaterials, 2006. **27**(36): p. 6052-6063.
10. Pisu, M., A. Concas, and G. Cao, *A novel simulation model for stem cells differentiation.* Journal of Biotechnology, 2007. **130**(2): p. 171-182.
11. Noël, D., et al., *Cell specific differences between human adipose-derived and mesenchymal-stromal cells despite similar differentiation potentials.* Experimental Cell Research, 2008. **314**(7): p. 1575-1584.
12. Vallée, M., J.F. Côté, and J. Fradette, *Adipose-tissue engineering: Taking advantage of the properties of human adipose-derived stem/stromal cells.* Pathologie Biologie, 2009. **57**(4): p. 309-317.
13. Casteilla, L. and C. Dani, *Adipose tissue-derived cells: from physiology to regenerative medicine.* Diabetes & Metabolism, 2006. **32**(5): p. 393-401.
14. Jagur-Grodzinski, J., *Polymers for tissue engineering, medical devices, and regenerative medicine. Concise general review of recent studies.* Polymers for advanced technologies, 2006. **17**(6): p. 395-418.
15. Furth, M.E., A. Atala, and M.E. Van Dyke, *Smart biomaterials design for tissue engineering and regenerative medicine.* Biomaterials, 2007. **28**(34): p. 5068-73.
16. Thomas, V., D.R. Dean, and Y.K. Vohra, *Nanostructured Biomaterials for Regenerative Medicine.* Current Nanoscience, 2006. **2**(3): p. 155-177.
17. Lutolf, M. and J. Hubbell, *Synthetic biomaterials as instructive extracellular microenvironments for morphogenesis in tissue engineering.* Nature biotechnology, 2005. **23**(1): p. 47-55.
18. Wert, G.d. and C. Mummery, *Human embryonic stem cells: research, ethics and policy.* Human Reproduction, 2003. **18**(4): p. 672-682.
19. Gonyon, D.L., Jr. and M.R. Zenn, *Simple approach to the radiated scalp wound using INTEGRA skin substitute.* Ann Plast Surg, 2003. **50**(3): p. 315-20.
20. Prystowsky, J.H., D.M. Siegel, and J.A. Ascherman, *Artificial skin for closure and healing of wounds created by skin cancer excisions.* Dermatol Surg, 2001. **27**(7): p. 648-53; discussion 653-4.
21. Minger, S.L., *Regenerative medicine.* Regenerative Medicine, 2005. **1**(1): p. 1-2.

22. Woolf, A.D. and B. Pfleger, *Burden of major musculoskeletal conditions.* Bulletin of the World Health Organization, 2003. **81** (9).
23. Hardingham, T., S. Tew, and A. Murdoch, *Tissue engineering: chondrocytes and cartilage.* Arthritis Res, 2002. **4 Suppl 3**: p. S63-8.
24. Rollín, R., et al., *Differential proteome of bone marrow mesenchymal stem cells from osteoarthritis patients.* Osteoarthritis and Cartilage, 2008. **16**(8): p. 929-935.
25. Im, G., II, Y.-W. Shin, and K.-B. Lee, *Do adipose tissue-derived mesenchymal stem cells have the same osteogenic and chondrogenic potential as bone marrow-derived cells?* Osteoarthritis and Cartilage, 2005. **13**(10): p. 845-853.
26. Csaki, C., P.R.A. Schneider, and M. Shakibaei, *Mesenchymal stem cells as a potential pool for cartilage tissue engineering.* Annals of Anatomy - Anatomischer Anzeiger, 2008. **190**(5): p. 395-412.
27. Ilic, D., *Industry Update: Latest developments in stem cell research and regenerative medicine.* Regenerative Medicine, 2012. **8**(1): p. 9-15.
28. Zuk, P.A., et al., *Human Adipose Tissue Is a Source of Multipotent Stem Cells.* Mol. Biol. Cell, 2002. **13**(12): p. 4279-4295.
29. Evans, M.J. and M.H. Kaufman, *Establishment in culture of pluripotential cells from mouse embryos.* Nature, 1981. **292**(5819): p. 154-6.
30. Spradling, A., D. Drummond-Barbosa, and T. Kai, *Stem cells find their niche.* Nature, 2001. **414**(6859): p. 98-104.
31. Bodnar, A.G., et al., *Extension of Life-Span by Introduction of Telomerase into Normal Human Cells.* Science, 1998. **279**(5349): p. 349-352.
32. Thomson, J.A., et al., *Embryonic Stem Cell Lines Derived from Human Blastocysts.* Science, 1998. **282**(5391): p. 1145-1147.
33. Pera, M.F., B. Reubinoff, and A. Trounson, *Human embryonic stem cells.* Journal of cell science, 2000. **113 (Pt 1)**: p. 5-10.
34. Nicol, D., D. Chalmers, and B. Gogarty, *Regulation Biomedical Advances: Embryonic Stem Cell Research.* Macquarie Law Journal, 2002. **2**.
35. *Prohibition of Human Cloning for Reproduction and the Regulation of Human Embryo Research Amendment Act No. 172 (Cth).* 2006.
36. Okita, K., T. Ichisaka, and S. Yamanaka, *Generation of germline-competent induced pluripotent stem cells.* Nature, 2007. **448**(7151): p. 313-317.
37. Friedenstein, A.J., R.K. Chailakhjan, and K.S. Lalykina, *The development of fibroblastic colonies in monolayer cultures of guineapig bone marrow and spleen cells.* Cell Tissue Kinet., 1970. **3**: p. 393-403.
38. Phinney, D.G. and D.J. Prockop, *Concise Review: Mesenchymal Stem/Multipotent Stromal Cells: The State of Transdifferentiation and Modes of Tissue Repair-Current Views.* Stem Cells, 2007. **25**: p. 2896-2902.
39. Bunnell, B.A., et al., *Adipose-derived stem cells: Isolation, expansion and differentiation.* Methods, 2008. **45**(2): p. 115-120.
40. Pittenger, M.F., et al., *Multilineage potential of adult human mesenchymal stem cells.* Science, 1999. **284**: p. 143 - 147.
41. Zeng, R., et al., *Electrophysiological study on differentiation of rat bone marrow stromal stem cells into neuron-like cells in vitro by edaravone.* Chinese Journal of Traumatology (English Edition), 2009. **12**(3): p. 167-172.
42. Wang, Y., et al., *Expansion and osteogenic differentiation of bone marrow-derived mesenchymal stem cells on a vitamin C functionalized polymer.* Biomaterials, 2006. **27**(17): p. 3265-3273.
43. Wang, L., et al., *Differentiation of human bone marrow mesenchymal stem cells grown in terpolyesters of 3-hydroxyalkanoates scaffolds into nerve cells.* Biomaterials, 2010. **31**(7): p. 1691-1698.

44. Taha, M.F. and V. Hedayati, *Isolation, identification and multipotential differentiation of mouse adipose tissue-derived stem cells.* Tissue and Cell, 2010. **42**(4): p. 211-216.
45. Shih, D.T.-B., et al., *Expansion of adipose tissue mesenchymal stromal progenitors in serum-free medium supplemented with virally inactivated allogeneic human platelet lysate.* Transfusion, 2011. **51**(4): p. 770-778.
46. Scuteri, A., et al., *Mesenchymal stem cells neuronal differentiation ability: a real perspective for nervous system repair?* Curr Stem Cell Res Ther, 2011. **6**(2): p. 82-92.
47. Rebelatto, C.K., et al., *Dissimilar Differentiation of Mesenchymal Stem Cells from Bone Marrow, Umbilical Cord Blood, and Adipose Tissue.* Experimental Biology and Medicine, 2008. **233**(7): p. 901-913.
48. Phillips, J.E., et al., *Human mesenchymal stem cell differentiation on self-assembled monolayers presenting different surface chemistries.* Acta Biomaterialia, 2010. **6**(1): p. 12-20.
49. Mauney, J.R., et al., *Engineering adipose-like tissue in vitro and in vivo utilizing human bone marrow and adipose-derived mesenchymal stem cells with silk fibroin 3D scaffolds.* Biomaterials, 2007. **28**(35): p. 5280-90.
50. Martin-Rendon, E., et al., *Autologous bone marrow stem cells to treat acute myocardial infarction: a systematic review.* Eur Heart J, 2008. **29**(15): p. 1807-18.
51. *Regenerative Medicine Glossary.* Regenerative Medicine, 2009. **4**(4s): p. S1-S88.
52. Schilling, T., et al., *Plasticity in adipogenesis and osteogenesis of human mesenchymal stem cells.* Molecular and Cellular Endocrinology, 2007. **271**(1-2): p. 1-17.
53. Clarke, D. and J. Frisén, *Differentiation potential of adult stem cells.* Current Opinion in Genetics & Development, 2001. **11**(5): p. 575-580.
54. Betre, H., et al., *Chondrocytic differentiation of human adipose-derived adult stem cells in elastin-like polypeptide.* Biomaterials, 2006. **27**(1): p. 91-99.
55. Xu, Y., et al., *Myelin-forming ability of Schwann cell-like cells induced from rat adipose-derived stem cells in vitro.* Brain Research, 2008. **1239**: p. 49-55.
56. Lee, J.-H. and D.M. Kemp, *Human adipose-derived stem cells display myogenic potential and perturbed function in hypoxic conditions.* Biochemical and Biophysical Research Communications, 2006. **341**(3): p. 882-888.
57. da Silva Meirelles, L., P.C. Chagastelles, and N.B. Nardi, *Mesenchymal stem cells reside in virtually all post-natal organs and tissues.* J Cell Sci, 2006. **119**(Pt 11): p. 2204-13.
58. Ahima, R.S., *Adipose Tissue as an Endocrine Organ.* Obesity, 2006. **14**(S8): p. 242S-249S.
59. Engeli, S., et al., *The adipose-tissue renin-angiotensin-aldosterone system: role in the metabolic syndrome?* The International Journal of Biochemistry & Cell Biology, 2003. **35**(6): p. 807-825.
60. Ailhaud, G., P. Grimaldi, and R. Negrel, *Cellular and molecular aspects of adipose tissue development.* Annu Rev Nutr, 1992(12): p. 207-233.
61. Chen, Y., et al., *Mesenchymal stem cells: A promising candidate in regenerative medicine.* The International Journal of Biochemistry & Cell Biology, 2008. **40**(5): p. 815-820.
62. Conrad, C. and R. Huss, *Adult stem cell lines in regenerative medicine and reconstructive surgery.* Journal of Surgical Research, 2005. **124**(2): p. 201-208.
63. Wagner, W., et al., *Replicative Senescence of Mesenchymal Stem Cells: A Continuous and Organized Process.* PLoS One, 2008. **3**(5): p. e2213.
64. Fischer, A.H., et al., *Hematoxylin and eosin staining of tissue and cell sections.* CSH Protoc, 2008. **2008**: p. pdb prot4986.
65. Takahashi, K., et al., *Induction of pluripotent stem cells from adult human fibroblasts by defined factors.* Cell, 2007. **131**(5): p. 861-72.
66. Lin, K.K. and M.A. Goodell, *Purification of Hematopoietic Stem Cells Using the Side Population*, in *Methods in Enzymology*, K. Irina and L. Robert, Editors. 2006, Academic Press. p. 255-264.

67. Simmons, D., et al., *Molecular cloning of a cDNA encoding CD34, a sialomucin of human hematopoietic stem cells.* The Journal of Immunology, 1992. **148**(1): p. 267-271.
68. Fackler, M.J., et al., *Activated protein kinase C directly phosphorylates the CD34 antigen on hematopoietic cells.* Journal of Biological Chemistry, 1990. **265**(19): p. 11056-11061.
69. Satterthwaite, A.B., et al., *Structure of the gene encoding CD34, a human hematopoietic stem cell antigen.* Genomics, 1992. **12**(4): p. 788-794.
70. Krause, D.S., et al., *CD34: Structure, Biology, and Clinical Utility.* The Journal of The American Society of Hematology, 1996. **87**(1): p. 1-13.
71. Sutherland, D.R. and A. Keating, *The CD34 Antigen: Structure, Biology, and Potential Clinical Applications.* Journal of Hematotherapy, 1992. **1**(2): p. 115-129.
72. Sanz-Ruiz, R., et al., *Adipose Tissue-derived Stem Cells: The Friendly Side of a Classic Cardiovascular Foe.* Journal of Cardiovascular Translational Research, 2008. **1**(1): p. 55-63.
73. Katz, A.J., et al., *Cell Surface and Transcriptional Characterization of Human Adipose-Derived Adherent Stromal (hADAS) Cells.* STEM CELLS, 2005. **23**(3): p. 412-423.
74. Mitchell, J.B., et al., *Immunophenotype of Human Adipose-Derived Cells: Temporal Changes in Stromal-Associated and Stem Cell–Associated Markers.* STEM CELLS, 2006. **24**(2): p. 376-385.
75. Strem, B.M., et al., *Multipotential differentiation of adipose tissue-derived stem cells.* Keio J Med, 2005. **54**(3): p. 132-41.
76. Cousin, B., et al., *Adult Stromal Cells Derived from Human Adipose Tissue Provoke Pancreatic Cancer Cell Death both In Vitro and In Vivo.* PLoS ONE, 2009. **4**(7): p. e6278.
77. Majumdar, M.K., et al., *Characterization and functionality of cell surface molecules on human mesenchymal stem cells.* J Biomed Sci, 2003. **10**: p. 228 - 241.
78. Young, H.E., et al., *Human pluripotent and progenitor cells display cell surface cluster differentiation markers CD10, CD13, CD56, and MHC class-I.* Proc Soc Exp Biol Med, 1999. **221**(1): p. 63-71.
79. Short, B., et al., *Mesenchymal stem cells.* Archives of Medical Research, 2003. **34**(6): p. 565-571.
80. Etheridge, S.L., et al., *Expression Profiling and Functional Analysis of Wnt Signaling Mechanisms in Mesenchymal Stem Cells.* STEM CELLS, 2004. **22**(5): p. 849-860.
81. Song, H.Y., et al., *Oncostatin M induces proliferation of human adipose tissue-derived mesenchymal stem cells.* The International Journal of Biochemistry & Cell Biology, 2005. **37**(11): p. 2357-2365.
82. Dicker, A., et al., *Functional studies of mesenchymal stem cells derived from adult human adipose tissue.* Experimental Cell Research, 2005. **308**(2): p. 283-290.
83. Sethe, S., A. Scutt, and A. Stolzing, *Aging of mesenchymal stem cells.* Ageing Research Reviews, 2006. **5**(1): p. 91-116.
84. Tuli, R., et al., *Characterization of Multipotential Mesenchymal Progenitor Cells Derived from Human Trabecular Bone.* STEM CELLS, 2003. **21**(6): p. 681-693.
85. Reyes, M. and C.M. Verfaillie, *Characterization of multipotent adult progenitor cells, a subpopulation of mesenchymal stem cells.* Ann N Y Acad Sci, 2001. **938**: p. 231 - 233.
86. Jones, E.A., et al., *Isolation and characterization of bone marrow multipotential mesenchymal progenitor cells.* Arthritis & Rheumatism, 2002. **46**(12): p. 3349-3360.
87. Lin, G., et al., *Defining stem and progenitor cells within adipose tissue.* Stem Cells Dev, 2008. **17**(6): p. 1053-63.
88. Corbi, A.L., et al., *The human leukocyte adhesion glycoprotein Mac-1 (complement receptor type 3, CD11b) alpha subunit. Cloning, primary structure, and relation to the integrins, von Willebrand factor and factor B.* J Biol Chem, 1988. **263**(25): p. 12403-11.
89. Haziot, A., et al., *The monocyte differentiation antigen, CD14, is anchored to the cell membrane by a phosphatidylinositol linkage.* The Journal of Immunology, 1988. **141**(2): p. 547-552.

90. Kozmik, Z., et al., *The promoter of the CD19 gene is a target for the B-cell-specific transcription factor BSAP.* Mol. Cell. Biol., 1992. **12**(6): p. 2662-2672.
91. Balzac, F., et al., *Expression of beta 1B integrin isoform in CHO cells results in a dominant negative effect on cell adhesion and motility.* J Cell Biol, 1994. **127**(2): p. 557-65.
92. Balzac, F., et al., *Expression and functional analysis of a cytoplasmic domain variant of the beta 1 integrin subunit.* J Cell Biol, 1993. **121**(1): p. 171-8.
93. Streuli, M., et al., *Differential usage of three exons generates at least five different mRNAs encoding human leukocyte common antigens.* J Exp Med, 1987 **166**(5): p. 1548-66.
94. Robker, R.L., et al., *Leukocyte migration in adipose tissue of mice null for ICAM-1 and Mac-1 adhesion receptors.* Obes Res, 2004. **12**(6): p. 936-40.
95. Kemshead, J.T., et al., *Human Thy-1: expression on the cell surface of neuronal and glial cells.* Brain Res. , 1982 **236** (2): p. 451-461
96. Al-Khalili, L., et al., *Human skeletal muscle cell differentiation is associated with changes in myogenic markers and enhanced insulin-mediated MAPK and PKB phosphorylation.* Acta Physiol Scand, 2004. **180**(4): p. 395-403.
97. Pilling, D., et al., *Identification of Markers that Distinguish Monocyte-Derived Fibrocytes from Monocytes, Macrophages, and Fibroblasts.* PLoS ONE, 2009. **4**(10): p. e7475.
98. Kiertscher, S.M. and M.D. Roth, *Human CD14+ leukocytes acquire the phenotype and function of antigen-presenting dendritic cells when cultured in GM-CSF and IL-4.* Journal of Leukocyte Biology, 1996. **59**(2): p. 208-18.
99. Middleton, J., et al., *A comparative study of endothelial cell markers expressed in chronically inflamed human tissues: MECA-79, Duffy antigen receptor for chemokines, von Willebrand factor, CD31, CD34, CD105 and CD146.* J Pathol, 2005. **206**(3): p. 260-8.
100. Zhang, H.-T., et al., *Neural differentiation ability of mesenchymal stromal cells from bone marrow and adipose tissue: a comparative study.* Cytotherapy, 2012. **14**(10): p. 1203-1214.
101. Technau, A., et al., *Adipose tissue-derived stem cells show both immunogenic and immunosuppressive properties after chondrogenic differentiation.* Cytotherapy, 2011. **13**(3): p. 310-7.
102. Taléns-Visconti, R., et al., *Human mesenchymal stem cells from adipose tissue: Differentiation into hepatic lineage.* Toxicology in Vitro, 2007. **21**(2): p. 324-329.
103. Schilling, T., et al., *Microarray analyses of transdifferentiated mesenchymal stem cells.* Journal of Cellular Biochemistry, 2008. **103**(2): p. 413-433.
104. Woodbury, D., et al., *Adult rat and human bone marrow stromal cells differentiate into neurons.* . J Neurosci Res, 2000 **61**: p. 364–370.
105. Tatard, V.M., et al., *Neurotrophin-directed differentiation of human adult marrow stromal cells to dopaminergic-like neurons.* Bone, 2007. **40**(2): p. 360-373.
106. Bryder, D., D.J. Rossi, and I.L. Weissman, *Hematopoietic stem cells: the paradigmatic tissue-specific stem cell.* The American journal of pathology, 2006. **169**(2): p. 338-346.
107. Reali, C., et al., *Differentiation of human adult CD34+ stem cells into cells with a neural phenotype: Role of astrocytes.* Experimental Neurology, 2006. **197**(2): p. 399-406.
108. Zhang, H.-t., et al., *Comparison of adult neurospheres derived from different origins for treatment of rat spinal cord injury.* Neuroscience Letters, 2009. **458**(3): p. 116-121.
109. Xu, Y., et al., *Neurospheres from rat adipose-derived stem cells could be induced into functional Schwann cell-like cells in vitro.* BMC Neuroscience, 2008(9): p. 21.
110. Al-Salleeh, F., et al., *Human osteogenic protein-1 induces osteogenic differentiation of adipose-derived stem cells harvested from mice.* Archives of Oral Biology, 2008. **53**(10): p. 928-936.
111. Ratanavaraporn, J., et al., *Growth and osteogenic differentiation of adipose-derived and bone marrow-derived stem cells on chitosan and chitooligosaccharide films.* Carbohydrate Polymers, 2009. **78**(4): p. 873-878.

112. Guo, X., et al., *In vitro generation of an osteochondral construct using injectable hydrogel composites encapsulating rabbit marrow mesenchymal stem cells.* Biomaterials, 2009. **30**(14): p. 2741-2752.
113. Pelttari, K., E. Steck, and W. Richter, *The use of mesenchymal stem cells for chondrogenesis.* Injury, 2008. **39**(1, Supplement 1): p. 58-65.
114. Im, G.-I., *Chondrogenesis from mesenchymal stem cells derived from adipose tissue on the fibrin scaffold.* Current Applied Physics, 2005. **5**(5): p. 438-443.
115. Miljkovic, N.D., G.M. Cooper, and K.G. Marra, *Chondrogenesis, bone morphogenetic protein-4 and mesenchymal stem cells.* Osteoarthritis and Cartilage, 2008. **16**(10): p. 1121-1130.
116. Guilak, F., et al., *Clonal analysis of the differentiation potential of human adipose-derived adult stem cells.* Journal of Cellular Physiology, 2006. **206**(1): p. 229-237.
117. Stastna, M., M.R. Abraham, and J.E. Van Eyk, *Cardiac stem/progenitor cells, secreted proteins, and proteomics.* FEBS Letters, 2009. **583**(11): p. 1800-1807.
118. Shim, W.S.N., et al., *Ex vivo differentiation of human adult bone marrow stem cells into cardiomyocyte-like cells.* Biochemical and Biophysical Research Communications, 2004. **324**(2): p. 481-488.
119. Hwang, K.C., et al., *Chemicals that modulate stem cell differentiation.* Proc Natl Acad Sci U S A, 2008. **105**(21): p. 7467-71.
120. Takahashi, K., et al., *Induction of pluripotent stem cells from adult human fibroblasts by defined factors.* cell, 2007. **131**(5): p. 861-872.
121. Cattaneo, E. and R. McKay, *Proliferation and differentiation of neuronal stem cells regulated by nerve growth factor.* Nature, 1990. **347**(6295): p. 762-765.
122. Caplan, A.I. and S.P. Bruder, *Mesenchymal stem cells: building blocks for molecular medicine in the 21st century.* Trends Mol Med, 2001. **7**(6): p. 259-64.
123. Hong, L., et al., *Adipose tissue engineering by human adipose-derived stromal cells.* Cells Tissues Organs, 2006. **183**(3): p. 133-40.
124. Cho, S.W., et al., *Enhancement of adipose tissue formation by implantation of adipogenic-differentiated preadipocytes.* Biochem Biophys Res Commun, 2006. **345**(2): p. 588-94.
125. Parsons, W.J., V. Ramkumar, and G.L. Stiles, *Isobutylmethylxanthine stimulates adenylate cyclase by blocking the inhibitory regulatory protein, Gi.* Molecular Pharmacology, 1988. **34**(1): p. 37-41.
126. Calker, D.v., M. Müller, and B. Hamprecht, *ADENOSINE REGULATES VIA TWO DIFFERENT TYPES OF RECEPTORS, THE ACCUMULATION OF CYCLIC AMP IN CULTURED BRAIN CELLS.* Journal of Neurochemistry, 1979. **33**(5): p. 999-1005.
127. Petersen, R.K., et al., *Cyclic AMP (cAMP)-Mediated Stimulation of Adipocyte Differentiation Requires the Synergistic Action of Epac- and cAMP-Dependent Protein Kinase-Dependent Processes.* Mol. Cell. Biol., 2008. **28**(11): p. 3804-3816.
128. Darlington, G.J., S.E. Ross, and O.A. MacDougald, *The Role of C/EBP Genes in Adipocyte Differentiation.* Journal of Biological Chemistry, 1998. **273**(46): p. 30057-30060.
129. Chawla, A., et al., *Peroxisome proliferator-activated receptor (PPAR) gamma: adipose-predominant expression and induction early in adipocyte differentiation.* Endocrinology, 1994. **135**(2): p. 798-800.
130. Lehmann, J.M., et al., *Peroxisome Proliferator-activated Receptors α and γ Are Activated by Indomethacin and Other Non-steroidal Anti-inflammatory Drugs.* Journal of Biological Chemistry, 1997. **272**(6): p. 3406-3410.
131. Prawitt, J., et al., *Characterization of lipid metabolism in insulin-sensitive adipocytes differentiated from immortalized human mesenchymal stem cells.* Experimental Cell Research, 2008. **314**(4): p. 814-824.
132. Enomoto, H., et al., *Runx2 deficiency in chondrocytes causes adipogenic changes in vitro.* Journal of Cell Science, 2004. **117**(3): p. 417-425.

133. Rubin, J.P., et al., *Collagenous microbeads as a scaffold for tissue engineering with adipose-derived stem cells.* Plast Reconstr Surg, 2007. **120**(2): p. 414-24.
134. von Heimburg, D., et al., *Human preadipocytes seeded on freeze-dried collagen scaffolds investigated in vitro and in vivo.* Biomaterials, 2001. **22**(5): p. 429-438.
135. WHO, *Osteoporosis: Both Health Organizations and Individuals must act now to avoid an impending epidemic.* http://www.who.int/inf-pr-1999/en/pr99-58.html, 1999. **Press Release WHO/58 11 October 1999**.
136. Wagner, W., et al., *Comparative characteristics of mesenchymal stem cells from human bone marrow, adipose tissue, and umbilical cord blood.* Experimental Hematology, 2005. **33**(11): p. 1402-1416.
137. Muschler, G.F., et al., *Age- and gender-related changes in the cellularity of human bone marrow and the prevalence of osteoblastic progenitors.* Journal of Orthopaedic Research, 2001. **19**(1): p. 117-125.
138. Flynn, L., et al., *Adipose tissue engineering with naturally derived scaffolds and adipose-derived stem cells.* Biomaterials, 2007. **28**(26): p. 3834-3842.
139. Liu, Y., et al., *Injectable tissue-engineered bone composed of human adipose-derived stromal cells and platelet-rich plasma.* Biomaterials, 2008. **29**(23): p. 3338-3345.
140. Liu, G., et al., *Evaluation of the viability and osteogenic differentiation of cryopreserved human adipose-derived stem cells.* Cryobiology, 2008. **57**(1): p. 18-24.
141. Jing, W., et al., *Effects of [gamma]-secretase inhibition on the proliferation and vitamin D3 induced osteogenesis in adipose derived stem cells.* Biochemical and Biophysical Research Communications, 2010. **392**(3): p. 442-447.
142. Matsubara, H., et al., *Vascular tissues are a primary source of BMP2 expression during bone formation induced by distraction osteogenesis.* Bone, 2012. **51**(1): p. 168-80.
143. Kramer, J., et al., *Embryonic stem cell-derived chondrogenic differentiation in vitro: activation by BMP-2 and BMP-4.* Mechanisms of Development, 2000. **92**(2): p. 193-205.
144. Dragoo, J.L., et al., *Bone induction by BMP-2 transduced stem cells derived from human fat.* Journal of Orthopaedic Research, 2003. **21**(4): p. 622-629.
145. Phillips, J.E., et al., *Glucocorticoid-induced osteogenesis is negatively regulated by Runx2/Cbfa1 serine phosphorylation.* Journal of Cell Science, 2006. **119**(3): p. 581-591.
146. Bell, T.D., M.B. Demay, and S.-A.M. Burnett-Bowie, *The biology and pathology of vitamin D control in bone.* Journal of Cellular Biochemistry, 2010. **111**(1): p. 7-13.
147. Hidalgo, A.A., D.L. Trump, and C.S. Johnson, *Glucocorticoid regulation of the vitamin D receptor.* The Journal of Steroid Biochemistry and Molecular Biology, 2010. **121**(1-2): p. 372-375.
148. Suh, J.H., et al., *Hes1 stimulates transcriptional activity of Runx2 by increasing protein stabilization during osteoblast differentiation.* Biochemical and Biophysical Research Communications, 2008. **367**(1): p. 97-102.
149. Ducy, P., *CBFA1: A molecular switch in osteoblast biology.* Developmental Dynamics, 2000. **219**(4): p. 461-471.
150. Nakashima, K. and B. de Crombrugghe, *Transcriptional mechanisms in osteoblast differentiation and bone formation.* Trends in Genetics, 2003. **19**(8): p. 458-466.
151. Coelho, M.J. and M.H. Fernandes, *Human bone cell cultures in biocompatibility testing. Part II: effect of ascorbic acid, β-glycerophosphate and dexamethasone on osteoblastic differentiation.* Biomaterials, 2000. **21**(11): p. 1095-1102.
152. Jun-Beom, P., *The Effects of Dexamethasone, Ascorbic Acid, and β-Glycerophosphate on Osteoblastic Differentiation by Regulating Estrogen Receptor and Osteopontin Expression.* Journal of Surgical Research, (0).
153. Franceschi, R.T., B.S. Iyer, and Y. Cui, *Effects of ascorbic acid on collagen matrix formation and osteoblast differentiation in murine MC3T3-E1 cells.* Journal of Bone and Mineral Research, 1994. **9**(6): p. 843-854.

154. Fratzl-Zelman, N., et al., *Matrix mineralization in MC3T3-E1 cell cultures initiated by β-glycerophosphate pulse.* Bone, 1998. **23**(6): p. 511-520.
155. Chung, C.H., et al., *Mechanism of action of beta-glycerophosphate on bone cell mineralization.* Calcif Tissue Int, 1992. **51**(4): p. 305-11.
156. Heng, B.C., T. Cao, and E.H. Lee, *Directing Stem Cell Differentiation into the Chondrogenic Lineage In Vitro.* STEM CELLS, 2004. **22**(7): p. 1152-1167.
157. Koga, H., et al., *Mesenchymal stem cell-based therapy for cartilage repair: a review.* Knee Surgery, Sports Traumatology, Arthroscopy, 2009. **17**(11): p. 1289-1297.
158. Peterson, L., et al., *Autologous chondrocyte transplantation. Biomechanics and long-term durability.* Am J Sports Med, 2002. **30**(1): p. 2-12.
159. Brittberg, M., et al., *Treatment of Deep Cartilage Defects in the Knee with Autologous Chondrocyte Transplantation.* New England Journal of Medicine, 1994. **331**(14): p. 889-895.
160. Bartlett, W., et al., *Autologous chondrocyte implantation versus matrix-induced autologous chondrocyte implantation for osteochondral defects of the knee: A PROSPECTIVE, RANDOMISED STUDY.* J Bone Joint Surg Br, 2005. **87-B**(5): p. 640-645.
161. Ponticiello, M.S., et al., *Gelatin-based resorbable sponge as a carrier matrix for human mesenchymal stem cells in cartilage regeneration therapy.* Journal of Biomedical Materials Research, 2000. **52**(2): p. 246-255.
162. Lee, S.-H. and H. Shin, *Matrices and scaffolds for delivery of bioactive molecules in bone and cartilage tissue engineering.* Advanced Drug Delivery Reviews, 2007. **59**(4-5): p. 339-359.
163. Li, W.-J., et al., *A three-dimensional nanofibrous scaffold for cartilage tissue engineering using human mesenchymal stem cells.* Biomaterials, 2005. **26**(6): p. 599-609.
164. Wu, S.-C., et al., *Enhancement of chondrogenesis of human adipose derived stem cells in a hyaluronan-enriched microenvironment.* Biomaterials. **31**(4): p. 631-640.
165. Hui, T.Y., et al., *In vitro chondrogenic differentiation of human mesenchymal stem cells in collagen microspheres: Influence of cell seeding density and collagen concentration.* Biomaterials, 2008. **29**(22): p. 3201-3212.
166. Liu, X., et al., *In vivo ectopic chondrogenesis of BMSCs directed by mature chondrocytes.* Biomaterials, 2010. **31**(36): p. 9406-9414.
167. Banka, S., et al., *A combination of chemical and mechanical stimuli enhances not only osteo- but also chondro-differentiation in adipose-derived stem cells.* Journal of Oral Biosciences, 2012. **54**(4): p. 188-195.
168. Her, G.J., et al., *Control of three-dimensional substrate stiffness to manipulate mesenchymal stem cell fate toward neuronal or glial lineages.* Acta Biomaterialia, 2013. **9**(2): p. 5170-5180.
169. Morgan, E.F., et al., *Vascular development during distraction osteogenesis proceeds by sequential intramuscular arteriogenesis followed by intraosteal angiogenesis.* Bone, 2012. **51**(3): p. 535-45.
170. Nii, M., et al., *The effects of interactive mechanical and biochemical niche signaling on osteogenic differentiation of adipose-derived stem cells using combinatorial hydrogels.* Acta Biomaterialia, 2013. **9**(3): p. 5475-5483.
171. Wong, M. and R.S. Tuan, *Nuserum, a synthetic serum replacement, supports chondrogenesis of embryonic chick limb bud mesenchymal cells in micromass culture.* In Vitro Cell Dev Biol Anim, 1993. **29A**(12): p. 917-22.
172. Chin, A.C., et al., *Defined and serum-free media support undifferentiated human embryonic stem cell growth.* Stem Cells Dev, 2010. **19**(6): p. 753-61.
173. Kawamura, M. and M.R. Urist, *Growth factors, mitogens, cytokines, and bone morphogenetic protein in induced chondrogenesis in tissue culture.* Dev Biol, 1988. **130**(2): p. 435-42.
174. Mendelson, A., *Chondrogenesis of Stem/Progenitor Cells by Chemotaxis Using Novel Cell Homing Systems.* 2012.

175. Hunziker, E., I. Driesang, and E. Morris, *Chondrogenesis in cartilage repair is induced by members of the transforming growth factor-beta superfamily.* Clinical orthopaedics and related research, 2001. **391**: p. S171-S181.
176. Sekiya, I., et al., *In vitro cartilage formation by human adult stem cells from bone marrow stroma defines the sequence of cellular and molecular events during chondrogenesis.* Proceedings of the National Academy of Sciences, 2002. **99**(7): p. 4397-4402.
177. De Luca, F., et al., *Regulation of growth plate chondrogenesis by bone morphogenetic protein-2.* Endocrinology, 2001. **142**(1): p. 430-436.
178. Ng, F., et al., *PDGF, TGF-β, and FGF signaling is important for differentiation and growth of mesenchymal stem cells (MSCs): transcriptional profiling can identify markers and signaling pathways important in differentiation of MSCs into adipogenic, chondrogenic, and osteogenic lineages.* Blood, 2008. **112**(2): p. 295-307.
179. Derynck, R. and Y.E. Zhang, *Smad-dependent and Smad-independent pathways in TGF-[beta] family signalling.* Nature, 2003. **425**(6958): p. 577-584.
180. Liu, D., B.L. Black, and R. Derynck, *TGF-β inhibits muscle differentiation through functional repression of myogenic transcription factors by Smad3.* Genes & Development, 2001. **15**(22): p. 2950-2966.
181. Grönroos, E., et al., *Control of Smad7 Stability by Competition between Acetylation and Ubiquitination.* Molecular cell, 2002. **10**(3): p. 483-493.
182. Chubinskaya, S., M. Hurtig, and D.C. Rueger, *OP-1/BMP-7 in cartilage repair.* Int Orthop, 2007. **31**(6): p. 773-81.
183. Pang, E.K., et al., *Effect of recombinant human bone morphogenetic protein-4 dose on bone formation in a rat calvarial defect model.* J Periodontol, 2004. **75**(10): p. 1364-70.
184. Hanada, K., et al., *BMP-2 induction and TGF-β1 modulation of rat periosteal cell chondrogenesis.* Journal of Cellular Biochemistry, 2001. **81**(2): p. 284-294.
185. Huang, J.I., et al., *Chondrogenic potential of multipotential cells from human adipose tissue.* Plast Reconstr Surg, 2004. **113**(2): p. 585-94.
186. Sakaguchi, Y., et al., *Comparison of human stem cells derived from various mesenchymal tissues: superiority of synovium as a cell source.* Arthritis Rheum, 2005. **52**(8): p. 2521-9.
187. Nakayama, N., et al., *Macroscopic cartilage formation with embryonic stem-cell-derived mesodermal progenitor cells.* J Cell Sci, 2003. **116**(Pt 10): p. 2015-28.
188. Pereira, R.C., A.N. Economides, and E. Canalis, *Bone Morphogenetic Proteins Induce Gremlin, a Protein That Limits Their Activity in Osteoblasts.* Endocrinology, 2000. **141**(12): p. 4558-4563.
189. Delcroix, G.J.R., et al., *Adult cell therapy for brain neuronal damages and the role of tissue engineering.* Biomaterials, 2009. **31**(8): p. 2105-2120.
190. McAleese, S.M., et al., *Complete amino acid sequence of the neurone-specific γ isozyme of enolase (NSE) from human brain and comparison with the non-neuronal α form (NNE).* European Journal of Biochemistry, 1988. **178**(2): p. 413-417.
191. Kingham, P.J., et al., *Adipose-derived stem cells differentiate into a Schwann cell phenotype and promote neurite outgrowth in vitro.* Experimental Neurology, 2007. **207**(2): p. 267-274.
192. Ishii, K., et al., *Effects of 2-mercaptoethanol on survival and differentiation of fetal mouse brain neurons cultured in vitro. .* Neurosci Lett 1993 **163**(159 -162.).
193. Choi, C.B., et al., *Analysis of neuron-like differentiation of human bone marrow mesenchymal stem cells.* Biochemical and Biophysical Research Communications, 2006. **350**(1): p. 138-146.
194. Romero-Ramos, M., et al., *Neuronal differentiation of stem cells isolated from adult muscle.* Journal of Neuroscience Research, 2002. **69**(6): p. 894-907.
195. Safford, K.M., et al., *Neurogenic differentiation of murine and human adipose-derived stromal cells.* Biochemical and Biophysical Research Communications, 2002. **294**(2): p. 371-379.

196. Barnabé, G.F., et al., *Chemically-Induced RAT Mesenchymal Stem Cells Adopt Molecular Properties of Neuronal-Like Cells but Do Not Have Basic Neuronal Functional Properties.* PLoS ONE, 2009. **4**(4): p. e5222.
197. Abello, P.A., S.A. Fidler, and T.G. Buchman, *Thiol reducing agents modulate induced apoptosis in porcine endothelial cells.* Shock, 1994. **2**(2): p. 79-83.
198. Chiao, C., et al., *Apoptosis and Altered Redox State Induced by Caffeic Acid Phenethyl Ester (CAPE) in Transformed Rat Fibroblast Cells.* Cancer Research, 1995. **55**(16): p. 3576-3583.
199. Kim, B.J., et al., *Differentiation of adult bone marrow stem cells into neuroprogenitor cells in vitro.* NeuroReport, 2002. **13**(9): p. 1185-1188.
200. Costa-Silva, B., et al., *Fibronectin promotes differentiation of neural crest progenitors endowed with smooth muscle cell potential.* Experimental Cell Research, 2009. **315**(6): p. 955-967.
201. Das, A.V., et al., *Neural stem cells in the adult ciliary epithelium express GFAP and are regulated by Wnt signaling.* Biochemical and Biophysical Research Communications, 2006. **339**(2): p. 708-716.
202. Radtke, C., et al., *Peripheral glial cell differentiation from neurospheres derived from adipose mesenchymal stem cells.* International Journal of Developmental Neuroscience, 2009. **27**(8): p. 817-823.
203. Greco, S.J. and P. Rameshwar, *Enhancing Effect of IL-1α on Neurogenesis from Adult Human Mesenchymal Stem Cells: Implication for Inflammatory Mediators in Regenerative Medicine.* The Journal of Immunology, 2007. **179**(5): p. 3342-3350.
204. Cho, K.J., et al., *Neurons Derived From Human Mesenchymal Stem Cells Show Synaptic Transmission and Can Be Induced to Produce the Neurotransmitter Substance P by Interleukin-1α.* STEM CELLS, 2005. **23**(3): p. 383-391.
205. Liesi, P., *Laminin and fibronectin and their cellular receptors during neural development.* Seminars in Neuroscience, 1991. **3**(4): p. 331-340.
206. Ogawa, S., et al., *Induction of oligodendrocyte differentiation from adult human fibroblast-derived induced pluripotent stem cells.* In Vitro Cell Dev Biol Anim, 2011. **47**(7): p. 464-9.
207. Takahashi, J., T.D. Palmer, and F.H. Gage, *Retinoic acid and neurotrophins collaborate to regulate neurogenesis in adult-derived neural stem cell cultures.* Journal of Neurobiology, 1999. **38**(1): p. 65-81.
208. Pankov, R. and K.M. Yamada, *Fibronectin at a glance.* Journal of Cell Science, 2002. **115**(20): p. 3861-3863.
209. George, E.L., et al., *Defects in mesoderm, neural tube and vascular development in mouse embryos lacking fibronectin.* Development, 1993. **119**(4): p. 1079-1091.
210. Bez, A., et al., *Neurosphere and neurosphere-forming cells: morphological and ultrastructural characterization.* Brain Research, 2003. **993**(1-2): p. 18-29.
211. Herbst, R.S., *Review of epidermal growth factor receptor biology.* International journal of radiation oncology, biology, physics, 2004. **59**(2): p. S21-S26.
212. Hermann, A., et al., *Efficient generation of neural stem cell-like cells from adult human bone marrow stromal cells.* Journal of Cell Science, 2004. **117**(19): p. 4411-4422.
213. Andrews, P.W., *Retinoic acid induces neuronal differentiation of a cloned human embryonal carcinoma cell line in vitro.* Developmental Biology, 1984. **103**(2): p. 285-293.
214. Katoh, M., *Regulation of WNT signaling molecules by retinoic acid during neuronal differentiation in NT2 cells: threshold model of WNT action (review).* Int J Mol Med, 2002. **10**(6): p. 683-7.
215. Kondo, T., et al., *Sonic hedgehog and retinoic acid synergistically promote sensory fate specification from bone marrow-derived pluripotent stem cells.* Proceedings of the National Academy of Sciences of the United States of America, 2005. **102**(13): p. 4789-4794.
216. di Summa, P.G., et al., *Adipose-derived stem cells enhance peripheral nerve regeneration.* Journal of Plastic, Reconstructive & Aesthetic Surgery, 2010. **63**(9): p. 1544-1552.

217. Mizuno, H., et al., *Myogenic differentiation by human processed lipoaspirate cells.* Plast Reconstr Surg, 2002. **109**(1): p. 199-209; discussion 210-1.
218. Kang, Y., et al., *Unsorted human adipose tissue-derived stem cells promote angiogenesis and myogenesis in murine ischemic hindlimb model.* Microvascular Research, 2010. **80**(3): p. 310-316.
219. Dezawa, M., et al., *Bone marrow stromal cells generate muscle cells and repair muscle degeneration.* Science, 2005. **309**(5732): p. 314-7.
220. Kim, M., et al., *Muscle regeneration by adipose tissue-derived adult stem cells attached to injectable PLGA spheres.* Biochemical and Biophysical Research Communications, 2006. **348**(2): p. 386-392.
221. Kim, Y.M., et al., *Angiotensin II-induced differentiation of adipose tissue-derived mesenchymal stem cells to smooth muscle-like cells.* The International Journal of Biochemistry & Cell Biology, 2008. **40**(11): p. 2482-2491.
222. Bacou, F., et al., *Transplantation of adipose tissue-derived stromal cells increases mass and functional capacity of damaged skeletal muscle.* Cell Transplant, 2004. **13**(2): p. 103-11.
223. Athanasuleas, C.L., et al., *Surgical ventricular restoration in the treatment of congestive heart failure due to post-infarction ventricular dilation.* Journal of the American College of Cardiology, 2004. **44**(7): p. 1439-1445.
224. Granger Cb, G.R.J.D.O. and et al., *PRedictors of hospital mortality in the global registry of acute coronary events.* Archives of Internal Medicine, 2003. **163**(19): p. 2345-2353.
225. Tang, C.C., G.S. Ma, and J.Y. Chen, *Transplantation of 5-azacytidine treated cardiac fibroblasts improves cardiac function of infarct hearts in rats.* Chin Med J (Engl), 2010. **123**(18): p. 2586-92.
226. Rangappa, S., et al., *Transformation of adult mesenchymal stem cells isolated from the fatty tissue into cardiomyocytes.* Ann Thorac Surg, 2003. **75**(3): p. 775-779.
227. Planat-Benard, V., et al., *Spontaneous cardiomyocyte differentiation from adipose tissue stroma cells.* Circ Res, 2004. **94**(2): p. 223-9.
228. Gaustad, K.G., et al., *Differentiation of human adipose tissue stem cells using extracts of rat cardiomyocytes.* Biochem Biophys Res Commun, 2004. **314**(2): p. 420-7.
229. Anderson, N.L. and N.G. Anderson, *Proteome and proteomics: New technologies, new concepts, and new words.* ELECTROPHORESIS, 1998. **19**(11): p. 1853-1861.
230. Blackstock, W.P. and M.P. Weir, *Proteomics: quantitative and physical mapping of cellular proteins.* Trends in biotechnology, 1999. **17**(3): p. 121-127.
231. Unwin, R.D., et al., *The potential for proteomic definition of stem cell populations.* Exp Hematol, 2003. **31**(12): p. 1147-59.
232. Canas, B., et al., *Trends in sample preparation for classical and second generation proteomics.* J Chromatogr A, 2007. **1153**(1-2): p. 235-58.
233. Rabilloud, T. and C. Lelong, *Two-dimensional gel electrophoresis in proteomics: a tutorial.* J Proteomics, 2011. **74**(10): p. 1829-41.
234. Corthals, G.L., et al., *The dynamic range of protein expression: A challenge for proteomic research.* Electrophoresis, 2000. **21**(6): p. 1104-1115.
235. Nagaraj, N., et al., *Deep proteome and transcriptome mapping of a human cancer cell line.* Mol Syst Biol, 2011. **7**: p. 548.
236. Righetti, P.G., et al., *Protein Equalizer™ Technology : The quest for a "democratic proteome".* PROTEOMICS, 2006. **6**(14): p. 3980-3992.
237. Thakur, S.S., et al., *Deep and highly sensitive proteome coverage by LC-MS/MS without prefractionation.* Mol Cell Proteomics, 2011. **10**(8): p. M110 003699.
238. Bononi, A., et al., *Protein Kinases and Phosphatases in the Control of Cell Fate.* Enzyme Research, 2011. **2011**: p. 26.
239. Szilagyi, A., et al., *Prediction of physical protein-protein interactions.* Phys Biol, 2005. **2**(2): p. S1-16.

240. Trakselis, M.A., S.C. Alley, and F.T. Ishmael, *Identification and Mapping of Protein−Protein Interactions by a Combination of Cross-Linking, Cleavage, and Proteomics.* Bioconjugate Chemistry, 2005. **16**(4): p. 741-750.
241. Farmer, T.B. and R.M. Caprioli, *Determination of protein–protein interactions by matrix-assisted laser desorption/ionization mass spectrometry.* Journal of Mass Spectrometry, 1998. **33**(8): p. 697-704.
242. Markwell, M.A. and C.F. Fox, *Protein-protein interactions within paramyxoviruses identified by native disulfide bonding or reversible chemical cross-linking.* Journal of Virology, 1980. **33**(1): p. 152-166.
243. Orlando, V., H. Strutt, and R. Paro, *Analysis of chromatin structure by in vivo formaldehyde cross-linking.* Methods, 1997. **11**(2): p. 205-14.
244. Sutherland, B.W., J. Toews, and J. Kast, *Utility of formaldehyde cross-linking and mass spectrometry in the study of protein-protein interactions.* J Mass Spectrom, 2008. **43**(6): p. 699-715.
245. Bader, S., S. Kuhner, and A.C. Gavin, *Interaction networks for systems biology.* FEBS Lett, 2008. **582**(8): p. 1220-4.
246. Marouga, R., S. David, and E. Hawkins, *The development of the DIGE system: 2D fluorescence difference gel analysis technology.* Analytical and Bioanalytical Chemistry, 2005. **382**(3): p. 669-678.
247. Unwin, R.D., J.R. Griffiths, and A.D. Whetton, *Simultaneous analysis of relative protein expression levels across multiple samples using iTRAQ isobaric tags with 2D nano LC-MS/MS.* Nat. Protocols, 2010. **5**(9): p. 1574-1582.
248. Thompson, A., et al., *Tandem Mass Tags: A Novel Quantification Strategy for Comparative Analysis of Complex Protein Mixtures by MS/MS.* Analytical Chemistry, 2003. **75**(8): p. 1895-1904.
249. Gygi, S.P., et al., *Quantitative analysis of complex protein mixtures using isotope-coded affinity tags.* Nature biotechnology, 1999. **17**(10): p. 994-999.
250. Ong, S.-E., et al., *Stable Isotope Labeling by Amino Acids in Cell Culture, SILAC, as a Simple and Accurate Approach to Expression Proteomics.* Molecular & Cellular Proteomics, 2002. **1**(5): p. 376-386.
251. Kondo, T. and S. Hirohashi, *Application of 2D-DIGE in Cancer Proteomics Toward Personalized Medicine*. 2009. p. 135-154.
252. Friedman, D.B. and K.S. Lilley, *Optimizing the Difference Gel Electrophoresis (DIGE) Technology*. 2008. p. 93-124.
253. Barthéléry, M., et al., *2-D DIGE identification of differentially expressed heterogeneous nuclear ribonucleoproteins and transcription factors during neural differentiation of human embryonic stem cells.* PROTEOMICS – Clinical Applications, 2009. **3**(4): p. 505-514.
254. Kantawong, F., et al., *Differential in-gel electrophoresis (DIGE) analysis of human bone marrow osteoprogenitor cell contact guidance.* Acta Biomaterialia, 2009. **5**(4): p. 1137-1146.
255. Ross, P.L., et al., *Multiplexed Protein Quantitation in Saccharomyces cerevisiae Using Amine-reactive Isobaric Tagging Reagents.* Molecular & Cellular Proteomics, 2004. **3**(12): p. 1154-1169.
256. Spooncer, E., et al., *Developmental Fate Determination and Marker Discovery in Hematopoietic Stem Cell Biology Using Proteomic Fingerprinting.* Molecular & Cellular Proteomics, 2008. **7**(3): p. 573-581.
257. Unwin, R.D., et al., *Quantitative proteomics reveals posttranslational control as a regulatory factor in primary hematopoietic stem cells.* Blood, 2006. **107**(12): p. 4687-94.
258. Williamson, A.J.K., et al., *Quantitative Proteomics Analysis Demonstrates Post-transcriptional Regulation of Embryonic Stem Cell Differentiation to Hematopoiesis.* Molecular & Cellular Proteomics, 2008. **7**(3): p. 459-472.

259. Ji, Y.-h., et al., *Quantitative Proteomics Analysis of Chondrogenic Differentiation of C3H10T1/2 Mesenchymal Stem Cells by iTRAQ Labeling Coupled with On-line Two-dimensional LC/MS/MS.* Molecular & Cellular Proteomics, 2010. **9**(3): p. 550-564.
260. Dayon, L., et al., *Combining low- and high-energy tandem mass spectra for optimized peptide quantification with isobaric tags.* Journal of Proteomics, 2010. **73**(4): p. 769-777.
261. Wang, J., et al., *A protein interaction network for pluripotency of embryonic stem cells.* Nature, 2006. **444**(7117): p. 364-368.
262. Gygi, S.P., et al., *Quantitative analysis of complex protein mixtures using isotope-coded affinity tags.* Nat Biotech, 1999. **17**(10): p. 994-999.
263. Lee, J.-H., et al., *Role of PI3K on the regulation of BMP2-induced [beta]-Catenin activation in human bone marrow stem cells.* Bone, 2010. **46**(6): p. 1522-1532.
264. Yang, L.Y., et al., *Adipose tissue-derived stromal cells express neuronal phenotypes.* Chin Med J (Engl), 2004. **117**(3): p. 425-9.
265. Huang, T., et al., *Neuron-like differentiation of adipose-derived stem cells from infant piglets in vitro.* J Spinal Cord Med, 2007. **30 Suppl 1**: p. S35-40.
266. Yang, L., J. Zheng, and C. Wang, *[The in vitro study of the human adipose tissue-derived stromal cells differentiating into the neuron-like cells].* Zhongguo Xiu Fu Chong Jian Wai Ke Za Zhi, 2006. **20**(8): p. 783-6.
267. Dhar, S., et al., *Long-term maintenance of neuronally differentiated human adipose tissue-derived stem cells.* Tissue Eng, 2007. **13**(11): p. 2625-32.
268. Wu, S.-C., et al., *Enhancement of chondrogenesis of human adipose derived stem cells in a hyaluronan-enriched microenvironment.* Biomaterials, 2010. **31**(4): p. 631-640.
269. Lepski, G., et al., *Limited Ca2+ and PKA-pathway dependent neurogenic differentiation of human adult mesenchymal stem cells as compared to fetal neuronal stem cells.* Experimental Cell Research, 2010. **316**(2): p. 216-231.
270. Sadie-Van Gijsen, H., et al., *Depot-specific and hypercaloric diet-induced effects on the osteoblast and adipocyte differentiation potential of adipose-derived stromal cells.* Molecular and Cellular Endocrinology, 2012. **348**(1): p. 55-66.
271. Hu, X., et al., *Histone Deacetylase Inhibitor Trichostatin A Promotes the Osteogenic Differentiation of Rat Adipose-Derived Stem Cells by Altering the Epigenetic Modifications on Runx2 Promoter in a BMP Signaling-Dependent Manner.* Stem Cells Dev, 2013. **22**(2): p. 248-55.
272. Chen, J., et al., *Transplantation of Adipose-Derived Stem Cells is Associated with Neural Differentiation and Functional Improvement in a Rat Model of Intracerebral Hemorrhage.* CNS Neuroscience & Therapeutics, 2012.
273. Lee, J.W., et al., *Chondrogenic differentiation of mesenchymal stem cells and its clinical applications.* Yonsei Med J, 2004. **45 Suppl**: p. 41-7.
274. Deng, J., et al., *Mesenchymal Stem Cells Spontaneously Express Neural Proteins in Culture and Are Neurogenic after Transplantation.* STEM CELLS, 2006. **24**(4): p. 1054-1064.
275. Saito, F., et al., *Spinal Cord Injury Treatment With Intrathecal Autologous Bone Marrow Stromal Cell Transplantation: The First Clinical Trial Case Report.* The Journal of Trauma and Acute Care Surgery, 2008. **64**(1): p. 53-59 10.1097/TA.0b013e31815b847d.
276. von Knoch, F., et al., *Effects of bisphosphonates on proliferation and osteoblast differentiation of human bone marrow stromal cells.* Biomaterials, 2005. **26**(34): p. 6941-6949.
277. Sabatino, M., et al., *The establishment of a bank of stored clinical bone marrow stromal cell products.* Journal of Translational Medicine, 2012. **10**(1): p. 23.
278. Mackay, A.M., et al., *Chondrogenic differentiation of cultured human mesenchymal stem cells from marrow.* Tissue Eng, 1998. **4**: p. 415 - 428.

279. Fujimura, J., et al., *Neural differentiation of adipose-derived stem cells isolated from GFP transgenic mice.* Biochemical and Biophysical Research Communications, 2005. **333**(1): p. 116-121.
280. Declercq, H., et al., *Isolation, proliferation and differentiation of osteoblastic cells to study cell/biomaterial interactions: comparison of different isolation techniques and source.* Biomaterials, 2004. **25**(5): p. 757-768.
281. Bellows, C.G., J.E. Aubin, and J.N.M. Heersche, *Initiation and progression of mineralization of bone nodules formed in vitro: the role of alkaline phosphatase and organic phosphate.* Bone and Mineral, 1991. **14**(1): p. 27-40.
282. Ovchinnikov, D., *Alcian Blue/Alizarin Red Staining of Cartilage and Bone in Mouse.* Cold Spring Harbor Protocols, 2009. **2009**(3): p. pdb.prot5170.
283. Herbert, B., et al., *Reduction and alkylation of proteins in preparation of two-dimensional map analysis: why, when, and how?* ELECTROPHORESIS, 2001. **22**(10): p. 2046-57.
284. Jobbins, S.E., et al., *Immunoproteomic approach to elucidating the pathogenesis of cryptococcosis caused by Cryptococcus gattii.* J Proteome Res, 2010. **9**(8): p. 3832-41.
285. Penolazzi, L., et al., *Evaluation of chemokine and cytokine profiles in osteoblast progenitors from umbilical cord blood stem cells by BIO-PLEX technology.* Cell Biology International, 2008. **32**(2): p. 320-325.
286. Dotti, C.G., C.A. Sullivan, and G.A. Banker, *The establishment of polarity by hippocampal neurons in culture.* J Neurosci, 1988. **8**(4): p. 1454-68.
287. Alderson, R.F., et al., *Brain-derived neurotrophic factor increases survival and differentiated functions of rat septal cholinergic neurons in culture.* Neuron, 1990. **5**(3): p. 297-306.
288. Wan Safwani, W.K.Z., et al., *The changes of stemness biomarkers expression in human adipose-derived stem cells during long-term manipulation.* Biotechnology and Applied Biochemistry, 2011. **58**(4): p. 261-270.
289. Guerne, P.A., D.A. Carson, and M. Lotz, *IL-6 production by human articular chondrocytes. Modulation of its synthesis by cytokines, growth factors, and hormones in vitro.* The Journal of Immunology, 1990. **144**(2): p. 499-505.
290. Yang, Y.Q., et al., *The role of vascular endothelial growth factor in ossification.* Int J Oral Sci, 2012. **4**(2): p. 64-8.
291. Bossolasco, P., et al., *Neuro-glial differentiation of human bone marrow stem cells in vitro.* Experimental Neurology, 2005. **193**(2): p. 312-325.
292. Marcus, A.J., et al., *Isolation, characterization, and differentiation of stem cells derived from the rat amniotic membrane.* Differentiation, 2008. **76**(2): p. 130-144.
293. Sanchez-Ramos, J.R., et al., *Expression of Neural Markers in Human Umbilical Cord Blood.* Experimental Neurology, 2001. **171**(1): p. 109-115.
294. Jaiswal, N., et al., *Osteogenic differentiation of purified, culture-expanded human mesenchymal stem cells in vitro.* Journal of Cellular Biochemistry, 1997. **64**(2): p. 295-312.
295. Chao, Y.X., et al., *Protein aggregate-containing neuron-like cells are differentiated from bone marrow mesenchymal stem cells from mice with neurofilament light subunit gene deficiency.* Neuroscience Letters, 2007. **417**(3): p. 240-245.
296. Franco Lambert, A.P., et al., *Differentiation of human adipose-derived adult stem cells into neuronal tissue: Does it work?* Differentiation, 2009. **77**(3): p. 221-228.
297. Battula, V.L., et al., *Prospective isolation and characterization of mesenchymal stem cells from human placenta using a frizzled-9-specific monoclonal antibody.* Differentiation, 2008. **76**(4): p. 326-336.
298. Gronthos, S., et al., *Surface protein characterization of human adipose tissue-derived stromal cells.* Journal of Cellular Physiology, 2001. **189**(1): p. 54-63.
299. Martin, I., et al., *A survey on cellular and engineered tissue therapies in europe in 2008.* Tissue Eng Part A, 2010. **16**(8): p. 2419-27.

300. Hadházy, C., et al., *Exogenous glycosaminoglycans modulate chondrogenesis, cyclic AMP level and cell growth in limb bud mesenchyme cultures.* Tissue and Cell, 1989. **21**(5): p. 673-685.
301. Han, Z.B., H.X. Chen, and J.X. Deng, *[Multipotential differentiation and potential applications of adipose-derived stem cells].* Sheng Wu Gong Cheng Xue Bao, 2007. **23**(2): p. 195-200.
302. Freyria, A.M. and F. Mallein-Gerin, *Chondrocytes or adult stem cells for cartilage repair: the indisputable role of growth factors.* Injury, 2012. **43**(3): p. 259-65.
303. Knudson, C.B., *Hyaluronan and CD44: strategic players for cell-matrix interactions during chondrogenesis and matrix assembly.* Birth Defects Res C Embryo Today, 2003. **69**(2): p. 174-96.
304. Lee, J.Y. and A.P. Spicer, *Hyaluronan: a multifunctional, megaDalton, stealth molecule.* Current Opinion in Cell Biology, 2000. **12**(5): p. 581-586.
305. Anderson, J.M., et al., *Osteogenic differentiation of human mesenchymal stem cells synergistically enhanced by biomimetic peptide amphiphiles combined with conditioned medium.* Acta Biomaterialia, 2011. **7**(2): p. 675-682.
306. Estes, B.T., et al., *Extended passaging, but not aldehyde dehydrogenase activity, increases the chondrogenic potential of human adipose-derived adult stem cells.* Journal of Cellular Physiology, 2006. **209**(3): p. 987-995.
307. Levi, B.P., et al., *Aldehyde dehydrogenase 1a1 is dispensable for stem cell function in the mouse hematopoietic and nervous systems.* Blood, 2009. **113**(8): p. 1670-1680.
308. Grün, F., et al., *Aldehyde Dehydrogenase 6, a Cytosolic Retinaldehyde Dehydrogenase Prominently Expressed in Sensory Neuroepithelia during Development.* Journal of Biological Chemistry, 2000. **275**(52): p. 41210-41218.
309. Atkinson, J.C., et al., *Collagen VI Regulates Normal and Transformed Mesenchymal Cell Proliferationin Vitro.* Experimental Cell Research, 1996. **228**(2): p. 283-291.
310. Lamande, S.R., et al., *The role of the alpha3(VI) chain in collagen VI assembly. Expression of an alpha3(VI) chain lacking N-terminal modules N10-N7 restores collagen VI assembly, secretion, and matrix deposition in an alpha3(VI)-deficient cell line.* J Biol Chem, 1998. **273**(13): p. 7423-30.
311. Kishi, S., et al., *SOX9 protein induces a chondrogenic phenotype of mesangial cells and contributes to advanced diabetic nephropathy.* J Biol Chem, 2011. **286**(37): p. 32162-9.
312. Roughley, P.J., et al., *Non-proteoglycan forms of biglycan increase with age in human articular cartilage.* Biochem J, 1993. **295 (Pt 2)**: p. 421-6.
313. Buckwalter, J.A. and H.J. Mankin, *Articular cartilage: tissue design and chondrocyte-matrix interactions.* Instructional course lectures, 1998. **47**: p. 477-486.
314. Sunil, P., et al., *Stem cell therapy in oral and maxillofacial region: An overview.* J Oral Maxillofac Pathol, 2012. **16**(1): p. 58-63.
315. Siddiqui, N.A. and J.M. Owen, *Clinical Advances in Bone Regeneration.* Curr Stem Cell Res Ther, 2013.
316. Katagiri, T. and N. Takahashi, *Regulatory mechanisms of osteoblast and osteoclast differentiation.* Oral Diseases, 2002. **8**(3): p. 147-159.
317. Koli, K., M.J. Ryynänen, and J. Keski-Oja, *Latent TGF-[beta] binding proteins (LTBPs)-1 and -3 coordinate proliferation and osteogenic differentiation of human mesenchymal stem cells.* Bone, 2008. **43**(4): p. 679-688.
318. Miner, J.H. and P.D. Yurchenco, *LAMININ FUNCTIONS IN TISSUE MORPHOGENESIS.* Annual Review of Cell and Developmental Biology, 2004. **20**(1): p. 255-284.
319. Xiao, Y., et al., *Gene expression profiling of bone marrow stromal cells from juvenile, adult, aged and osteoporotic rats: with an emphasis on osteoporosis.* Bone, 2007. **40**(3): p. 700-15.
320. Yoshikawa, M., et al., *Effects of Laminin For Osteogenesis in Porous Hydroxyapatite.* Macromolecular Symposia, 2007. **253**(1): p. 172-178.

321. Yang, D.H., et al., *Renal collecting system growth and function depend upon embryonic gamma1 laminin expression.* Development, 2011. **138**(20): p. 4535-44.
322. Mittag, F., et al., *Laminin-5 and type I collagen promote adhesion and osteogenic differentiation of animal serum-free expanded human mesenchymal stromal cells*. 2012. Vol. 4. 2012.
323. Schwartz-Filho, H.O., et al., *The Effect of Laminin-1-Doped Nanoroughened Implant Surfaces: Gene Expression and Morphological Evaluation.* International Journal of Biomaterials, 2012. **2012**: p. 9.
324. Damsky, C.H., *Extracellular matrix–integrin interactions in osteoblast function and tissue remodeling.* Bone, 1999. **25**(1): p. 95-96.
325. Zimmerman, D., et al., *Impaired Bone Formation in Transgenic Mice Resulting from Altered Integrin Function in Osteoblasts.* Developmental Biology, 2000. **220**(1): p. 2-15.
326. Jing, L., et al., *Differential expression of galectin-1 and its interactions with cells and laminins in the intervertebral disc.* J Orthop Res, 2012. **30**(12): p. 1923-31.
327. Aubin, J.E., et al., *Expression and regulation of galectin 3 in rat osteoblastic cells.* J Cell Physiol, 1996. **169**(3): p. 468-80.
328. Stock, M., et al., *Expression of Galectin-3 in Skeletal Tissues Is Controlled by Runx2.* Journal of Biological Chemistry, 2003. **278**(19): p. 17360-17367.
329. Bruder, S.P., et al., *Monoclonal antibodies reactive with human osteogenic cell surface antigens.* Bone, 1997. **21**(3): p. 225-235.
330. James, A.W., et al., *Sonic Hedgehog influences the balance of osteogenesis and adipogenesis in mouse adipose-derived stromal cells.* Tissue Eng Part A, 2010. **16**(8): p. 2605-2616.
331. Linde, A. and B. Persliden, *Cathepsind activity in isolated odontoblasts.* Calcified Tissue Research, 1977. **23**(1): p. 33-38.
332. Xynos, I.D., et al., *Ionic Products of Bioactive Glass Dissolution Increase Proliferation of Human Osteoblasts and Induce Insulin-like Growth Factor II mRNA Expression and Protein Synthesis.* Biochemical and Biophysical Research Communications, 2000. **276**(2): p. 461-465.
333. Zheng, M.H., D.J. Wood, and J.M. Papadimitriou, *What's new in the role of cytokines on osteoblast proliferation and differentiation?* Pathol Res Pract, 1992. **188**(8): p. 1104-21.
334. Shen, F., et al., *Cytokines link osteoblasts and inflammation: microarray analysis of interleukin-17- and TNF-α-induced genes in bone cells.* Journal of Leukocyte Biology, 2005. **77**(3): p. 388-399.
335. Bussard, K.M., D.J. Venzon, and A.M. Mastro, *Osteoblasts are a major source of inflammatory cytokines in the tumor microenvironment of bone metastatic breast cancer.* Journal of Cellular Biochemistry, 2010. **111**(5): p. 1138-1148.
336. Greenfield, E.M., et al., *Regulation of cytokine expression in osteoblasts by parathyroid hormone: Rapid stimulation of interleukin-6 and leukemia inhibitory factor mRNA.* Journal of Bone and Mineral Research, 1993. **8**(10): p. 1163-1171.
337. Canalis, E., *Interleukin-1 has independent effects on deoxyribonucleic acid and collagen synthesis in cultures of rat calvariae.* Endocrinology, 1986. **118**(1): p. 74-81.
338. LORENZO, J.A., et al., *Comparison of the Bone-Resorbing Activity in the Supernatants from Phytohemagglutinin-Stimulated Human Peripheral Blood Mononuclear Cells with That of Cytokines Through the Use of an Antiserum to Inter leukin 1.* Endocrinology, 1987. **121**(3): p. 1164-1170.
339. Dennis, J.E., et al., *The STRO-1+ marrow cell population is multipotential.* Cells Tissues Organs, 2002. **170**(2-3): p. 73-82.
340. Hanazawa, S., et al., *Human purified interleukin-1 inhibits DNA synthesis and cell growth of osteoblastic cell line (MC3T3-E1), but enhances alkaline phosphatase activity in the cells.* FEBS letters, 1986. **203**(2): p. 279-284.
341. Frost, A., et al., *Inflammatory cytokines regulate proliferation of cultured human osteoblasts.* Acta Orthopaedica, 1997. **68**(2): p. 91-96.

342. Rickard, D.J., M. Gowen, and B.R. MacDonald, *Proliferative responses to estradiol, IL-1α and TGFβ by cells expressing alkaline phosphatase in human osteoblast-like cell cultures.* Calcified Tissue International, 1993. **52**(3): p. 227-233.
343. Chaudhary, L., T. Spelsberg, and B. Riggs, *Production of various cytokines by normal human osteoblast-like cells in response to interleukin-1 beta and tumor necrosis factor-alpha: lack of regulation by 17 beta-estradiol.* Endocrinology, 1992. **130**(5): p. 2528-2534.
344. Ishimi, Y., et al., *IL-6 is produced by osteoblasts and induces bone resorption.* The Journal of Immunology, 1990. **145**(10): p. 3297-3303.
345. Jimi, E., et al., *Molecular mechanisms of BMP-induced bone formation: cross-talk between BMP and NF-κB signaling pathways in osteoblastogenesis.* Japanese Dental Science Review, 2010. **46**(1): p. 33-42.
346. Lee, Y., et al., *Differences in the cytokine profiles associated with prostate cancer cell induced osteoblastic and osteolytic lesions in bone.* Journal of Orthopaedic Research, 2003. **21**(1): p. 62-72.
347. Walsh, et al., *Cytokine expression by cultured osteoblasts from patients with osteoporotic fractures.* International Journal of Experimental Pathology, 2000. **81**(2): p. 159-163.
348. Dudziak, M.E., et al., *The effects of ionizing radiation on osteoblast-like cells in vitro.* Plastic and reconstructive surgery, 2000. **106**(5): p. 1049-1061.
349. Bilbe, G., et al., *PCR phenotyping of cytokines, growth factors and their receptors and bone matrix proteins in human osteoblast-like cell lines.* Bone, 1996. **19**(5): p. 437-445.
350. Mareschi, K., et al., *Neural differentiation of human mesenchymal stem cells: evidence for expression of neural markers and eag K+ channel types.* Experimental Hematology, 2006. **34**(11): p. 1563-1572.
351. Lu, P., A. Blesch, and M.H. Tuszynski, *Induction of bone marrow stromal cells to neurons: Differentiation, transdifferentiation, or artifact?* Journal of Neuroscience Research, 2004. **77**(2): p. 174-191.
352. Grill, R.J., Jr. and S.K. Pixley, *2-Mercaptoethanol is a survival factor for olfactory, cortical and hippocampal neurons in short-term dissociated cell culture.* Brain Res, 1993. **613**(1): p. 168-72.
353. Wislet-Gendebien, S., et al., *Astrocytic and neuronal fate of mesenchymal stem cells expressing nestin.* Brain Research Bulletin, 2005. **68**(1–2): p. 95-102.
354. Tan, B., et al., *AMP-activated kinase mediates adipose stem cell-stimulated neuritogenesis of PC12 cells.* Neuroscience, 2011. **181**: p. 40-47.
355. James, A.W., et al., *Use of Human Perivascular Stem Cells for Bone Regeneration.* J Vis Exp, 2012(63): p. e2952.
356. Arvidson, K., et al., *Bone regeneration and stem cells.* J Cell Mol Med, 2011. **15**(4): p. 718-46.
357. Marolt, D., M. Knezevic, and G. Vunjak-Novakovic, *Bone tissue engineering with human stem cells.* Stem Cell Research & Therapy, 2010. **1**(2): p. 10.
358. Ray, J. and F.H. Gage, *Differential properties of adult rat and mouse brain-derived neural stem/progenitor cells.* Molecular and Cellular Neuroscience, 2006. **31**(3): p. 560-573.
359. Moraleda, J.M., et al., *Adult stem cell therapy: Dream or reality?* Transplant Immunology, 2006. **17**(1): p. 74-77.
360. Yang, Y., et al., *NRSF silencing induces neuronal differentiation of human mesenchymal stem cells.* Experimental Cell Research, 2008. **314**(11-12): p. 2257-2265.
361. White, K., J.V. Bruckner, and W.L. Guess, *Toxicological studies of 2-mercaptoethanol.* Journal of Pharmaceutical Sciences, 1973. **62**(2): p. 237-241.
362. Ho, M., et al., *Comparison of standard surface chemistries for culturing mesenchymal stem cells prior to neural differentiation.* Biomaterials, 2006. **27**(24): p. 4333-4339.
363. Li, Q.-m., et al., *MSCs guide neurite directional extension and promote oligodendrogenesis in NSCs.* Biochemical and Biophysical Research Communications, 2009. **384**(3): p. 372-377.

364. Pothos, E.N., et al., *D2-Like dopamine autoreceptor activation reduces quantal size in PC12 cells.* J Neurosci, 1998. **18**(15): p. 5575-85.
365. Quesnel, C., et al., *Alveolar fibroblasts in acute lung injury: biological behaviour and clinical relevance.* European Respiratory Journal, 2010. **35**(6): p. 1312-1321.
366. Yamauchi, H., M. Kouhei, and A. Masahiro, *Proteomic assessment of important proteins for motor recovery in a rat model of photochemically-induced thrombosis.(Report).* Journal of Applied Research. Therapeutic Solutions L.L.C. 2009. HighBeam Research. , 2009.
367. Marangos, P.J. and D.E. Schmechel, *Neuron Specific Enolase, A Clinically Useful Marker for Neurons and Neuroendocrine Cells.* Annual Review of Neuroscience, 1987. **10**(1): p. 269-295.
368. Buniatian, G., et al., *The immunoreactivity of glial fibrillary acidic protein in mesangial cells and podocytes of the glomeruli of rat kidney in vivo and in culture.* Biol Cell, 1998. **90**(1): p. 53-61.
369. Maunoury, R., et al., *Glial fibrillary acidic protein immunoreactivity in adrenocortical and Leydig cells of the Syrian golden hamster (Mesocricetus auratus).* J Neuroimmunol, 1991. **35**(1-3): p. 119-29.
370. Davidoff, M.S., et al., *Leydig cells of the human testis possess astrocyte and oligodendrocyte marker molecules.* Acta Histochem, 2002. **104**(1): p. 39-49.
371. Kasantikul, V. and S. Shuangshoti, *Positivity to glial fibrillary acidic protein in bone, cartilage, and chordoma.* J Surg Oncol, 1989. **41**(1): p. 22-6.
372. Caccamo, D., et al., *Immunohistochemistry of a spontaneous murine ovarian teratoma with neuroepithelial differentiation. Neuron-associated beta-tubulin as a marker for primitive neuroepithelium.* Laboratory investigation; a journal of technical methods and pathology, 1989. **60**(3): p. 390-398.
373. Hoffman, P.N. and D.W. Cleveland, *Neurofilament and tubulin expression recapitulates the developmental program during axonal regeneration: induction of a specific beta-tubulin isotype.* Proceedings of the National Academy of Sciences, 1988. **85**(12): p. 4530-4533.
374. Katsetos, C.D., et al., *Class III beta-tubulin isotype: a key cytoskeletal protein at the crossroads of developmental neurobiology and tumor neuropathology.* J Child Neurol, 2003. **18**(12): p. 851-66; discussion 867.
375. Kilroy, G.E., et al., *Cytokine profile of human adipose-derived stem cells: Expression of angiogenic, hematopoietic, and pro-inflammatory factors.* Journal of Cellular Physiology, 2007. **212**(3): p. 702-709.
376. Taha, M.F. and V. Hedayati, *Isolation, identification and multipotential differentiation of mouse adipose tissue-derived stem cells.* Tissue Cell, 2010. **42**(4): p. 211-6.
377. Safford, K.M., et al., *Characterization of neuronal/glial differentiation of murine adipose-derived adult stromal cells.* Experimental Neurology, 2004. **187**(2): p. 319-328.
378. Jacque, C.M., et al., *Determination of glial fibrillary acidic protein (GFAP) in human brain tumors.* J Neurol Sci, 1978. **35**(1): p. 147-55.
379. Wislet-Gendebien, S., et al., *Regulation of neural markers nestin and GFAP expression by cultivated bone marrow stromal cells.* Journal of Cell Science, 2003. **116**(16): p. 3295-3302.
380. Michalczyk, K. and M. Ziman, *Nestin structure and predicted function in cellular cytoskeletal organisation.* Histol Histopathol, 2005. **20**(2): p. 665-71.
381. Maragakis, N.J., et al., *Glutamate transporter expression and function in human glial progenitors.* Glia, 2004. **45**(2): p. 133-143.
382. Jin, K., et al., *Heparin-Binding Epidermal Growth Factor-Like Growth Factor: Hypoxia-Inducible Expression In Vitro and Stimulation of Neurogenesis In Vitro and In Vivo.* The Journal of Neuroscience, 2002. **22**(13): p. 5365-5373.
383. Enwere, E., et al., *Aging Results in Reduced Epidermal Growth Factor Receptor Signaling, Diminished Olfactory Neurogenesis, and Deficits in Fine Olfactory Discrimination.* The Journal of Neuroscience, 2004. **24**(38): p. 8354-8365.

384. Müller, S., et al., *Neurogenesis in the Dentate Gyrus Depends on Ciliary Neurotrophic Factor and Signal Transducer and Activator of Transcription 3 Signaling.* STEM CELLS, 2009. **27**(2): p. 431-441.
385. Dziennis, S. and J. Alkayed Nabil, *Role of Signal Transducer and Activator of Transcription 3 in Neuronal Survival and Regeneration*, in *Reviews in the Neurosciences*. 2008. p. 341.
386. Benaud, C., et al., *AHNAK interaction with the annexin 2/S100A10 complex regulates cell membrane cytoarchitecture.* The Journal of Cell Biology, 2004. **164**(1): p. 133-144.
387. Lee, I.H., et al., *Ahnak Protein Activates Protein Kinase C (PKC) through Dissociation of the PKC-Protein Phosphatase 2A Complex.* Journal of Biological Chemistry, 2008. **283**(10): p. 6312-6320.
388. Amagai, M., *A Mystery of AHNAK//Desmoyokin Still Goes On.* J Investig Dermatol, 2004. **123**(4): p. xiv-xiv.
389. Thomson, S., et al., *A systems view of epithelial–mesenchymal transition signaling states.* Clinical and Experimental Metastasis, 2011. **28**(2): p. 137-155.
390. Borgonovo, B., et al., *Regulated exocytosis: a novel, widely expressed system.* Nature Cell Biology, 2002. **4**(12): p. 955-962.
391. Warner-Schmidt, J.L., et al., *Role of p11 in Cellular and Behavioral Effects of 5-HT4 Receptor Stimulation.* The Journal of Neuroscience, 2009. **29**(6): p. 1937-1946.
392. Gerasimenko, J.V., et al., *Bile Acids Induce Ca2+ Release from Both the Endoplasmic Reticulum and Acidic Intracellular Calcium Stores through Activation of Inositol Trisphosphate Receptors and Ryanodine Receptors.* Journal of Biological Chemistry, 2006. **281**(52): p. 40154-40163.
393. Ritter, B., et al., *PACSIN 2, a novel member of the PACSIN family of cytoplasmic adapter proteins.* FEBS Letters, 1999. **454**(3): p. 356-362.
394. Modregger, J., et al., *All three PACSIN isoforms bind to endocytic proteins and inhibit endocytosis.* Journal of Cell Science, 2000. **113**(24): p. 4511-4521.
395. Lee, I.H., et al., *AHNAK-mediated Activation of Phospholipase C-γ1 through Protein Kinase C.* Journal of Biological Chemistry, 2004. **279**(25): p. 26645-26653.
396. Olalla, L.a., et al., *Nuclear Localization of L-type Glutaminase in Mammalian Brain.* Journal of Biological Chemistry, 2002. **277**(41): p. 38939-38944.
397. Bak, L.K., A. Schousboe, and H.S. Waagepetersen, *The glutamate/GABA-glutamine cycle: aspects of transport, neurotransmitter homeostasis and ammonia transfer.* Journal of Neurochemistry, 2006. **98**(3): p. 641-653.
398. Márquez, J., et al., *Glutaminase: A multifaceted protein not only involved in generating glutamate.* Neurochemistry International, 2006. **48**(6–7): p. 465-471.
399. Fon, E.A. and R.H. Edwards, *Molecular mechanisms of neurotransmitter release.* Muscle & Nerve, 2001. **24**(5): p. 581-601.
400. Curthoys, N.P. and M. Watford, *Regulation of glutaminase activity and glutamine metabolism.* Annu Rev Nutr, 1995. **15**: p. 133-59.
401. Albrecht, J. and M.D. Norenberg, *Glutamine: a Trojan horse in ammonia neurotoxicity.* Hepatology, 2006. **44**(4): p. 788-94.
402. Sulzer, D., et al., *Dopamine neurons make glutamatergic synapses in vitro.* J Neurosci, 1998. **18**(12): p. 4588-602.
403. Borg, J., et al., *Selective culture of neurons from rat cerebral cortex: Morphological characterization, glutamate uptake and related enzymes during maturation in various culture media.* Developmental Brain Research, 1985. **18**(1–2): p. 37-49.
404. Paulus, W., C. Huettner, and J.C. Tonn, *Collagens, integrins and the mesenchymal drift in glioblastomas: a comparison of biopsy specimens, spheroid and early monolayer cultures.* Int J Cancer, 1994. **58**(6): p. 841-6.
405. Tabatabaie, L., et al., *l-Serine synthesis in the central nervous system: A review on serine deficiency disorders.* Molecular Genetics and Metabolism, 2010. **99**(3): p. 256-262.

406. Heil, S.G., et al., *Is Mutated Serine Hydroxymethyltransferase (SHMT) Involved in the Etiology of Neural Tube Defects?* Molecular Genetics and Metabolism, 2001. **73**(2): p. 164-172.
407. Page-McCaw, A., A.J. Ewald, and Z. Werb, *Matrix metalloproteinases and the regulation of tissue remodelling.* Nat Rev Mol Cell Biol, 2007. **8**(3): p. 221-33.
408. Yong, V.W., *Metalloproteinases: mediators of pathology and regeneration in the CNS.* Nature Reviews. Neuroscience, 2005. **6**(12): p. 931-944.
409. Fujioka, H., et al., *Neural Functions of Matrix Metalloproteinases: Plasticity, Neurogenesis, and Disease.* Biochemistry Research International, 2012. **2012**: p. 8.
410. Smiley, J.F., A.I. Levey, and M.M. Mesulam, *Infracortical interstitial cells concurrently expressing m2-muscarinic receptors, acetylcholinesterase and nicotinamide adenine dinucleotide phosphate-diaphorase in the human and monkey cerebral cortex.* Neuroscience, 1998. **84**(3): p. 755-769.
411. Bray, S.J., *Notch signalling: a simple pathway becomes complex.* Nat Rev Mol Cell Biol, 2006. **7**(9): p. 678-89.
412. Kikuchi, G., T. Yoshida, and M. Noguchi, *Heme oxygenase and heme degradation.* Biochem Biophys Res Commun, 2005. **338**(1): p. 558-67.
413. Vile, G.F., et al., *Heme oxygenase 1 mediates an adaptive response to oxidative stress in human skin fibroblasts.* Proceedings of the National Academy of Sciences, 1994. **91**(7): p. 2607-2610.
414. Motterlini, R., et al., *Curcumin, an antioxidant and anti-inflammatory agent, induces heme oxygenase-1 and protects endothelial cells against oxidative stress.* Free Radical Biology and Medicine, 2000. **28**(8): p. 1303-1312.
415. Hayashi, S., et al., *Induction of Heme Oxygenase-1 Suppresses Venular Leukocyte Adhesion Elicited by Oxidative Stress: Role of Bilirubin Generated by the Enzyme.* Circulation Research, 1999. **85**(8): p. 663-671.
416. Mehindate, K., et al., *Proinflammatory cytokines promote glial heme oxygenase-1 expression and mitochondrial iron deposition: implications for multiple sclerosis.* J Neurochem, 2001. **77**(5): p. 1386-95.
417. Kim, Y.S., et al., *The anti-inflammatory role of heme oxygenase-1 in lipopolysaccharide and cytokine-stimulated inducible nitric oxide synthase and nitric oxide production in human periodontal ligament cells.* J Periodontol, 2009. **80**(12): p. 2045-55.
418. Choi, A.M. and J. Alam, *Heme oxygenase-1: function, regulation, and implication of a novel stress-inducible protein in oxidant-induced lung injury.* American journal of respiratory cell and molecular biology, 1996. **15**(1): p. 9-19.
419. Chen, K., K. Gunter, and M.D. Maines, *Neurons Overexpressing Heme Oxygenase-1 Resist Oxidative Stress-Mediated Cell Death.* Journal of Neurochemistry, 2000. **75**(1): p. 304-313.
420. Radtke, S., et al., *Cross-regulation of cytokine signalling: pro-inflammatory cytokines restrict IL-6 signalling through receptor internalisation and degradation.* J Cell Sci, 2010. **123**(Pt 6): p. 947-59.
421. Ivashkiv, L.B., *A signal-switch hypothesis for cross-regulation of cytokine and TLR signalling pathways.* Nat Rev Immunol, 2008. **8**(10): p. 816-22.
422. Le, W.D., W.J. Xie, and S.H. Appel, *Protective role of heme oxygenase-1 in oxidative stress-induced neuronal injury.* J Neurosci Res, 1999. **56**(6): p. 652-8.
423. Krzywanski, D.M., et al., *Variable regulation of glutamate cysteine ligase subunit proteins affects glutathione biosynthesis in response to oxidative stress.* Archives of Biochemistry and Biophysics, 2004. **423**(1): p. 116-125.
424. Koide, S.-i., et al., *Association of polymorphism in glutamate-cysteine ligase catalytic subunit gene with coronary vasomotor dysfunction and myocardial infarction.* Journal of the American College of Cardiology, 2003. **41**(4): p. 539-545.
425. Dasgupta, A., S. Das, and P. Kumar Sarkar, *Thyroid hormone promotes glutathione synthesis in astrocytes by up regulation of glutamate cysteine ligase through differential stimulation of*

its catalytic and modulator subunit mRNAs. Free Radical Biology and Medicine, 2007. **42**(5): p. 617-626.
426. Lavoie, S., et al., *Curcumin, quercetin, and tBHQ modulate glutathione levels in astrocytes and neurons: importance of the glutamate cysteine ligase modifier subunit.* Journal of Neurochemistry, 2009. **108**(6): p. 1410-1422.
427. Efferth, T., et al., *Role of glucose-6-phosphate dehydrogenase for oxidative stress and apoptosis.* Cell Death Differ, 2006. **13**(3): p. 527-8; author reply 529-30.
428. Zhang, Z., et al., *High glucose inhibits glucose-6-phosphate dehydrogenase, leading to increased oxidative stress and β-cell apoptosis.* The FASEB Journal, 2010. **24**(5): p. 1497-1505.
429. Mejías, R., et al., *Neuroprotection by Transgenic Expression of Glucose-6-Phosphate Dehydrogenase in Dopaminergic Nigrostriatal Neurons of Mice.* The Journal of Neuroscience, 2006. **26**(17): p. 4500-4508.
430. Herschman, H. and W. Hall, *Regulation of prostaglandin synthase-1 and prostaglandin synthase-2.* Cancer and Metastasis Reviews, 1994. **13**(3-4): p. 241-256.
431. O'Banion, M.K., et al., *Interleukin-1β Induces Prostaglandin G/H Synthase-2 (Cyclooxygenase-2) in Primary Murine Astrocyte Cultures.* Journal of Neurochemistry, 1996. **66**(6): p. 2532-2540.
432. Feng, L., et al., *Involvement of reactive oxygen intermediates in cyclooxygenase-2 expression induced by interleukin-1, tumor necrosis factor-alpha, and lipopolysaccharide.* J Clin Invest, 1995. **95**(4): p. 1669-75.
433. Hollebeeck, S., et al., *Dimethyl sulfoxide (DMSO) attenuates the inflammatory response in the in vitro intestinal Caco-2 cell model.* Toxicology Letters, 2011. **206**(3): p. 268-275.
434. Asmis, L., et al., *DMSO inhibits human platelet activation through cyclooxygenase-1 inhibition. A novel agent for drug eluting stents?* Biochem Biophys Res Commun, 2010. **391**(4): p. 1629-33.
435. Benagiano, M., et al., *Human 60-kDa Heat Shock Protein Is a Target Autoantigen of T Cells Derived from Atherosclerotic Plaques.* The Journal of Immunology, 2005. **174**(10): p. 6509-6517.
436. Tavaria, M., et al., *A hitchhiker's guide to the human Hsp70 family.* Cell Stress Chaperones, 1996. **1**(1): p. 23-8.
437. Morano, K.A., *New tricks for an old dog: the evolving world of Hsp70.* Ann N Y Acad Sci, 2007. **1113**: p. 1-14.
438. Paul Chapple, J., G.R. Smerdon, and A.J.S. Hawkins, *Stress-70 protein induction in Mytilus edulis: Tissue-specific responses to elevated temperature reflect relative vulnerability and physiological function.* Journal of Experimental Marine Biology and Ecology, 1997. **217**(2): p. 225-235.
439. Ritossa, F., *Discovery of the heat shock response.* Cell Stress Chaperones, 1996. **1**(2): p. 97-8.
440. Ritossa, F., *A new puffing pattern induced by temperature shock and DNP in drosophila.* Experientia, 1962. **18**(12): p. 571-573.
441. Ricaniadis, N., et al., *Long-term prognostic significance of HSP-70, c-myc and HLA-DR expression in patients with malignant melanoma.* Eur J Surg Oncol, 2001. **27**(1): p. 88-93.
442. Luders, J., J. Demand, and J. Hohfeld, *The ubiquitin-related BAG-1 provides a link between the molecular chaperones Hsc70/Hsp70 and the proteasome.* J Biol Chem, 2000. **275**(7): p. 4613-7.
443. Jakob, U., et al., *Small heat shock proteins are molecular chaperones.* Journal of Biological Chemistry, 1993. **268**(3): p. 1517-20.
444. Kiang, J.G. and G.C. Tsokos, *Heat shock protein 70 kDa: molecular biology, biochemistry, and physiology.* Pharmacol Ther, 1998. **80**(2): p. 183-201.
445. Deverman, B.E. and P.H. Patterson, *Cytokines and CNS development.* Neuron, 2009. **64**(1): p. 61-78.

446. Perrier, S., F. Darakhshan, and E. Hajduch, *IL-1 receptor antagonist in metabolic diseases: Dr Jekyll or Mr Hyde?* FEBS Lett, 2006. **580**(27): p. 6289-94.
447. Goshen, I., et al., *Brain interleukin-1 mediates chronic stress-induced depression in mice via adrenocortical activation and hippocampal neurogenesis suppression.* Mol Psychiatry, 2008. **13**(7): p. 717-28.
448. Molina-Holgado, E. and F. Molina-Holgado, *Mending the broken brain: neuroimmune interactions in neurogenesis.* J Neurochem, 2010. **114**(5): p. 1277-90.
449. Villeda, S.A., et al., *The ageing systemic milieu negatively regulates neurogenesis and cognitive function.* Nature, 2011. **477**(7362): p. 90-4.
450. Whitney, N.P., et al., *Inflammation mediates varying effects in neurogenesis: relevance to the pathogenesis of brain injury and neurodegenerative disorders.* Journal of Neurochemistry, 2009. **108**(6): p. 1343-1359.
451. Beck Jr, R.D., et al., *Changes in hippocampal IL-15, related cytokines, and neurogenesis in IL-2 deficient mice.* Brain Research, 2005. **1041**(2): p. 223-230.
452. Gómez-Nicola, D., et al., *Interleukin-15 regulates proliferation and self-renewal of adult neural stem cells.* Molecular Biology of the Cell, 2011. **22**(12): p. 1960-1970.
453. Trendelenburg, G. and U. Dirnagl, *Neuroprotective role of astrocytes in cerebral ischemia: Focus on ischemic preconditioning.* Glia, 2005. **50**(4): p. 307-320.
454. Miossec, P., T. Korn, and V.K. Kuchroo, *Interleukin-17 and type 17 helper T cells.* N Engl J Med, 2009. **361**(9): p. 888-98.
455. Chiricozzi, A., et al., *Integrative responses to IL-17 and TNF-alpha in human keratinocytes account for key inflammatory pathogenic circuits in psoriasis.* J Invest Dermatol, 2011. **131**(3): p. 677-87.
456. Chisholm, S.P., et al., *Interleukin-17A Increases Neurite Outgrowth from Adult Postganglionic Sympathetic Neurons.* The Journal of Neuroscience, 2012. **32**(4): p. 1146-1155.
457. Pitzer, C., et al., *Granulocyte-colony stimulating factor improves outcome in a mouse model of amyotrophic lateral sclerosis.* Brain, 2008. **131**(Pt 12): p. 3335-47.
458. Schneider, A., et al., *The hematopoietic factor G-CSF is a neuronal ligand that counteracts programmed cell death and drives neurogenesis.* The Journal of Clinical Investigation, 2005. **115**(8): p. 2083-2098.
459. Kawada, H., et al., *Administration of Hematopoietic Cytokines in the Subacute Phase After Cerebral Infarction Is Effective for Functional Recovery Facilitating Proliferation of Intrinsic Neural Stem/Progenitor Cells and Transition of Bone Marrow-Derived Neuronal Cells.* Circulation, 2006. **113**(5): p. 701-710.
460. Sehara, Y., et al., *Potentiation of neurogenesis and angiogenesis by G-CSF after focal cerebral ischemia in rats.* Brain Research, 2007. **1151**(0): p. 142-149.
461. Butovsky, O., et al., *Microglia activated by IL-4 or IFN-γ differentially induce neurogenesis and oligodendrogenesis from adult stem/progenitor cells.* Molecular and Cellular Neuroscience, 2006. **31**(1): p. 149-160.
462. Butovsky, O., et al., *Microglia can be induced by IFN-γ or IL-4 to express neural or dendritic-like markers.* Molecular and Cellular Neuroscience, 2007. **35**(3): p. 490-500.
463. Lee, Y.W., et al., *IL-4-induced Oxidative Stress Upregulates VCAM-1 Gene Expression in Human Endothelial Cells.* Journal of Molecular and Cellular Cardiology, 2001. **33**(1): p. 83-94.
464. Mesplès, B., et al., *Neuronal TGF-ß1 mediates IL-9/mast cell interaction and exacerbates excitotoxicity in newborn mice.* Neurobiology of Disease, 2005. **18**(1): p. 193-205.
465. Vane, J.R., Y.S. Bakhle, and R.M. Botting, *CYCLOOXYGENASES 1 AND 2.* Annual Review of Pharmacology and Toxicology, 1998. **38**(1): p. 97-120.
466. Iosif, R.E., et al., *Tumor Necrosis Factor Receptor 1 Is a Negative Regulator of Progenitor Proliferation in Adult Hippocampal Neurogenesis.* The Journal of Neuroscience, 2006. **26**(38): p. 9703-9712.

467. Widera, D., et al., *MCP-1 induces migration of adult neural stem cells.* European Journal of Cell Biology, 2004. **83**(8): p. 381-387.
468. Villa, P., et al., *The interleukin-8 (IL-8/CXCL8) receptor inhibitor reparixin improves neurological deficits and reduces long-term inflammation in permanent and transient cerebral ischemia in rats.* Mol Med, 2007. **13**(3-4): p. 125-33.
469. Di Sebastiano, P., et al., *Expression of interleukin 8 (IL-8) and substance P in human chronic pancreatitis.* Gut, 2000. **47**(3): p. 423-8.
470. Ekdahl, C.T., Z. Kokaia, and O. Lindvall, *Brain inflammation and adult neurogenesis: The dual role of microglia.* Neuroscience, 2009. **158**(3): p. 1021-1029.
471. Jin, K., et al., *Vascular endothelial growth factor (VEGF) stimulates neurogenesis in vitro and in vivo.* Proceedings of the National Academy of Sciences, 2002. **99**(18): p. 11946-11950.
472. Sun, Y., et al., *VEGF-induced neuroprotection, neurogenesis, and angiogenesis after focal cerebral ischemia.* The Journal of Clinical Investigation, 2003. **111**(12): p. 1843-1851.
473. Ogunshola, O.O., et al., *Paracrine and Autocrine Functions of Neuronal Vascular Endothelial Growth Factor (VEGF) in the Central Nervous System.* Journal of Biological Chemistry, 2002. **277**(13): p. 11410-11415.
474. Khaibullina, A.A., J.M. Rosenstein, and J.M. Krum, *Vascular endothelial growth factor promotes neurite maturation in primary CNS neuronal cultures.* Developmental Brain Research, 2004. **148**(1): p. 59-68.
475. Rothwell, N.J. and P.J.L.M. Strijbos, *Cytokines in neurodegeneration and repair.* International Journal of Developmental Neuroscience, 1995. **13**(3–4): p. 179-185.
476. Vallières, L., et al., *Reduced Hippocampal Neurogenesis in Adult Transgenic Mice with Chronic Astrocytic Production of Interleukin-6.* The Journal of Neuroscience, 2002. **22**(2): p. 486-492.
477. Monje, M.L., H. Toda, and T.D. Palmer, *Inflammatory Blockade Restores Adult Hippocampal Neurogenesis.* Science, 2003. **302**(5651): p. 1760-1765.
478. Taga, T. and S. Fukuda, *Role of IL-6 in the neural stem cell differentiation.* Clinical Reviews in Allergy & Immunology, 2005. **28**(3): p. 249-256.
479. März, P., et al., *Activation of gp 130 by IL-6/soluble IL-6 receptor induces neuronal differentiation.* European Journal of Neuroscience, 1997. **9**(12): p. 2765-2773.
480. Penkowa, M., et al., *Impaired inflammatory response and increased oxidative stress and neurodegeneration after brain injury in interleukin-6-deficient mice.* Glia, 2000. **32**(3): p. 271-285.
481. McKinnon, R.D., et al., *FGF modulates the PDGF-driven pathway of oligodendrocyte development.* Neuron, 1990. **5**(5): p. 603-614.
482. Cedar, S.H., et al., *From embryos to embryonic stem cells: biopolitics and therapeutic potential.* Reprod Biomed Online, 2006. **13**(5): p. 725-31.
483. Choi, Y.S., et al., *Adipogenic differentiation of adipose tissue derived adult stem cells in nude mouse.* Biochemical and Biophysical Research Communications, 2006. **345**(2): p. 631-637.
484. Beltrami, A.P., D. Cesselli, and C.A. Beltrami, *Pluripotency rush! Molecular cues for pluripotency, genetic reprogramming of adult stem cells, and widely multipotent adult cells.* Pharmacology & Therapeutics. **In Press, Corrected Proof**.
485. Abdanipour, A. and T. Tiraihi, *Induction of adipose-derived stem cell into motoneuron-like cells using selegiline as preinducer.* Brain Research, 2012. **1440**(0): p. 23-33.
486. Ullian, E.M., et al., *Schwann cells and astrocytes induce synapse formation by spinal motor neurons in culture.* Molecular and Cellular Neuroscience, 2004. **25**(2): p. 241-251.
487. Qian, D.-X., et al., *Comparison of the Efficiencies of Three Neural Induction Protocols in Human Adipose Stromal Cells.* Neurochemical Research, 2010. **35**(4): p. 572-579.
488. Sagisaka, T., et al., *Directed neural lineage differentiation of adult hippocampal progenitor cells via modulation of hippocampal cholinergic neurostimulating peptide precursor expression.* Brain Research, 2010. **1327**: p. 107-117.

489. Wilkison, W.O. and J. Gimble, *Adipose tissue-derived stromal cell that expresses characteristics of a neuronal cell.* US patent 7078230 2006.
490. Tao, H., R. Rao, and D.D.F. Ma, *Cytokine-induced stable neuronal differentiation of human bone marrow mesenchymal stem cells in a serum/feeder cell-free condition.* Development, Growth & Differentiation, 2005. **47**(6): p. 423-433.
491. Hensley, K., K. Venkova, and A. Christov, *Emerging biological importance of central nervous system lanthionines.* Molecules, 2010. **15**(8): p. 5581-94.
492. Dupre, S., et al., *Characterization of [35S] Lanthionine Ketimine Specific Binding to Bovine Brain Membranes.* Biochemical and Biophysical Research Communications, 1993. **195**(2): p. 673-678.
493. Fontana, M., et al., *[35S]Lanthionine ketimine binding to bovine brain membranes.* Biochemical and Biophysical Research Communications, 1990. **171**(1): p. 480-486.
494. Watts, P.J. and L. Illum, *Pectin compositions and methods of use for improved delivery of drugs to mucosal surfaces*. 2002, Google Patents.
495. Watts, P.J. and L. Illum, *IMPROVED DELIVERY OF DRUGS TO MUCOSAL SURFACES*. 2004, EP Patent 0,975,367.
496. Kong, X., et al., *Compounds for the treatment of CNS and amyloid associated diseases.* US patent 0167057 A1, 2006.
497. Edgar, D.M., et al., *CNS target modulators.* US patent 7317026, 2008.
498. Hensley, K., et al., *Proteomic identification of binding partners for the brain metabolite lanthionine ketimine (LK) and documentation of LK effects on microglia and motoneuron cell cultures.* J Neurosci, 2010. **30**(8): p. 2979-88.
499. Hensley, K., *Lanthionine-related compounds for the treatment of inflammatory diseases.* US patent 7683055, 2007.
500. Hensley, K., K. Venkova, and A. Christov, *Emerging Biological Importance of Central Nervous System Lanthionines.* Molecules, 2010. **15**(8): p. 5581-5594.
501. Cavallini, D., et al., *Sulfur-containing cyclic ketimines and imino acids. A novel family of endogenous products in the search for a role.* Eur J Biochem, 1991. **202**(2): p. 217-23.
502. Nardini, M., et al., *Bovine brain ketimine reductase.* Biochimica et Biophysica Acta (BBA) - Protein Structure and Molecular Enzymology, 1988. **957**(2): p. 286-292.
503. Ricci, G., et al., *Detection of 2H-1,4-thiazine-5,6-dihydro-3,5-dicarboxylic acid (lanthionine ketimine) in the bovine brain by a fluorometric assay.* Biochimica et Biophysica Acta (BBA) - General Subjects, 1989. **990**(2): p. 211-215.
504. Hensley, K., et al., *Collapsin response mediator protein-2: an emerging pathologic feature and therapeutic target for neurodisease indications.* Mol Neurobiol, 2011. **43**(3): p. 180-91.
505. Solinas, S.P., et al., *The reducing activity of S-aminoethylcysteine ketimine and similar sulfur-containing ketimines.* Biochemical and Biophysical Research Communications, 1992. **183**(2): p. 481-486.
506. Marcoux, F.W., J.E. Goodrich, and M.A. Dominick, *Ketamine prevents ischemic neuronal injury.* Brain Research, 1988. **452**(1–2): p. 329-335.
507. Nada, S.E., et al., *A derivative of the CRMP2 binding compound lanthionine ketimine provides neuroprotection in a mouse model of cerebral ischemia.* Neurochemistry International, 2012. **61**(8): p. 1357-1363.
508. Sheen, V.L., et al., *Filamin A and Filamin B are co-expressed within neurons during periods of neuronal migration and can physically interact.* Human Molecular Genetics, 2002. **11**(23): p. 2845-2854.
509. Nagano, T., S. Morikubo, and M. Sato, *Filamin A and FILIP (Filamin A-Interacting Protein) Regulate Cell Polarity and Motility in Neocortical Subventricular and Intermediate Zones during Radial Migration.* The Journal of Neuroscience, 2004. **24**(43): p. 9648-9657.
510. Vadodaria, K.C., et al., *Stage-Specific Functions of the Small Rho GTPases Cdc42 and Rac1 for Adult Hippocampal Neurogenesis.* The Journal of Neuroscience, 2013. **33**(3): p. 1179-1189.

511. Dong, S., et al., *Curcumin enhances neurogenesis and cognition in aged rats: implications for transcriptional interactions related to growth and synaptic plasticity.* PLoS One, 2012. **7**(2): p. e31211.
512. Gualdoni, S., et al., *Normal levels of Rac1 are important for dendritic but not axonal development in hippocampal neurons.* Biol Cell, 2007. **99**(8): p. 455-64.
513. Tahirovic, S., et al., *Rac1 Regulates Neuronal Polarization through the WAVE Complex.* The Journal of Neuroscience, 2010. **30**(20): p. 6930-6943.
514. Kim, S.Y., et al., *H2O2-dependent hyperoxidation of peroxiredoxin 6 (Prdx6) plays a role in cellular toxicity via up-regulation of iPLA2 activity.* J Biol Chem, 2008. **283**(48): p. 33563-8.
515. Rhee, S.G., H.Z. Chae, and K. Kim, *Peroxiredoxins: a historical overview and speculative preview of novel mechanisms and emerging concepts in cell signaling.* Free Radic Biol Med, 2005. **38**(12): p. 1543-52.
516. Claiborne, A., et al., *Protein-sulfenic acids: diverse roles for an unlikely player in enzyme catalysis and redox regulation.* Biochemistry, 1999. **38**(47): p. 15407-16.
517. Simzar, S., et al., *Contrasting Antioxidant and Cytotoxic Effects of Peroxiredoxin I and II in PC12 and NIH3T3 Cells.* Neurochemical Research, 2000. **25**(12): p. 1613-1621.
518. Holmgren, A., *Thioredoxin and glutaredoxin systems.* J Biol Chem, 1989. **264**(24): p. 13963-6.
519. Nordberg, J. and E.S. Arner, *Reactive oxygen species, antioxidants, and the mammalian thioredoxin system.* Free Radic Biol Med, 2001. **31**(11): p. 1287-312.
520. Ahsan, M.K., et al., *Redox regulation of cell survival by the thioredoxin superfamily: an implication of redox gene therapy in the heart.* Antioxid Redox Signal, 2009. **11**(11): p. 2741-58.
521. Zhou, F., et al., *Attenuation of neuronal degeneration in thioredoxin-1 overexpressing mice after mild focal ischemia.* Brain Res, 2009. **1272**: p. 62-70.
522. Tanaka, J. and K. Sobue, *Localization and characterization of gelsolin in nervous tissues: gelsolin is specifically enriched in myelin-forming cells.* J Neurosci, 1994. **14**(3 Pt 1): p. 1038-52.
523. Sun, H.Q., et al., *Gelsolin, a multifunctional actin regulatory protein.* J Biol Chem, 1999. **274**(47): p. 33179-82.
524. Burtnick, L.D., et al., *Structure of the N-terminal half of gelsolin bound to actin: roles in severing, apoptosis and FAF.* EMBO J, 2004. **23**(14): p. 2713-22.
525. Harms, C., et al., *Neuronal gelsolin prevents apoptosis by enhancing actin depolymerization.* Mol Cell Neurosci, 2004. **25**(1): p. 69-82.
526. Carro, E., *Gelsolin as therapeutic target in Alzheimer's disease.* Expert Opin Ther Targets, 2010. **14**(6): p. 585-92.
527. de la Chapelle, A., et al., *Gelsolin-derived familial amyloidosis caused by asparagine or tyrosine substitution for aspartic acid at residue 187.* Nat Genet, 1992. **2**(2): p. 157-60.
528. Bazinet, C., et al., *The Drosophila clathrin heavy chain gene: clathrin function is essential in a multicellular organism.* Genetics, 1993. **134**(4): p. 1119-1134.
529. Zagon, I.S., et al., *Spectrin subtypes in mammalian brain: an immunoelectron microscopic study.* J Neurosci, 1986. **6**(10): p. 2977-86.
530. Goodman, S.R., B.M. Riederer, and I.S. Zagon, *Spectrin subtypes in mammalian brain.* Bioessays, 1986. **5**(1): p. 25-9.
531. Riederer, B.M., I.S. Zagon, and S.R. Goodman, *Brain spectrin(240/235) and brain spectrin(240/235E): two distinct spectrin subtypes with different locations within mammalian neural cells.* J Cell Biol, 1986. **102**(6): p. 2088-97.
532. Lynch, G. and M. Baudry, *Brain spectrin, calpain and long-term changes in synaptic efficacy.* Brain Res Bull, 1987. **18**(6): p. 809-15.
533. Goodman, S.R., et al., *Brain spectrin: of mice and men.* Brain Res Bull, 1995. **36**(6): p. 593-606.

534. Pasquini, L.A., et al., *Galectin-3 drives oligodendrocyte differentiation to control myelin integrity and function.* Cell Death Differ, 2011. **18**(11): p. 1746-56.
535. Comte, I., et al., *Galectin-3 maintains cell motility from the subventricular zone to the olfactory bulb.* J Cell Sci, 2011. **124**(Pt 14): p. 2438-47.
536. Pesheva, P., et al., *Galectin-3 promotes neural cell adhesion and neurite growth.* J Neurosci Res, 1998. **54**(5): p. 639-54.
537. Pesheva, P., et al., *Murine microglial cells express functionally active galectin-3 in vitro.* J Neurosci Res, 1998. **51**(1): p. 49-57.
538. Iglehart, J.D., et al., *Increased erbB-2 Gene Copies and Expression in Multiple Stages of Breast Cancer.* Cancer Research, 1990. **50**(20): p. 6701-6707.
539. Bailleul, B., et al., *Skin hyperkeratosis and papilloma formation in transgenic mice expressing a ras oncogene from a suprabasal keratin promoter.* Cell, 1990. **62**(4): p. 697-708.
540. Battifora, H. and M.I. Kopinski, *Distinction of mesothelioma from adenocarcinoma. An immunohistochemical approach.* Cancer, 1985. **55**(8): p. 1679-1685.
541. Ayene, I.S., et al., *Mutation in G6PD gene leads to loss of cellular control of protein glutathionylation: mechanism and implication.* J Cell Biochem, 2008. **103**(1): p. 123-35.
542. Bota, D.A., J.K. Ngo, and K.J.A. Davies, *Downregulation of the human Lon protease impairs mitochondrial structure and function and causes cell death.* Free Radical Biology and Medicine, 2005. **38**(5): p. 665-677.
543. Svitkina, T.M., A.B. Verkhovsky, and G.G. Borisy, *Plectin sidearms mediate interaction of intermediate filaments with microtubules and other components of the cytoskeleton.* J Cell Biol, 1996. **135**(4): p. 991-1007.
544. Wiche, G., *Role of plectin in cytoskeleton organization and dynamics.* Journal of Cell Science, 1998. **111**(17): p. 2477-2486.
545. Steinboeck, F. and D. Kristufek, *Identification of the cytolinker protein plectin in neuronal cells - expression of a rodless isoform in neurons of the rat superior cervical ganglion.* Cell Mol Neurobiol, 2005. **25**(7): p. 1151-69.
546. Tsuruta, D. and J.C.R. Jones, *The vimentin cytoskeleton regulates focal contact size and adhesion of endothelial cells subjected to shear stress.* Journal of Cell Science, 2003. **116**(24): p. 4977-4984.
547. Bechtold, D. and I. Brown, *Induction of Hsp27 and Hsp32 Stress Proteins and Vimentin in Glial Cells of the Rat Hippocampus Following Hyperthermia.* Neurochemical Research, 2003. **28**(8): p. 1163-1173.
548. Ding, M., et al., *Altered taurine release following hypotonic stress in astrocytes from mice deficient for GFAP and vimentin.* Molecular Brain Research, 1998. **62**(1): p. 77-81.
549. Janmey, P.A., et al., *Viscoelastic properties of vimentin compared with other filamentous biopolymer networks.* The Journal of Cell Biology, 1991. **113**(1): p. 155-160.
550. Buzzard, K.A., et al., *Heat Shock Protein 72 Modulates Pathways of Stress-induced Apoptosis.* Journal of Biological Chemistry, 1998. **273**(27): p. 17147-17153.
551. Calvo, J., A. Carbonell, and J. Boya, *Co-expression of glial fabrillary acidic protein and vimentin in reactive astrocytes following brain injury in rats.* Brain Research, 1991. **566**(1): p. 333-336.
552. Joshi, R., et al., *Primary structure and domain organization of human alpha and beta adducin.* J Cell Biol, 1991. **115**(3): p. 665-75.
553. Sakaki, M., et al., *Interaction between emerin and nuclear lamins.* J Biochem, 2001. **129**(2): p. 321-7.
554. Guo, C.J., et al., *Interleukin-1beta stimulates macrophage inflammatory protein-1alpha and -1beta expression in human neuronal cells (NT2-N).* J Neurochem, 2003. **84**(5): p. 997-1005.
555. Biber, K., et al., *Chemokines in the brain: neuroimmunology and beyond.* Curr Opin Pharmacol, 2002. **2**(1): p. 63-8.

556. Ma, Q., et al., *Impaired B-lymphopoiesis, myelopoiesis, and derailed cerebellar neuron migration in CXCR4- and SDF-1-deficient mice.* Proc Natl Acad Sci U S A, 1998. **95**(16): p. 9448-53.
557. Pease, J., *Tails of the unexpected–an atypical receptor for the chemokine RANTES/CCL5 expressed in brain.* British journal of pharmacology, 2009. **149**(5): p. 460-462.
558. Proudfoot, A.E.I., et al., *Extension of Recombinant Human RANTES by the Retention of the Initiating Methionine Produces a Potent Antagonist.* Journal of Biological Chemistry, 1996. **271**(5): p. 2599-2603.
559. Hu, S., et al., *Morphine inhibits human microglial cell production of, and migration towards, RANTES.* Journal of Psychopharmacology, 2000. **14**(3): p. 238-243.
560. Keswani, S.C., et al., *Schwann cell chemokine receptors mediate HIV-1 gp120 toxicity to sensory neurons.* Annals of neurology, 2003. **54**(3): p. 287-296.
561. Dejda, A., P. Sokolowska, and J.Z. Nowak, *Neuroprotective potential of three neuropeptides PACAP, VIP and PHI.* Pharmacol Rep, 2005. **57**(3): p. 307-20.
562. Huang, Y.S., et al., *Effects of interleukin-15 on neuronal differentiation of neural stem cells.* Brain Res, 2009. **1304**: p. 38-48.
563. Gomez-Nicola, D., et al., *Interleukin-15 regulates proliferation and self-renewal of adult neural stem cells.* Mol Biol Cell, 2011. **22**(12): p. 1960-70.
564. Shichita, T., et al., *Pivotal role of cerebral interleukin-17-producing gammadeltaT cells in the delayed phase of ischemic brain injury.* Nat Med, 2009. **15**(8): p. 946-50.
565. Kramer, J.M. and S.L. Gaffen, *Interleukin-17: a new paradigm in inflammation, autoimmunity, and therapy.* J Periodontol, 2007. **78**(6): p. 1083-93.
566. Friedenstein, A.J.P. and K.V. Petrokova, *Osteogenesis in transplants of bone marrow cells.* Journal of Embyological Experimental Morphology, 1966. **16**: p. 381 - 390.
567. Chou, J., et al., *Strontium- and magnesium-enriched biomimetic beta-TCP macrospheres with potential for bone tissue morphogenesis.* J Tissue Eng Regen Med, 2012.
568. Green, D., et al., *A Therapeutic Potential for Marine Skeletal Proteins in Bone Regeneration.* Marine Drugs, 2013. **11**(4): p. 1203-1220.